ABSTRACT

Title of Document: REMEDIATION OF PETROLEUM CONTAMINATED SOILS AND GROUNDWATER USING HIGH CARBON CONTENT FLY ASH

Mehmet Melih Demirkan, Ph.D., 2008

Directed By: Associate Professor, Ahmet H. Aydilek, and Associate Professor, Eric A. Seagren, Department of Civil and Environmental Engineering

Class F fly ash, a by-product of coal-burning power plants, is generated in large quantities and occasionally contains significant amounts of unburned carbon (i.e., high loss on ignition) as a result of equipping the power plants with the low nitrogen oxide burners. The overall goal of this research was to assess the feasibility of using high carbon content fly ash (HCCFA) as a stabilizing agent for petroleum contaminated soils (PCSs) and as a reactive medium in permeable sorptive barriers (PSBs) for remediation of petroleum hydrocarbon contaminated groundwater. A battery of laboratory tests was conducted to evaluate the geotechnical and environmental suitability of stabilized PCSs. The test program included batch adsorption, compaction, long-term column leaching, column sorption-desorption, and column biodegradation tests. Naphthalene and *o*-xylene sorption onto seven different fly ashes and powder activated carbon (PAC) was studied in a series of batch adsorption tests. A tertiary model non-aqueous phase liquid was used as

the pollutant in column leaching tests conducted on PCS-fly ash mixtures. Retardation performance of HCCFA or PAC mixed with sand was investigated through column sorption-desorption and column biodegradation experiments to study the mass transfer behavior of the medium in a PRB application.

Batch sorption tests demonstrated a nonlinear sorption behavior for naphthalene and *o*-xylene onto HCCFA. Sorption was strongly correlated with carbon content of the ashes. Compaction test results indicated that the maximum unit weights and optimum liquid contents of the stabilized soils satisfy the limits set for highway embankment construction. Column leaching test results indicated that the naphthalene and *o*-xylene concentrations in the effluents collected from the stabilized PCS columns were lower than those collected from the control (soil only) columns. Column sorption-desorption tests revealed a retardation capacity of 48 to 78% for naphthalene and 15 to 48% for o-xylene. The biodegradation tests showed that high levels of biodegradation occurred when fly ash was employed as reactive medium. The study indicated that HCCFA can be effective in remediation of PCSs, and has good hydraulic and adsorption properties which may justify its potential use as a PSB material in remediation of groundwater contaminated with petroleum residues.

REMEDIATION OF PETROLEUM CONTAMINATED SOILS AND GROUNDWATER USING HIGH CARBON CONTENT FLY ASH

By

Mehmet Melih Demirkan

Dissertation submitted to the Faculty of the Graduate School of the
University of Maryland, College Park, in partial fulfillment
of the requirements for the degree of
[Doctor of Philosophy]
[2008]

Advisory Committee:
Associate Professor [Ahmet H. Aydilek], Chair
Associate Professor [Eric A. Seagren], Co-Chair
Professor [Sherif Aggour]
Professor [Alba Torrents]
Professor [Martin C. Rabenhorst]

Dedication

To my wife, Fatma, and my parents, Hatice and Cevdet Demirkan.

Acknowledgements

I would like to express my gratitude to Dr. Ahmet Aydilek. Starting from my application process to UMD, he supported me enthusiastically and gave me the opportunity to work with him. For almost five years, Dr. Aydilek has been my advisor and guide technically on my research but more importantly a mentor in my career decisions and a friend in my personal matters. The support he provided in so many ways cannot possibly be expressed in words adequately. I feel blessed that I had the opportunity to learn from him and become his friend.

I also want to acknowledge the invaluable help of Dr. Eric A. Seagren as my co-advisor. None of the laboratory work that has been done in this research would have been possible without his guidance, participation and care. Dr. Seagren has been an endless source of support in the laboratory and I feel proud to have worked with him, but more importantly I feel privileged that I had the opportunity to know him in person.

My appreciation also goes to my other committee members; Dr. Torrents, Dr. Aggour, and Dr. Rabenhorst for spending time in reviewing this work and assisting me to complete the degree.

There are people whom I greatly acknowledge their contributions to this study and I would like to thank them all for their support and company during the course of this research. Regis Carvalho, Neha Rustagi, Zack Knight, Kristin Loomis, Alice Tsai, Doina Morar, Xin Song, Eunyoung Hong, Philip Jones, Bora Cetin and Lan Zhang; many thanks.

My mom and dad are my strongest supporters at every stage of my life. I would like to express my deep love and gratitude for their sincere encouragement to reach my

objectives. Last but not least, I am very thankful to Fatma. Her continuous support to my goals is my greatest motivation. Without her, this study could not been completed.

For the funding support of this research, Maryland State Highway Administration, Maryland Department of Natural resources, Graduate School of University of Maryland, Maryland Water Resources Research Center is also gratefully acknowledged.

.

Table of Contents

List of Tables

List of Figures

Chapter 1 Introduction

Remediation of contaminated soil and groundwater has been an important task for engineers and scientists in recent years. As a result, the difficulty of reducing subsurface contamination levels has resulted in the research and development of several innovative and cost-effective treatment technologies. One of the sources of soil and groundwater contamination in the United States is petroleum spills. Petroleum-based contamination contains significant quantities of naphthalene, pyrene, benzene, toluene, and xylenes, which are listed as hazardous waste compounds by the U.S. Environmental Protection Agency. The presence of such compounds in the subsurface environment presents a significant health hazard (Agency for Toxic Substances and Disease Registry 2001).

Approximately 90% of the coal used in United States is burned to produce electricity. As a result, the power plants produce vast quantities of coal combustion by-products (CCBs) that present another environmental challenge. One of these CCBs, Class F fly ash, is generated in large quantities and occasionally contains significant amounts of unburned carbon (i.e., high loss on ignition) due to the common use of low nitrogen oxides (NO_x) burners in recent years. For instance, twelve power plants in Maryland that use the cyclone process to burn coal produce about 600,000 tons of high-carbon content Class F fly ash each year. This fly ash has a carbon content of 12-20% and has no value as a concrete additive, as the maximum carbon content allowed in the ASTM C618 is 6%. Recent data indicate that approximately 68% of this high-carbon content fly ash (HCCFA) is placed in landfills, thereby consuming valuable land space and creating the potential to impact aquatic resources (Petzrick 2001). Therefore, Class F fly ash represents an abundant solid waste for which there is a significant need to find a use.

Large-volume use of fly ash in highway applications can aid in solving this waste disposal problem as well as providing economic savings to users by replacing more costly raw materials. For example, recent investigations indicate that petroleum hydrocarbons in the soil will inhibit the cementitious reactions between the petroleum-contaminated soil and the stabilizing agent, and the pollutant will eventually emanate from the stabilized block as a result of leakage or chemical diffusion. One way to retard or limit the movement of the petroleum hydrocarbons is to provide a sorptive agent that sorbs these pollutants as they move through the soil. The organic carbon in Class F fly ashes is ideally suited for this purpose, as its adsorption of various organic contaminants such as phenols, dyes, herbicides, and polychlorinated biphenyls has been documented (Akgerman and Zardkoohi 1996, Konstantinou and Albanis 2000, Janos et al. 2003, Nollet et al. 2003). Attempts have also been made to stabilize petroleum contaminated wastes using Class F fly ash for their potential use in highway environments; however, this previous work generally included creating a monolithic medium and encapsulating the petroleum contaminants rather than adsorbing them (Tuncan et al. 2000).

Contamination of groundwater with petroleum hydrocarbons is also a commonly encountered phenomenon. Pump-and-treat is a traditionally used method for remediating these products; however, the technique has various drawbacks: (1) necessity of large water volume and long time periods (5-50 years) for effective treatment, (2) difficulty to reach drinking water standards, and (3) high operational costs. These disadvantages prompted researchers to develop alternative methods for in-situ remediation of petroleum contaminants (Khan et al. 2004). One of the passive remediation technologies gaining wide acceptance is the use of permeable reactive barriers (PRB). In this technology, the

pollutants are immobilized permanently or their levels are reduced to the Maximum Contamination Limits (MCL) while the plume is passing through an underground barrier system. One relatively new variation on the PRB concept is to use an immobilization process, in which the organic pollutants are adsorbed onto sorptive surface of the barrier material. The reaction mechanism in these PRBs is often adsorption, and a term "permeable sorptive barriers (PSB)" has been recently introduced (Woinarski et al. 2003). Typical compounds of interest treated with such systems are trichloroethylene (TCE), petroleum hydrocarbons as well as trace elements and heavy metals.

Laboratory studies have demonstrated the effectiveness of various natural and synthetic sorbents as potential reactive/sorptive medium for treatment of groundwater containing both organic and inorganic pollutants. Specific materials tested include such as wood chips, limestone, manure (USEPA 2006), peat (Guerin et al. 2002), and lignitic coal (Jenk et al. 2003) have been investigated. For example, Schad and Gratwohl (1998) reported a successful field application of sorptive barrier using activated carbon as sorbent for a groundwater contaminated with petroleum hydrocarbons. Furthermore, there is growing interest in the utilization of recycled materials for remediation of contaminated groundwater as a part of sorptive barrier investigations. Recycled materials, such as waste tires (Kershaw et al. 1997, Kim et al 1997) and foundry sand (Lee et al. 2004) have also been studied to investigate their feasibility as sorptive medium in these barrier systems. Accordingly, HCCFA has the potential to be another PRB medium as recent research studies suggest that it posses good sorption characteristics for various organic contaminants.

The current study had two main objectives: First objective was to investigate the geotechnical performance and environmental suitability of HCCFA as a binder for stabilization of petroleum contaminated soils. Second one was to address the effectiveness of HCCFA as a sorptive medium in a reactive barrier for groundwater clean-up. To meet these objectives following tests and numerical analyses were performed: (1) Batch adsorption tests were conducted in order to determine the sorption capacity and characteristics of the seven different HCCFA, (2) compaction and column leaching tests were performed on petroleum contaminated soils stabilized with HCCFA, (3) column sorption desorption tests were conducted on HCCFA-sand mixtures to assess the organic pollutant sorption and desorption properties of the HCCFA, (4) column biodegradation experiments were conducted on inoculated HCCFA-sand mixtures to study biodegradation, and (5) biosorptive barriers were designed using the column-derived parameters.

A detailed literature review about remediation of petroleum-contaminated soil and groundwater,, sorption isotherm and biokinetic models, and high carbon content fly ash are presented in Chapter 2. Chapter 3 provides methodology and results of the batch adsorption tests conducted on seven different HCCFA. The utilization of a Maryland HCC fly ash in remediating petroleum contaminated soils for highway application is presented in Chapter 4. Chapter 5 describes methods and results of column sorption-desorption experiments conducted on fly ash-sand mixtures. Chapter 6 provides the procedure and results of the column biodegradation experiments. The barrier design methodology is also given in Chapter 6. Summary and conclusions along with future recommendations are given in Chapter 7.

Chapter 2 Literature Review

Contamination of the subsurface environment by organic pollutants is a growing problem that needs to be addressed by environmental and geotechnical engineers. Pollutants enter the subsurface directly as a result of accidents, spills during transportation, leakage from industrial facilities, waste disposal sites, as well as aboveground storage tanks and underground storage tanks (USTs) (Kamnikar 2001).

Of the sources of subsurface contamination, USTs represent a significant contribution. According to U.S. Environmental Protection Agency (USEPA), state agencies are spending more than $1 billion annually for the clean-up of 26,000 leakage sites (USEPA 2004). In spite of the strict regulatory measures, nearly 30 % of the 700,000 USTs around the country are not equipped with leak detection and corrosion protection systems and, thus, become a continuous source for petroleum hydrocarbon release (USEPA 2004). Furthermore, according to a National Cooperative Highway Research Program (NCHRP) study in 1996, there were 1000 UST leaking cases reported to the state agencies weekly and each leakage contaminated approximately 40 m^3 of surrounding subsurface soils including vadose zone and soils below groundwater table (Friend 1996) as illustrated in Figure 2.1. Many of the USTs contain petroleum products and their leachate contaminated drinking water supplies in various cases (Kamnikar 2001).

Petroleum products are often called non aqueous phase liquids (NAPLs) due to their immiscible nature in water. As a category of contaminants NAPLs are considered to present a considerable a threat to subsurface environment because: (1) their low liquid

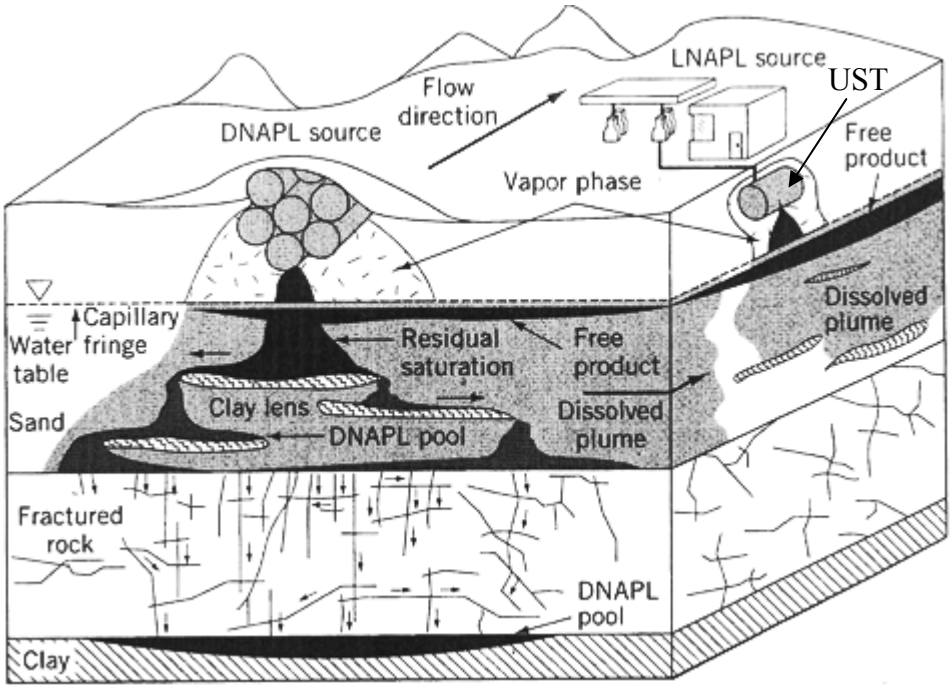

Figure 2.1 Complex nature of NAPL movements in the subsurface due to UST leakage (LNAPL: Light non-aqueous phase liquid, DNAPL: Dense non-aqueous phase liquid) (adopted Pankow and Cherry 1996)

viscosities enable them to move easily into subsurface, (2) they have relatively high solubilities with respect to drinking water limits, which results in significant contamination even they dissolve in small quantities, and (3) they exhibit very low partitioning behavior in aquifer soils. The toxicity of NAPL related compounds is also noteworthy. For example, NAPLs that originated from petroleum hydrocarbons contain significant quantities of naphthalene, pyrene, benzene, toluene, and xylenes, which are listed as hazardous waste compounds by the U.S. Environmental Protection Agency (U.S.EPA). The presence of such compounds in the subsurface environment presents a significant health hazard (Agency for Toxic Substances and Disease Registry 2001).

The goal of this chapter is to review the remediation technologies available for NAPL contamination with a particular emphasis on petroleum hydrocarbon contaminants and their remediation via stabilization and permeable reactive barrier. In addition, given its key role in these technologies, the topic of sorption is reviewed in detail, as well as the innovative use of high carbon content fly ash as sorptive material. Finally, the key points of this review are summarized to develop the motivation for the current research.

2.1 NAPL Remediation Technologies

Regulatory agencies and industry recognize the potential dangers that petroleum spills and associated organic pollutants pose to human health and the environment. Currently, treatment and removal of harmful constituents, such as NAPLs from contaminated soils is considered to be preferable to disposal without treatment, e.g., in a landfill. In addition, the availability and cost of landfilling for petroleum contaminated soils is constantly changing as many landfills refuse to accept these soils due to strict regulations or increase in their dumping fees (Friend 1996).

In response to the growing need to address contamination of the subsurface, several remediation technologies based on chemical, physical, or biological processes have been developed to treat soil and groundwater that is contaminated by petroleum hydrocarbon NAPLs (Khan et al. 2004). Most common technologies for remediation of petroleum contaminated soils (PCSs) are: soil washing, soil vapor extraction, soil flushing, vitrification, thermal desorption, biopiles, landfarming, bioslurry systems, bioventing, encapsulation, and stabilization (Kamnikar 2002). On the other hand, air sparging, pump-and-treat, biosparging, groundwater circulation wells, natural attenuation, and permeable reactive/sorptive barriers are the technologies that are commonly used for the remediation of NAPL-contaminated groundwater. Each of these techniques have advantages and disadvantages depending on factors such as site characteristics and contamination type.

Among these methods, the pump-and-treat method is perhaps the one most commonly known, in terms of NAPL clean-up from subsurface. However, as an ex-situ remediation method, pump and treat has a poor success record. Some of the problems associated with conventional ex-situ groundwater treatments are: (1) the need to manage large volumes of water containing very low concentrations of contaminants, (2) significant disruptions of normal operations for long time periods, and (3) the high cost of operating a large-scale project for a long time (Cantrell and Kaplan 1999).

In recent decades, the problems with the pump-and-treat methods have led to an increasing interest in alternative, innovative treatments some of which are outlined above. Of these other technologies, of particular relevancy to this research are stabilization of

contaminated soils and permeable reactive/sorptive barriers which are reviewed further below.

2.1.1 Stabilization of Petroleum Contaminated Soils

Stabilization is the process that reduces the mobility of the hazardous substances and contaminants in the environment through both physical and chemical means (FRTR 1999). Stabilization should be distinguished from solidification, which is the encapsulation of waste materials in an inflexible monolithic solid of high structural integrity.

Stabilization of contaminated waste soils (e.g., PCSs) and their beneficial reuse as part of landfill caps and highway embankments had been encouraged by the U.S.EPA (Meegoda et al. 1998). For example, petroleum contaminated soils have been utilized in various stabilization applications such as a substitute for a fine aggregate in concrete (Ezeldin et al. 1992), in mixture for asphalt concrete (Meegoda 1999), as well as in highway construction as fill material (Meegoda et al. 1998).

One alternative and cost effective way of stabilizing PCS is through the use of coal combustion by products (CCB) as stabilizing agents. According to the American Coal Ash Association, more than 70 millions tons of these products are landfilled each year; therefore their beneficial use, e.g, in construction, is highly desirable (Kulaots et al. 2004). One of the CCBs of current concern is high carbon content (HCC) fly ash, which to date has seen liitle use in environmental remediation. Tuncan et al. (2000) did attempt to use fly ash in stabilizing petroleum spills; however, their approach relied on creating a monolithic medium and encapsulating the petroleum contaminants rather than adsorption of the pollutants inside contaminated soils. Nevertheless, petroleum hydrocarbons can be

adsorbed by the available carbon present in high carbon content fly ash, and stabilized PCS stabilization using such an approach can be potentially reused in highway constructions, as reviewed further in section 2.4 below.

Even though fly ash is classified as non-hazardous waste by the U.S. EPA, it is common to conduct metal leaching tests on soil-fly ash mixtures to evaluate their use for engineering applications (Marota-Valler et al. 1999). This mainly due to the fact that most of the fly ashes contain traces of heavy metals. The amount and distribution of metals in fly ash depend mainly on the type of coal and the burning process. Bin-Shafique et al. (2006) addressed the behavior of heavy metal leaching from soils stabilized with fly ash. Heavy metal leaching performance of fly ash-stabilized soils was evaluated through laboratory water leach and column tests as well as through analysis of leachate collected in lysimeters in a field highway test cell. The results indicated that concentrations of metals in leachate from soil-fly ash mixtures prepared with various soil and fly ashes at different fly ash content tend to be lower (1.5 to 2.5 times) than those from fly ash alone. Leaching potential of a metal from a soil-fly ash mixture depends on the metal concentration in the fly ash as well as in the soil, pH of the leachate, the cation exchange capacity (CEC) of the soil, and type of the fly ash.

The release pattern of metals from the soil-fly ash mixtures appears to be adsorption-controlled. Adsorption of metals is highly dependent on the pH of the pore fluid. However, the pH of the soil-fly ash mixtures appears to be persistent, which yields a limited leaching for at least 30 pore volumes of flow, which corresponds to at least 30-years of flow in the field for a roadway application (Bin-Shafique et al. 2006).

2.1.2 Permeable Sorptive Barriers for Contaminated Groundwater Clean up

Permeable treatment barriers have been increasingly used for groundwater remediation in the last decade. Typical contaminants of concern are chlorinated solvents, radioactive isotopes, petroleum compounds, mine waste, or septic discharge (Lee and Benson 2002). The concept of permeable treatment barriers is relatively simple. Reactive material is placed in the subsurface where a plume of contaminated groundwater must pass through it as it flows, typically under a natural gradient (creating a passive treatment system) and treated groundwater comes out the other side. Composition of the reactive zone may vary; however, in all cases the hydraulic conductivity of the zone is designed to be greater than or equal to the surrounding aquifer so that the barrier does not impede groundwater flow. Most commonly used treatment barriers are currently permeable reactive barriers (PRB), where zero valent iron is employed as the reactive media for converting contaminants to non-toxic or immobile species (FRTR 1999).

Permeable treatment barriers provide a versatile containment option because they are a passive means of removing contaminants from groundwater and they can be applied to different sites and contaminants by choosing an appropriate reactive media. Reactive media are selected based on their effectiveness to treat site-specific contaminants (Lee et al. 2004), and constitute the major cost for the PRB application. Cost of the reactive material for in-situ barrier technology is particularly important because much larger quantities are generally required than ex-situ applications (Cantrell and Kaplan 1999). Due to high cost of conventional manufactured filling materials such as zero valent iron and activated carbon, current research is underway to investigate the effectiveness of alternative reactive materials.

The concept of incorporating alternative materials into permeable reactive barriers is fairly new, but the compounds of interest treated with such alternative media cover a wide range including Trichloroethylene (TCE), petroleum hydrocarbons as well as trace elements and heavy metals. The reaction mechanism in these PRBs is typically sorption and the term "permeable sorptive barriers" (PSBs) recently been adopted for this as innovative clean-up technology (Woinarski et al. 2003). Like PRBs, PSBs contain media that remove contaminants from the groundwater, however, in this case the removal mechanism is an immobilization process, in which the organic pollutants are adsorbed onto the sorptive medium surface (Khan et al. 2004).

Laboratory studies have demonstrated the effectiveness of various natural and synthetic sorbents in removing contaminants from aqueous solutions. Materials that have been investigated as a potential reactive/sorptive medium for treatment of groundwater containing both organic and inorganic pollutants in permeable barriers include: ground rubber from scrap tires (Kershaw et al. 1997), foundry sand (Lee et al. 2004) and peat (Guerin et al. 2002, Ramussen et al 2002), metal oxides, bottom ash, fly ash (Cantrell and Kaplan 1999), organic carbon (USEPA 2006a), wood chips, limestone, manure (USEPA 2006b), paper sludge (Moo-Young and Zimmie 1997), and tire chips (Kim et al 1997), lignitic coal (Jenk et al. 2003).

Of these materials use of ground rubber, foundry sand and peat as a permeable sorptive barrier is discussed further below. In a study on ground rubbers shredded from scrap tires, Kershaw et al. (1997) examined the ability of ground rubber to remove benzene and *o*-xylene from groundwater. The results of batch scale sorption tests revealed that ground rubber can sorb up to 1.3 and 8.2 mg/g-tire rubber of benzene and *o*-

xylene, respectively, mainly due to the interaction of the polymer chains present in the rubber with BTEX compounds. Column tests also indicated that ground tire rubber has a high sorption capacity, which makes it a possible sorptive medium for permeable reactive barriers (Kershaw et al. 1997).

Lee and Benson (2002) studied the use of foundry sand as a PRB medium. Specifically, batch tests were performed to investigate the applicability of foundry sand as a sorptive medium for herbicides such as alachlor and metolachlor as well as a reactive media for chlorinated solvents such as trichloroethylene (TCE), 1-1 dicholoroethylene, 1-2 dicholoroethylene and 1-2 cisdicholoroethylene. Column tests were performed to simulate the field conditions more realistically. The columns had a diameter of 25 mm and a height ranging from 200 mm to 450 mm with simulated groundwater flow maintained in a range of 20-60 mL/day. Column sorption test results indicated that foundry sand a high sorption capacity for all chemicals tested with linear partitioning coefficients ranging between 1.0 and 54.8 L/kg. A 25 % difference between the partition coefficients obtained from batch and column tests was attributed to the variation of solid to solution ratio in two tests.

Guerin et al. (2002) studied peat as a sorptive medium in a full scale PSB application to treat groundwater that was contaminated with petroleum hydrocarbons. A permeable sorptive barrier was constructed in front of a hydrocarbon plume that originated from an UST facility. Peats mixed with cocoa fiber were placed in a 27 m long, 0.6 m deep and 0.6 m wide trench. A 10-month monitoring of the plume suggested that the removal efficiency of petroleum hydrocarbons such as BTEX compounds was relatively high (i.e., up to 97 % removal of toluene).

In a recent study, Doherty et al. (2006) has tested ammonium sorption capacity of fly ash from a peat burning power plant. The fly ash produced on a by-product of combustion of this organic material, was highly effective in removing the ammonium compounds in a field sequential barrier system. The fly ash also did not inhibit the microbial medium in this field application.

2.1.3 Bio-reactive Barriers

PSBs have great potential for removing the organic compounds from contaminated groundwater via sorption; however, they can be improved by incorporating the biodegradation (biotransformation) capabilities of the natural microorganism (Kalin 2004). Accordingly, these barriers combine the two processes in a unique way in that they can be engineered to prevent via sorption the contaminant movement across the site boundaries before risk receptors are impacted and confine contaminant plume in the barrier. Subsequently the pollutants may then dissipate via biodegradation by naturally existing microorganisms (Kalin 2004). Several recent studies have shown the potential for utilization of an engineered passive barrier in front of contaminated plume to take the advantage of potential microbial degradation of the hazardous contaminants. These passive biodegradation barriers are often called bioreactive barriers (Kalin 2004).

For example, Warith et al (1999) conducted a laboratory study on bioreactive barriers, in which they simulated the biodegradation process using soil columns composed of sand inoculated with non-indigenous microorganism. A contaminated groundwater plume was modeled using an aqueous naphthalene solution. After determining the optimum biomass concentration and optimum hydraulic conductivity through soil column tests, they determined the naphthalene biodegradation potential

using non-indigenous bacteria harvested from municipal activated sludge. The results indicated a 100% naphthalene removal under aerobic conditions, emphasizing the fact that ultimate transport and fate of naphthalene was strongly affected by adsorption to barrier medium. A sensitivity analysis conducted on the column test results indicated that the parameters like the first order biodegradation rate, sorption retardation factor, dispersivity, porosity and hydraulic gradient have an equal effect on the naphthalene removal. Hydraulic conductivity, however, had the highest influence on the fate of the contaminant in a bioreactive barrier.

The results from other laboratory and filed studies suggest that PAHs (Ramussen et al 2002), MTBE (Salanitro et al. 2001, Liu et al 2006), BTEX (Tiehm et al,2001, Lorbeer et al. 2002, Guerin et al 2002), and TCE (Tiehm et al,2001, Lorbeer et al. 2002) can be successfully removed from groundwater using bioreactive barriers. Although the microorganisms and barrier medium varied depending on the application Table (2,1). All these studies rely on the biodegradation capacity of the bioreactive barrier under aerobic conditions.

Activated carbon, a commonly used sorptive medium due to its high adsorption capacity, has also been incorporated into bioreactive barriers as a substratum to support the growth of microbial population during the biodegradation process. It has been used either sequentially (Lohbeer et al. 2002) or mixed (Shirazi et al. 2001) with the biodegradation process to extend the life time of the barrier. Recently, Leglize et al. (2006) evaluated the applicability of activated carbon as a reactive medium for bioreactive barrier applications. In these experiments, phenanthrene was used the model contaminant and the microorganism used was a phenanthrene-degrading strain isolated

from PAH contaminated soil. They determined that phenanthrene removal via adsorption to the activated carbon and studied the biodegradation process. While expressing the necessity of dynamic test techniques (i.e. column experiments) in order to determine the role of each process, they showed the complementary effect of biodegradation and sorption-based removal system for a successful barrier.

Given the importance of understanding the biodegradation and sorption processes for successful optimization and design of bioreactor systems, the next three sections review three topics in more detail. First, biodegradation of naphthalene and *o*-xylene, the two model contaminants in this study, is reviewed. Then sorption and fly ash, the sorptive material used in this research, are reviewed.

2.2 Biodegradation

Naturally occurring microorganism induced biological processes have been utilized for mitigation of organic contaminants from subsurface. Biological processes, which involve enzymes as catalysts, frequently bring extensive modification in the structure and toxicological properties of pollutants. These transformation or mineralization processes, commonly known as biodegradation, can be defined as the biologically catalyzed reduction in the complexity of the chemical, wherein organic molecules converted into basic organic elemental form (i.e., C, N, O, H) or simpler organic compounds (i.e., CH_4, CO_2, H_20) during their transport in the subsurface (Alexander 1999).

In natural systems biodegradation occur in many different of conditions such as aerobic, anaerobic, metagenic, sulfate reducing and nitrate reducing conditions. Among these aerobic degradation of PAHs like naphthalene has been studied extensively (Wraith

et al 1999). Because the bacterial metabolism of naphthalene under aerobic and is of importance for this research, it is reviewed in this section.

During naphthalene degradation NH_4Cl and Na_2HPO_4 present in the synthetic groundwater served as the N and P source, respectively. The overall stoichiometry for aerobic naphthalene degradation, including biomass synthesis, with ammonia as the nitrogen source, is as follows (McCarty 1987):

$$C_{10}H_8 + 6O_2 + 1.2\ NH_3 \rightarrow 1.2\ C_5H_7O_2N + 4CO_2 + 1.6H_2O \quad (2.1)$$

This equation was used as the for the nutrient requirement calculation based on stoichiometry of biological reaction of naphthalene. Similarly, biodegradation of xylene isomers is shown below with Equation (2.2) including cell synthesis.

$$C_6H_4(CH_3)_2 + 4.234\ O_2 + 1.256\ HCO_3 + 1.256\ NH_4^+ \rightarrow 1.256\ C_5H_7O_2N + 2.986\ CO_2 + 3.746\ H_2O \quad (2.2)$$

2.3 Sorption

Sorption is the process in which the chemicals become associated with solid phases. It is extremely important because it may dramatically affect the fate and impacts of chemicals in the subsurface environment (Schwarzenbach 1999). The term "sorption" is used to denote the uptake of a contaminant by soils or sediments without referring to a specific mechanism. The term adsorption and absorption are used to define specific processes involved (Chiou 2002). Adsorption refers to when molecule attachs to two dimensional surfaces, whereas absorption is reserved for the phenomena in which the organic molecules penetrate (partition) into three-dimensional matrix of a solid.

Sorption of organic chemicals in the subsurface is controlled by several factors including soil type (e.g.: mineral and organic matter content) and physico-chemical

properties of the contaminant(s) (e.g., aqueous solubility, polarity, hydrophobicity, lipophilicity and molecular structure) (Semple et al. 2003). Therefore, prediction of the fate of the organic compounds in a soil environment is difficult due to the highly complex interaction between organic molecules (sorbate) and solid phases (sorbent). For example, a non-polar organic chemical in aqueous solution may escape from water and penetrate into the soil organic matter. Additionally, a nonpolar organic chemical may displace water molecules from the region near a mineral surface and be held there by London dispersive forces (van der Waals bonds) and by polar interactions (Schwarzenbach et al. 1993). On the contrary, polar molecules attach to charged surface molecules (i.e., negatively charged mineral surfaces) and nonpolar substances may attach to the surface or diffuse inside to organic matter in the system. All of these interactions occur simultaneously, and the combination that dominates the overall solution-solid distribution will depend on the structural properties of the organic sorbate and the solid sorbent of interest.

Previous research indicates that the sorption of organic contaminants in solids occur in five different ways: (1) absorption via diffusion through rubbery ”soft” organic matter, (2) absorption via diffusion through glassy “hard” organic matter, (3) adsorption on to surface of organic matter, (4) adsorption onto mineral surfaces, and (5) adsorption into micropores of minerals with porous surface (Luthy et al. 1997). These processes are illustrated in Figure 2.2. The terms refer to phases of solid the solid organic content, rubbery or ”soft” and glassy or “hard” both of which phases contain dissolution sites. The glassy phase is thought to contain more rigid cavities (holes) than glassy phase where contaminants can interact with the organic matter. A contaminant thus diffuses into this

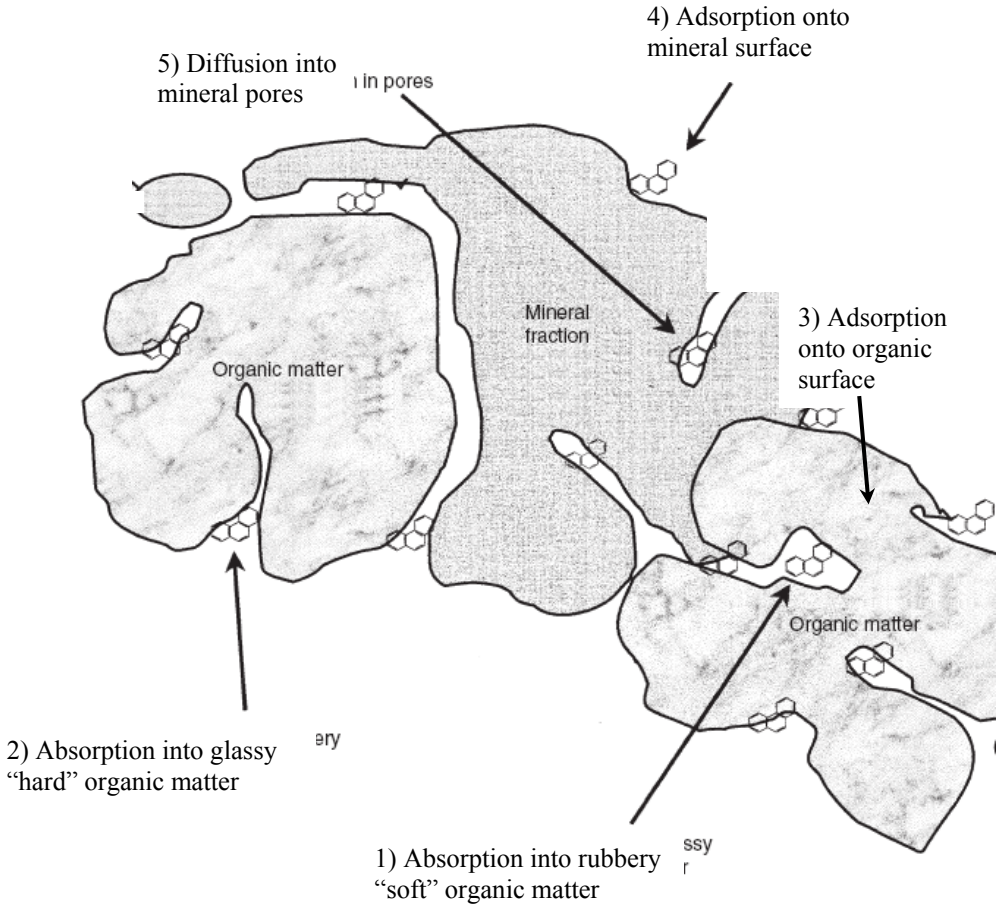

Figure 2. 2 Diagram showing five concepts sorption of an organic contaminant sorption onto a sorbent (Adapted from Semple et al. 2003)

complex structure and is sequestered into the organic matter. The rates of diffusion are controlled by radii of soil particles, and shape of the pores (Semple et al. 2003).

The reaction kinetics of the organic chemicals also play a significant role on the adsorption of the contaminants. Organic contaminants generally exhibit two kinetic stages within the solid gepsorbent phases (e.g., sediments, natural soils). Initially, a portion of the contaminant can be sorbed quickly (in minutes to a few hours), whereas the remaining fraction is sorbed more slowly over weeks or months (Xing and Pignatello 1997). The initial rapid sorption is generally constitutes the significant proportion and is due to hydrogen bonding and van der Waals forces, mechanisms that are expected to occur instantaneously upon contact of the organic chemical with the solid surface, especially the surface of the organic content (Chiou 2002, Semple et al. 2003).

2.3.1 Sorption Equilibrium Isotherms

In the laboratory, the sorption behavior of the solids and organic chemicals under equilibrium conditions is generally studied using sorption isotherms. Isotherms are graphic representations of the distribution of a given compound between a liquid phase and a solid phase at a constant temperature (Carmo et al. 2000). Sorption isotherms are commonly employed in evaluating the organic or inorganic contaminant sorption capacity of soils and other geomaterials. The isotherm type and its degree of nonlinearity is consistent with the sorption mechanism(s) prevailing in a given system (Schwerzenbach 1993). Experimentally determined sorption isotherms generally exhibit different shapes. The first case is the one in which the affinity of the compound for the solid remains the same over an observed concentration range (Schwerzanbach et al. 1993).

This type of the isotherm is called a linear isotherm. It is applicable to the conditions where partitioning of the contaminants into the homogeneous organic phase is dominating the overall sorption and where the strongest adsorption sites are far from being saturated at low concentrations. The general equation for a linear isotherm is:

$$q = K_d C_f \tag{2.3}$$

where q is the sorbed amount at equilibrium (mg/kg), K_d is the partition coefficient (L/kg) and C_f is the equilibrium (final) concentration (mg/L).

Even though linear isotherms are commonly employed, the heterogeneous structure of soils may suggest nonlinear sorption behavior. There are four previously studied phenomena that cause isotherm nonlinearity: (1) retention by the heterogeneous solid organic matter that contains both ”rubbery” (or soft) and “glassy” (or hard) polymer like sorption domains, (2) the presence of small quantities of high surface area carbonaceous materials such as soot, black carbon (Carmo et al. 2000) (3) the availability of different sets of internal pores in organic matter for adsorption of different organic chemicals and (4) the presence of specific interactions between polar organics and limited active sites in organic matter (Chiou and Kile 1998).

The common approaches for accounting this nonlinearity are use of the Langmuir and Freundlich isotherms. The Langmuir sorption isotherm is preferred when the sorption of chemicals occur on a solid surface that contains a fixed number of identical active sorption sites. The equation for Langmuir isotherm is,

$$q = \frac{Q_{\max} K_L C_f}{1 + K_L C_f} \tag{2.4}$$

where q is the sorbed equilibrium concentration (mg/kg), Q_{max} is the sorption capacity of particular solid (mg/kg), K_L is the Langmuir isotherm coefficient (L/kg), and C_f is the equilibrium (final) aqueous concentration (mg/L). One conceptual difficulty of the Langmuir isotherm is that, in some cases, the estimated sorption capacity greatly exceeds that theoretically allowed by monolayer coverage on solid surface (Xia and Ball 1999).

The Freundlich equation was developed mainly to account for the empirical observation of a variation in adsorption with concentration of the sorbate on an heterogeneous surface (Haws et al. 2006). The Freundlich isotherm has the following form:

$$q = K_F C_f^{\ n} \tag{2.5}$$

where q is the sorbed equilibrium concentration (mg/kg), K_F is the Freundlich isotherm coefficient (mg/kg)/(L/kg)$^{-n}$, C_f is the equilibrium (final) aqueous concentration (mg/L), and n is the dimensionless parameter that denotes degree of deviation from isotherm linearity. Freundlich isotherm assumes that there are multiple types of sorption sites acting in parallel, with each site type exhibiting a different sorption free energy and total site abundance (Schwarzenbach et al. 1993). In case of n=1, the isotherm is linear and indicates constant sorption free energies at all sorbate sites, whereas when n<1, the isotherm is concave downward and suggests that the added sorbates are bound with weaker free energies. The case when n>1 indicates that the isotherm is convex upward and suggests that the more sorbate present in the sorbent enhances further sorption.

In the case of sorbents with a complex nature, the nonlinearity can not be fully described by a Langmuir or a Freundlich isotherm. Therefore, Cooney (1999) and

Maurya and Mittal, (2006) have offered a combination of Freundlich and Langmuir isotherm. This combined isotherm has three unknowns, and can be defined as,

$$q = \frac{bQmCf^{n}}{1 + bCf^{n}} \tag{2.6}$$

where q is the sorbed equilibrium concentration (mg/kg), b is the combined isotherm coefficient (mg/kg)/(L/kg)$^{-n}$, C_f is the equilibrium (final) aqueous concentration (mg/L), n is the dimensionless parameter, and Q_m is the sorption capacity of particular solid (mg/kg).

Even though empirical models like the Freundlich isotherm (Equation 2.5), can have some qualitative mechanistic relevance assigned to its parameters, more theoretically-based models have been increasingly used (Nguyen et al 2004). For instance, the Polanyi adsorption model has been successfully implemented by many researchers to model the adsorption of non-polar hydrocarbons onto activated carbon (Xia and Ball, 1999, Crittenden et al 1999, Kleineidam et al 2002). The theory was first applied by Polanyi for gas adsorption. Polanyi adsorption theory explains the adsorption as a sorbate molecule (e.g., organic chemical) comes in the close vicinity of a sorbent surface. According to the theory, an adsorption potential (ε) exists in this vicinity and depends on the distance to the surface and the physical and chemical properties of the sorbents (Xia and Ball 1999). More specifically, ε defines equal values that form equipotential surfaces that together withhold volume with the solid surface. The schematic representation of the Polanyi adsorption theory is shown in Figure 2.3. Equation 2.5 defines ε for the gas adsorption:

$$\varepsilon = RT \ln(P^{o} / P) \tag{2.7}$$

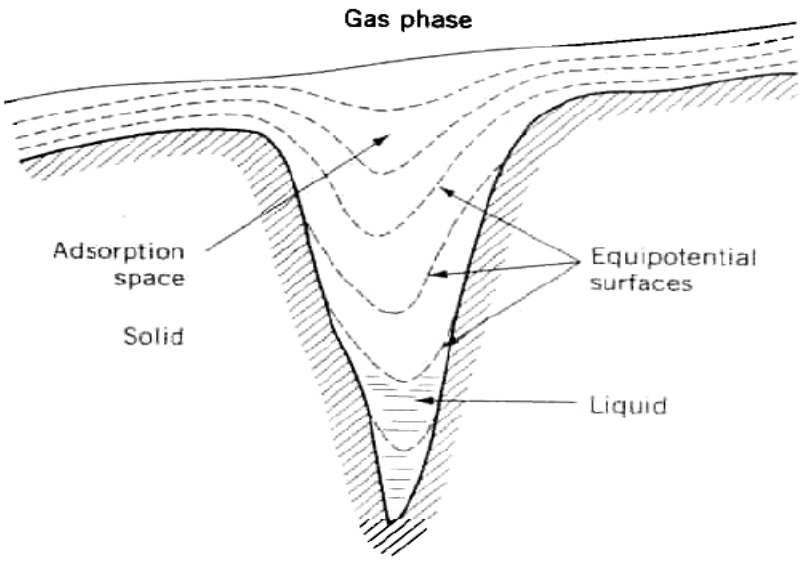

Figure 2. 3 Representation of the pore surface with equipotential surfaces corresponding to adsorption potential for lower values with increasing pore size (Manes 1998).

where R (J K^{-1} mol^{-1})is the ideal gas constant, T (K) is the temperature at equilibrium, P^o/P is the partial pressure.

Polanyi describes how the volume of the adsorbed molecules can be plotted against the adsorption potential (ε) to a obtain characteristic curve for adsorption (Allen-King et al. 2002). According to Manes (1998) characteristic curve can be used to provide a relationship between the sorbent surface with multiple sorbates by applying a correlation divisor or normalization factor to (ε) so that one can obtain a correlation curve between adsorbed volume (q') and adsorption potential for multiple solutes. For example, Dubinin and Ashtakhov (1960) further applied the Polanyi theory to sorption of organic chemical in highly porous solids via pore filling mechanism by fitting a line through a correlation curve:

$$\frac{q'}{q'_{max}} = \exp\left[-\left[\frac{RT\ln(P^o/P)}{\beta_i E_o}\right]^d\right] \tag{2.8}$$

where q'_{max} stands for maximum sorption capacity , d is the characteristic curve fitting parameter, and $\beta_i E_o$ is normalization factor, which is a characteristic energy of adsorption (Allen-King et al. 2002).

Manes (1998) further developed the Polanyi theory for aqueous adsorption of partially miscible solutes and defined the adsorption potential as:

$$\varepsilon_{sw} = RT\ln(Cs/Cf) \tag{2.9}$$

where ε_{sw} is the effective adsorption potential (J/L) of partially miscible solutes, C_s is the solute solubility (mg/L) and C_f is the equilibrium concentration of the solute (mg/L). Manes (1998) modified the normalization factor as molar volume of the sorbate, although he suggested using an additional correlation factor (γ).

The final version of the Polanyi theory used in this study was developed by Xia and Ball (1999). Xia and Ball (1999) named their approach the Polanyi-Manes (PM) model; however, in this work this approach to the Polanyi theory is hereafter refered to the Polanyi-Dubinin-Manes (PDM) model, consistent with other researchers (Allen-King et al 2002, Haws et al 2006). The characteristic curve equation developed by Xia and Ball (1999) is given as follows:

$$q' = q'_{\max} \exp\left[(-c) \left[\frac{\varepsilon_{sw}}{N} \right]^d \right] \tag{2.10}$$

where q' is the adsorbed volume per unit mass of sorbent (L/kg), q'_{max} is the adsorption volume capacity at the saturation (L/kg), ε_{sw} is the adsorption potential (J/L), and N is the normalizing factor for weakly polar solutes, which is taken as the molar volume (V_S), where V_s is the ratio between molecular mass (cm^3/mol) and solute density (g/cm^3). c and d are the fitting parameters. c corrects for the use of V_s and normalizing sorption potential and d reflects the nature of the stochastic distribution of ε_{sw}/N (Nguyen et al. 2007). The molar volume, which represents the molecular size of the organic molecule, was determined to be the best method of normalization compared to other factors like polarity, and hydrogen-bonding parameters, which are indication of a molecule's hydrophobicity and van der Waals forces predominant during adsorption, respectively (Crittenden et al. 1999).

The PDM model isotherm has great potential to simulate the equilibrium sorption data ion for multiple organic chemical as a single data set by using the appropriate q'_{max}, d and c/N^d. Thus the PDM equation has two main potential benefits for environmental engineers. First, it predicts the same volumetric loading (q') for all compounds having the

same value of C_s/C_f, on the abscissa of the characteristic curve. Second, for a reference compound at single temperature, the correlation curve can be applicable to predications at different temperatures (Allen-King et al. 2002).

An improved adsorption model known as the Fritz-Schluender isotherm goes beyond the current empirical and mechanistic models, with five fitting parameters, has been implemented by Fritz and Schluender (1974), Mollah and Robinson (1996), Yang and Al-Duri (2000) and Maurya and Mittal (2006) for sorption of various hydrophobic organic compound adsorption onto different sorbents like activated carbon. The model equation is given as:

$$q = \frac{\alpha_1 . Cf^{\beta 1}}{\alpha_1' + \alpha_2 . Cf^{\beta 2}} \tag{2.11}$$

where q is the sorbed concentration at equilibrium (mg/kg), C_f is the equilibrium (final) aqueous concentration (mg/L). α_1 (mg/g)/(mg/L)$^{\beta 1}$and α_2 (mg/L)$^{\beta 2}$ are the Fritz-Schluender isotherm parameters, and β_1, β_2 and α_1' are the dimensionless Fritz-Schluender isotherm parameters, which indicate the sorbent heterogeneity (Yang and Al-Duri 2000).

The Fritz-Schluender isotherm model was selected for evaluation in this work because it is a hybrid model between the Freundlich and Langmuir models with a substantial number of fitting parameters. Due to the difficulties associated with estimating the chemical heterogeneity of the surface and complex sequestration processes, a model with greater number of model constants can possibly yield a better prediction (Maurya and Mittal 2006).

Numerous studies have been conducted to relate the sorption behavior of numerous organic and inorganic chemicals with various sorbents using different isotherm

models. More importantly, it has been widely investigated whether one isotherm model is superior to others for explaining the sorption isotherms by means of physical and chemical interactions, such as, the pore structure of the sorbent and the types of the bonds between sorbent and sorbate (Malek and Farooq 1996, Crittenden et al 1999, Maurya and Mittal 2006). For example, Malek and Farooq (1996) compared seven different nonlinear models using equilibrium adsorption data for three alkane hydrocarbons in activated carbon adsorption tests. Among the isotherm models analyzed, a combined approach of Freundlich and Langmuir isotherms (Equation 2.6 in Section 2.3.1) performed reasonably well and provides the better prediction than the other isotherm models.

In a more recent study, the applicability of sixteen different equilibrium models for sorption of basic dyes on activated carbon and bio-sorptive materials were studied by Maurya and Mittal (2006). The study evaluated isotherm models that incorporated different number of model parameters, ranging from one independent parameter (the linear model) to five independent parameters (the Fritz-Schulender model). There were several key conclusions from their study. The first was that the accuracy of the model fit to the experimental data improves with the number of model parameters. However, they have also concluded that isotherms having two model parameters (i.e., Freundlich and Langmuir isotherms) can be used to predict the adsorption process. Secondly, they used the theories behind the isotherm models and the data to understand the sorption mechanisms of the different sorbents tested. For example, they concluded that physicosorption may be responsible for adsorption onto activated carbon, and that chemisorption or other mechanisms based on ion exchange, chemical complexation and electrostatic forces may be the cause behind the sorption onto biosorptive materials.

2.4 High Carbon Content Fly Ash

Fly ash is a byproduct of coal-burning electrical power plants. Fly ash exits in the combustion chamber flue gas, and it is captured by air pollution control equipment such as electrostatic precipitators, bag-houses, or wet scrubbers (Kalyoncu 2001). According to ASTM C- 618 fly ash can be categorized in two general classes: Class C and Class F. Class C fly ash has a lignite and sub-bituminous coal source and has a minimum silicon dioxide (SiO_2) plus aluminum oxide (Al_2O_3) plus iron oxide (Fe_2O_3) level of 50 percent. In comparison, Class F fly ash has an anthracite and bituminous coal source and with a minimum SiO_2 plus Al_2O_3 plus Fe_2O_3 level of 70 percent (ASTM 2005).

According to American Coal Ash Association (ACAA), the total ash production of 858 power electrical plants in the Unites States is approximately 108 millions tons per year. Currently, only 30 % of this ash is being beneficially reused, with the remaining having to be landfilled (Kulaots et al. 2004). The potential for beneficial reuse of fly ash is related to the chemical constituents in the ash. These chemical constituents mainly depend on the chemical composition of the coal. However, fly ash that is produced from the same source and which has very similar chemical composition may have significantly different ash mineralogy depending on the coal combustion technology used (Bin-Shafique 2002). This highly variable nature of the fly ash defines its utilization rate in construction applications as concrete grout, structural fill, cement clinker raw feed and road base or sub-base material. The concrete industry is the largest consumer of fly ash, and, the ASTM classifications help in understanding the pozzolanic behavior of the ash and, therefore, the potential for its reuse as a concrete additive. For example, Class C fly

ash with self-cementing properties due to its high calcium oxide –quick lime- (CaO) level, is commonly being used as a concrete additive.

Unfortunately, the beneficial reuse percentage of fly ash in the concrete industry has been in a decline due to an increase in the amount of unburned carbon in the fly ash. This increase in unburned carbon is a result of the introduction of low nitrogen oxide (NO_x) burners into the coal combustion system of power plants. In order to address the environmental concerns about NO_x emissions, the U.S. Congress passed the Clean Air Act Amendments (CAAA) in 1990. With the start of the implementation of Phase II of the CAAA, all power plants have to install continuous emission monitoring systems, which are instruments that monitor SO_2 and NO_x emissions (Kalyoncu 2001). In order to fulfill the requirements of the CAAA by reducing NO_x emissions, many electric utilities installed no-NO_x burners or retrofitted their current boilers according to the new regulations. The installation of low- or no-NO_x burners changes the flame temperature profile as well as the flame chemistry. In essence, a hot oxygen rich flame was replaced by cooler and longer fuel rich flame (Maroto-Valer et al. 1999).

As a result, low-or no-NO_x burners reduce NO_x emissions by yielding a lower combustion efficiency, however, they also lead to a significant increase in the unburned carbon content in fly ash. In certain cases, the unburned carbon content exceeds the ASTM limit of 6%, for use in concrete application. This is due to the fact that the excess unburned carbon in concrete-containing fly ash cement reduces the freeze-thaw resistance of concrete by capturing the air-entraining agents that are used to modify the microstructure through introducing controlled porosity (Kalyoncu 2001).

Researchers are looking for innovative ways to utilize the unburned carbon inside the fly ash by separating it from the fly ash and using it as a raw material for activated carbon (Maroto-Valer et al.2001). Nevertheless, this operation is costly and alternatives to directly use high carbon content fly ash in geotechnical and environmental applications need to be assessed.

The Loss on ignition (LOI) value is the most important parameter that controls the beneficial reuse of fly ash. For the fly ashes defined as Class F, which are commonly derived from Eastern U.S. coals, the LOI value is essentially equal to the unburned carbon content (Maroto-Valer et al. 1999). However, it is generally known that the ASTM LOI value is not sufficient to identify the suitability of fly ash for beneficial reuse, because this value only gives a rough approximation to the carbon content of sample. Plus it does not directly correlate with the capacity to adsorb some organic molecules such as the air entrainment additives of concrete industry (Maroto-Valer et al. 2001).

In order to have a better understanding of the adsorption mechanisms between organic molecules and the high carbon content fly ash, the physical and chemical properties of the carbon have to be identified. In general this necessitates an investigation of the effects of surface area, and the chemical nature of the carbon surfaces on sorption (Kulaots et al. 2004). For instance, petrographic analyses of high carbon content fly ash conducted in previous studies indicated that carbon in fly ash exists in three different forms: i) inertinite particles, ii) isotropic coke and iii) anisotropic coke. These three carbon forms have different densities, surface characteristics, pore structure and particle size (Maroto-Valler et al. 2001). Therefore, it is anticipated that each carbon forms may have specific sorption behavior.

Numerous studies are available in the existing literature that confirm the capacity of fly ash for removal of organic contaminants from aqueous solutions. For example, Banerjee et al. (1995) conducted a study to investigate seven different fly ashes as a sorbent material to isolate and immobilize alcohols and ketones from aqueous solution. The results of that study indicate that fly ash has a significant adsorption capacity for organic compounds. Unburned carbon was the only constituent in the fly ash that correlated well with the adsorption capacity.

Akgerman and Zardkoohi (1996) studied the adsorption capacity of a fly ash with a surface area of 1.87 m^2 /g. for phenolic compounds. The ash adsorbed 67, 20 and 22 mg/g phenol, cholorophenol and 2,4-dicholorophenol, respectively. Freundlich isotherms were successfully used to model the observed adsorption capacity. Similarly, Banerjee et al (1997) found that the Freundlich isotherm describes the removal of *o*-xylene by fly ash. However, the rate of adsorption of *o*-xylene observed by Banerjee et al (1997) was dependent on the size and carbon content of the fly ash used. This "size effect" was also evident in the adsorption capacity of fly ash for other organic compounds. (Kulaots et al. 2004). Previous research also suggested that high carbon content fly ashes can be beneficial for removal of herbicides (Konstantinou and Albanis 2000), PCBs (Nollet et al. 2003) and dyes (Jonas et al. 2003, Wang et al. 2005a) via adsorption.

Mott and Weber (1992) investigated the effectiveness of Class F fly ash as a sorptive barrier medium in a low permeability slurry wall. Fly ash, containing varying amounts of unburned carbon (i.e., 6.5 % to 10.3%), exhibited a significant sorption capacity as a barrier medium. Even though numerous studies have been conducted on alternative barrier materials as described above, there is still relatively little information

available on sorption and reaction properties of CCBs, particularly on Class F fly ash, as a sorptive medium for permeable reactive barriers.

2.5 Synthesis of Previous Studies and Motivation for the Current Research

Past research indicates that petroleum spills are one of the most common sources of soil and groundwater contamination (Mercer and Cohen 1990). Removal of these pollutants from subsurface environment is essential and use of waste and recycled materials in remediation technologies is becoming popular due to economic reasons. For instance, legislation have been promulgated in many states to incorporate recycled materials into engineering applications. One alternative material that is abundant in Maryland as well as in various parts of the U.S. is high carbon content (HCC) Class F fly ash (Petzrick 2001). Two potential ways of incorporating HCC fly ash into environmental remediation are to: (1) use it as a binder in stabilization of petroleum contaminated natural soils (e.g., borrow material) for their further beneficial reuse in highway construction, and (2) use it as part of a PRB medium in remediation of contaminated groundwater plumes.

Traditionally, borrow materials have been derived from natural materials (soil). As a result, testing and approval processes are geared to evaluate natural materials. Furthermore historically, the natural material approval process has not required an environmental review. However, many producers of recycled soil-based materials use a reclamation process to stabilize the contaminants. After the reclamation process, the soil may still contain the original contaminant(s), which may, in turn, affect the engineering properties of the material. Therefore, normal testing procedures may be inappropriate for approval and construction quality assurance. Currently, there are no definitive criteria for

determining the suitability of these products for use in a transportation project although there is a generic acceptance process for recycled materials. To make progress in this area, additional information concerning the geotechnical and environmental properties of recycled or reclaimed soil is needed.

Moreover, although several studies have been conducted on alternate barrier materials, as discussed above, limited information exists about the sorption properties of CCBs, and particularly the HCC Class F fly ash. Such information is highly essential if these ashes are to be used as part of a permeable reactive barrier. Although fly ash has been considered as an alternative material for removal of inorganic heavy metals and trace elements from groundwater (Czuda and Has 2002, Komnitsas et al. 2006), further research is needed to show its feasibility as a reactive medium in a barrier application. For any type of sorptive barrier, the development of a predictive model and further design requires accurate characterization of sorption capacity using laboratory column tests (Rabideau et al. 2001).

Bioreactive barriers are gaining momentum as viable alternative to traditional remediation techniques, because contaminants are biologically degraded instead of only being immobilized via sorption. Incorporation biotransformation processes is also logical way of extending the lifetime of permeable reactive/sorptive barriers. Accordingly, research efforts are needed to study the behavior of biodegradation processes coupled with sorption mechanism, within a bioreactive barrier, and modeling of full-scale permeable reactive barrier systems to address the bioremediation and sorption capacities in operational parameters.

In order to respond to these needs, standard compaction tests and column leaching tests were undertaken to evaluate the geotechnical performance and environmental suitability of petroleum-contaminated soils stabilized by using HCC fly ash. For adsorption capacity assessments, a series of batch adsorption tests were conducted with two petroleum hydrocarbons and seven Maryland fly ashes. A series of composite column sorption-desorption were also conducted on the same fly ashes. Finally biodegradation processes within the sorptive media was evaluated using column biodegradation tests. The results coupled with a numerical model were used to define a set of design parameters for a barrier system that is capable of operation for the long term, with little or no maintenance.

Chapter 3: Batch Adsorption Tests on HCC Fly Ash

A series of batch adsorption tests were performed to characterize the organic contaminant adsorption capacity of the high carbon content fly ash for selected non-polar organic compounds specifically, Naphthalene and *o*-xylene. The batch adsorption technique is one of the most commonly used laboratory methods for determining adsorption isotherms and estimating partitioning coefficients of geologic materials (USEPA 1999). This test method is generally listed under the category of screening tests and is applicable to a large group of pollutants and geomaterials (Kim et al. 1997, Kim et al. 2001, Headley et al. 2001, ASTM 2003).

3.1 *Materials*

3.1.1 Physical and Chemical Properties of the Fly Ashes

Seven different fly ashes obtained from six different electrical power plants located in Maryland were employed in the testing program. The fly ashes were named after their plant of origin as follows: Morgantown (MT), Potomac River (PR), Brandon Shores (BS), Chalk Point (CP), Paul Smith (PS), Dickerson Precipitator (DP), and Dickerson Baghouse (DB) ashes. They were all produced as a result of burning pulverized bituminous coal and classified as Class F fly ash according to ASTM C 610.

The chemical properties of these fly ashes are summarized in Table 3.1. These values are determined in the analytical testing facility of ALS laboratory group Portland, Oregon. In addition, several physical properties of the fly ashes were determined. Mechanical sieving and hydrometer analyses were conducted following ASTM D 422.

Table 3.1Chemical properties of the Maryland fly ashes employed in the testing program.

Constituent	PS	DB	DP	BS	CP	MT	PR
SiO_2 (%)	50.8	37.73	34.91	45.13	50.16	49.15	52.47
Al_2O_3 (%)	26.88	27.26	24.42	23.06	23.09	25.48	24.9
Fe_2O_3 (%)	5.51	11.53	12.59	3.16	14.51	13.74	6
CaO (%)	0.73	3.77	3.18	7.82	2.67	2.48	1.47
MgO (%)	0.57	0.53	0.52	0.83	1.27	0.87	1.28
Na_2O (%)	0.21	0.25	0.26	0.25	0.56	0.58	0.79
K_2O (%)	2.19	1.02	1.05	1.68	2.25	1.86	2.85
Cr_2O_3 (%)	0.02	0.04	0.03	0.02	0.02	0.03	0.02
TiO_2 (%)	1.48	1.5	1.29	1.42	1.21	1.37	1.29
MnO (%)	0.01	0.01	0.01	0.01	0.04	0.02	0.03
P_2O_5 (%)	0.17	1.33	1.02	0.09	0.32	0.58	0.23
SrO (%)	0.03	0.24	0.21	0.06	0.11	0.13	0.15
BaO (%)	0.05	0.1	0.11	0.06	0.14	0.08	0.17
LOI (%)	10.7	14.9	20.5	13.4	3.2	3.1	8.3

Note: LOI=Loss on ignition, i.e., unburned carbon content. Gs=Specific Gravity, SSA= Specific Surface Area, PS=Paul Smith, DB=Dickerson Baghouse, DP=Dickerson Precipitator, BS=Brandon Shores, CP=Chalk Point, MT=Morgantown, PR=Potomac River.

Table 3.2 Physical properties of the Maryland fly ashes employed in the testing program.

Property	PS	DB	DP	BS	CP	MT	PR
Gs	2.20	2.37	2.34	2.17	2.43	2.45	2.29
SSA(m2/g)	5.15	6.96	11.08	5.46	1.23	1.36	1.67

The resulting grain size distributions of these fly ashes are presented in Figure 3.1. Attempts made to measure the Atterberg limits (ASTM D 4318) indicated that the fly ashes are non-plastic. The measured values for the specific gravity (Gs) (ASTM D 792) and specific surface area (SSA) of the fly ashes are provided in Table 3.2. It is known that there are relationships between the physicochemical properties of geosorbents and SSA (Yukselen and Kaya 2006). The SSA measurements were conducted by Material Synergy laboratory in Oxnard CA following five point Brunauer-Emmett-Teller (BET) analysis by using a Micromeritic Gemini 2360. The samples were degassed under flowing UHP grade nitrogen for two hours at a temperature of 200 before the SSA measurements.

3.1.2 Light Microscopy and Petrographic Analyses of Fly Ashes

Recent studies conducted by Maroto-Valer et.al. (2001) and Kulaots et. al. (2004) have suggested that the type of unburned carbon present in fly ash plays an important factor on its sorption characteristics. Therefore, the formation and presence of carbon in the fly ashes collected from Maryland power plants was evaluated using two different analysis techniques. First, digital images of the fly ashes were captured using a Zeiss polarizing microscope equipped with a Nikon D1 digital SLR camera. The microscope provided a magnification level in a range of 2.5 to 50X. The captured images had an image resolution of 2000 by 1312 pixels, and the corresponding pixel size was approximately 2.5×10^{-3} mm. The specimens were illuminated from the top using American Optical external light stand providing incident light. The light intensity was adjusted so that the fly ash particles were clearly visible. Figure 3.2 shows one of the digital images of

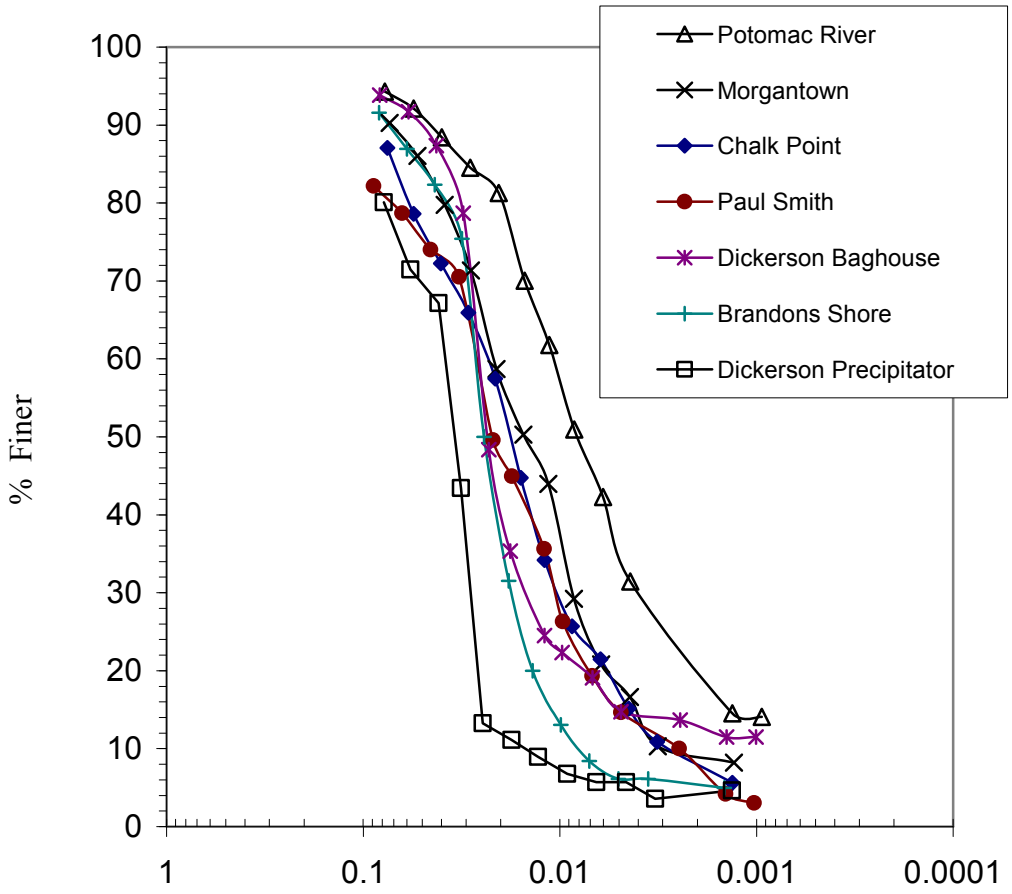

Figure 3.1 Grain size distribution of the materials employed in the batch adsorption tests.

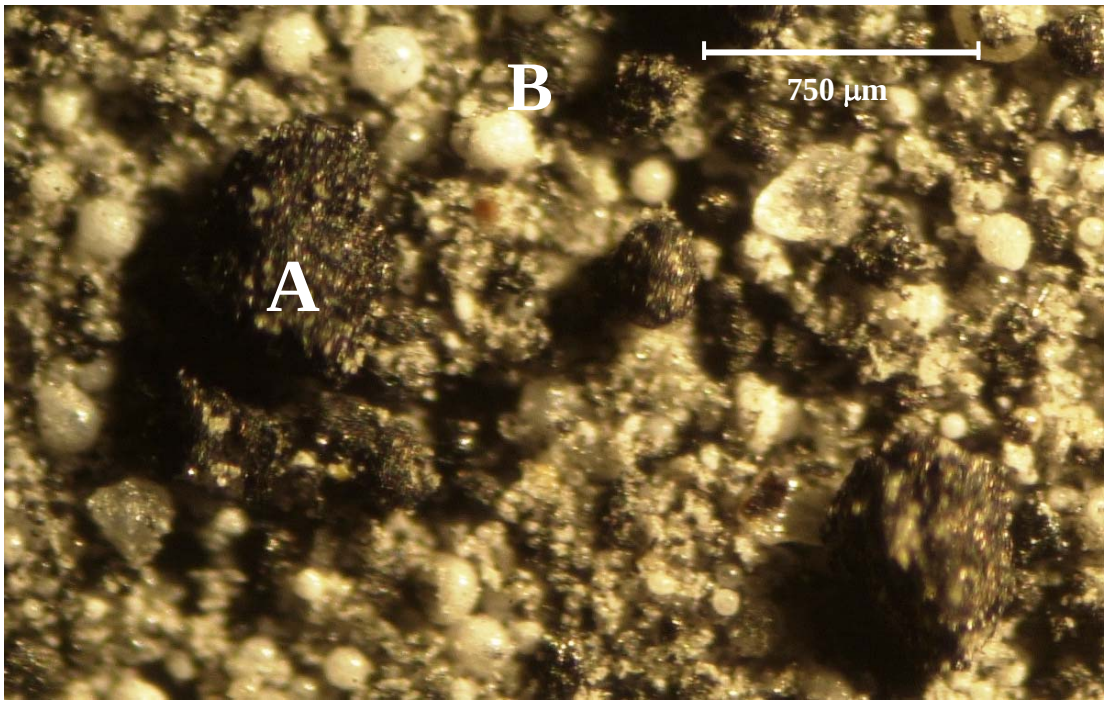

Figure 3.2 Different types of particles in Brandon shores fly ash
A: Carbon particles, B: Inorganic particles .

Brandon Shores fly ash captured by this method. The digital images were mainly used to provide qualitative comparison of the fly ashes, which are primarily silica (Table 3.1) and the carbon particles present. Additional simple measurements conducted on the images indicated that the size of the carbon, and inorganic particles (silica and spinel) present in Maryland fly ashes varied from 100 to 1500 μm and from 10 to 100 μm, respectively.

The second method used to study the carbon type was petrographic analyses. These analyses were performed at the University of Kentucky Center for Applied Energy Research Laboratories using a Leitz Orthoplan microscope equipped with a 50X oil immersion objective. The system utilized for the analyses employed a reflected-light optics technique. The fly ash specimens were impregnated in Sudan Blackdoped epoxy to eliminate the subsurface reflections that are common with a non-dyed epoxy (Maroto-Valer et al. 1999). Previous petrographic studies of fly ashes have identified three distinct forms of unburned carbon in fly ash: (i) inertinites, which appeared to be nonfused particles; (ii) isotropic coke, which are the particles that extensively reacted and passed through a molten stage; and (iii) anisotropic coke, which are the particles more highly aligned with carbon particles (Hower and Mastalerz 2001). Inertinite particles were identified by morphology while isotropic particles were distinguished from the anisotropic particles by their optical activity. A summary of the results obtained from of the petrographic analyses is given in Table 3.3. Duplicate specimens of BS and DP fly ashes were subjected to petrographic analyses for quality control purposes. Table 3.3 provides the amounts of the three different carbons as well as other inorganic constituents in terms of their percentages by volume.

Table 3.3 Inorganic and carbon constitutes of Maryland fly ashes determined through petrographic analysis (all values are given in percentages by volume).

Fly ash[1]	**Glass (%)**	**Mullite (%)**	**Spinel (%)**	**Quartz (%)**	**Isotropic Carbon (%)**	**Anisotropic Carbon (%)**	**Inertinite (%)**	**Total Carbon[2] (%)**
DP	53.8±3.11	_	5.4±1.98	_	2.4±1.13	33.8±7.64	4.6±1.41	40.8±5.1
BS	88.2±0.85	_	0.6±0.28	_	3.8±1.41	6.4±2.26	0.6±0.28	10.8±1.13
CP	90.4	_	3.6	_	1.2	2.8	2.0	6.0
DB	66.8	_	2.0	_	1.2	26.4	3.6	31.2
MT	85.6	_	6.8	_	2.4	4.4	0.8	7.6
PR	86.4	_	1.2	_	1.6	8.4	1.6	11.6
PS	85	_	0.4	_	0.4	12.6	1.2	14.2

[1]Note: PS=Paul Smith, DB=Dickerson Baghouse, DP=Dickerson Precipitator, BS=Brandon Shores, CP=Chalk Point, MT=Morgantown, PR=Potomac River.
2 Total Carbon = Isotropic carbon + anisotropic carbon

Reporting these values as percentages by volume is preferable to percentages by weight (i.e., loss on ignition, LOI) as the carbon particles typically have lower densities than inorganic particles (Maroto-Valler et al. 2001).

The inorganic particles were counted and classified as glass (solid and non-crystalline aluminosilicates), quartz (non-melted silicates), mullite (a typical composition $Al_6Si_2O_{13}$), or spinel (iron oxides) (Maroto-Valler et al. 1999). The petrographic analyses showed that the ashes exhibit a structure commonly observed in Class F fly ashes, i.e., the ashes were dominated by Al^{3+} and Si^{2+} with varying amounts of spinel. Figure 3.3 presents the images of the glass and spinel components of the Morgantown fly ash. The three different types of carbon (i.e., anisotropic, inertinite, and isotropic) are also clearly visible in the petrographic images. This is illustrated in Figure 3.4, which demonstrates the presence of these formations in the Brandon Shores fly ash. The three different types of carbon were present together (Figure 3.5a) or separately (Figures 3.4b through d) in the fly ash.

It is interesting to look at the relationships between the properties of the fly ashes. For example, the relationship between LOI and percent total carbon by volume measured in petrographic analyses for all the fly ash is presented in Figure 3.5. The volumetric percentages tend to yield higher values than LOI; however, a clear trend is still visible between the two sets of measurements. Figure 3.6 reveals the strong correlation exists when LOI or total carbon by volume is plotted against SSA. Clearly, the higher LOI fly ashes have higher surface area. These observations are in good agreement with previous studies, which indicate that carbon fraction generally increases with increasing specific

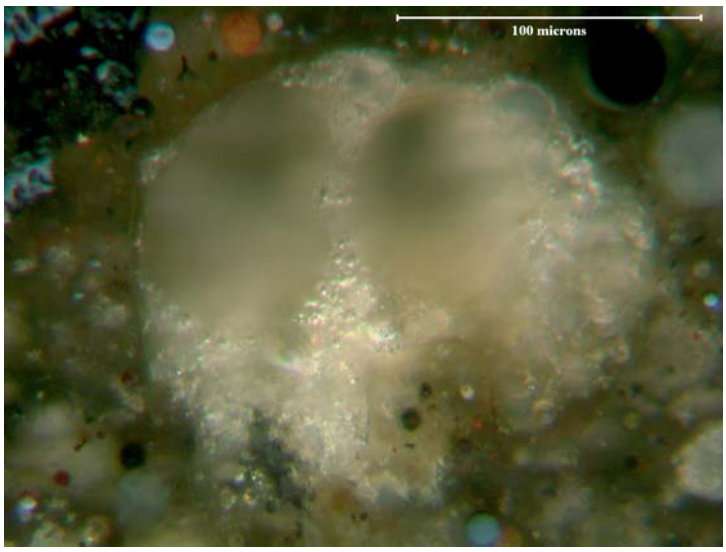

a)

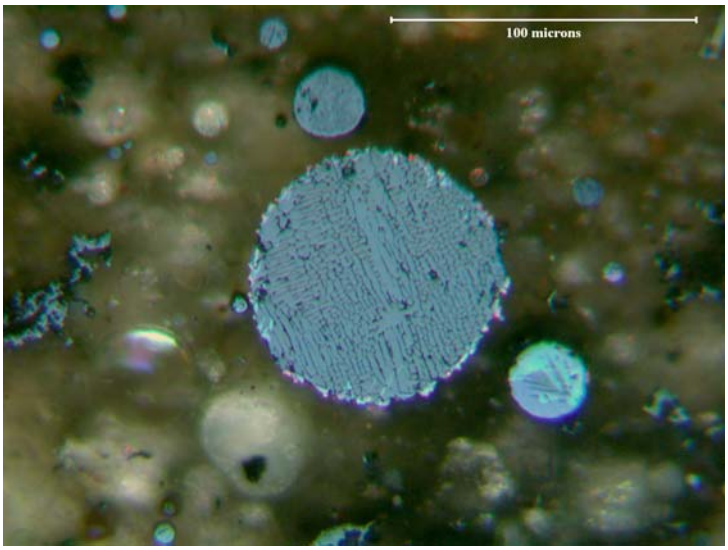

b)

Figure 3.3 Inorganic components of Morgantown (MT) fly ash: a) Al-Si (i.e., glass) and b) spinel.

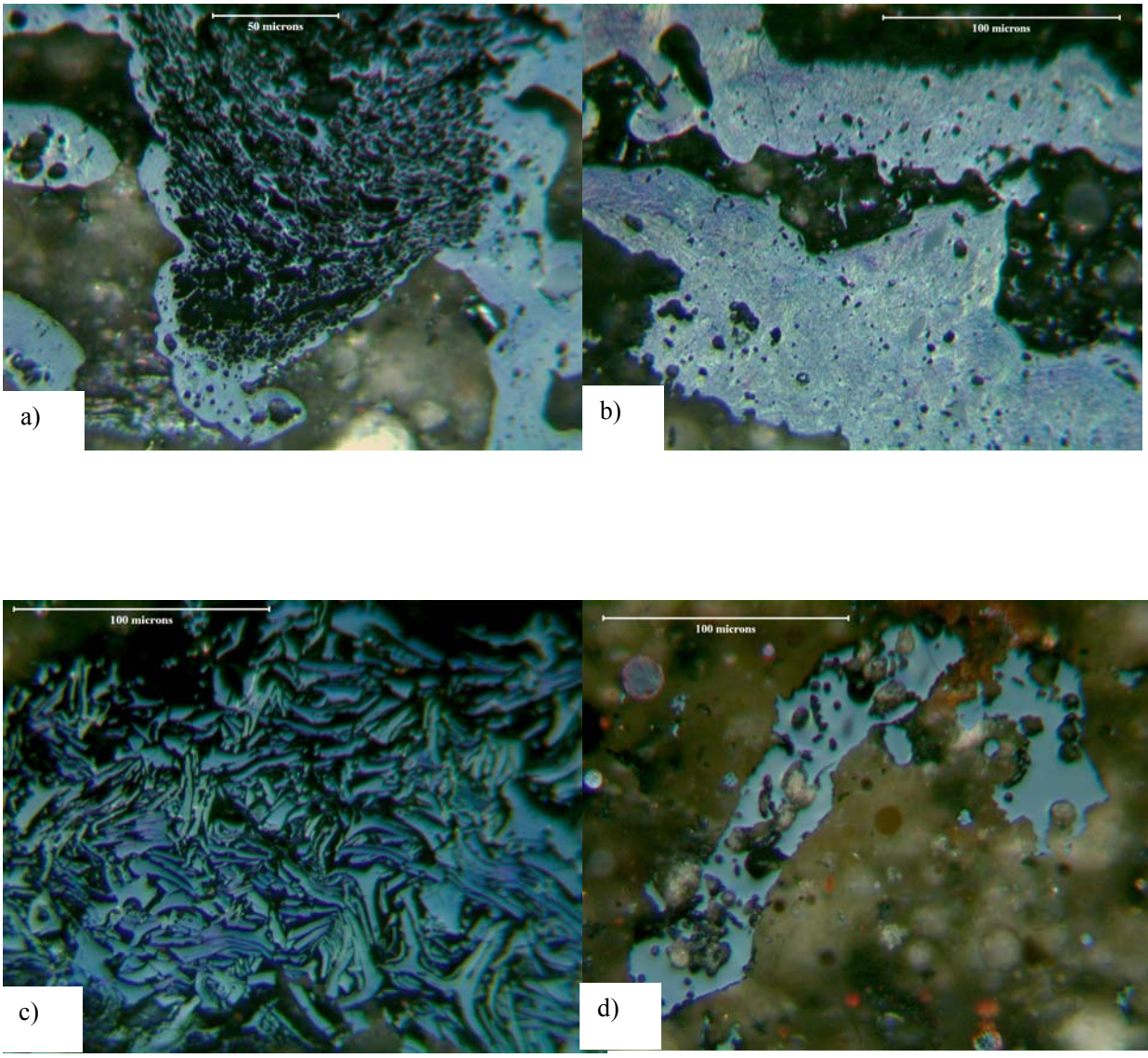

Figure 3.4 Images from petrographic analysis of Brandon Shores (BS) fly ash a) All three carbon forms on one carbon particle, b) anisotropic carbon, c) inertinite, and d) Isotropic carbon.

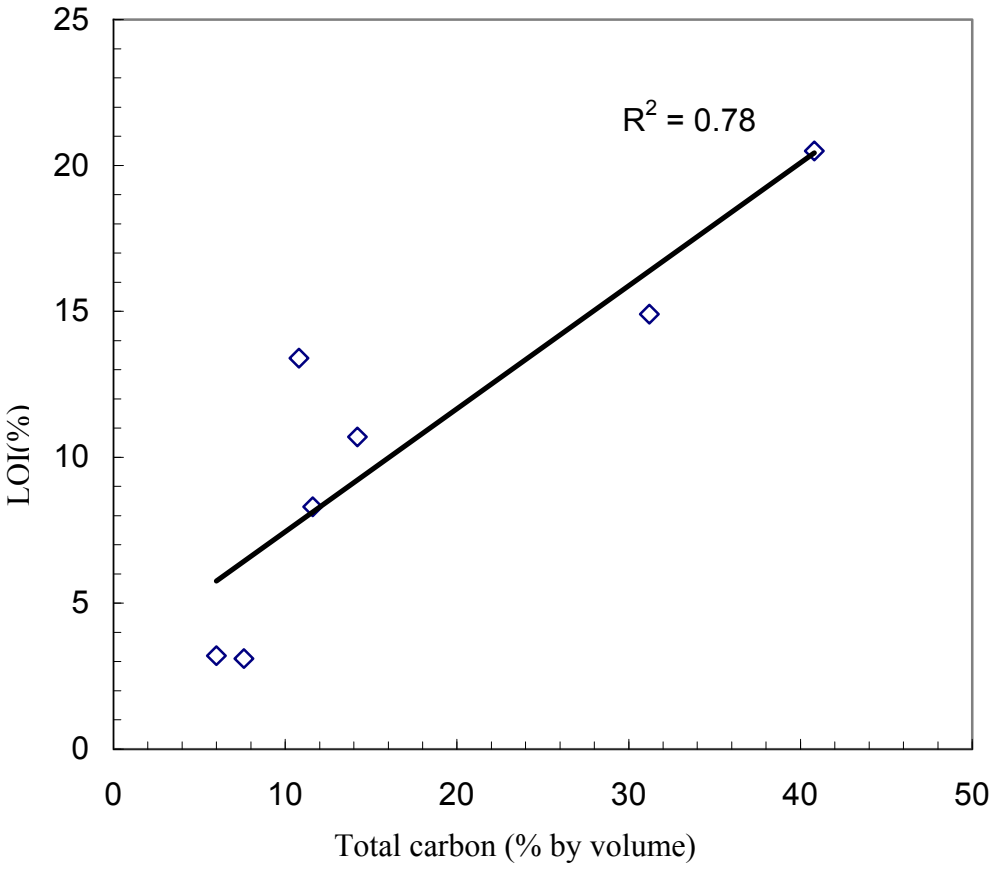

Figure 3. 5Relationship between loss on ignition (by weight) and percent total carbon determined in the petrographic analyses.

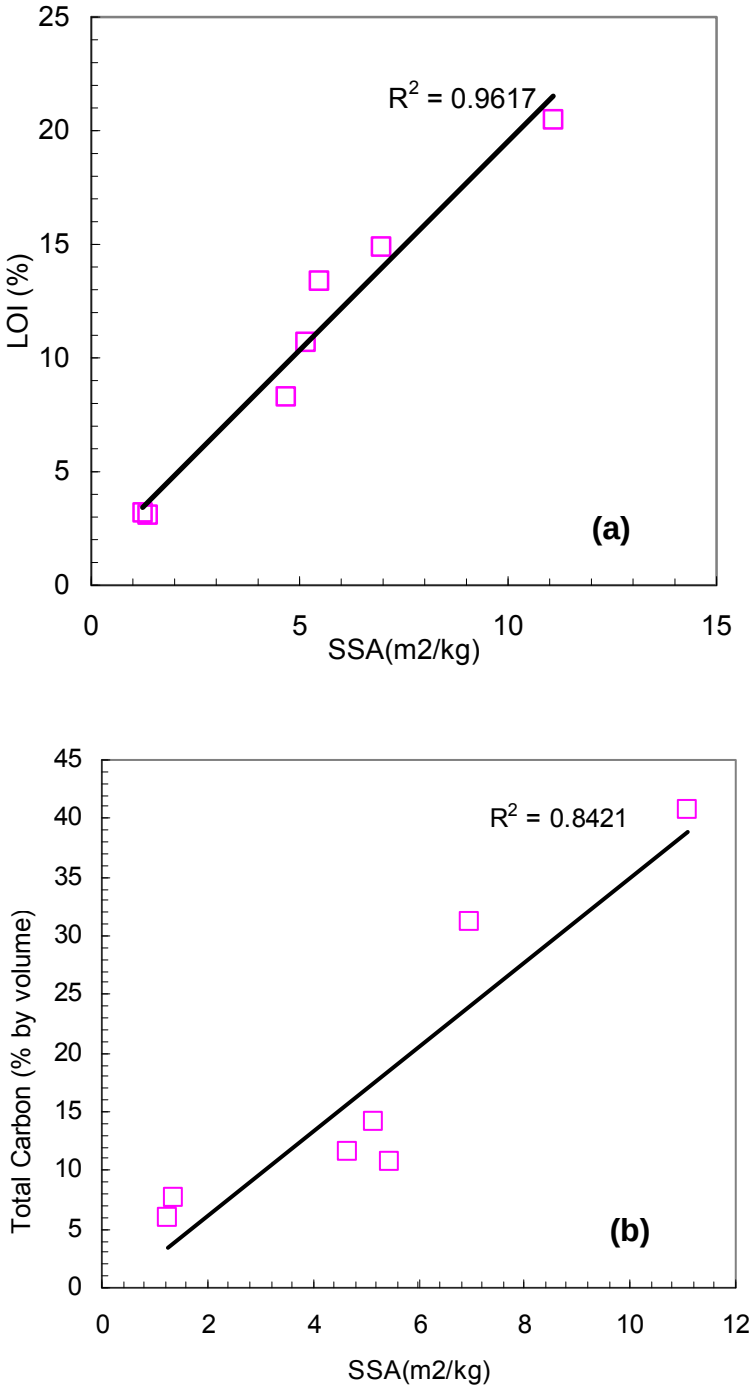

Figure 3. 6Correlation curves between a) percent LOI and specific surface area b) Total carbon from petrographic analyses of the Maryland Fly ashes

surface area of the fly ash due to unburned carbon particles, regardless of the type and source of the coal (Baltrus et al. 2001).

3.1.3 Reference Soil

A natural soil was employed as a reference material in the adsorption tests. The soil utilized in the current study is commonly used as a borrow material in construction of highways in the state of Maryland. The soil was classified as clayey sand (SC) according to the Unified Soil Classification System (USCS) and A-2-4 according to the American Association of State Highway and Transportation Officials (AASHTO) Classification System. Grain size distribution analyses indicated that the soil had approximately 34% particles passing the U.S. No. 200 sieve. The fines content (particle size smaller than 2 μm) of the borrow material was 10%. Specific gravity (G_s) of the material was 2.65, and it had very low plasticity (PI = 5). Based on an analysis performed using a SHIMADZU 500 carbon analyzer, the soil had a total organic content (TOC) of about 0.5% by weight. The cation exchange capacity (CEC) and pH of the material were 2.9 meq/100g and 7.2, respectively, as determined by Agri Analysis Inc. (Leola, Pennsylvania).

3.1.4 Powdered Activated Carbon (PAC)

Activated carbon, strong sorbent, which is commonly used for experimental and practical purposes, was used in this work as a control sorbent. Specifically, powdered activated carbon (PAC) HYDRODARCO B from Norit Americas Inc. was chosen due to its comparable grain size distribution with fly ashes. The specific surface area of this PAC range from 500 to 600 m^2/g (Norit Inc. 2007).

3.1.5 Contaminants

Refined petroleum products (e.g., diesel fuel) typically contain more than 100 chemical compounds (Lee et al. 1992). Therefore, to avoid analytical and data analysis complications, naphthalene, a representative polycyclic aromatic hydrocarbon (PAH), and *o*-xylene, a compound from the benzene-toluene- ethylbenzene-xylene (BTEX) group, were selected as the target model contaminants for the batch adsorption tests. A PAH was chosen as the target compound in this study mainly for two reasons. First, aromatic hydrocarbons, including PAHs represent a significant fraction of the hydrocarbons in diesel fuels. Second, PAHs have relatively low solubility, high sorption, and low volatility which facilitate sorption and leaching studies. Furthermore, naphthalene is listed as one of the pollutants in the U.S. EPA priority list (Schwarzenbach et. al. 1999). *O*-xylene was included in testing because the BTEX group compounds are commonly encountered as subsurface pollutants, and are also included in the U.S. EPA's priority pollutant list. The physical and chemical properties of naphthalene and *o*-xylene are listed in Table 3.4. The naphthalene and *o*-xylene used in this research were purchased from VWR Scientific, Inc. (99% purity).

3.2 Experimental Methods

Three different series of batch sorption tests were conducted. The first series of preliminary batch tests was conducted on one of the fly ashes, Brandon Shores

Table 3.4 Physical and Chemical properties of naphthalene and o-xylene (Schwarzenbach et al. 1999).

	Naphthalene	*O*-xylene
Chemical Formula	$C_{10}H_8$	C_8H_{10}
Molecular Weight	128.2	106.16
Melting Point	80.5 ºC	-25 ºC
Boling Point	218 ºC	144.4 ºC
Density at 20 ºC	1.145 g/mL	0.88 g/mL
Solubility	31.7 mg/L	178 mg/L
Log K_{ow}	3.29	3.12
Vapor Pressure	0.087 mmHg	5 mmHg
Henry's law Constant	4.6 10^{-4} atm-m^3/mol	5.19 10^{-3} atm-m^3/mol

(BS) fly ash, to study the solid-to-solution ratios, i.e., the ratio of the weight of the solid to the volume of the aqueous naphthalene or *o*-xylene solution, and to identify the optimum ratio for further testing. Second, a series of batch kinetic tests were conducted on the Brandon Shores fly ash to study the reaction kinetics with the two organic compounds. Finally, the optimum solid-to-solution ratio and equilibrium time defined by these two series of tests were used for the batch adsorption tests conducted on the remaining fly ashes. The method of concentration analyses was selected considering the initial concentration of the organic compound and detection limit of the equipment.

3.2.1 Batch Adsorption Tests to Optimize Solid to Solution Ratios

To perform these batch adsorption tests, three different amounts (0.5 g, 1 g, and 2 g) of fly ash were placed in duplicate 60 mL glass centrifuge tubes. A 20 mg/L naphthalene or 10 mg/L *o*-xylene aqueous solution was prepared 24 hours before the test, and 60 mL were mixed with the fly ash at room temperature (24 ± 2 ºC). These fly ash masses and solution volume corresponded to solid-to-solution ratios of 1/120, 1/60, and 1/30, respectively. Additionally, two control samples were prepared by adding only the aqueous naphthalene or *o*-xylene solution to the vials. The centrifuge tubes were sealed with Teflon® lined caps and then were placed and rotated for 24 hours using the end-over-end rotator (ATR Scientific-24). The agitated samples were then separated by centrifugation (Beckman GPR centrifuge) at 3000 rpm for 15 min. A 2 mL-sample of the supernatant was transferred to a clean 8 mL amber vial and the vial was capped using an open-top screw-thread closed with a polytetrafluoroethylene (PTFE)-faced rubber septa and saved for analysis of naphthalene and *o*-xylene concentrations as described in the

following section. Amber vials were chosen for sample storage in order to prevent the possible photolytic decomposition of the contaminants, which are known to be light sensitive (APHA, 1995). A PTFE membrane filter with 0.45 μm opening size was used during transfer of the supernatant into the vials to remove any solid phase particles remaining in suspension after centrifugation.

The ASTM D 5285 procedure for recommends a solid-to-solution ratio that would result in 20 to 80% sorption of the contaminant. However, the first series of batch adsorption tests conducted on Brandon Shores fly ash indicated that the fly ash specimens prepared at high solid-to-solution ratios such as 1/30 and 1/60 resulted in ≈100% sorption of the naphthalene and o-xylene (Figure 3.7). Therefore, the remaining batch kinetic and adsorption tests were conducted on specimens prepared at a ratio of 1/120 which gave approximately 60-80 % sorption.

3.2.2 Batch Kinetic Tests

Similar to the preliminary batch adsorption tests, Brandon Shores (BS) fly ash was used in the batch kinetic tests. A total of thirty fly ash/o-xylene and fly ash/naphthalene solutions were prepared at a solid-to-solution ratio of 1/120. An initial naphthalene or o-xylene concentration of 20 mg/L was employed in these experiments. A series of batch kinetic tests were performed in which, the solutions were equilibrated on an end-over-end rotator shaker for 3, 6, 12, 24, and 48 hours. The procedures for specimen preparation and analysis followed those described in section 3.2.1. The batch kinetic test data presented in Figure 3.9 show that the final aqueous concentrations of naphthalene measured at the different equilibrium times are comparable. The results suggested an equilibrium time of 24 hours for future tests. The results presented in

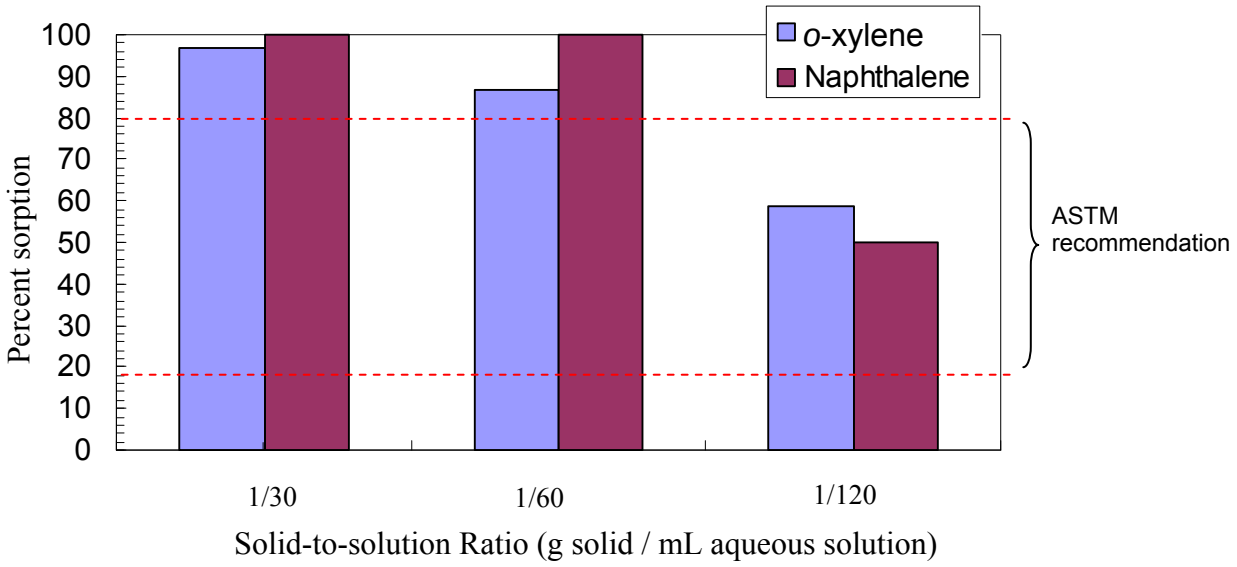

Figure 3. 7 Preliminary batch adsorption tests for solid-to-solution ratio determination. Bars represent the average of triplicate measurements.

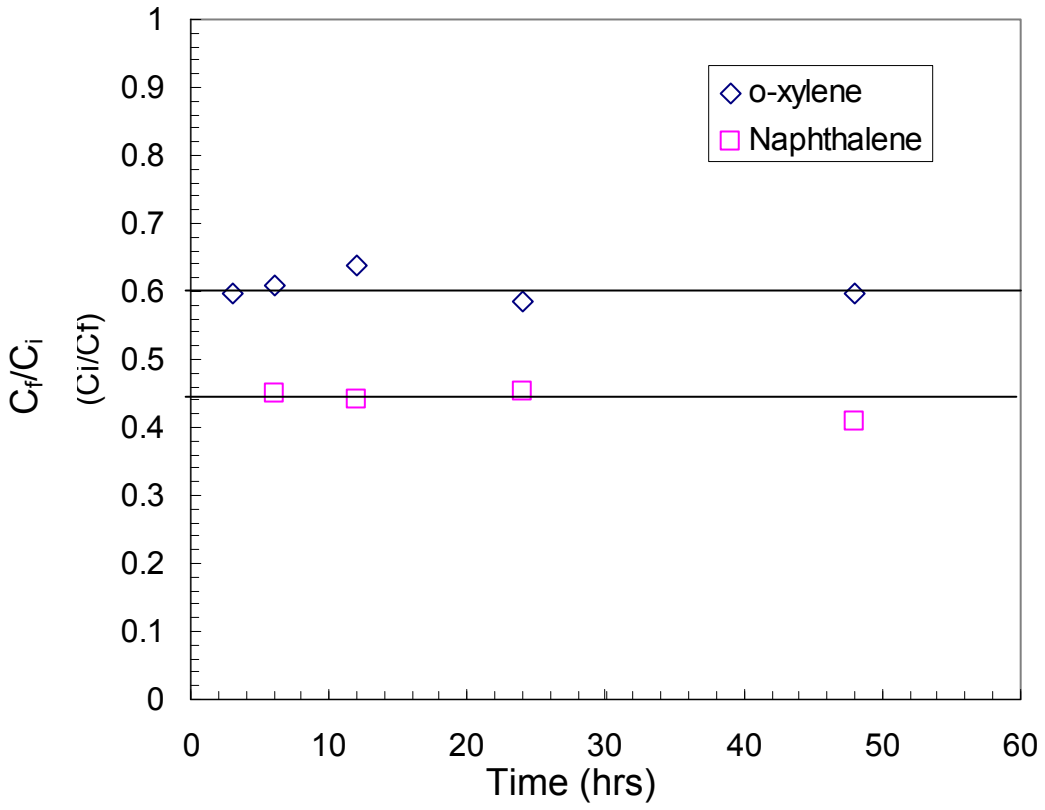

Figure 3. 8Batch kinetic tests conducted fly ash and solutions of o-xylene and naphthalene (Ci=Initial concentration, Cf=Final concentration).

Figure 3.8 also suggest that the sorption of both naphthalene and *o*-xylene onto fly ash is a quick process. A large percentage of the contaminant was sorbed in a short period of time (in minutes to a few hours), whereas the remaining fraction was sorbed more slowly within the next few days. The observed trends are meaningful as the initial sorption generally occurs by hydrogen bonding and van der Waals forces, and is expected to occur instantaneously upon contact of the nonpolar organic chemical with the fly ash (Semple et al. 2003). A separate series of batch kinetic tests were not performed on the reference soil; however, the 24-hr period was deemed acceptable based on the equilibrium times reported for similar materials (Chiou 2002).

3.2.3 Batch Adsorption Tests for all Fly ashes

Based on the results of the first two series of tests, batch adsorption tests were performed for all fly ashes, following the procedure of Section 3.2.1, with a solid-to-solution ratio of 1/120 and an equilibrium time of 24 hrs. The initial concentration of naphthalene and *o*-xylene in this third series of batch adsorption tests ranged from 0.5 to 25 mg/L and from 0.2 to 85 mg/L, respectively. The reference soil (borrow material) was included in the third series of batch adsorption tests. Naphthalene solutions were prepared at concentrations of 0.5, 1, 2, 3, 4, 5, 7.5, 10, 15, and 20 mg/L and added in 60 mL centrifuge tubes along with 0.5 g of borrow material. The procedures for centrifuging and collecting of supernatant were the same of the ones followed for fly ash. The solutions were equilibrated with end-over-end rotator shaker for 24 hours.

3.3 Mathematical Methods

In this work the database was evaluated by six equilibrium isotherm models, namely Linear (Henry's law) model, Freundlich model, Langmuir model, a Combined model of Freundlich and Langmuir (CFL), Polanyi-Dubinin-Manes (PDM) model, and the Fritz-Schluender model. These six different isotherm models how various numbers of model constants, linear isotherm having one, the Freundlich and Langmuir isotherms having two, CFL and PDM isotherms having three, and the Fritz Schluender isotherm having five model constants. A detailed explanation of the six isotherms models used in the current study was given at Section 2.3.1. For all isotherms except the PDM model, the sorbed amount q_i (mg/kg) was plotted against the final equilibrium concentration C_f (mg/L). In case of the PDM model, q_i/density of the sorbate (q'_{max}) was plotted against effective adsorption potential normalized by molar volume of the sorbate (E_{sw}/V_s). Parameters such as the surface characteristics of the sorbent or the hydrophobicity of the organic molecule have a great influence on the adsorption behavior. Therefore by using seven different fly ashes and PAC, two difficult organic contaminants, and applying the different isotherm models, the goal was to attempt to provide a better understanding of the adsorption mechanism.

The adsorption test data were analyzed using a nonlinear regression analysis. Specifically, the isotherm models were fit to the collected experimental data using a curve fitting method, which employs Levenberg-Marquardt algorithm. The goodness of the curve fit was evaluated based on the adjusted value of R^2 and the relative standard error (RSE), which is the ratio of root mean squared error (RMSE) over standard deviation. The isotherm that gave the highest adjusted R^2 value and lowest RSE was

considered to give the best fit. It is important to note that; both the R^2 value and RSE were "adjusted" to account the number of independent parameters in the model. Therefore, they can be used to provide an accurate relative comparison for the goodness of the fit between models with different number of parameters. The adjusted R^2 expression is given Equation 3.1 below,

$$Adjusted \cdot R^2 = 1 - \left[\frac{(n-1)}{v}\right](1 - R^2) \tag{3.1}$$

where n is the number of data points, v indicates the number of independent model parameters. The regular (unadjusted) R^2 values which do not account for the degree of freedom of the model were also calculated for all models; however, are not presented herein as the values are higher than the adjusted ones and provided an unconservative estimate. The residual analysis of the best fit results and experimental data were also examined for all fits.

3.4 Analytical Methods

3.4.1 Fluorescence Analysis

A Shimadzu 5301 Fluorescence Spectrophotometer was utilized to measure the final concentrations of naphthalene and *o*-xylene in the batch adsorption test specimens. Excitation and emission wavelengths for naphthalene and *o*-xylene in aqueous solution were 273 and 336 nm, and 267 and 289 nm, respectively. Preliminary investigations indicated that the detection limits of the equipment for naphthalene and *o*-xylene were 0.0165mg/L and 1.273 mg/L, respectively. Thus, the specimens with initial naphthalene and *o*-xylene concentrations greater than 2 mg/L could be accurately determined using

the spectrofluorophotometer. The supernatants in the amber vials were analyzed with fluorescence as follows. First, the supernatant was transferred into a Quartz sample cell, and the cell was then immediately placed into the sample compartment of the spectrofluorophotometer. Subsequently, the fluorescence intensities corresponding to excitation and emission wavelengths of the specimens were measured.

Fluorescence intensity reading were converted to concentrations based on standard curves derived using duplicate standard solutions that were prepared for each compound. The concentrations of supernatants were then calculated using the standard calibration curves. The standard concentrations for naphthalene were 0, 0.4, 0.8, 1.6, 4.0, 8.0, and 16 mg/L, while the standard concentrations for *o*-xylene were 0, 5.63, 10.14, 11.3, 22.6, 40.6, 45.2, 81.7 mg/L in aqueous solutions.

3.4.2 Gas Chromatography (GC) Analysis

Due to the relatively high detection limits for *o*-xylene using the fluorescence method, low concentrations (<2mg/L) of *o*-xylene were determined using a gas chromatograph (GC). Gas chromatography is an analytical method for separation and identification of chemical compounds. The details of the GC analysis employed in the current study are provided in the following paragraphs.

First, 10 μl of 500 mg/L acenaphthene in methanol internal standard solution were spiked into the 2mL supernatant sample using a 100 μl Hamilton gas-tight syringe that was inserted into the sample vial through the septum in the cap. The internal standard acenaphthene was used to minimize the sensitivity of the *o*-xylene concentration to the extraction procedure (Hong 2003). After addition of the internal

standard, the vial was shaken by hand for one minute to thoroughly mix the solution. Subsequently, a liquid-liquid extraction procedure was applied before the GC analysis. The extraction solvent was GC grade hexane (Fisher Scientific, Inc., 99% purity). Following the internal standard mixing process, 1 mL of hexane was introduced into the vial and the vial was shaken for 10 minutes using an end-over-end rotator. The vial was then allowed to sit for at least two minutes to allow the liquid phases to separate. The GC analysis of *o*-xylene in hexane was performed as soon as possible after the extraction. If the samples could not be analyzed immediately, they were stored at 4°C up to 3 days to eliminate any possible volatilization or biological degradation.

Analysis of *o*-xylene in the hexane extracts was performed using a Hewlett Packard (HP) Model 6980 GC equipped with a flame ionization detector (FID). A software program Chemistation Version 6.03 was used for analysis. The GC column was a 30-m long HP-5 (crosslinked 5% phenyl/metyl siloxane) column with an internal diameter of 0.32 mm and a film thickness of 0.25 μm. The GC system and operating conditions used in the analysis of *o*-xylene and acenaphthene were adopted from Hong (2003). A summary of the system and operating conditions is provided in Table 3.4. The mode of operation was splitless injection and the septum purge time was 0.75 minutes. The running time for each injection was 10 minutes, because the retention times for the *o*-xylene and acenaphthene were 4.8 and 8.9 minutes, respectively (Figure 3.9).

A 1 μl aliquot of the hexane extract was manually injected into the GC using a 10 μL Hewlett Packard analytical syringe. Any air bubbles in the syringe were

Table 3.5 Operating conditions for GC analysis of o-xylene

Gas Flowrates	Carrier Gas	Helium
	Septum Purge	60 mL/min
	Column Flow rate	8.2 mL/min
	Make up Gas (Nitrogen)	17.7 mL/cm
	Flame Oxidant (Air)	400 mL/min
	Flame Combustible(Hydrogen)	40 mL/min
Oven	Initial Temperature	40 ºC
	Initial Hold Time	4 min
	Temperature Increase	30 ºC/min
	Hold Time	1 min
	Final Temperature	215 ºC
Injector	Temperature	250 ºC
Detector	Temperature	300 ºC

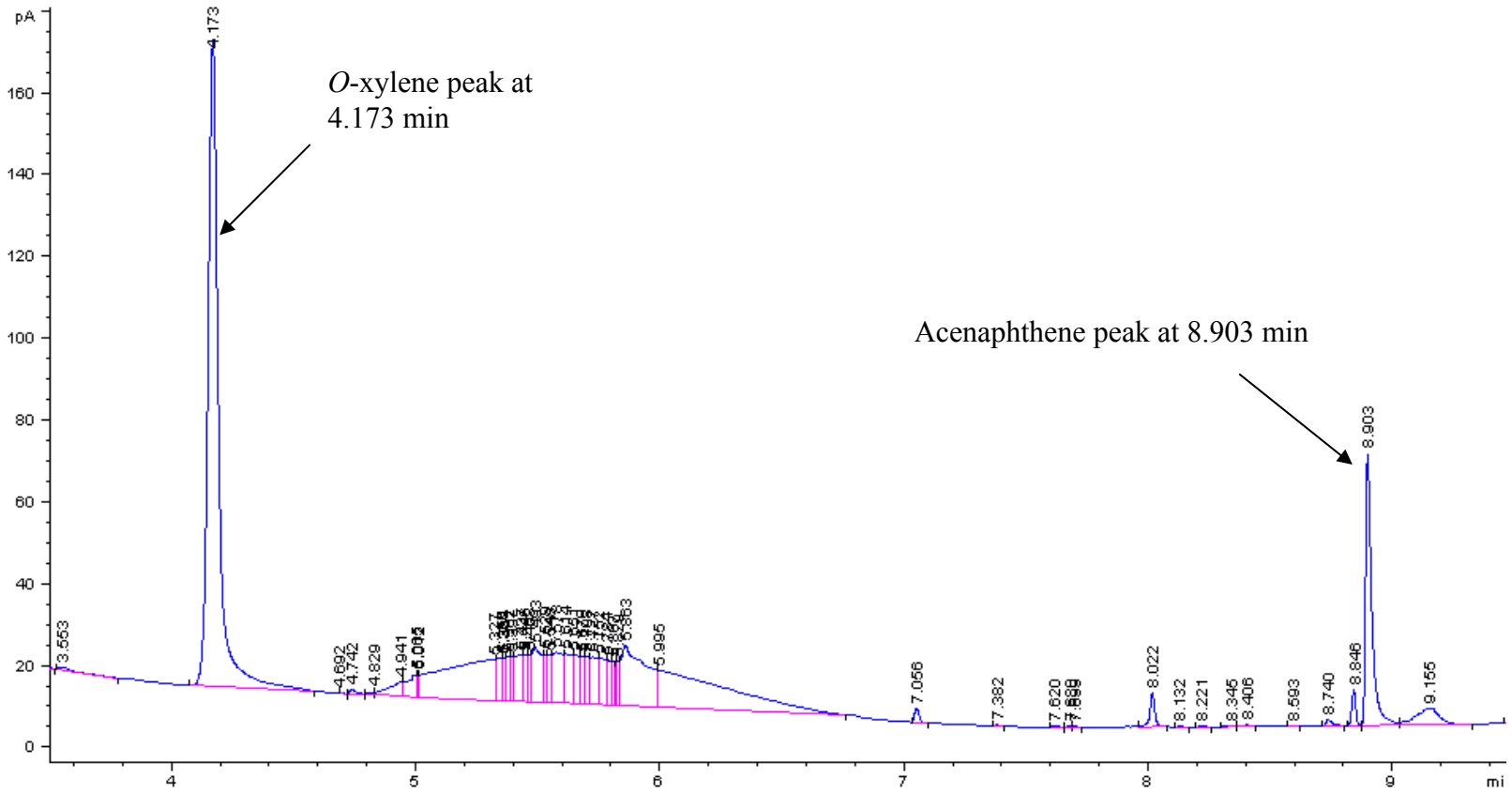

Figure 3 9 A typical GC plot for o-xylene and acenaphthene as an internal standard.

manually removed before the injection. The syringe was rinsed with extract three times before and five times after each injection. Injections were performed in duplicate for every sample to ensure good reproducibility.

This GC method adopted herein was calibrated for each set of experiments with standard solutions of *o*-xylene and acenaphthene in hexane. Calibration was performed by using three different concentrations of acenapthene and four different concentrations of *o*-xylene as summarized in Table 3.5. Each Standard was injected in triplicates. The linear regression equations that best defined the relationship between the GC peak area and the measured concentrations of the *o*-xylene and acenaphthene in hexane, respectively, are also provided in Table 3.5. Preliminary analyses indicated that the higher concentration points of a given standard calibration curve had a weighted effect on the overall standard curve when range in the concentrations covered greater than one order of magnitude. This adverse effect was eliminated by using a weighted linear regression (Relative Least Squares, RLS) analysis, for the *o*-xylene standard curve. However, an unweighted linear regression (Absolute Least Squares, ALS) was found to be acceptable for the analyses of acenapthene in hexane. The detailed explanations of the two regression analyses are provided by Berthouex and Brown (2000). By following this method, detection limits for naphthalene and *o*-xylene are 0.0216 mg/L and 0.0656 mg/L respectively.

The aqueous concentration of *o*-xylene was calculated from the measured concentration in hexane by using the following equation:

$$\left[C_{aq}\right]_{OX} = \frac{\left[C_{hex}\right]_{ox}}{\left[C_{hex}\right]_{Ace}}\left(\frac{V_{is}}{V_{sam}}\right)\left[C_{is}\right]_{Ace} \qquad (3.2)$$

Table 3 6 Standard solutions and equations used for o-xylene and acenapthene in hexane

Compound	Standard Solutions used (mg/L)	Curve Equations	R^2
o-xylene	0.1442, 1.442, 3.605, 36.05	$A_{ox} = 35.318\ [C_{hex}]_{ox} + 3.377$ [(a)]	0.999
Acenaphthene	0.5, 5, 10	$A_{Ace} = 29.476[C_{hex}]_{Ace} - 4.599$ [(b)]	0.994

Note: A_{ox} – area of the *o*-xylene peak in the chromatogram, A_{Ace} – area of the acenaphthene peak in the chromatogram, $[C_{hex}]_{ox}$ - the *o*-xylene concentration in hexane, $[C_{hex}]_{Ace}$ - the acenaphthene concentration in hexane
[(a)]- calculated by RLS [(b)] - calculated by ALS

where $[C_{aq}]_{ox}$ is the concentration of *o*-xylene in the aqueous sample, $[C_{hex}]_{ox}$ and $[C_{hex}]_{Ace}$ are measured concentrations of *o*-xylene and acenaphthene in hexane, respectively, V_{is} is volume of the internal standard solution (10 μL), V_{sam} is the volume of aqueous sample, and $[C_{is}]_{Ace}$ is the concentration of the internal solution (500 mg/L in this case).

The amount of the adsorbate (i.e., naphthalene or *o*-xylene) sorbed on the solid phase per dry unit weight of solid (q_i) was then calculated by using the mass balance approach:

$$q_i = \frac{V_w\left([C_i]_{ox} - [C_{aq}]_{ox}\right)}{M_{solid}} \tag{3.3}$$

where q_i is in (mg/g), V_w is the volume of the solution (mL), $[C_i]_{ox}$ is the initial concentration of *o*-xylene (mg/L), $[C_{aq}]_{ox}$ is the concentration of *o*-xylene in aqueous solution after sorption (mg/L), and M_{solid} is the dry mass of solid particles (g).

3.5 Results and Discussions

The results of the batch adsorption test using the seven HCCFAs and PAC are presented in two sections first looking at naphthalene sorption, and the o-xylene. It is common to relate qi (mg of sorbed contaminant per kg of sorbent), to the final equilibrium concentration Cf (mg/L) of the contaminant in solution by using sorption isotherm models.

3.5.1 Naphthalene Adsorption onto Maryland Fly Ashes and Activated Carbon

The parameters and regression statistics for the fly ash/PAC-naphthalene isotherm models are given in Table 3.6. None of the data sets for the sorbents could be fit using the linear model. This appears to be reasonable. Chiou et al. (2000) reported that the linear isotherm is an indication of partitioning of the non-polar organic chemical with humic substances of the sorbent, and that highly thermally altered materials, like HCCFA, could deviate from a linear isotherm. They noted that even small amounts of thermally altered carbonaceous material can cause substantial nonlinearity in the sorption isotherm.

The sorption data and best fit sorption isotherm models for naphthalene on all fly ashes and PAC are plotted on the standard basis (q_i (mg/kg) versus C_f (mg/L))(Figure 3.10). Note that the data for two fly ashes (DB and CP) and PAC are also plotted in this figure for comparison purposes, although the PDM model was the best model these sorbents as discussed below.

The nonlinearity in the naphthalene sorption data could be explained by the heterogeneous structure of the HCCFA. It is well known that thermally altered materials (e.g., fly ash) have non-polar surfaces with potentially high surface area and porosity, which were created by thermal alteration processes at extremely high temperatures (>1000 °C degree). These changes in the chemical and physical of structure of the material promote adsorption, and possibly result in nonlinear sorption isotherms that are characterized by a high sorption capacity at low concentrations (Allen-King et al 2002). Such nonlinearity was also reported by Kleinidam et al.

Table 3 7 The isotherm parameters and goodness of fit statistics for the applied adsorption isotherm models from naphthalene adsorption tests.

		BS			**DP**			**DB**			**PR**		
Isotherm type	Isotherm parameters		R^2	RSE		R^2	RSE		R^2	RSE		R^2	RSE
Linear	K_d (L/kg)	N/A	N/A	N/A	N/A	N/A	N/A	381.6	0.10	0.958	N/A	N/A	N/A
Freundlich	K_f (mg/kg)(mg/L)$^{-n}$	637.1	0.87	0.386	1416	0.94	0.249	873.2	0.97	0.173	454.4	0.87	0.369
	n (-)	0.195			0.194			0.3179			0.314		
Langmuir	Q_{max} (g/kg)	885.9	0.83	0.414	1332	0.80	0.458	1411	0.94	0.256	933.1	0.78	0.474
	K_L (L/kg)	5.274			60.96			2.484			0.966		
CFL	Q_m (mg/kg)	1117	0.88	0.360	115400	0.93	0.269	2250	0.99	0.138	2206	0.84	0.396
	b (mg/kg)(mg/L)$^{-n}$	1.592			0.013			0.699			0.265		
	n (-)	0.512			0.196			0.521			0.423		
PDM	q'_{max} (L/kg)	0.849	0.87	0.001	3.394	0.93	0.275	1.512	0.99	0.014	0.98	0.85	0.395
	c (mL/J)	0.001			0.113			0.005			0.021		
	d (-)	2.007			0.757			1.681			1.302		
Fritz-Schluender	α_1(mg/kg)/(mg/L)$^{\beta 1}$	2.851	0.82	0.436	420.5	0.91	0.309	9.823	0.98	0.158	19.52	0.73	0.524
	α_2(mg/L)$^{\beta 2}$	0.004			-0.025			0.011			-1.217		
	α_1' (-)	4.10^{-4}			0.319			0			1.26		
	β_1(-)	0.885			0.174			4.138			0.253		
	β_2(-)	0.770			2.385			3.841			0.002		

Linear Isotherm: $q_i=K_d C_f$, Freundlich Isotherm: $q_i=K_f C_f^n$, Langmuir Isotherm: $q_i=(K_L Q_{max} C_f)/(1+ K_L C_f)$
CFL Isotherm: $q_i=(K_L Q_{max} C_f^n)/(1+ K_L C_f^n)$ PDM Isotherm: $q'_i= q'_{max} \exp [© (E_{sw}/V_s)^d]$
Fritz-Schluender Isotherm: $q_i=(\alpha_1 C_f \beta_1)/(\alpha_1' + \alpha_2 C_f \beta_2)$
N/A: Not available

Table 3.7. (continued)

		CP			**MT**			**PS**			**PAC**		
Isotherm type	Isotherm parameters		R^2	RSE		R^2	RSE		R^2	RSE		R^2	RSE
Linear	K_d (L/kg)	N/A	N/A	N/A	N/A	N/A	N/A	N/A	N/A	N/A	N/A	N/A	N/A
Freundlich	K_f (mg/kg)(mg/L)$^{-n}$	88.43	0.85	0.361	102	0.99	0.096	696.1	0.97	0.185	72570	0.82	0.439
	n (-)	0.174			0.306			0.339			0.169		
Langmuir	Q_{max} (g/kg)	110.9	0.87	0.337	194	0.90	0.321	1355	0.91	0.302	81690	0.99	0.109
	K_L (L/kg)	5.189			1.25			1.240			11.65		
CFL	Q_m (mg/kg)	124.7	0.88	0.327	603.3	0.99	0.104	2955	0.96	0.194	78820	0.99	0.096
	b (mg/kg)(mg/L)$^{-n}$	2.723			0.205			0.318			20.99		
	n (-)	0.655			0.391			0.469			1.242		
PDM	q'_{max} (L/kg)	0.101	0.88	0.326	0.225	0.99	0.105	1.521	0.96	0.210	68.44	0.99	0.095
	c (mL/J)	$1.2\ 10^{-4}$			0.028			0.018			$1.8\ 10^{-8}$		
	d (-)	2.625			1.213			1.367			5.096		
Fritz-Schluender	α_1(mg/kg)/(mg/L)$^{\beta 1}$	7.145	0.87	0.334	15.66	0.95	0.164	27.34	0.87	0.369	$28\ 10^5$	0.98	0.116
	α_2(mg/L)$^{\beta 2}$	0.004			0.007			-0.033			38.25		
	α_1' (-)	0.075			0.143			0.007			0.533		
	β_1(-)	0.266			0.398			0.334			1.681		
	β_2(-)	1.218			1.205			0.007			1.638		

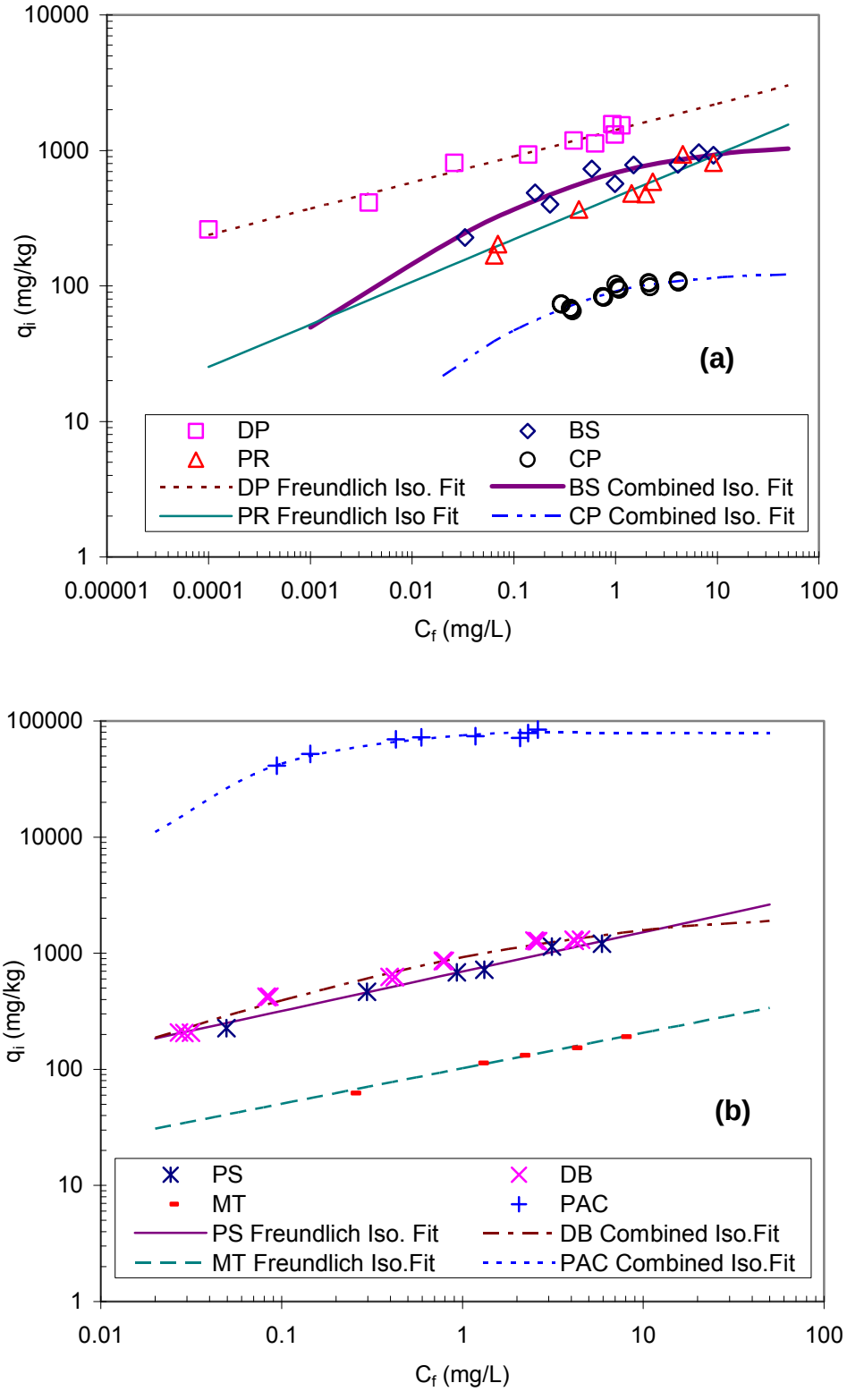

Figure 3 10 Adsorption isotherms with best fit models after naphthalene adsorption experiments. Symbols are from test data. Lines are isotherm from regression results

(2002) for sorption of heterogeneous sorbents like coal combustion by-products (i.e., fly ash) and by Luthy et al. (1997) for sorption of natural soils and sediments.

The goodness of fit statistics for the naphthalene sorption for all fly ashes and PAC are given in Table 3.7. Table 3.7 show that four of the fly ashes (DP, MT, PR, and PS) yielded Freundlich isotherm, two of them (DB, CP) along with PAC yielded PDM isotherm model and BS fly ash yielded CFL isotherm. On the other hand, statistically insignificant differences (at 95% confidence level) in R^2 values of some fits (e.g., CFL and PDM isotherm fit for CP fly ash and PAC) suggested that more than one isotherm model can possibly be used for the interpretation of the sorption data.

The goodness of the fit criteria (R^2 and RSE) generally indicated that the Freundlich isotherm provided a better fit than the Langmuir isotherm, with the exception of CP fly ash and PAC. This is mainly due to the basic assumptions upon which these models are based. The Langmuir isotherm assumes a monolayer surface adsorption with a maximum capacity, which limits the capacity of the sorbent. On the other hand, the Freundlich isotherm has no limiting capacity, rather than the shape of the curves, it depends on the value of the Freundlich exponent "n".

In the Freundlich isotherm "n" is measure of how the affinity of the adsorbate changes to the sorbed concentration changes. Table 3.7 shows that the "n" values for naphthalene adsorption on DP, PR, PS, and MT fly ashes were significantly lower than 1.0, indicating a strong nonlinearity and that affinities decrease with increasing sorbed concentration. The "n" values for fly ash ranged from 0.194 to 0.339 and were lower than an "n" of 0.67 previously reported for sorption of pyrene onto activated carbon (Accardi-Dey and Gschwend 2002). A highly heterogeneous structure and uneven distribution of

the unburned carbon present in the fly ash (i.e., presence of different carbon forms at different amounts in a given fly ash) may be responsible for the observed behavior.

For one of the fly ashes (BS), the CFL isotherm model provided the best fit to the laboratory data. Using three fitting parameters, the CFL model enables the prediction of the naphthalene adsorption of CP, BS, and DB fly ashes slightly better than the Freundlich and Langmuir isotherms. Naphthalene with the limited data available, it is not yet possible to make any claims regarding to the superiority of CFL isotherm to Freundlich or Langmuir in predicting the sorption properties of fly ash.

Recent studies indicated that the Polanyi-Dubinin Manes –PDM- isotherm model provides both mechanistic and modeling advantages, while aiding in identifying the adsorption process (Allen-King et al. 2002). For two of the seven fly ashes (DB and CP) and PAC, the PDM isotherm provided the best fit data. Similarly, PDM isotherm was utilized by Kleineidam et al. (2002) for non-polar organic chemicals tested with various geosorbents that had meso and micro-pores (i.e., pore sizes varying between 2 nm and 50 nm, and smaller than 2 nm, respectively). These range of meso-pore sizes also exist in fly ashes (Kulaots et al 1998). Maroto-Valer et al. (2001) reports that more than 50% of the pores inside the fly ash can be characterized as meso-pores, regardless of the carbon type. They attribute the existence of such large pores sizes to the extensive and rapid devolatilization of coal during the combustion process. Accordingly, a pore filling mechanism, such ash explained by the PDM isotherm, is believed to be the dominant mechanism for adsorption of non-polar organic chemical onto highly heterogonous sorbents like fly ash (Kleineidam et al. 2002).

It has been suggested that if the number of fitting parameters (degree of freedom) of the sorption isotherm is increased, it could yield a better fit (Mauraya and Mittal 2006). However, the Fritz-Schulender isotherm with five degree freedom did not provide a better fit for naphthalene sorption data onto any of the sorbents tested. The numerical complexities stemmed five degree of freedom also reduced the potential for model likes Fritz-Schulender.

As described above, not all the fly ashes exhibited same type of isotherm (e.g., the Freundlich, combined and PDM were among the best fits). Therefore, in order to compare the adsorption performance of the seven fly ashes on a common basis, the average amounts of sorbed organic compound per mass of fly ash (qi average) were plotted against LOI in Figure 3.11. As expected, the adsorbed amount increases with increasing total carbon content. The effect of LOI on adsorption of organic compounds has previously been documented for chlorinated benzenes (Mott and Weber 1992), for o-xylene (Banerjee et al. 1995), for dodecyl benzene sulfonate (Kulaots et al. 2004), and for methylene blue (Wang et al. 2005b).

There is also the question the contribution of the inorganic portion of the fly ashes to the contaminant sorption. Mott and Weber (1992) investigated the sorption properties of three bituminous fly ashes, which had a comparable source to the fly ashes tested in this work, and concluded that samples with no LOI did not show any adsorption capacity. However, raw fly ashes with LOI showed significant adsorption capacity for chlorinated solvents.

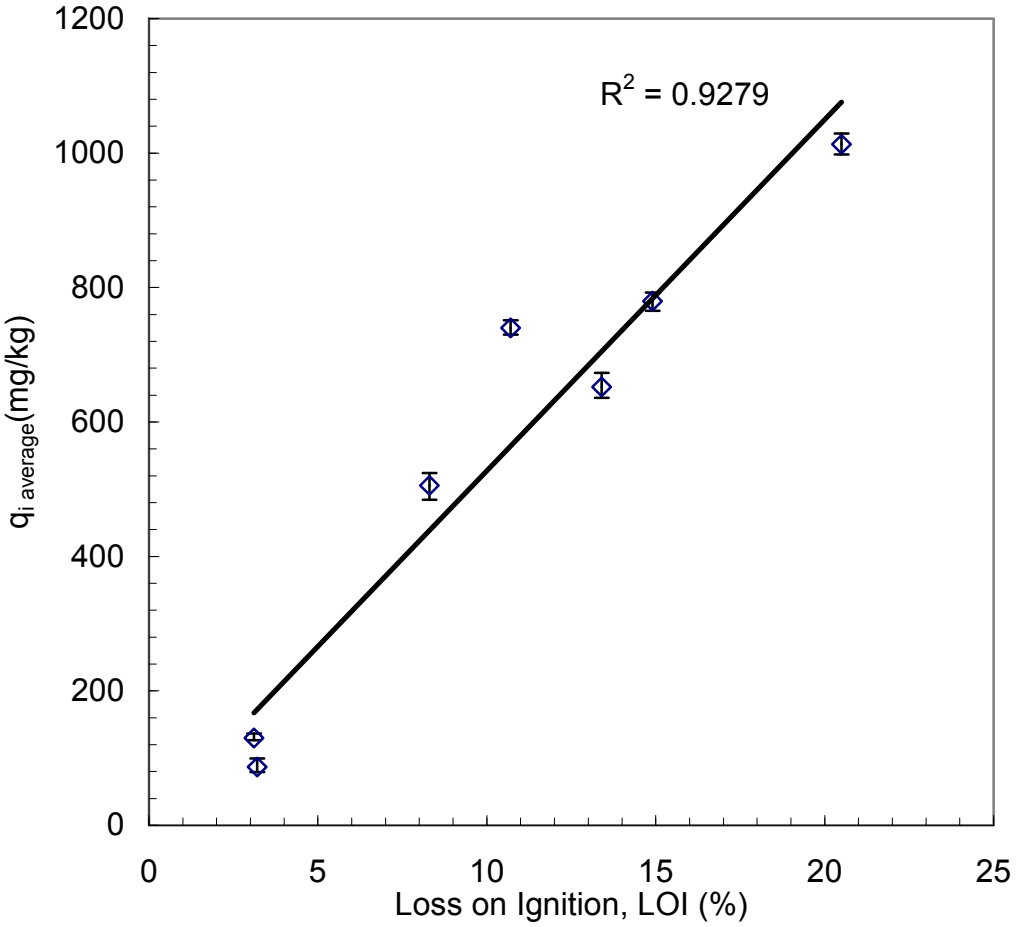

Figure 3.11 The relationship between average sorbed amount $q_{i\ average}$ (mg/kg) of naphthalene and percent LOI (%) of Maryland fly ashes

Thus, in this study we attributed the adsorption capacity to the unburned carbon constituents of the fly ashes and examined the contribution of each fraction of carbon content on the adsorption capacity of the compounds tested.

As discussed above, the fly ashes contain three different forms of carbon: inertinite, anisotropic carbon and isotropic carbon. It has previously been well documented in the literature that the pollutant sorption properties of coal combustion by-products are dependent on the anisotropic and isotropic carbons due to soft surface structure of these two carbon forms. Conversely, inertinite is known to have low sorption properties due to its glassy, hard surface structure (Morata-Valler et al. 1999, 2001). To study the effect of carbon type on naphthalene adsorption properties in the current study, $q_{i\ average}$ was plotted against the percentages of the different carbon forms by volume in Figure 3.12. The trends are clear; with $q_{i\ average}$ increasing on the total carbon content (by vol.) increases. As expected, the anisotropic and isotropic carbons are somewhat better correlated with sorption, as evidenced by the slightly higher coefficient of determination (R^2) (Figure 3.12b). This may suggest that soft surface nature of these carbons facilitated the adsorption of naphthalene. It should be noted that the statistical significance level of the correlation was more than 95% for the data plotted in Figure 3.12. Finally as expected, there was no correlation between $q_{i\ average}$ and the inertinite content (% vol.).

As illustrated in Figure 3.13, there was also a strong relationship between the specific surface area (SSA) for the naphthalene sorption tests. Specifically, fly ashes with higher surface area generally have higher sorption capacity. For example, DP fly ash (SSA=11.08 m^2/g) has an average sorbed amount of 1012.94 mg/kg whereas CP

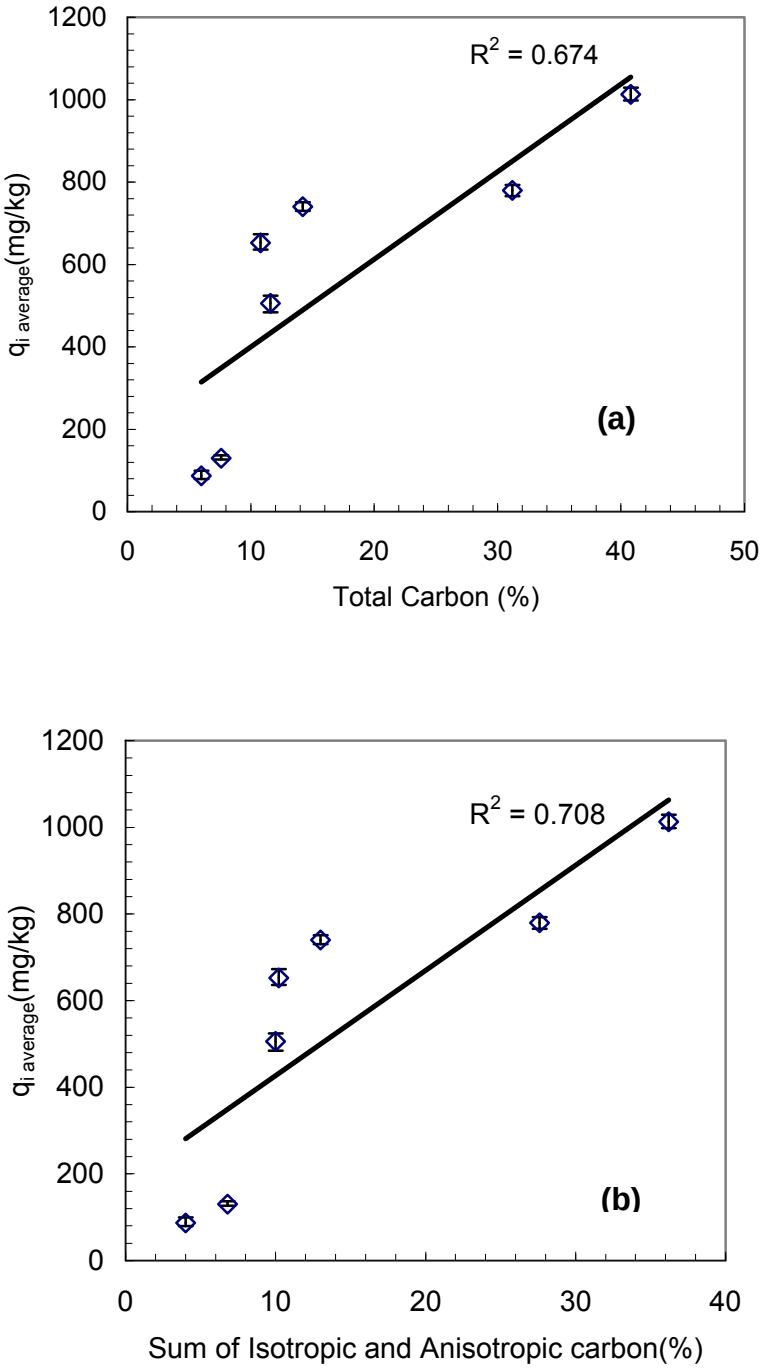

Figure 3.12 The relationship between averaged sorbed amount of naphthalene and a) total carbon [inertinite + isotropic + anisotropic carbon](by volume), and b) sum of isotropic and anisotropic carbon from petrographic analysis (by volume)

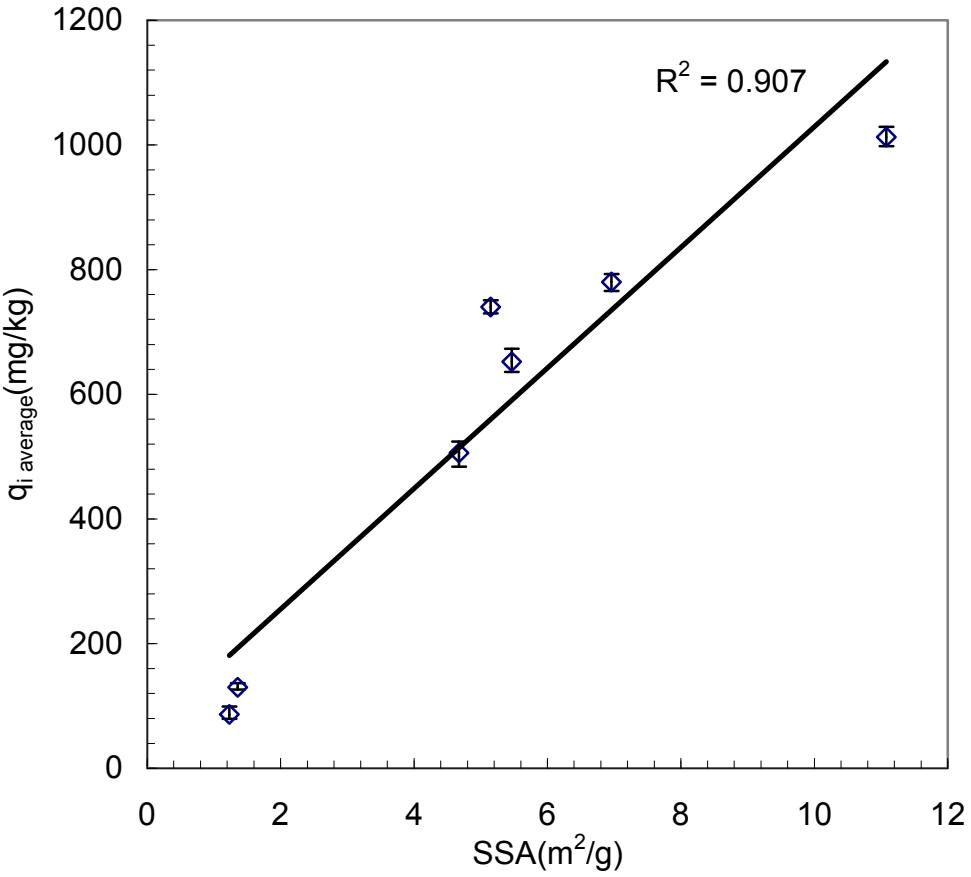

Figure 3 13 The correlation between average naphthalene sorbed amount $q_{i\ average}$ (with percent error) (mg/kg) and specific surface area (SSA m^2/g).

fly ash (SSA=1.23 m^2/g) has substantially low average sorbed amount of 86.64 mg/kg. This is not surprising, that it was shown above that $q_{i\ average}$ was highly correlated with LOI (%) (Figure 3.11) and that LOI was correlated with SSA (Figure 3.6). Wang et al. (2005b) also derived a correlation between SSA and the sorption capacity of fly ashes for hydrophobic dyes.

Finally the PDM isotherms are plotted for the seven fly ashes and PAC in Figure 3.14. The PDM isotherms for naphthalene sorption also indicate a trend among the sorbent. In particular, the PDM isotherms for the high LOI fly ashes (e.g., DP) lie above the ones with relatively low LOI values (e.g., CP) (Figure 3. 14a). PAC, with its superior adsorption capacity, lies well above the fly ashes (Figure 3.14b). This trend is examined further in Figure 3.15, which relates the maximum adsorption volume capacity at saturation (q'_{max}) to LOI. The capacity is generally well-correlated to the LOI. For instance, DP fly ash (LOI=20.5%) yielded a q'_{max} of 1562 L/kg, whereas the same maximum adsorption volume capacity was 482.48 L/kg for PR fly ash (LOI=8.3%). The q'_{max} data are also highly correlated with the total carbon content (R^2=0.836) and the percent of isotropic and anisotropic carbon (R2=0.840), as shown in Figure 3.16, indicating that these carbon forms are likely to play the major role on overall adsorption capacity. In addition, there is no correlation between q'_{max} and the percent inertinite, further confirming the importance of the isotropic and anisotropic carbon.

Figure 3.17 shows that q'_{max} is strongly correlated to the specific surface area of fly ashes. Kleineidam et al. (2002) have reported a similar increase in the q'_{max} with increasing SSA of two different sorbents, activated carbon and bituminous coal.

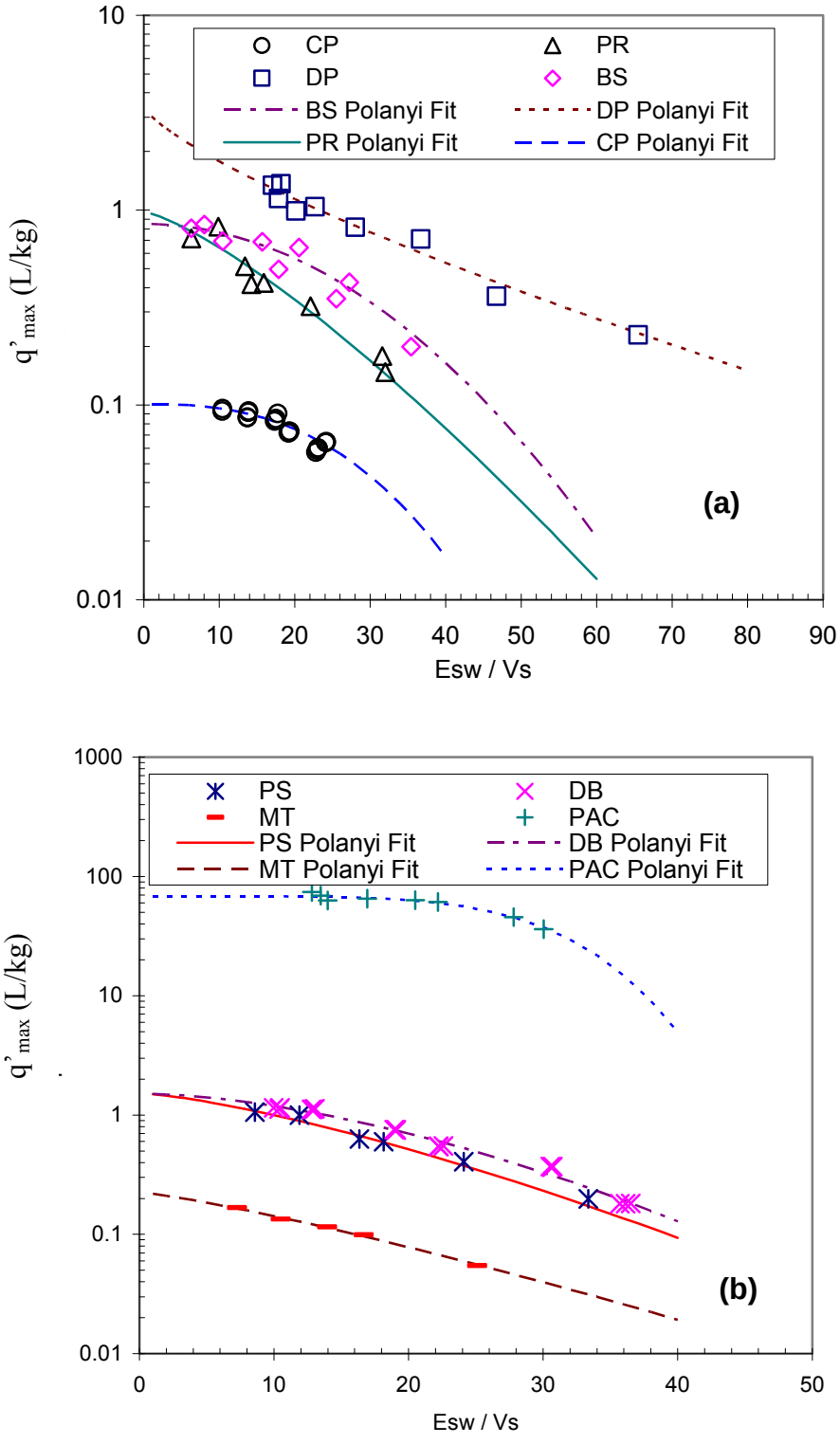

Figure 3 14 PDM isotherms for (a)CP, PR, BS, DP fly ashes, (b)PS, MT, DB fly ashes and PAC for naphthalene adsorption. . Symbols are from test data. Lines are isotherm from regression results

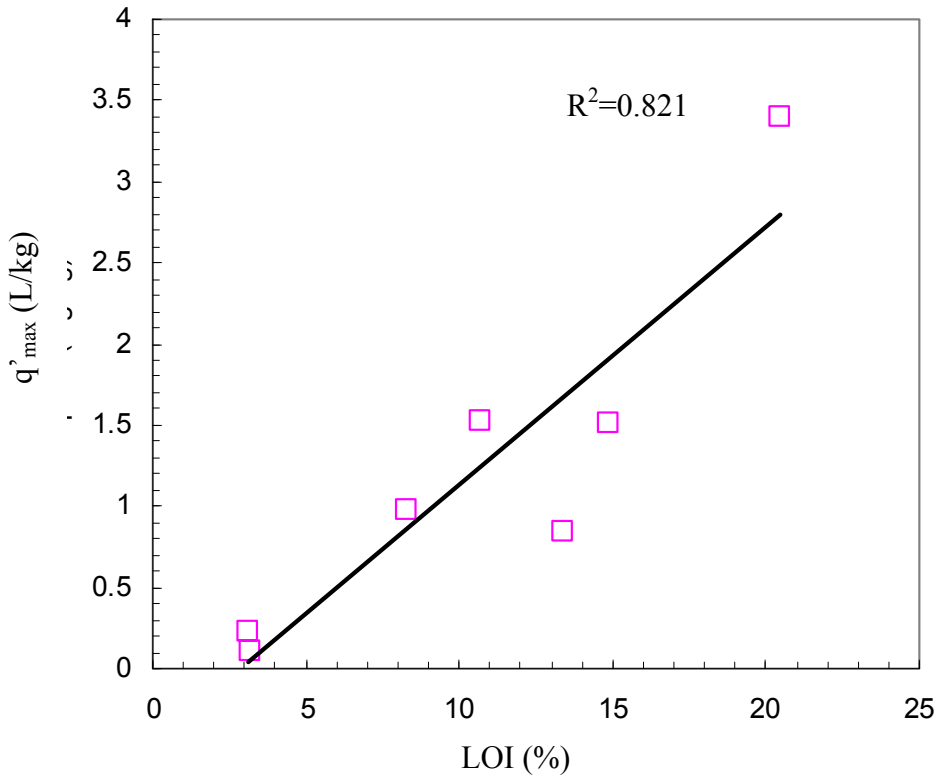

Figure 3 15 The correlation between LOI (%) and q'_{max}(L/kg) for all fly ashes.

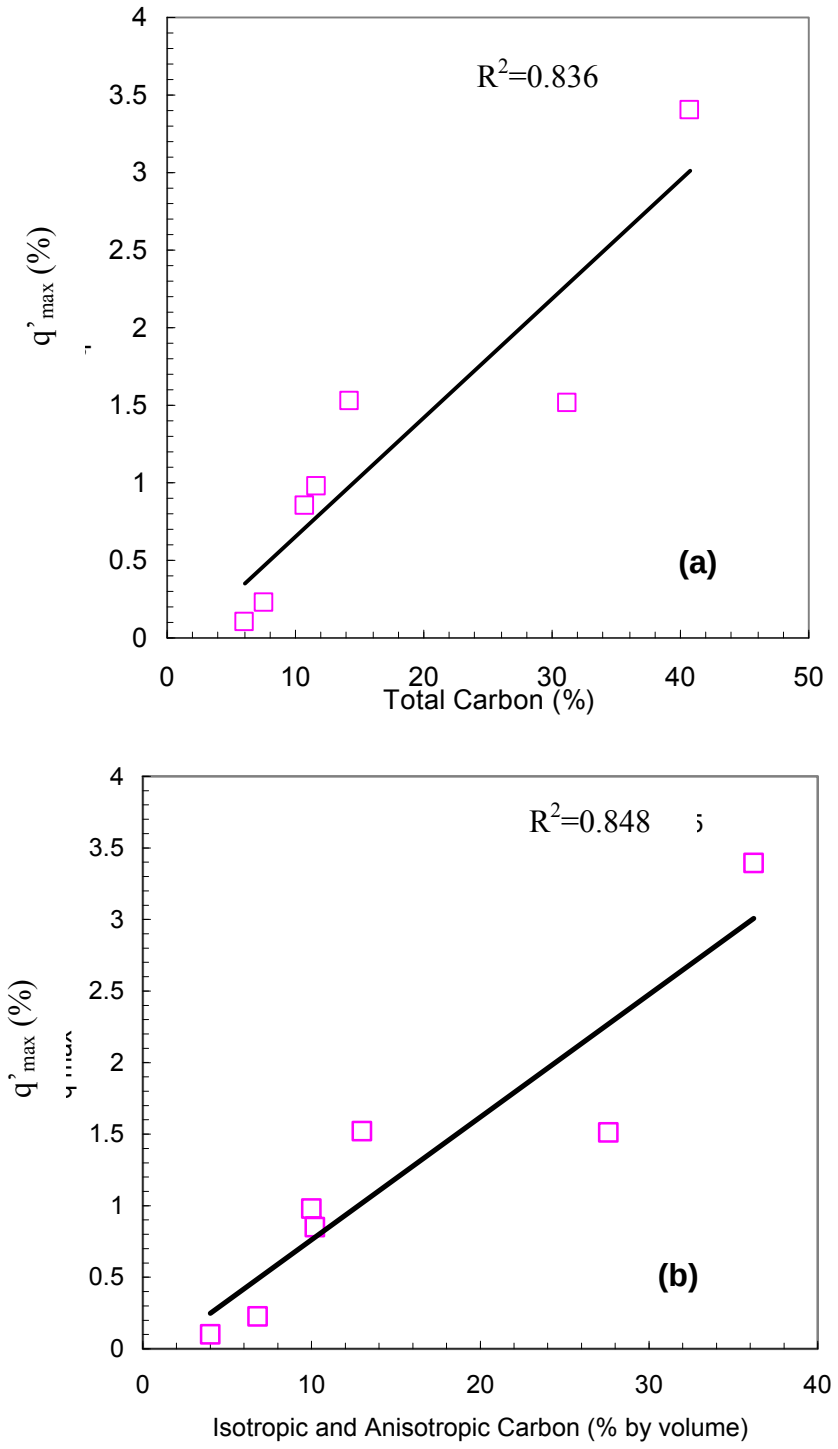

Figure 3 16 The relationship between maximum adsorption capacity (q'_{max}) of naphthalene and a) total carbon [inertinite + isotropic + anisotropic carbon](by volume), and b) sum of isotropic and anisotropic carbon from petrographic analysis (by volume)

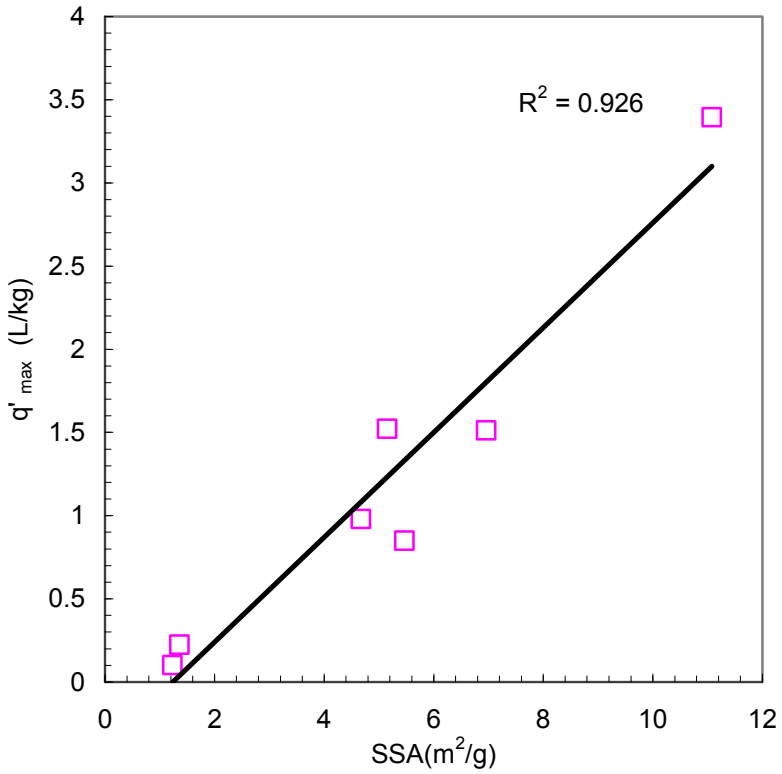

Figure 3 17 Naphthalene q'_{max} from PDM Isotherm versus specific surface area SSA (m^2/g) of the fly ashes tested

3.5.2 *O*-xylene Adsorption onto Maryland Fly Ashes and Activated Carbon

A battery of batch adsorption tests using *o*-xylene were as the adsorbate also conducted with the seven Maryland fly ashes and PAC. Nonlinear regression analyses of the data were performed by following the same procedures as described above for the naphthalene tests. The results from the regression analysis are summarized in Table 3.8. Based on the goodness of fit statistics, in the case of o-xylene, the BS and CP fly ash data were best fit by the Freundlich isotherm. Interestingly, unlike naphthalene adsorption where the Langmuir isotherm never rendered a best fit, the data for *o*-xylene adsorption onto the DB and PR fly ashes was fit by a Langmuir isotherm. For the remaining fly ashes, the CFL isotherm was determined as providing the best fit for the DP and PS fly ash data, and the PDM isotherm model was best fit for the CP fly ash data. Finally, the PAC adsorption results revealed that the CFL isotherm and the PDM isotherm have same goodness of fit parameters: the determination coefficient R^2 was 0.99, and relative standard error RSE was 0.105 for both isotherms.

The isotherms providing the best fit are plotted along with the experimental data from the *o*-xylene batch adsorption tests in Figure 3.18. Similar to the naphthalene adsorption data, the isotherms for the fly ashes with the high carbon content are located above the isotherms of the fly ashes with relatively low carbon content. This trend is further investigated further below by determining unburned carbon fractions and adsorption capacity.

Table 3 8 The isotherm parameters and goodness of fit statistics for the applied adsorption isotherm models from o-xylene adsorption tests.

		BS			**DP**			**DB**			**PR**		
Isotherm type	Isotherm parameters		R^2	RSE		R^2	RSE		R^2	RSE		R^2	RSE
Linear	K_d (L/kg)	32.99	0.17	0.911	N/A	N/A	N/A	N/A	N/A	N/A	N/A	N/A	N/A
Freundlich	K_f (mg/kg)(mg/L)$^{-n}$	289.7	0.98	0.172	803.4	0.89	0.344	525.7	0.75	0.507	379.4	0.65	0.599
	n (-)	0.387			0.260			0.224			0.209		
Langmuir	Q_{max} (g/kg)	1397	0.93	0.266	1983	0.92	0.283	1197	0.85	0.392	770.2	0.86	0.385
	K_L (L/kg)	0.128			0.396			0.518			0.642		
CFL	Q_m (mg/kg)	4401	0.97	0.178	2369	0.93	0.280	1241	0.80	0.449	720	0.85	0.394
	b (mg/kg)(mg/L)$^{-n}$	0.066			0.410			0.514			0.606		
	n (-)	0.474			0.659			0.880			1.426		
PDM	q'$_{max}$ (L/kg)	2.09	0.97	0.195	2.419	0.92	0.285	1.346	0.80	0.211	0.812	0.85	0.390
	c (mL/J)	0.039			0.002			8.1 10^{-5}			1.3 10^{-7}		
	d (-)	1.212			2.082			2.934			4.911		
Fritz-Schluender	α_1(mg/kg)/(mg/L)$^{\beta 1}$	1298	0.96	0.211	45.39	0.88	0.339	19.44	0.45	0.747	49.81	0.75	0.500
	α_2(mg/L)$^{\beta 2}$	4.101			0.029			0.027			0.088		
	α_1' (-)	0.377			0.036			0.004			0.091		
	β_1(-)	0.382			0.822			6.114			2.094		
	β_2(-)	-0.005			0.737			6.012			2.021		

Linear Isotherm: $q_i=K_d C_f$, Freundlich Isotherm: $q_i=K_f C_f^n$, Langmuir Isotherm: $q_i=(K_L Q_{max} C_f)/(1+ K_L C_f)$
CFL Isotherm: $q_i=(K_L Q_{max} C_f^n)/(1+ K_L C_f^n)$ PDM Isotherm: $q'_i= q'_{max} \exp [© (E_{sw}/V_s)^d]$
Fritz-Schluender Isotherm: $q_i=(\alpha_1 C_f \beta_1)/(\alpha_1' + \alpha_2 C_f \beta_2)$
N/A: Not available

Table 3.8. (continued)

		CP			MT			PS			PAC		
Isotherm type	Isotherm parameters		R^2	RSE		R^2	RSE		R^2	RSE		R^2	RSE
Linear	K_d (L/kg)	N/A	N/A	N/A	7.927	0.68	0.569	N/A	N/A	N/A	N/A	N/A	N/A
Freundlich	K_f (mg/kg)(mg/L)$^{-n}$	34.04	0.97	0.177	79.08	0.90	0.327	305.2	0.86	0.376	46940	0.98	0.142
	n (-)	0.381			0.388			0.3796			0.200		
Langmuir	Q_{max} (g/kg)	176.6	0.83	0.413	375.2	0.84	0.402	1019	0.95	0.240	71240	0.84	0.398
	K_L (L/kg)	0.090			0.195			0.2993			3.461		
CFL	Q_m (mg/kg)	81150	0.95	0.235	27030	0.86	0.377	861.7	0.96	0.207	127600	0.99	0.105
	b (mg/kg)(mg/L)$^{-n}$	4 10^{-4}			0.003			0.2497			0.604		
	n (-)	0.423			0.385			1.571			0.357		
PDM	q'$_{max}$ (L/kg)	0.570	0.98	0.181	0.927	0.87	0.413	0.9788	0.96	0.225	108.4	0.99	0.105
	c (mL/J)	0.452			0.213			4.6 10^{-7}			0.004		
	d (-)	0.532			0.735			4.689			1.675		
Fritz-Schluender	α_1(mg/kg)/(mg/L)$^{\beta 1}$	41.00	0.88	0.354	0.098	0.58	0.655	1.6 10^4	0.72	0.530	66.59	0.98	0.162
	α_2(mg/L)$^{\beta 2}$	1.296			0.002			53.95			0.0013		
	α_1' (-)	0.100			0.030			68.22			6 10^{-6}		
	β_1(-)	57.38			27.76			20.46			1.879		
	β_2(-)	37.00			27.36			20.07			1.692		

N/A: Not available

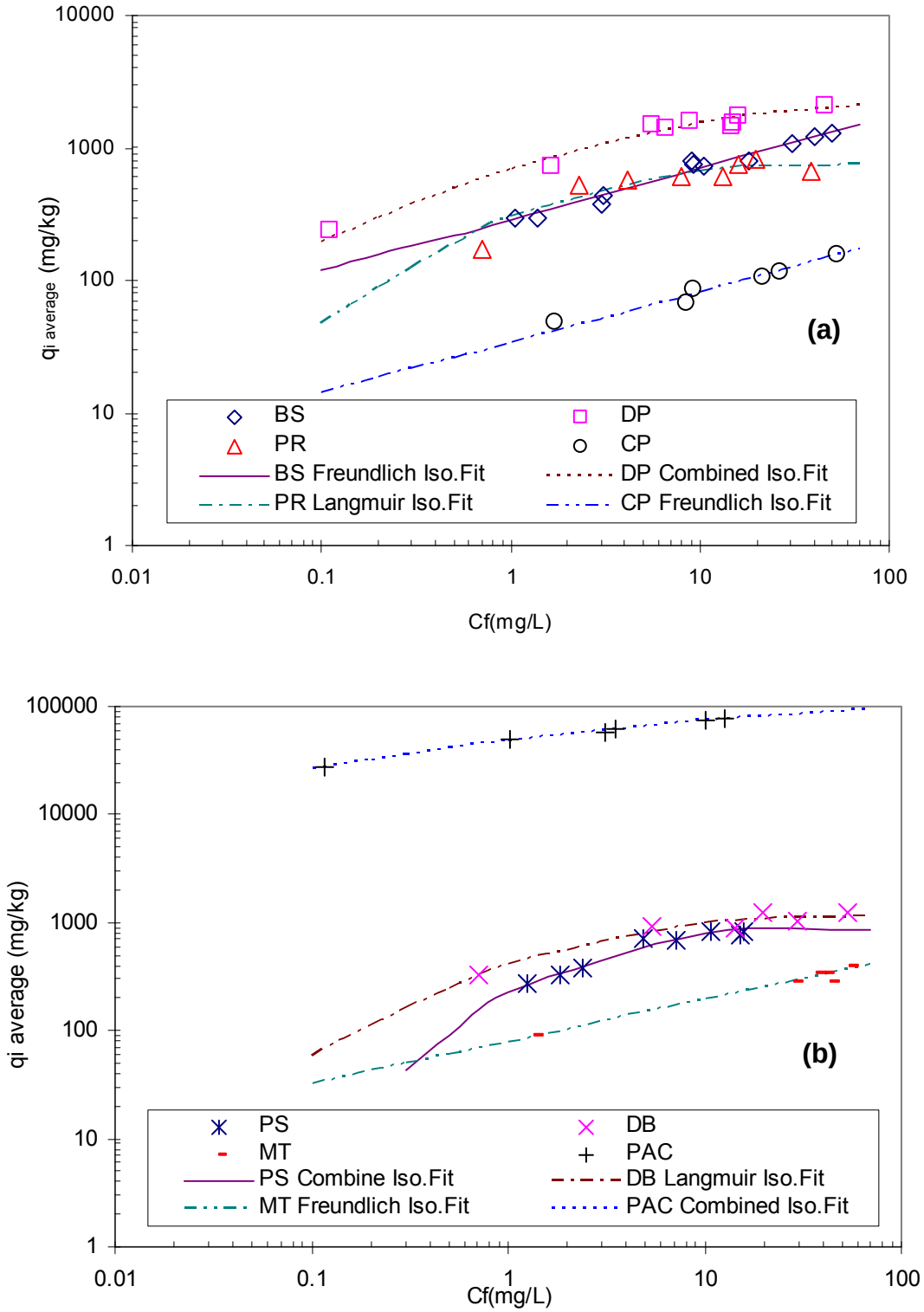

Figure 3 18 Adsorption isotherms with best fit models for the o-xylene adsorption experiments. Symbols are average of triplicate data. Lines are isotherm from regression results

Similar to the case for the naphthalene sorption, none of the fly ashes were best fit by a linear isotherm probably due to the strongly heterogeneous structure, for the *o*-xylene adsorption. Thermally altered materials, like fly ash, do not contain constituents that hydrophobic organic chemicals could easily partition into (AllenKing et al. 2002).

The Freundlich isotherm, which is provided the best fit for BS and MT fly ashes, is one of most commonly employed isotherms for nonlinear sorption modeling. The best fit values for the Freundlich coefficient (n) which can be taken as indication of how the affinity of the adsorbate changes sorbed concentration increases, were 0.387 and 0.388 for BS and MT, respectively. Being smaller than 1.0 these number indicated the highly nonlinear nature of the *o*-xylene adsorption, and the affinity of the fly ashes for the o-xylene decrease with increasing sorbed o-xylene concentration, as was observed for naphthalene. Similarly, Mott and Weber (1992) presented "n" values ranging from 0.267-0.498 for fly ashes with comparable LOI and SSA values during BTEX adsorption.

The *o*-xylene data for the PR and DB fly ashes, which have a relatively high LOI (8.3% and 14.9%, respectively) were best fit with a Langmuir isotherm. Similar observations were made by Bartelt-Hunt et al. (2005) when benzene and *o*-xylene were tested with organophilic clays. Organophilic clays are clayey soils modified with hydrophobic surfactants and, as a result, exhibit very high hydrophobic (sorptive) chemical structure. Even though the chemistry of sorption in organophilic clays and high LOI fly ashes are different, the trends in sorption are the same in both cases.

The CFL isotherm, with three degree of freedom, was determined as to provide the best fit for the DP and PS fly ash data, and yielded the same fit statistics as obtained with the PDM model for PAC. Interestingly, the fit statistics for the CFL isotherm was

similar to other models, indicating that the numerical difficulties added by introducing one more fit parameter were not justified. The PDM model, in addition to providing the best fit to the PAC data along with the CFL model, also provided the best fit to the CP fly ash data. The PDM model fits are describeb in more detail below.

Based on the goodness of the fit statistics, none of the *o*-xylene adsorption data sets were fit best by the Fritz Schulender isotherm. The naphthalene adsorption results also revealed the same trend. Considering the available data from the *o*-xylene and naphthalene tests, it can be inferred that an isotherm model with a higher degree of freedom will not necessarily perform better than models with a low degree of freedom contrary to expectation.

Consistent with the naphthalene data no matter what isotherm model provided the best fit to the data, when all of the o-xylene data are compared, the adsorbed amount increases with the carbon content of the fly ash. This is illustrated for the *o*-xylene data by the plot of the averaged sorbed amount ($q_{i\ average}$) against LOI (%) in Figure 3.19, which demonstrates the strong correlation between these values. Consistent with this trend, $q_{i\ average}$ is also highly correlated with the total carbon amount (by volume) (Figure 3.20a) and $q_{i\ average}$, and with the sum of isotropic and anisotropic carbon amounts (by volume) (Figure 3.20b). However, no correlation is observed with $q_{i\ average}$ and inertinite (% vol.). Similar trends were observed with

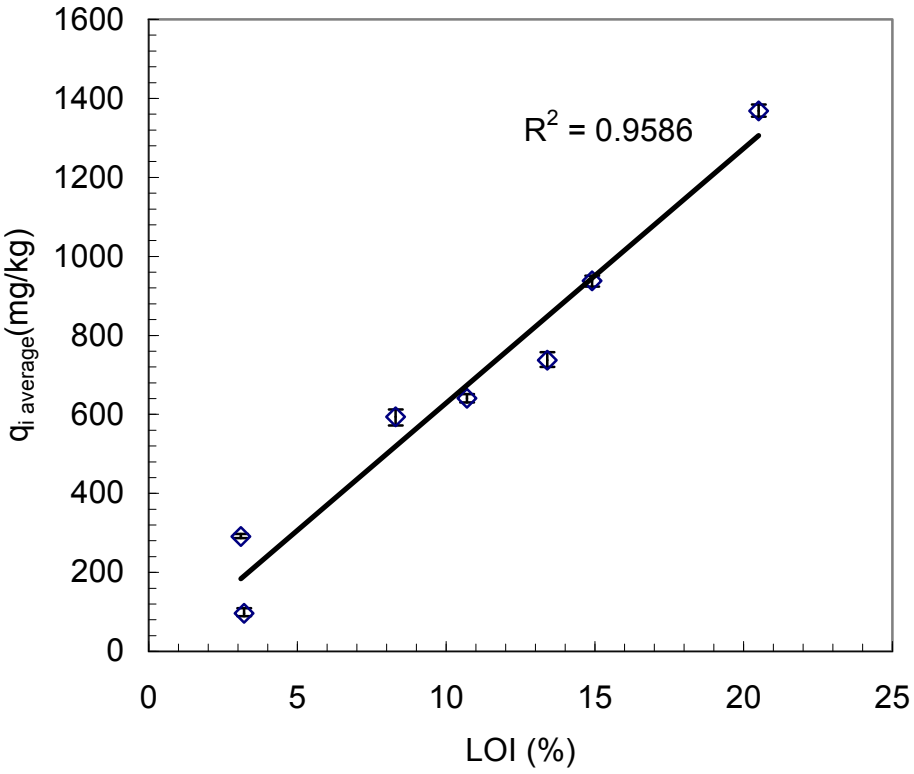

Figure 3 19 The correlation between the averaged sorbed amount versus loss on ignition from o-xylene adsorption experiments.

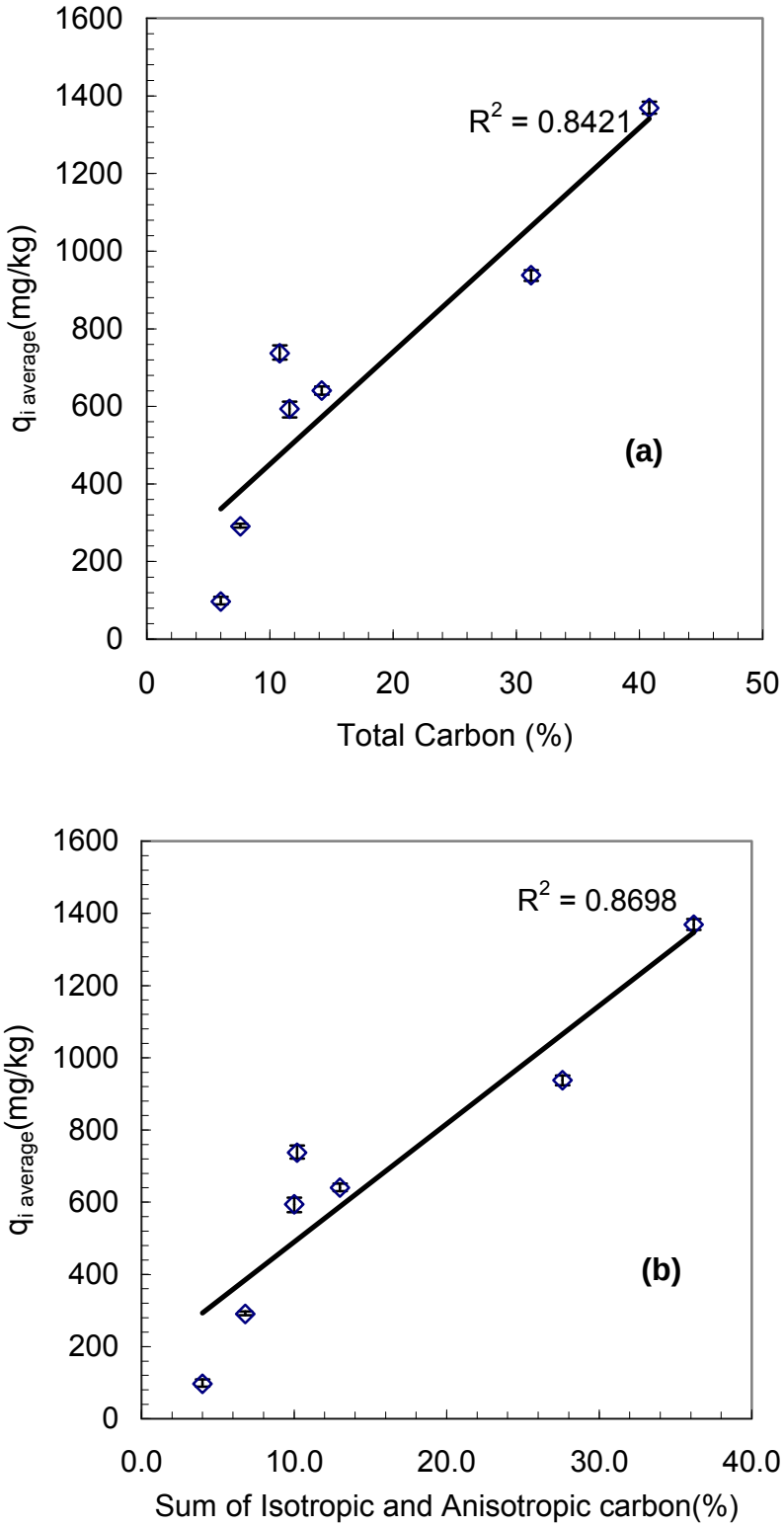

Figure 3 20 The relationship between averaged sorbed amount of o-xylene and a) total carbon [inertinite + isotropic + anisotropic carbon](by volume), and b) sum of isotropic and anisotropic carbon from petrographic analysis (by volume)

naphthalene adsorption, as discussed above. Additionally, as with naphthalene, the correlation of $q_{i\ average}$ with the sum of the isotropic and anisotropic carbon amounts yielded a slightly better R^2 value than the correlation with the total carbon amount. This is probably because the reactive carbon types like isotropic and anisotropic carbons are more available for adsorption than the carbon forms like inertinite.

As observed with naphthalene, there is a strong correlation between $q_{i\ average}$ and the specific surface area (SSA) (Figure 3.21). This is consistent with the observation discussed with the naphthalene data that LOI is correlated with surface area of the fly ashes. Thus, fly ashes with a high SSA may have a higher capacity for sorption of organic chemicals than ones have a low SSA. Same observation was made for naphthalene adsorption.

PDM isotherms for all the fly ashes and the PAC are shown in Figure 3.22. As discussed above for naphthalene adsorption, the PDM isotherms were evaluated in detail for a better understanding of *o*-xylene adsorption. The PDM isotherms for *o*-xylene uptake demonstrated similar trends as the naphthalene data when examined as a function of the sorbent characteristics. These of trends were evaluated by assessing the correlation between the maximum adsorption volume capacity (q'_{max}) from PDM isotherm parameters and the unburned carbon amounts and Figure 3.23 shows the correlation between q'_{max} (L/kg) and LOI (%). The determination coefficient (R^2) value of 0.746 indicates a good correlation between q'_{max} and LOI(%). Figures 3.24a and 3.24b depict the relationship between q'_{max} and the total carbon by volume and q'_{max} and the sum of the isotropic and anisotropic carbon, respectively.

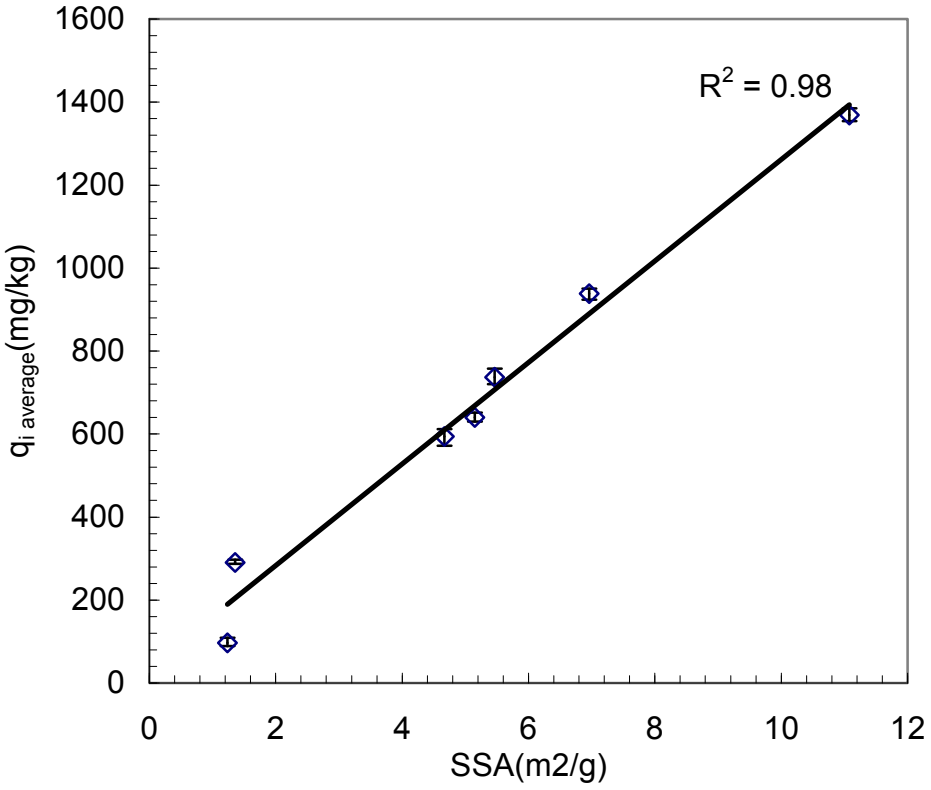

Figure 3 21 The correlation between the averaged sorbed amount versus specific surface area SSA (m^2/g) from o-xylene adsorption experiments.

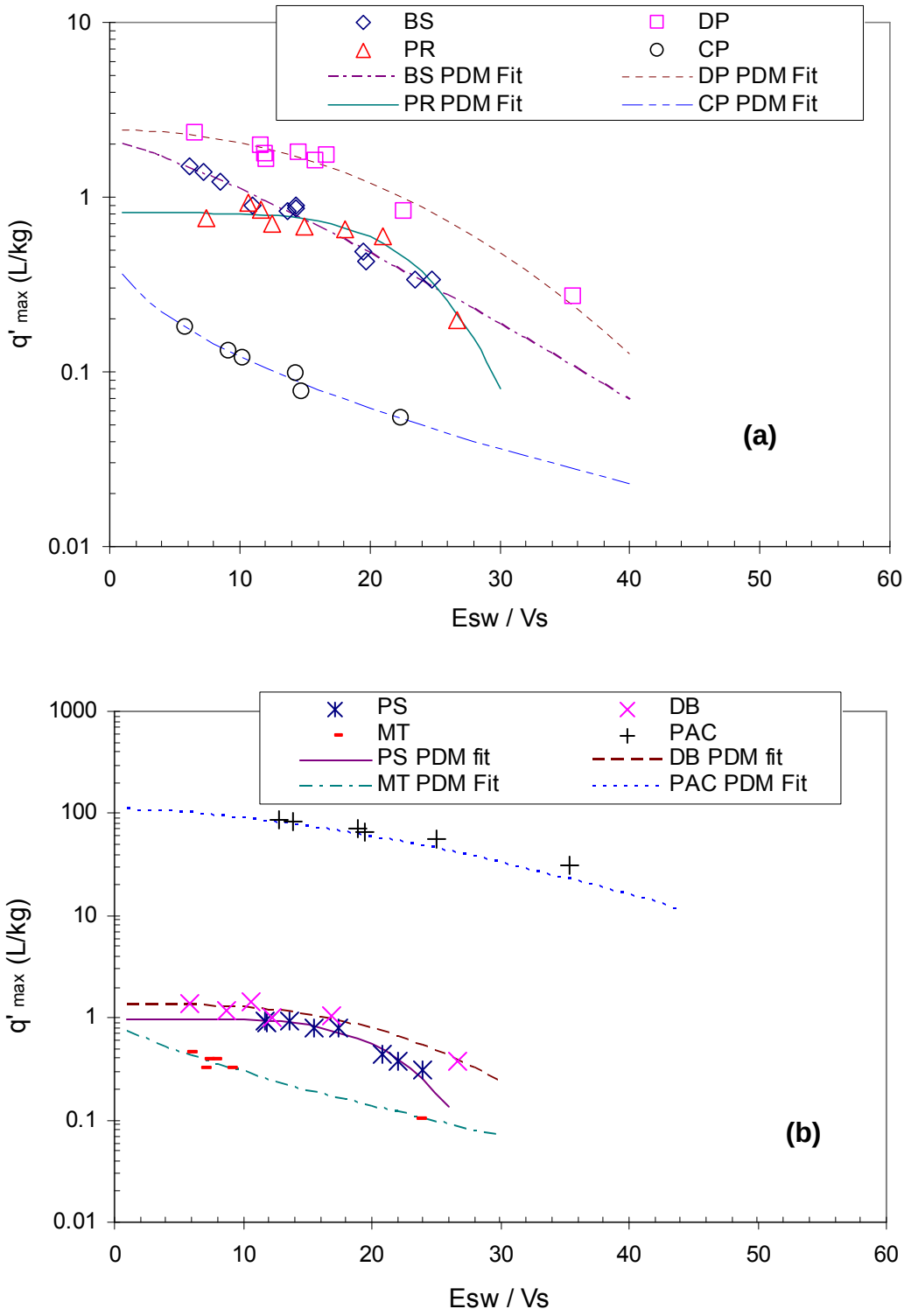

Figure 3 22 PDM isotherms for (a)CP, PR, BS, DP fly ashes, (b)PS, MT, DB fly ashes and PAC for o-xylene adsorption. . Symbols are from test data. Lines are isotherm from regression results

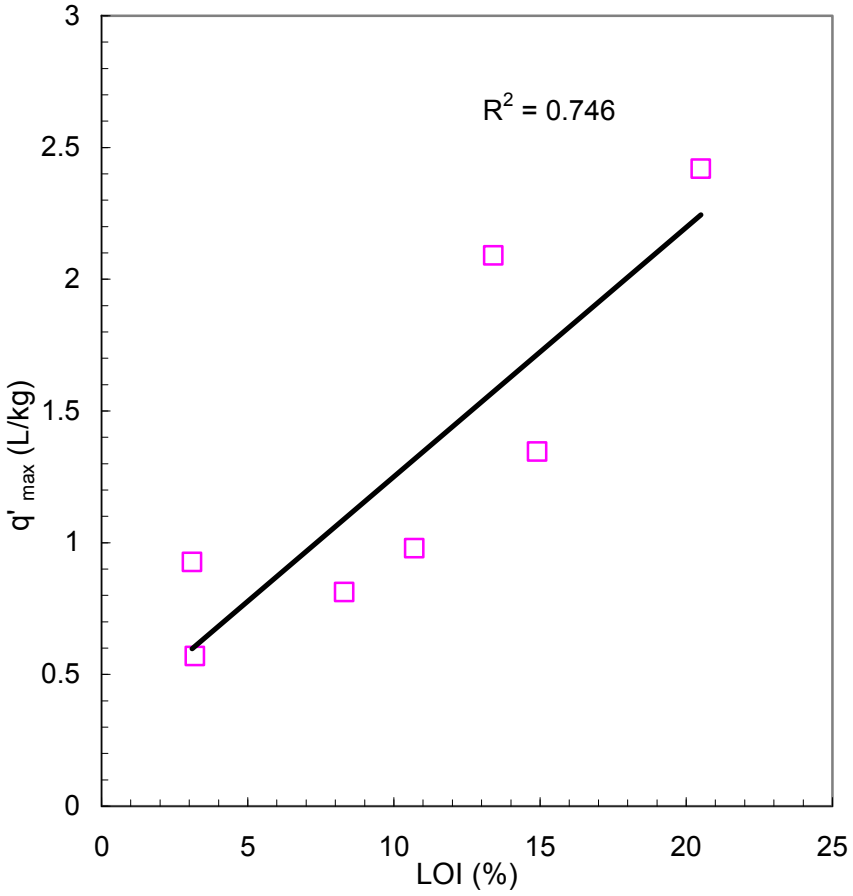

Figure 3 23 O-xylene q'$_{max}$ from Polanyi Isotherm versus loss on ignition LOI (%) of the fly ashes tested

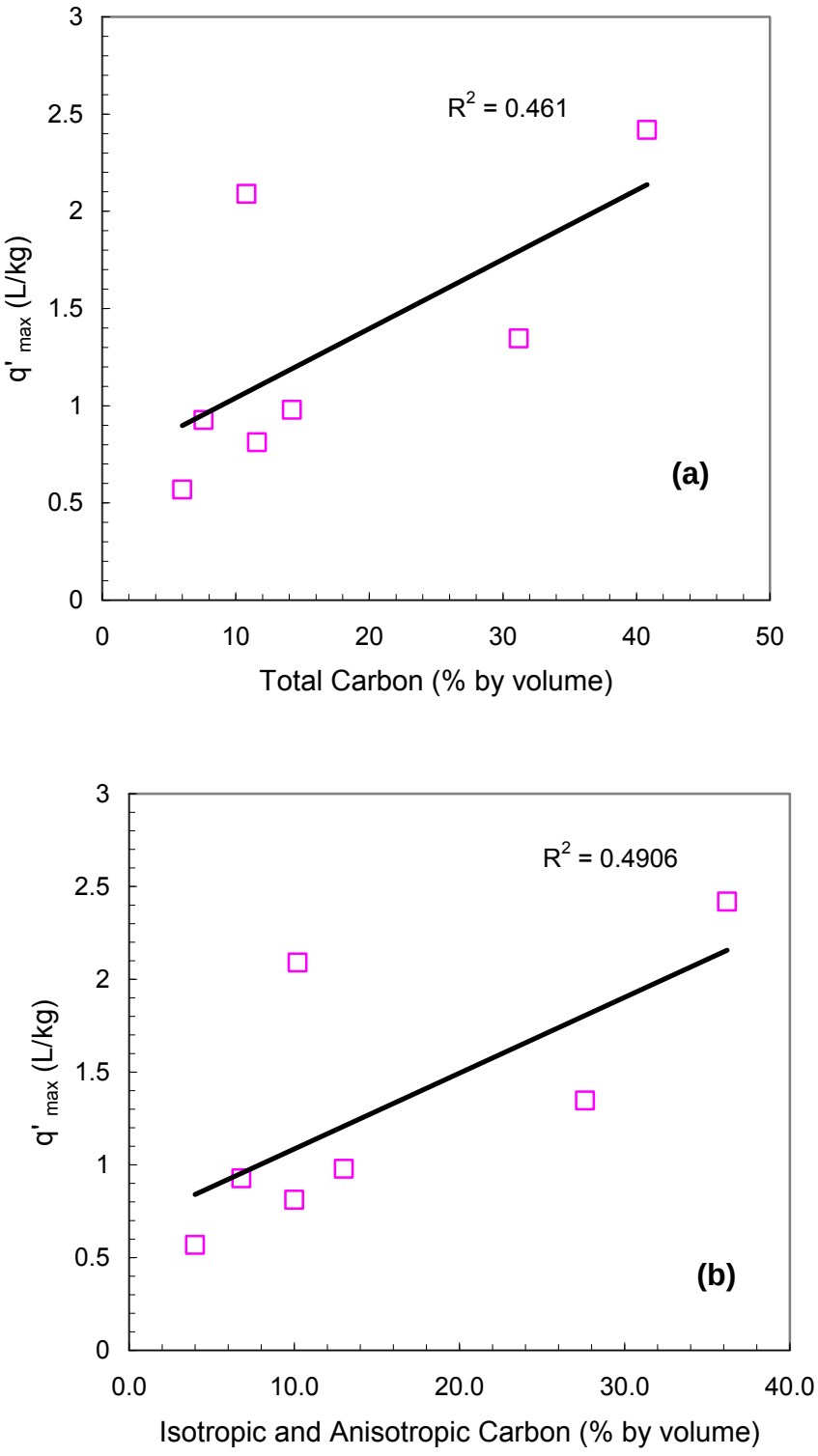

Figure 3 24 The relationship between maximum adsorption capacity (q'_{max}) of o-xylene and a) total carbon [inertinite + isotropic + anisotropic carbon](by volume), and b) sum of isotropic and anisotropic carbon from petrographic analysis (by volume)

Similar to the naphthalene results, *o*-xylene sorption capacity is well correlated with the sum of the isotropic and anisotropic carbon with a slightly better correlation in the latter case. Figure 3.25 shows the correlation between q_{max} and SSA, which yielded a correlation with a R^2 of 0.666.

3.5.3 Effect of Adsorbate on Adsorption to Maryland Fly ashes and PAC

By running batch adsorption tests with different organic compounds is possible to assess the sorption affinity of compounds that have different chemical properties. For example, the octanol water partition coefficient (K_{ow}) is often taken as a good indicator of the hydrophobicity of non-polar organic chemicals. Chiuo et al. (2000) has reported the effect of hydrophobicity on sorption of organic compounds onto geo-sorbents and indicated that compounds with a higher log K_{ow} have higher sorption affinity than compounds with a lower log K_{ow}. Based on these results and others, log K_{ow} widely used to quantify the sorption affinity for organic chemicals. On this basis, naphthalene with log K_{ow} of 3.29, is more hydrophobic than *o*-xylene which has log K_{ow} of 3.12 (Schwarzenbach et al. 1999). Another chemical property commonly used as a measure of hydrophobicity and sorption affinity is water solubility. Here it is also important note that the water solubility of *o*-xylene (Cs=178 mg/L) is substantially higher than naphthalene (Cs=31 mg/L), again indicating a greater hydrophobicity of naphthalene. Accordingly, it is expected that naphthalene should have slightly higher sorption affinity for the fly ash than *o*-xylene.

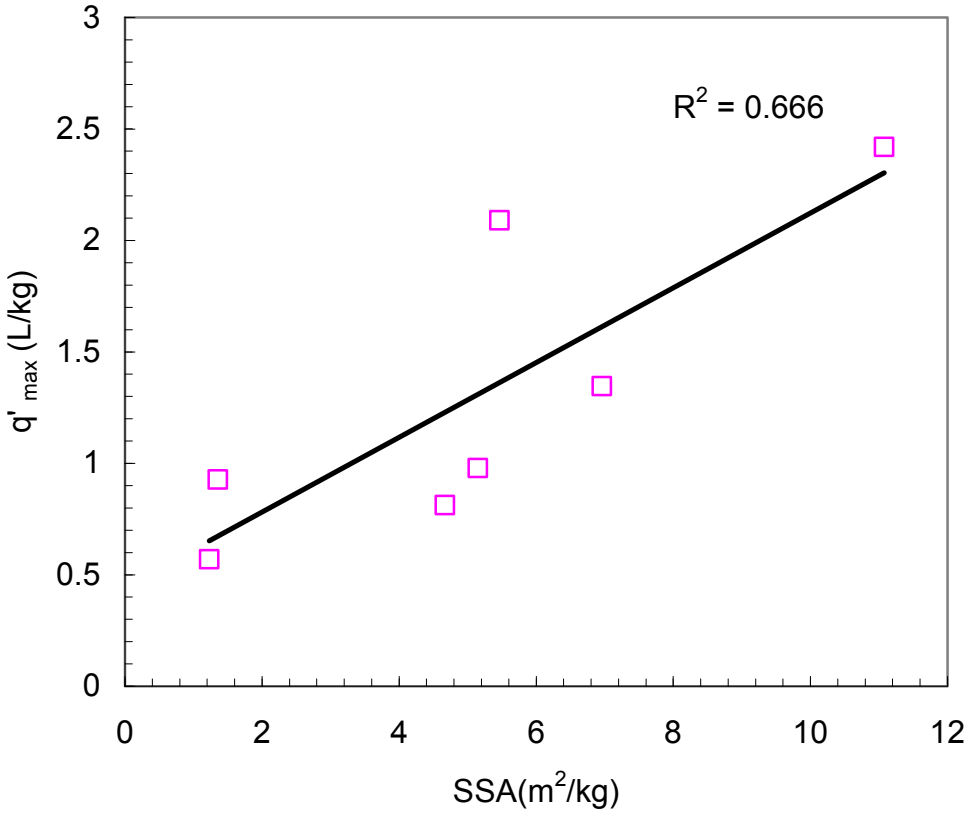

Figure 3 25 O-xylene q'_{max} from Polanyi Isotherm versus specific surface area SSA (m^2/g) of the fly ashes tested

The influence of the hydrophobic nature of the non-polar organic chemicals was determined using the naphthalene and *o*-xylene data for the seven fly ashes and PAC sorption. Figure 3.22 shows the adsorption isotherms for selected fly ashes and PAC for naphthalene and *o*-xylene. The data in Figure 3.26 suggests that for relatively low concentrations, naphthalene was sorbed more than *o*-xylene molecule as expected. For example DP fly ash sorbed 240 mg/kg of *o*-xylene at 0.11 mg/L, however at 0.13 mg/L final concentration naphthalene was sorbed at the amount of 929.68 mg/kg.

Another factor that needs to be considered when adsorption of two non polar compounds having different molecular sizes is the level of comparing the adsorption nonlinearity. Malek and Farooq (1996) explicitly studied the effect of molecular size on the adsorption nonlinearity by comparing the Freundlich isotherm exponents "n" from separate adsorption tests using various organic compounds. They reported that for given sorbate compounds with larger molecular weights had best fit Freundlich isotherm exponents "n" that were smaller than also 1.0 and smaller relative to "n" values obtained for from compounds with smaller molecular weights. In this study, naphthalene has larger molecular weight (MW=128.6 g/mol) than *o*-xylene (MW=106.17 g/mol). In order to examine the effect of molecular size on the level of nonlinearity for the fly ashes, the Freundlich isotherm exponents were compared for naphthalene and *o*-xylene adsorption.

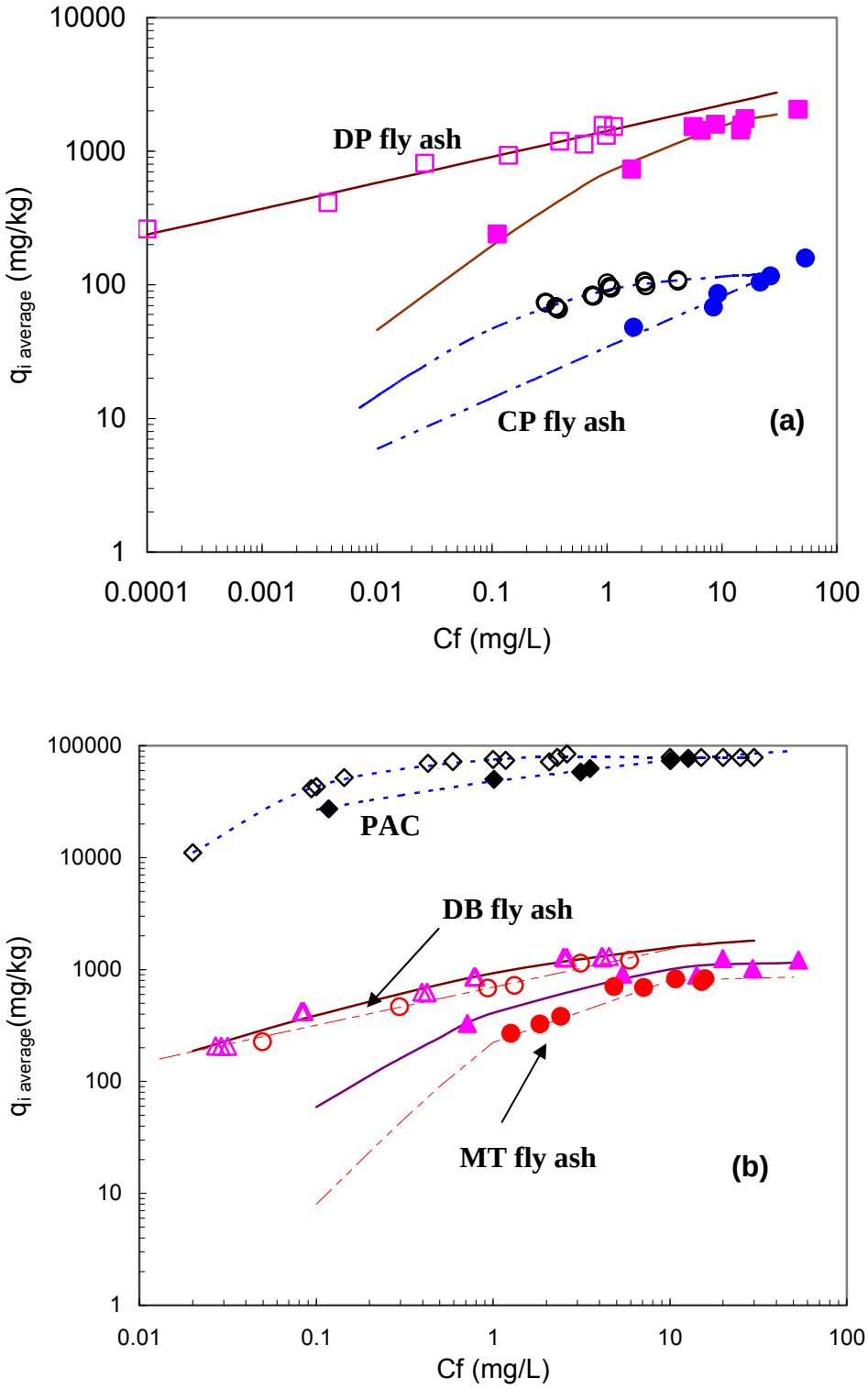

Figure 3 26 Adsorption isotherms for comparison of sorption nonlinearity. Solid symbols are for o-xylene. Open symbols are for naphthalene.

In general, the results of this research were consistant with the conclusions of Malek and Farooq (1996), with all n values for naphthalene, and 5 out of 7 values less than the corresponding n value for *o*-xylene. For example, for the BS fly ash, the naphthalene data yielded an "n" value of 0.195 which is smaller than 1, and smaller relative to the "n" value of 0.387 obtained for *o*-xylene adsorption. Similarly, MT fly ash with relatively low unburned carbon (LOI=3.1 %) has yielded "n" value of 0.306 for the naphthalene and 0.388 for *o*-xylene adsorption. However, for DB and PR, the "n" value for the naphthalene was greater than the value to *o*-xylene.

3.5.4 Discussion on PDM Isotherm

PDM model explicitly accounts for the role of molar volume in determining the adsorption capacity, while also accounting for the effect of temperature and solubility and chemical size through the definition of the adsorption potential by normalization using those properties (Nguyen et al. 2007). Here it is important to note that when using sorbates that are solid at the test temperature, the subcooled liquid solubility could be used inplace of with the water solubility. However, previous studies have indicated that the PDM parameters calculated using sub-cooled liquid solubility are only "slightly better" than the PDM isotherm parameters taken from the results calculated using the water solubililty (Kleineidam et al 2002). Allen King et al. (2002) also discussed the usage of water solubility instead of subcooled liquid solubility for solid compounds. They reported non-detectable differences in the results, within the precision of the experiment for sorbents tested. There were also similar efforts to detect the influence of the

crystalline phase adsorption by accounting for the sub-cooled liquid solubility by Xia and Pignatello (2001), who observed insufficient precision to confirm or refuse the expected effect when sub-cooled liquid solubility was used. Most recently, Nguyen et al. (2007) suggested a change of 10% to 50% between the PDM parameters when sub-cooled liquid solubilities of the solid compounds were replaced with water solubility. In their study, naphthalene was in the lower end of their spectrum (10% change), therefore for practical purposes in this study, the water solubility of naphthalene was used during PDM isotherm parameter analysis.

One of the practical advantages of using PDM model is the ability to derive the isotherm by normalizing the aqueous concentration to the water solubilities and molecular sizes of the organic compounds. This provides a unified sorption isotherm for a group of similar organic compounds and a specific sorbent material (e.g., activated carbon, fly ash). By using such a normalized PDM isotherm (usually referred to as a correlation curve when used for multiple sorbates), the sorption capacity of one sorbent for a group of chemical can be determined. This approach has been successfully employed by many researchers for numerous organic compounds and wide variety of sorbent types (Manes 1998, Xia and Ball 1999, Kleineidam et al. 2002, Allen King et al. 2002, Nguyen et al. 2007).

In order to follow a similar approach, the batch adsorption test data of naphthalene and *o*-xylene were combined (unified) for all the fly ashes and the PAC. The correlation curves were then plotted using the combined data (Figure 3.27). The PDM model parameters for the combined adsorption data were calculated using the

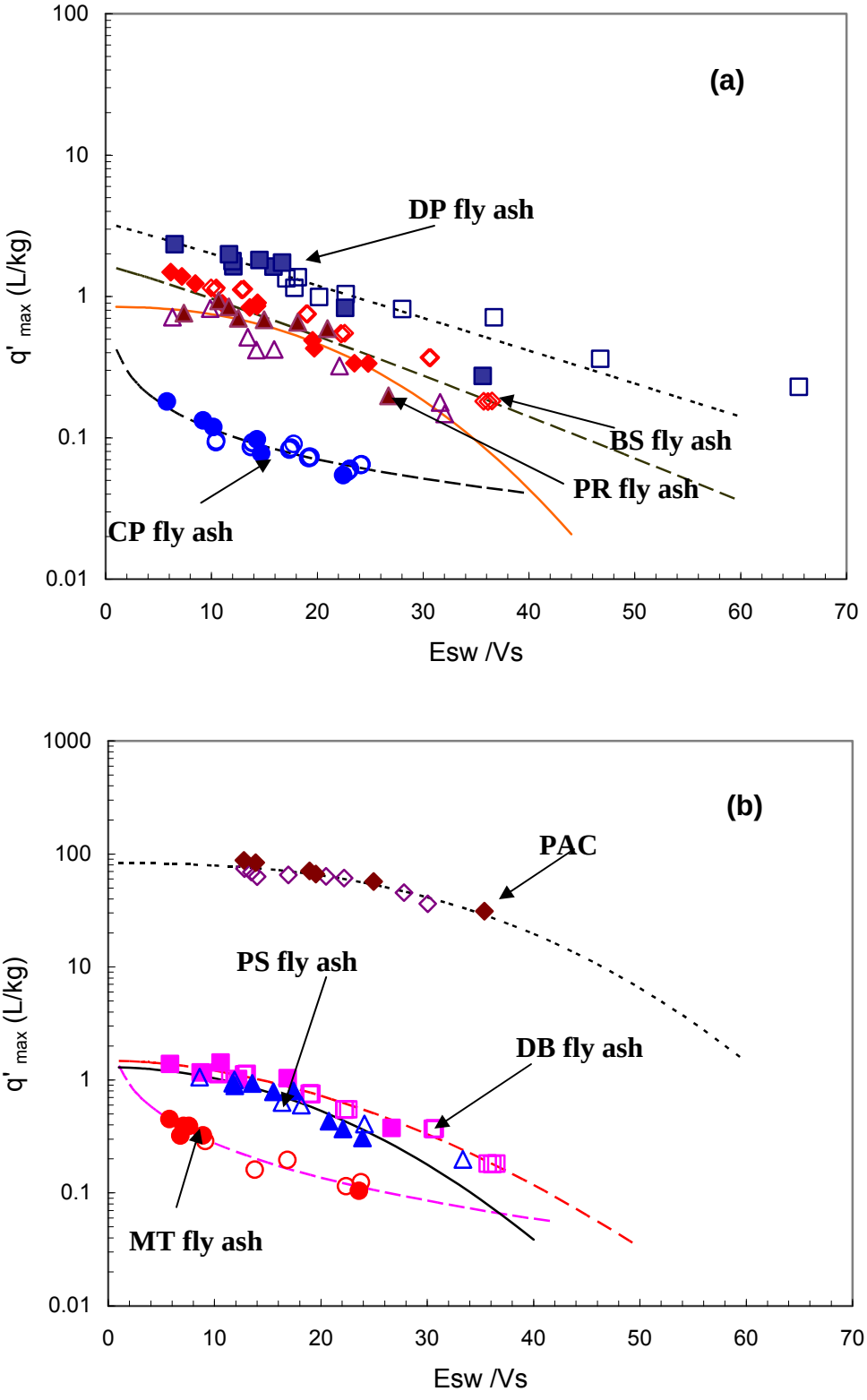

Figure 3 27 Correlation curves from PDM isotherm using naphthalene and o-xylene data. Open symbols are from naphthalene tests Solid symbols are from o-xylene

same nonlinear regression technique as was described earlier. The results of the regression analyses are given in Table 3.9. Clearly, the combined data can be described well by a single best-fit regression for each sorbent.

The exponent "d" in PDM isotherm model has been used as an indicator of the dependence of the adsorbate distribution on the adsorption energy with values usually reported between 1 and 5 (Allen King et al. 2002). For example, widely used Dubinin-Raduskevich equation assumes "d" equals 2 by relating it to the complete Van der-waals interaction between the non-polar organic compound and a particular sorbate (Mauraya and Mittal 2006). Similarly, Xia and Ball (1999) has obtained d values between 1.4 and 2.7 when correlation curves were fitted to nine individual sorbates.

Examining the "d" values obtained in this work from the PDM isotherms (correlation curves) using the combined naphthalene and *o*-xylene sorption data, it appears that they are in good agreement with the recently cited values from literature. All of the d values range between 1.031 and 2.547 with the exception of the MT and CP fly ashes. The "d" values for these two fly ashes, which are 0.1594 and 0.2633 for the CP and MT fly ashes, respectively, are substantially lower compared to ones from other fly ashes results. The reasons behind these low values are not clear. However, the relatively low unburned carbon contents of these fly ashes (LOI_{CP} = 3.2 % and LOI_{MT} = 3.1 %) may cause these low distributions of the adsorption energies along the adsorption surfaces.

Table 3 9 PDM model parameters from nonlinear regression analysis using combined naphthalene and o-xylene batch adsorption data

Sorbent	q'_{max} (L/kg)	*c* (mL/J)	*d* (-)	R^2	RSE
DP	3.311	0.0464	1.031	0.92	0.192
BS	1.657	0.0434	1.095	0.75	0.506
PR	0.845	$5.7\ 10^{-4}$	2.319	0.72	0.558
CP	7.867	2.925	0.1594	0.90	0.323
DB	1.481	0.0031	1.824	0.96	0.213
PS	1.291	0.023	1.987	0.93	0.268
MT	8.957	1.9	0.2633	0.93	0.277
PAC	82.6	$1.2\ 10^{-4}$	2.547	0.84	0.412

Based on this analysis, we can suggest that the PDM isotherm could potentially be used to simulate adsorption of multiple organic compounds onto one particular sorbent. In turn, the PDM isotherm can be used to estimate the same volumetric adsorption capacity (q'_{max}) for all compounds having similar abscissa values on PDM isotherm (Allen King et al. 2002). Additionally, PDM isotherms at a single temperature can be employed to predict adsorption volume capacity at other temperatures.

Like all isotherm models, the PDM isotherm is strictly constrained by the concentration range for which it was determined. However, environmental engineers and scientists can model the concentration-dependent sorption of similar chemical compounds by determining the PDM isotherm for a single compound. By this approach, substantial simplicity can be provided in sorption capacity assessments. Similar recommendations were also provided by Critenden et al. (2000), and Allen King et al. (2002).

3.6 Conclusions

Based on the results of the analysis on seven Maryland fly ashes with high carbon content, it was determined that the loss on ignition (LOI) of the Maryland high carbon content Class F fly ashes varied between 3.1% and 20.5% and contained three distinct carbon forms, namely anisotropic, isotropic and inertinite. Batch adsorption tests indicated that the naphthalene and *o*-xylene adsorption capacity of these fly ashes was strongly correlated with LOI and total amount of carbons forms by volume. Correlation with more reactive carbon forms (i.e. anisotropic and isotropic) resulted in higher R^2 values.

A solid-to-solution ratio of 1/120 was determined as optimum value for batch tests. Batch kinetic tests revealed the quick adsorption process and 24 hours of equilibrium was maintained during the course of batch tests. The results of the series of batch adsorption tests on seven fly ashes with naphthalene and *o*-xylene revealed that the chemical and physical of structure of the fly ash promoted adsorption and yielded nonlinear sorption isotherms that are characterized by high sorption capacity at low concentrations. This nonlinear sorption trend was supported by the Freundlich isotherm coefficient "n" values that are ranging between 0.194 and 0.339 for naphthalene sorption and between 0.381 and 0.387 for o-xylene sorption. Furthermore, fly ashes with higher surface area generally exhibited high sorption capacities. Batch adsorption test data revealed that naphthalene was sorbed more than o-xylene when same fly ash data was compared, and this was explained by the relatively high hydrophobicity of naphthalene.

The goodness of fit for six different isotherm models to batch adsorption data was assessed using coefficient of determination and RMSE as the fit criteria. Isotherm models with five fitting parameters did not show superiority over other models with lower fit parameters. Among the adsorption isotherm models used to evaluate adsorption test data. Polanyi-Dubinin-Manes (PDM) model posed great potential for explaining the petroleum contaminant adsorption on to fly ash. Pore filling mechanism, explained by PDM isotherm, was believed to be the dominant mechanism for adsorption of non-polar organic chemical onto highly heterogonous sorbents like fly ash. One of the practical advantages of the PDM model is the normalization of the aqueous concentrations to water solubilities of the organic compounds. This provides unified sorption isotherm for a group of similar organic compounds for specific sorbent material (i.e, activated carbon,

fly ash). By use of PDM isotherm (usually referred to as correlation curve when used for multiple sorbates), sorption capacity of a particular sorbent can be determined for a group of chemicals.

Chapter 4 Stabilization of Petroleum Contaminated Soils Using High Carbon Content Fly Ash

Reclamation of soils contaminated by petroleum spills has been a challenge for state agencies during the last two decades. In the late 1980s and early 1990s, cleanup philosophies emphasized excavation of large volumes of petroleum-contaminated soils (PCSs) from sites, frequently attempting to achieve total removal and landfilling of those materials. Regulatory agencies departed from this philosophy in the mid-1990s. As a result, some ex-situ treatment methods such as landspreading, thermal treatment and bioremediation, as well as in situ methods like bioventing and soil vapor excavation have been applied in recent years (Kamnikar 2001). Remediation of contaminated waste materials and their beneficial reuse as part of landfill caps and highway embankments have also been encouraged by the United States Environmental Protection Agency (U.S.EPA) (Meegoda 1999). One alternative remediation method is to stabilize these soils by adding a binder to adsorb the pollutant(s) while maintaining its good engineering properties. Materials stabilized in such a manner could be reused in highway construction, and the most common application being their use as a borrow fill material.

Traditionally, borrow materials have been derived from natural materials (soil). As a result, testing and approval processes are geared to evaluate natural materials. Historically, the natural material approval process has not required an environmental review. Many producers of recycled soil-based materials use a reclamation process to stabilize the contaminants. After the reclamation process, the soil may still contain the original contaminant(s), which might, in turn, affect the engineering properties of the

material. Therefore, normal testing procedures may be inappropriate for approval and construction quality assurance. Currently there are no definitive criteria for determining the suitability of these products for use in a transportation project, although there is a generic acceptance process for recycled materials being developed by a national center, the Recycled Materials Resource Center. To make progress in this area, additional information concerning the geotechnical and environmental properties of recycled or reclaimed soil is needed (Ezeldin et al. 1992, Meegoda and Ratnaweera 1995). In order to respond to this need, a study was undertaken to evaluate stabilization of petroleum contaminated soils by using high carbon content fly ash (HCCFA). This section explains preparation and testing of PCSs in the laboratory, and presents and discusses the results of a series of geotechnical (i.e., compaction) and environmental tests (column leaching tests) conducted on PCSs stabilized with HCCFA.

4.1 Materials

4.1.1 Borrow Material

The reference soil employed in the compaction and leaching tests was a borrow material commonly used in embankment construction in Maryland. The borrow material was classified as clayey sand (SC) according to the Unified Soil Classification System (USCS) and A-2-4 according to the American Association of State Highway and Transportation Officials (AASHTO) Classification System. Grain size analyses indicated that the soil had approximately 34% particles passing through the U.S. No. 200 sieve, and 10% particles that were smaller than 2 μm in diameter. Based on an analysis performed using a SHIMADZU 500 carbon analyzer, the borrow material had a total organic content

(TOC) of about 0.5% by weight. The cation exchange capacity (CEC) and pH of the material were 2.9 meq/100g and 7.2, respectively, as determined by Agri Analysis, Inc. located in Leola, Pennsylvania. PCSs were prepared by mixing borrow material with contaminants in a laboratory setting. The water-density relationship of the borrow material was determined by running standard Proctor compaction tests following the procedures outlined in ASTM D 698 (Figure 4.1). The tests indicated that the maximum dry density and optimum water content were 20.1 kN/m^3 and 10%, respectively.

4.1.2 Fly ash

The fly ash used in the current study was obtained from the Brandon Shores (BS) Power Plant located in Baltimore, Maryland. It was produced as a result of burning pulverized bituminous coal and classified as Class F fly ash according to ASTM C 610. According to the grain size distribution, it has 92 % fines passing through #200 sieve. Detailed physical and chemical properties of BS fly ash are in given in section 3.1.1.

4.1.3 Contaminants

Diesel fuel was chosen as the contaminant for the compaction tests, because it is one of the most commonly encountered pollutants in sites contaminated with petroleum residues. The diesel fuel was purchased from a local gas station and added to the borrow material at 1% to 2% by weight. These percentages were selected because soils exhibiting higher concentrations, e.g., greater than 3% by weight, are accepted as hazardous waste and are generally disposed in hazardous waste landfills (Kamnikar 2001).The chemical composition of diesel fuel can be variable and is highly dependent on the source of the crude oil and the degree of chemical modification. A chemical analysis was not conducted on the diesel fuel employed in the testing program; however, in general diesel

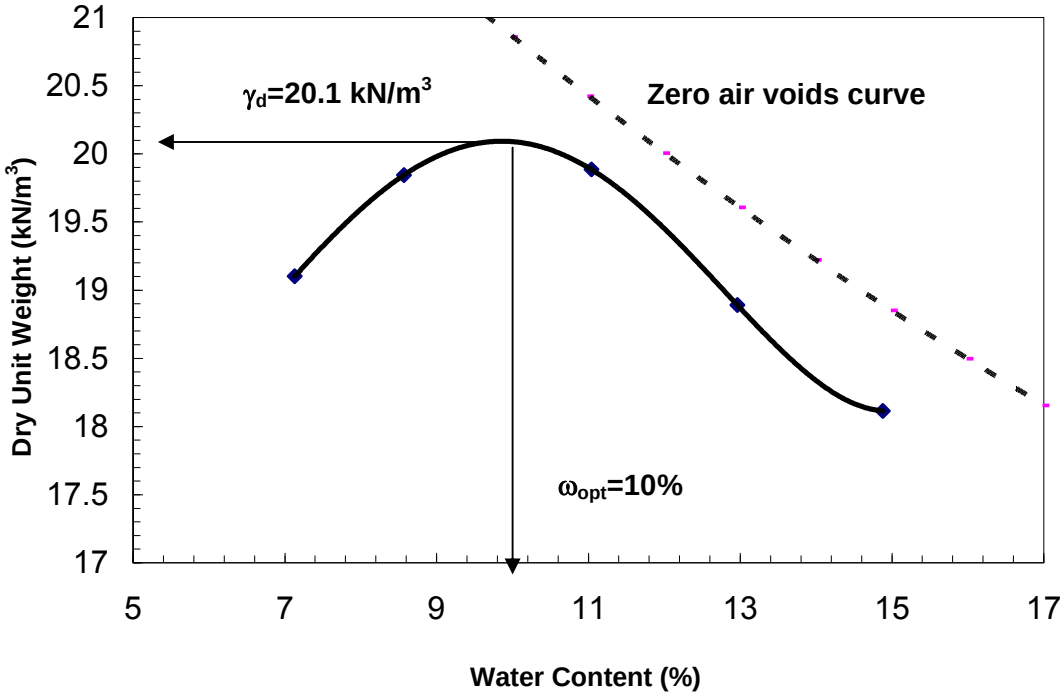

Figure 4. 1 Standard proctor compaction curve for the borrow material

fuels have been reported to contain about 40% n-alkanes, 40% iso-and cycloalkanes, 20% polycyclic aromatic hydrocarbons (PAH), and a few percent isoprenoids, sulfur, nitrogen, and oxygenated compounds (Lee et al. 1992).

The contaminant used during the column leaching tests was a simplified tertiary model nonaqueous phase liquid (NAPL) that consisted of naphthalene and o-xylene dissolved in dodecane.(described further below) These three compounds represented the PAH, monocyclic aromatics, and n-alkane groups, respectively. Detailed description of the chemicals of interest is given Section 3.1.5. The NAPL concentration was designed to give nominal aqueous equilibrium concentrations of 5 mg/L and 10 mg/L for naphthalene and o-xylene, respectively. The former value is higher than the reported aqueous equilibrium concentration of naphthalene in diesel fuel (Lee et al. 1992), but was selected mainly due to analytical and experimental constraints.

4.2. Methods

4.2.1 Laboratory Preparation of Contaminated Soils

The borrow materials are contaminated with petroleum hydrocarbons by following spiking procedure which the compounds were introduced into the soil medium (Doick et al. 2003). Spiking is defined by the ASTM E1676 as “the experimental addition of a test material such as a chemical or mixture of chemicals, sewage sludge, oil, particulate matter or highly contaminated matter sediment/soil to a clean negative control or reference sediment/soil to determine the toxicity of the material added.” Preliminary investigations indicated that interpretation of test data is highly dependent on the spiking

procedure. Therefore, in order to prepare homogenous and reproducible soil–diesel fuel mixtures, the protocol explained by Doick et al. (2003) was adopted A stainless steel spoon was used, which has been reported to produce good spike homogeneity and to be a more reliable approach as compared to other spiking methodologies (e.g., using a blender or a modified bench drill) (Doick et al. 2003). The spiking protocol applied during both compaction and column leaching tests is briefly discussed below:

As part of the methodology, 3500 g of soil (borrow material) was hydrated by adding 3% water by weight. A 700 g of this hydrated soil was then placed into a stainless steel bowl. Diesel fuel or NAPL solution for column tests were added at 1% and 2% by weight in compaction tests and 0.5% and 2% in column leaching tests. The mixture was blended by hand using the stainless steel spoon for about 90 seconds. The remaining 2800 g of hydrated soil was divided into four aliquots equal in weight. Each aliquot was contaminated and blended for about 90 seconds following the same procedure. The spiked sand samples were then placed into 2L amber glass jars with no headspace and kept in 4 °C room for 30 days before starting the tests as discussed further below.

4.2.2 Model NAPL Design, Preparation and Equilibrium Concentration Tests

The model NAPL was composed with naphthalene, *o*-xylene as main constituents of interest and using dodecane as the main solvent. The mole fractions of naphthalene in the NAPL mixture were back-calculated using the Raoult's law described by the following equation:

$$(C_N)eq = (\gamma_N)_{NAPL}(X_N)_{NAPL}(C_N)_{eq}^{Pure}(\frac{f^L}{f^S})^{Pure} \quad (4.1)$$

where $(C_N)_{eq}$ is the equilibrium concentration of naphthalene in the aqueous phase, $(\gamma_N)_{NAPL}$ is activity coefficient for naphthalene in NAPL mixture, $(X_N)_{NAPL}$ is the mole fraction of naphthalene in NAPL mixture, $(C_N)_{eq}^{Pure}$ is the aqueous thermodynamic equilibrium concentration of naphthalene in the pure solid form (aqueous solubility) and is equal to 31 mg/L, and (f^L/f^S) is the ratio of naphthalene fugacities in the subcooled liquid and solid state and is equal to 3.53 (Schwarzenbach et al. 1999). In this formula, the activity coefficient for naphthalene in the aqueous phase, $(\gamma_N)_{aq.}$ is assumed to aqual to 1, i.e., the aqueous solution behaves ideally. The design equilibrium concentration of naphthalene in the aqueous phase $(C_N)_{eq}$ of naphthalene was set at 5 mg/L. Using this value, the following two assumptions were made in order to calculate the mole fraction of naphthalene in the NAPL mixture; (1) the solute- solute interactions in the aqueous phase are small, and (2) NAPL phase is ideal, therefore $(\gamma_N)_{NAPL}$ is unity.

Following the same assumptions, the *o*-xylene mole fractions in the aqueous phase was also back-calculated using the equation below:

$$(C_O)eq = (\gamma_O)_{NAPL}(X_O)_{NAPL}(C_O)_{eq}^{Pure} \tag{4.2}$$

where $(C_O)_{eq}$ is the equilibrium concentration of *o*-xylene in aqueous phase, $(\gamma_O)_{NAPL}$ is the activity coefficient for *o*-xylene in NAPL mixture, $(X_O)_{NAPL}$ is the mole fraction of *o*-xylene in NAPL mixture, $(C_O)_{eq}^{Pure}$ is the aqueous thermodynamic equilibrium concentration of *o*-xylene in the pure solid form (aqueous solubility) and is equal to 170 mg/L. The design equilibrium concentration of *o*-xylene in the aqueous phase $(C_O)_{eq}$ was set at 10 mg/L in Equation (4.2), and corresponding mole fraction calculated by assuming that $(\gamma_N)_{NAPL}$ is equal to 1.

After calculating the required mole fractions of naphthalene and *o*-xylene in dodecane based on Equations (4.1) and (4.2), the corresponding testing NAPL solution was prepared. Subsequently, experiments were conducted to determine the aqueous equilibrium concentrations of each compound , by following a two-stage nested sampling design described by Mendenhall and Sincich (1984). The experimental procedure was as follows. First, 30 mL of the aqueous solution and a 10 mL of the NAPL mixture were placed in 40 mL amber vials and capped using screw caps with Teflon® septa. The volumes of aqueous phase and NAPL phase were selected such that NAPL phase concentration of the tertiary naphthalene, *o*-xylene and dodecane mixture would not significantly change when at equilibrium with aqueous phase (Seagren et al. 1994). Five replicate NAPL-aqueous solution mixtures were prepared and the inverted vials were shaken for three days on the horizontal shaker at a moderate speed. After shaking, they were kept at controlled temperature (22 ± 2 ºC) for five days to allow for phase separation. Two aqueous samples were then withdrawn from each of the shaken vials by using a 2.5 mL gastight syringe. To dose, 1 mL air was first pulled into the syringe, the syringe was inserted through the septum, and the air inside the syringe was injected into the vial to prevent NAPL intrusion into the syringe. Afterwards, 2.5 mL of aqueous solution was slowly withdrawn and 2 mL of this solution was subjected to liquid-liquid hexane extraction, followed by analysis using gas chromatography, as explained in detail in Section 3.3.2.

The measured aqueous equilibrium concentrations of each compound in the samples from the batch equilibrium test were different than expected based on Equation (4.1) and (4.2), with the sated assumptions. It is well known that when more than one

organic compound is present in aqueous solution, cosolvent effect may cause changes in their chemical properties. In order to investigate the cosolvent effect of *o*-xylene and naphthalene, the Yalkowsky model was applied (Schwarzenbach et al. 1999). The results indicated that a cosolvent effect was not present mainly due to presence of low volumes of naphthalene and *o*-xylene in the aqueous solution. Therefore, it was concluded the assumption of ideality in the aqueous phase was correct, but the assumption of ideal NAPL phase [$(\gamma_N)_{NAPL} = 1$] was not valid. Similar observations were made by Seagren and Moore (2003). Therefore, the measured equilibrium concentrations were used in Equation (4.1) and (4.2) to back calculate activity coefficients of 1.77 and 1.21 for naphthalene and *o*-xylene, respectively. Correspondingly, the mole fractions of each compound in the NAPL mixture used in the column tests, described below, were prepared considering the new activity coefficients. The equilibrium concentrations of *o*-xylene and naphthalene in the aqueous phase were successfully maintained at the nominal target value of 10 mg/L and 5 mg/L, respectively, with the new activity coefficients after performing a second set of equilibrium tests by following the same procedure described above.

4.2.3 Aging of Contaminated Soils

Previous research indicated that contact time between soil and contaminant has a significant effect on the laboratory test results. This contact time is often called aging and is defined as the diffusion of organic contaminants into the nano and micro-scale pores of the soil. As a result of aging, often physical entrapment and partitioning into soil organic matter or its organic carbon fraction occurs (Doick et al. 2003). The generally

recommended aging time ranges from 2 to 4 weeks to replicate these effects in laboratory prepared spiked soils (Reid et al. 1998, Northcott and Jones 2000, Brinch et al. 2002). In the current study, soil-contaminant combinations were aged at 4°C for a period of two and four-week(s) to investigate the effect of aging on geotechnical properties (i.e, compaction) as well as to select the optimal chemical equilibrium time for further testing. Additionally, a set of one-year aged samples were tested in order to understand the long-term aging effects on the geotechnical properties of soils. Column leaching specimens were aged for 4 weeks at 4°C.

4.2.4 Compaction Tests

4.2.4.1 Water Content and Liquid Content Determination

Laboratory compaction tests were conducted on soils and soil-fly ash mixtures following the procedures outlined in ASTM D 698. Standard Proctor effort was used during compaction. However, instead of the term "water content" commonly used in interpreting the compaction test data, a term "liquid content" was adopted. Liquid content herein represents the total amount of water and diesel fuel inside a specimen (Meegoda 1995). To determine the liquid content, two separate techniques were studied before the compaction tests: surfactant desorption and thermal method.

The surfactant desorption technique was performed using the TX-100 nonionic surfactant, [$C_{14}H_{22}O(C_2H_4O)_n$, MW= 625 g/mol] (99% purity) was used. Surfactants can enhance the water dissolution of nonionic organic compounds, and increase the desorption of organic pollutants from contaminated soils. For example, nonionic surfactants have been commonly employed in testing the desorption characteristics of soils contaminated with PAHs (Zhu et al. 2004) and pesticides (Mata-Sandoval et al.

2002). For this study, an aqueous solution of TX-100 was first prepared at a concentration of 10 mM. An 80 mL aliquot of this solution was mixed with 20 grams of diesel fuel-spiked soil, which was then placed in a 125 mL amber bottle equipped with a Teflon® septum cap. The bottles were shaken for 24 hours and the solution was allowed to sit for about two hours. After the sedimentation, decantation of the supernatant was performed by a glass pipette, taking care not to remove the emulsion. The remaining sample (emulsion plus soil) was then kept in the oven at 105 °C for 24 hours. The dry weight of the emulsion plus soil mixture was determined, and the difference between that dry weight and the initial soil weight (20 g) was used to calculate the liquid content. The results indicated that this particular nonionic surfactant might not be the best compound for desorption of diesel fuel from the borrow material. A similar conclusion was reached in a study conducted by You and Liu (1996) in which TX-100 first adsorbed onto the soil through hydrophobic interactions and increased the hydrophobicity of soil; however, it then acted as an additional organic component on the soil surface and enhanced organic pollutant partitioning. Further trials with different concentrations of TX-100 or different types of surfactants were not carried out, because it was beyond the scope of the current project.

Ultimately, the thermal method was chosen for determining the liquid content. As part of the thermal method, the contaminated soil was kept in an oven at 105 °C for 48 hours and its gravimetric water content was determined. However, the boiling points of the organic constituents inside the diesel fuel did not allow accurate determination of the total liquid content at 105 °C and higher temperatures were necessary. Considering the reported boiling temperature of 250 °C for diesel fuel as well as the observations made by

Meegoda et al. (1998), a temperature of 400 °C was selected in the current study to burn the organics present inside the soil medium. The specimens were kept in the oven at 400 °C for 24 hours. It was assumed that all the organic material was combusted at 400 °C, and the liquid content was calculated by using the following equation :

$$LC = TO - TOC \tag{4.3}$$

where LC is the liquid content (% by weight), TOC is the total natural organic content of the borrow material (% by weight), and TO is a total content of natural organic matter in the borrow material (TOC), plus diesel fuel and the gravimetric water content. For all practical purposes, LC represents the summation of the diesel fuel and gravimetric water content. However, calculating the liquid content by simply adding the initial water and diesel fuel contents, for instance, may not be accurate since there may have been small deviations in the diesel fuel content during specimen preparation. This procedure can be helpful to the practicing engineers, and the organic contaminant level can be identified by the thermal technique if the natural organic content of the soil is known a priori.

4.2.5 Column Leaching Tests

Soils contaminated with petroleum hydrocarbons can be stabilized by using binders that exhibit significant sorptive capacity; however, the long-term leaching of undesired constituents from the stabilized end-product must be studied. Leaching is the process by which inorganic or organic contaminants are released from the solid phase into the water phase under the influence of mineral dissolution, desorption, or complexation processes. The water that contains the dissolved and desorbed (removed) hazardous constituents, which is often called leachate, can potentially contaminate the groundwater or surface water (Bin-Shafique 2002). Laboratory leaching tests have

traditionally been used to evaluate the leachability of various hazardous compounds. Leaching test results are often used to define the transport properties of chemical pollutants in a soil medium under controlled conditions, e.g., hydraulic gradient, climatic stresses. Column tests have been used to determine the leaching performance of PAHs from sewage farm soils (Reemtsma and Mehrtens 1997), VOC's from clay liners (Kim et al. 2001), and TCE and pesticides from foundry sand (Lee and Benson 2002).

Column leaching tests performed in this study consisted of continuous flow of liquid through a solid matrix (i.e., the petroleum-contaminated soil). A schematic diagram of the column leaching test set up is shown in Figure 4.2. Stainless steel was used to fabricate the column cylinders and top and bottom plates. The column cylinder fit into grooves in the top and bottom plates, which were equipped with Viton O-rings, and the entire assembly was hold together by 4 threaded rods over with nuts and knobs on each end. When assembled, the column reactor had an inside diameter of 101.6 mm and height of 177.8mm. The borrow material and borrow material/fly ash mixture specimens were spiked with the model NAPL, as discussed above, and then compacted in the column using standard Proctor energy giving the test specimen height of 114.3 mm. The remaining upper 63.5 mm-section inside the column was used as an influent reservoir for sampling. A supply (influent) tank containing DI water was placed above the columns, and the influent was provided at a nominal flow rate of 10 μL/min. This rate was selected based on the desired hydraulic gradient of 4 to 5. The specimen was underlined by a glass fiber filter and stainless steel screen. An effluent reservoir was located between the bottom of the specimen and lower base of the column. The effluent leaving the specimen

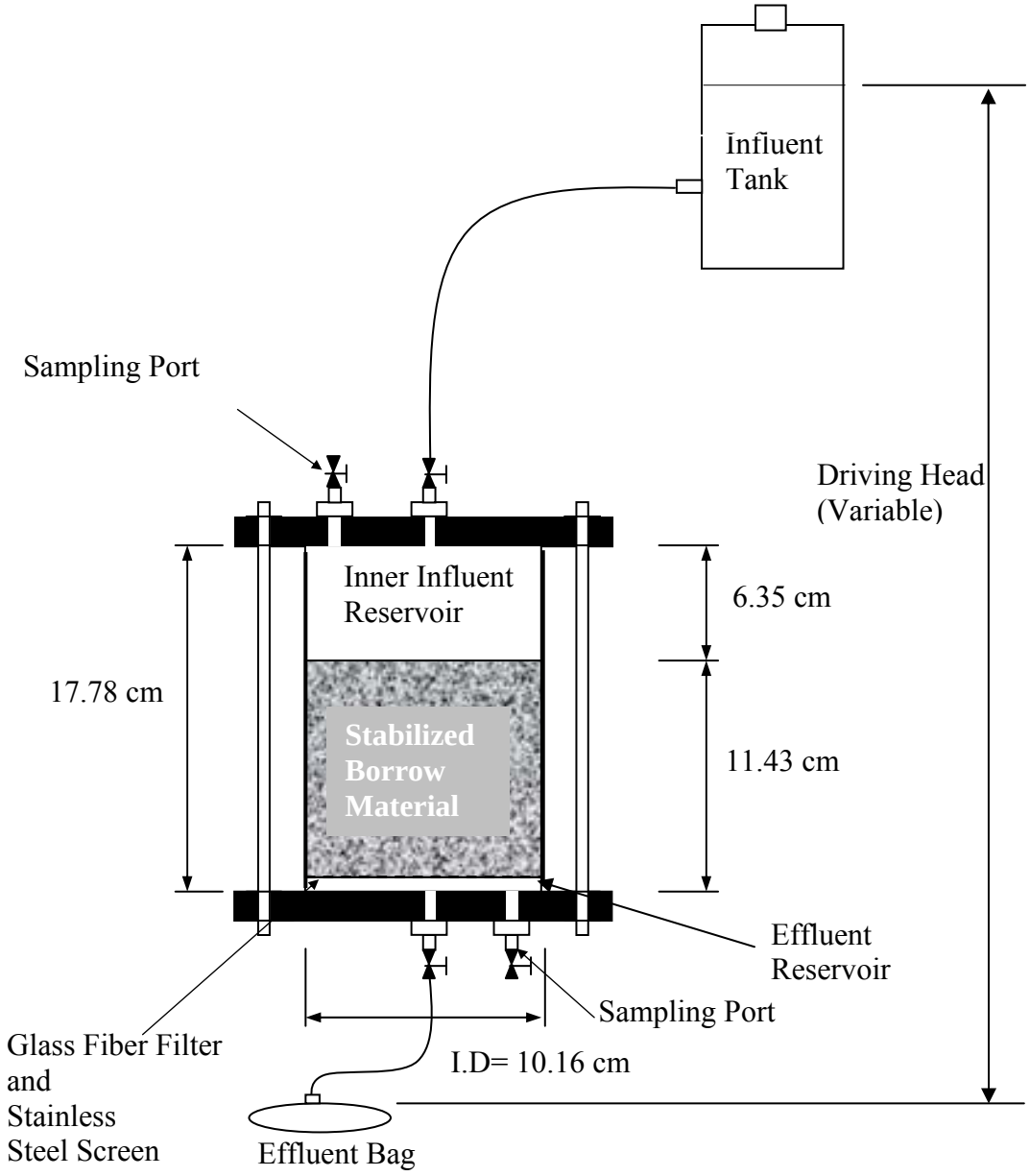

Figure 4.2 Schematic of column leaching Test Set-up (Not to scale).

was collected in Teflon® effluent bags. All of the tubing was Teflon® and the fittings were Teflon® or brass. As part of the current research study, two sets of column leaching tests were conducted. In the first set of experiments, the model tertiary NAPL, a mixture of naphthalene, *o*-xylene and dodecane, as described in Chapter 4, was added to the borrow material at 2%, and in the second set, the model NAPL was added at 0.5% by weight.

Each set of experiments included four columns, for a total of eight columns. One of the four columns in each set was a control column filled contaminated borrow material only. Duplicate control columns were performed in the second set of experiments to test for reproducibility. In the other three columns in each set, the contaminated borrow material was amended with 5%, 10%, and 20% Brandon Shores (BS) fly ash by weight, respectively. The physical and chemical properties of BS fly ash are given in Chapter 3. The NAPL-contaminated column specimens were prepared by following the same spiking procedure as used for the compaction tests, with the exception that the spiking was performed using the naphthalene- and *o*-xylene-in-dodecane model NAPL mixture instead of the diesel fuel used in compaction tests. The spiked specimens were aged for a total of 4 weeks. Control column specimens were prepared by compacting the 4-week aged NAPL-spiked borrow material in the columns. For the remaining column specimens, NAPL-spiked and 4-week aged borrow material was amended with 5%, 10% or 20% BS fly ash and kept in closed amber glass containers for 2 days to achieve an equilibrium. After 2 days, the mixtures were compacted inside the test columns.

As discussed previously, based on a fugacity model, the naphthalene and *o*-xylene in dodecane mole fractions of 0.026 and 0.0472 in the NAPL mixture provided nominal

naphthalene and *o*-xylene aqueous equilibrium concentrations of 5 and 10 mg/L, respectively. Thus, the maximum possible aqueous contaminant concentrations expected in the column leaching tests were the same as for the batch adsorption tests. The model NAPL was used in these experiments to simplify the analysis of the leachate collected from the specimen and focus on evaluation of the dissolution and sorption/desorption characteristics of the specific target organic compounds (i.e., naphthalene and *o*-xylene). As mentioned before, there are several different types of compounds in diesel fuel and it would be difficult to define the leaching behavior and the effect of binder on the stabilization of all of the pertinent organic pollutants.

The hydraulic properties of all columns are given in Table 4.1. Falling head hydraulic conductivity tests conducted on the borrow material compacted with the standard Proctor effort indicated that the material had an average hydraulic conductivity of $5x10^{-6}$ cm/sec. The measured hydraulic conductivities, coupled with the selected hydraulic gradient, resulted in the actual flow rates provided in Table 4.1. The columns were terminated after ensuring the stabilization of the flow and a steady-state effluent concentration of the contaminants.

Using the sampling port attached to the base of column, the effluent was monitored daily for the first two months of the tests. Due to relatively stabilized flow rates, weekly monitoring was adopted after two months. The aqueous effluent samples were collected using a luer-lock gas-tight syringe (VWR 60375-522) and a syringe pump (Harvard Apparatus 22). A constant extraction rate equal to the flow rate (10 μL/min) was used in order not to cause a disturbance in the continuous flow. The collected samples were

Table 4. 1 Hydraulic conductivity and flow rate of the columns employed in the current study

Contamination Level	Column Type	Hydraulic Conductivity (cm/sec)	Flow Rate (□l/min)
2 % NAPL	Control	$4.1\ 10^{-7} \pm 2.4\ 10^{-7}$	8.74 ± 3.4
	Column with 5% fly ash	$2.1\ 10^{-7} \pm 3.2\ 10^{-8}$	10.50 ± 1.6
	Column with 10% fly ash	$3.3\ 10^{-7} \pm 5.4\ 10^{-8}$	14.90 ± 6.2
0.5 % NAPL	Control 1[c]	$4.2\ 10^{-6} \pm 1.8\ 10^{-7}$	9.8 ± 0.4
	Control 2[c]	$2.9\ 10^{-6} \pm 7.8\ 10^{-8}$	6.5 ± 0.1
	Column with 5% fly ash	$3.9\ 10^{-6} \pm 7.1\ 10^{-7}$	8.6 ± 0.1
	Column with 10% fly ash	$5.1\ 10^{-6} \pm 1.3\ 10^{-6}$	11.4 ± 2.9

subjected to liquid-liquid hexane extraction, and the naphthalene and *o*-xylene concentrations in the hexane extracts were determined via GC analysis, as described in Section 3.3.2. The NAPL present inside the soil specimens were extracted and analyzed as discussed in the following section.

4.2.6 Analytical methods

4.2.6.1 Extraction of NAPL Compounds from Column Specimens

A mass balance analysis of the NAPL-contaminated borrow materials, as well as the fly ash-amended ones, required an assessment of the organic compound loss during each step of the laboratory preparation procedure. The losses occurred as a result of mass reduction of organics inside the column specimen, because the contaminated specimens were exposed to the atmosphere during the spiking, fly ash addition, compaction and aging. The losses are primarily attributed to volatilization, in particular for the *o*-xylene, a BTEX compound well-known for its relatively high volatility.

Another potential reason for loss during spiking is the sorption of the contaminants onto the stainless steel bowl or the stainless steel spoon used for the spiking, or onto the amber glass jars that the NAPL spiked soils were kept in for aging. In order to quantify these losses as well as to measure the concentrations of each organic compound that remained in the columns after the leaching test, an extraction of the soil specimens by means of a mechanical shaking extraction method was employed.

4.2.6.2 Extraction of Contaminants from the Soil

Two highly hydrophobic solvents, namely acetone and hexane were utilized to extract the NAPL mixture from soils after each step. Extraction of petroleum

hydrocarbons from soils has commonly been conducted through Soxhlet extraction method (ASTM 2002). However, there are three main problems associated with the Soxhlet method: (1) the soil sample is static during the extraction process, which may limit contact between solvent and soil microspores, (2) the method requires a long testing time of up to 24 hours and specialized apparatus, which may be prohibitive for large number of samples, and (3) high moisture content in soil samples may increase the variability due to difficulties associated with obtaining representative sub-samples (Schwab et. al. 1999). Because of these disadvantages, a more practical and efficient method, the mechanical shaking extraction method was adopted, using acetone as the main solvent. The details of the technique were described by Schwab et al. (1999). The objective of the mechanical shaking extraction was to remove and measure the contaminant mass in soil samples after each step of column specimen preparation, as well at the termination of the column tests.

As part of the extraction procedure, 1-g soil samples were collected and placed into 15-mL round-bottom glass vials. The vials were weighed before and after placement of the soil specimens to determine the wet soil mass. A 10 mL aliquot of solvent (hexane or acetone) was then added immediately to each vial containing 1 g of soil sample and the vials were capped using open-top caps with PTFE septum. The solvent amended vials were shaken using a reciprocal horizontal shaker at the maximum speed for 30 minutes. Then, the extracts were centrifuged for 10 min at 200 g, and the extraction solvent was decanted and transferred to amber glass vials capped with Teflon® septum. This process completed the first cycle of the extraction procedure. The soil samples were then subjected to two more extraction cycles following the same procedure and using fresh

solvent during each cycle. The extracts were combined and then kept at 4 ºC until it was possible to determine the concentrations of each compound in the extract.

Hexane was used as the solvent during extraction of NAPL from soil samples after the spiking, aging and post-compaction steps. There were two reasons for using hexane as solvent: (1) the analytical determination of the compound concentrations in the aqueous phase was performed using a hexane extraction, and (2) hexane is an effective solvent for most of the organic chemicals used in this study. However, the extraction efficiency of hexane, as a nonpolar solvent, was not satisfactory for extraction of the soil inside the column at the end of leaching tests due to the presence of high amounts of water (Schwab et al. 1999). Specifically, the nonpolar nature of hexane caused the formation of clumps rather than dispersion of soil particles, which prevented the removal of all the entrained hydrocarbons. Therefore, a polar solvent, acetone, was chosen for extractions of the compounds in the soil after the first set of columns were dismantled, and for extraction from the aqueous as well as solid phase samples for the second set of column experiments (at 0.5 %). Because acetone has both nonpolar and polar properties (it is fully miscible in water), its use as a solvent overcomes the problems associated with the hydrophobicity of hexane. Schwab et al. (1999) compared the extraction efficiencies of the mechanical shaking method using acetone and the ASTM Soxhlet extraction procedures and concluded that the efficiencies were comparable for clayey sandy soils, similar to the borrow material used in this study. Specifically, acetone extraction yielded a recovery efficiency of above 95% and was considered acceptable.

4.2.6.3. GC Method for Naphthalene, *O*-xylene and Dodecane Mixture

Because of the use of the testing model NAPL mixture, in the column tests, it was necessary to determine the aqueous concentrations of each compound of the model NAPL (i.e., *o*-xylene, naphthalene and dodecane). A GC procedure similar to that for *o*-xylene was utilized to analyze these components. Hexane or acetone was used as the main solvent during extraction, as described above. The same GC method was employed for both of the solvents; however, separate standard curves were prepared for each compounds (*o*-xylene, naphthalene, dodecane, and acenaphthene) in each solvent. The GC analyze of *o*-xylene, naphthalene, dodecane, and acenaphthene in the hexane and acetone were performed as follows: the oven temperature was held at 40 ºC for 4 minutes after injection of 1 μL of the extracted sample in hexane or acetone, and then the temperature was increased at a rate of 40 ºC/min up to a final temperature of 220 ºC. The retention times for the *o*-xylene, naphthalene, dodecane and acenaphthene were 4.27, 7.23, 7.37 and 8.9 minutes, respectively. The example chromatogram is shown in Figure 4.3.

Standard calibration curves of all three compounds and the internal standard in hexane, as well as acetone, were prepared. Tables 4.2 and 4.3 summarize the results of the calibration tests. When the difference between concentrations of the standard solutions was greater than 2 orders of magnitude, the higher points had dominant effect on the standard curve. Elimination of the adverse effect of one point to the overall curve was made by using weighted linear regression (Relative Least Squares- RLS) analysis, except an un- weighted linear regression (Absolute Least Squares - ALS) was used for the analyses of acenapthene in both solvents and naphthalene in acetone.

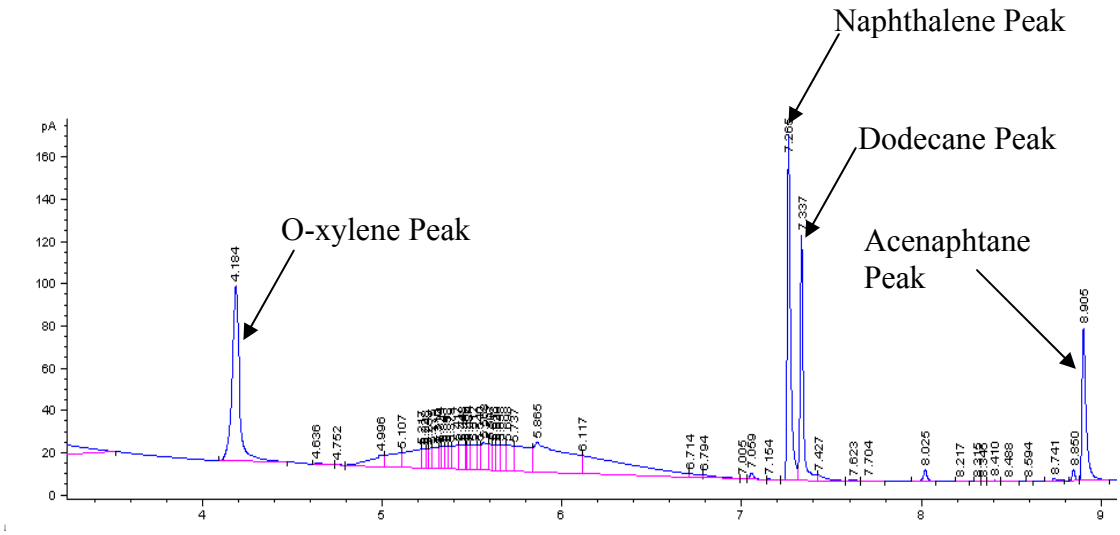

Figure 4.3 The GC plot for the *o*-xylene, naphthalene, dodecane and acenaphthene

Table 4.2 Standard solutions used for NAPL Compounds and equations for hexane

Compound	Standard Solutions Used (mg/L)	Curve Equations
O-xylene	0.1442 – 1.442 – 3.605 – 36.05	$A_{Ox} = 34.476\ [C_{hex}]_{Ox} + 0.9412$ [(a)]
Naphthalene	0.1 – 1 – 4.21 – 10.025	$A_{Naph} = 46.012\ [C_{hex}]_{Naph} + 0.2$ [(a)]
Dodecane	0.218 – 4.375 – 8.75	$A_{Dod} = 50.788\ [C_{hex}]_{Dod} + 6.377$ [(a)]
Acenaphthene	0.5 – 5 – 10	$A_{Ace} = 38.154[C_{hex}]_{Ace} - 8.93$ [(b)]

Notes: A – area of the peak of compound in the chromatogram [C_{hex}] - the naphthalene concentration in hexane. (a) calculated by Relative Least Squares (RLS); (b) - calculated by Absolute Least Squares, ALS.

Table 4. 3 Standard solutions used for NAPL Compounds and equations for acetone

Compound	Standard Solutions Used (mg/L)	Curve Equations
O-xylene	0.107 – 1.072 – 10.72 – 107.2	$A_{Ox} = 35.318\ [C_{Acet}]_{Ox} + 3.377$ [(a)]
Naphthalene	0.12 – 0.61 – 2.44 – 4.88 – 12.2	$A_{Naph} = 41.20\ [C_{Acet}]_{Naph} + 4.272$ [(b)]
Dodecane	0.072 – 0.748 – 3.744 – 7.48- 74.88 – 187.2 - 1872	$A_{Dod} = 33.706\ [C_{Acet}]_{Dod} + 1.5733$ [(a)]
Acenaphthene	1.6 – 8 – 16	$A_{Ace} = 29.476[C_{Acet}]_{Ace} – 4.599$ [(b)]

Notes: A – area of the peak of compound in the chromatogram [C_{Acet}] - the naphthalene concentration in acetone. (a) calculated by Relative Least Squares (RLS); (b) - calculated by Absolute Least Squares, ALS.

4.2.6.4 Measurement of NAPL Degraders

The occurrence of biodegradation during the column leaching experiments was evaluated as a possible cause for the reduction in the organic contaminant concentrations in contaminated soils. To monitor for biodegradation in the contaminated soils, microbial numbers in the leachate was measured on a periodic basis in the column effluent. Changes in the bacterial populations were taken as an indication of the level of biodegradation i.e., whether it is increasing or decreasing by the time. To enumerate the NAPL degrader bacterial populations in the column effluent samples, a 96 well microtiter plate most probable number (MPN) method was employed (Haines et al. 1996, Hong et al. 2006). A 180 μL sterilized Bushnell-Hass medium (Difco, No. 0578-17) was aseptically added to each well except the first row. Extraction of 2 mL of effluent samples from the columns was conducted by using syringe pump at a rate of 10 μL/min. 200 μL of effluent sample was then added to each well in the first row, whereupon 10-fold dilutions were performed from the first through 11^{th} row, leaving the 12^{th} row empty of sample as a sterile control. After the dilution procedure, 2 μL of filter sterilized model NAPL was added to each well in the plate (enough to cover the surface of each well) as the sole hydrocarbon source for enumeration. The plates were then sealed, covered from light in an plastic bag, and incubated for 7 days at the same temperature as the columns (24 ± 2 °C).

After 7 days of incubation, 50 μL of filtered 2-(p-iodophenyl)-3-(p-nitrophenyl)-5-phenyl tetrazolium chloride (3 g/L) (INT, Sigma No. I-1040-6) was added as an indicator to each well. The INT competes with O_2 for electrons from the respiratory electron transport chain, and once the INT is reduced to an insoluble formazan that

deposits a red precipitate in the presence of active respiring microorganisms (Hong 2003). Wells were scored as positive for NAPL-degrading organisms if the well turned a red or pink color. The total numbers of positive wells for each dilution row (each row except theoretically the last sterile row) were then counted and input into the computer program to calculate the most probable number (MPN).

To enumerate the number of NAPL-degrading colonies in the sample, a computer program, developed by the U.S. EPA Risk Reduction Engineering Laboratory was used. Inputs to the program include the number of dilutions, number of tubes per dilution, size of the initial volume, and dilution factor used (10-fold in this case). The program estimated the MPN using a maximum likelihood method assuming that the microbes exhibit an independent Poisson distribution. However, the estimation is biased for a small number of tubes, and even the 96-well plate has significant bias within. Thus, a bias-corrected MPN was calculated and used as the MPN of the effluent sample. In addition, 95% confidence intervals were calculated for each plate count to quantify the reliability of the MPN data. Due to intense laboratory work and labor, MPN measurements were conducted weekly during the course of the experiments on selected columns. These included the 0.5% NAPL-contaminated control column, and the 0.5% and 2% NAPL-contaminated 20 % fly ash amended columns.

4.3 Results

4.3.1 Compaction Tests Results.

4.3.1.1 Effect of Diesel Fuel Content on Compaction Tests

Compaction tests were performed on specimens spiked with 1% and 2% diesel fuel. As shown in Figure 4.4, the compaction curve shifts to the right and downward with increasing diesel fuel content. As a result of this shift, the maximum dry unit weight decreases and optimum liquid content increases for both 1% and 2% diesel fuel-spiked borrow material. Visual observations after the compaction tests indicated that the soil particles were coated by diesel fuel as a result of spiking and a clod-type porous matrix was visible. Due to this structure, it is speculated that unconnected voids increased the porosity of the soil matrix. The increase in porosity decreased the dry unit weight and increased the optimum liquid content. with increasing diesel fuel content. Attachment of NAPL to the soil phase, formation of clumps, and an increase in porosity were also reported in the studies conducted by Schwab et al. (1999) and Schwartz and Krizek (2006).

4.3.1.2 Effect of Aging on Compaction of Contaminated Borrow Material

Compaction tests were performed on specimens aged for two weeks, four weeks and one year. The aging process undertaken in this study was aimed at simulating field conditions by providing sufficient time for partitioning of the organic contaminants within the borrow material. This partitioning mechanism has an effect on the environmental fate of these compounds, discussed further below.

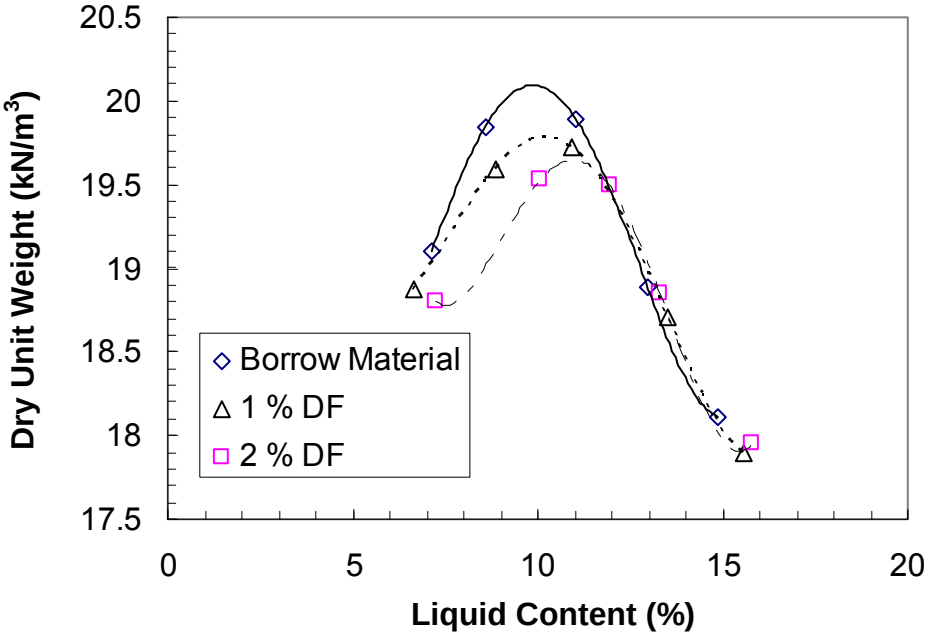

Figure 4.4 The effect of diesel fuel inside the contaminated soils from compaction tests (DF= Diesel fuel) Expected compaction curves were in solid lines.

The compaction curves for soils contaminated with 2% or 1% diesel fuel, and aged for 2 weeks, 4 weeks, and 1 year are presented in Figure 4.5. There was almost no change in the compaction parameters when the samples were tested after 2 and 4 weeks of aging.

On the other hand, when the aging period is increased to one year, the maximum dry weight of the compacted specimens slightly decreases (about 2%) with almost no significant change in the optimum liquid content. Similar observations were made for soils contaminated with 1% as well as 2% diesel fuel. Considering these factors, and testing limitations associated with relatively longer aging periods (e.g., one year), a 4-week aging period was adopted in the current study.

4.3.1.3 Effect of Fly Ash on the Contaminated Borrow Material

Based on the compaction test results summarized in Figures 4.4 and 4.5, a diesel fuel content of 1% and an aging time of 4 weeks were selected for preparation of fly ash-amended specimens. The fly ash was added at 5, 10 and 20% by weight to the diesel-fuel spiked and aged borrow material. Compaction curves developed for mixtures with varying fly ash contents (See Figure 4.6) indicate that dry unit weight decreases, and optimum water content increases, with increasing fly ash, i.e., the compaction curve shifts to down as well as right. This is a trend generally observed for soils with increasing fines content consistent with addition of the finer fly ash to

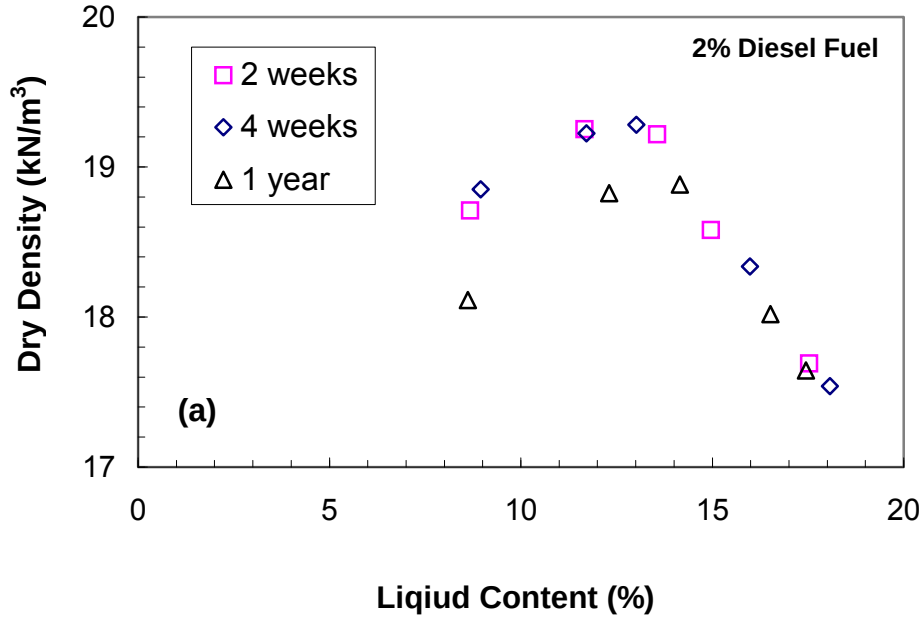

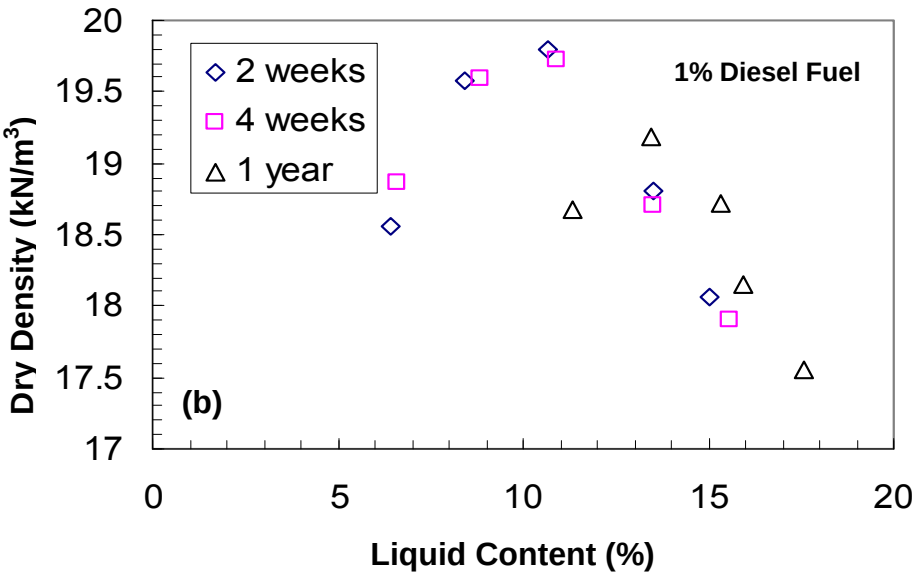

Figure 4.5 Compaction tests results on (a) 2%, and (b) 1% diesel fuel spiked soils after 1 week, 2 weeks and 4 weeks of aging

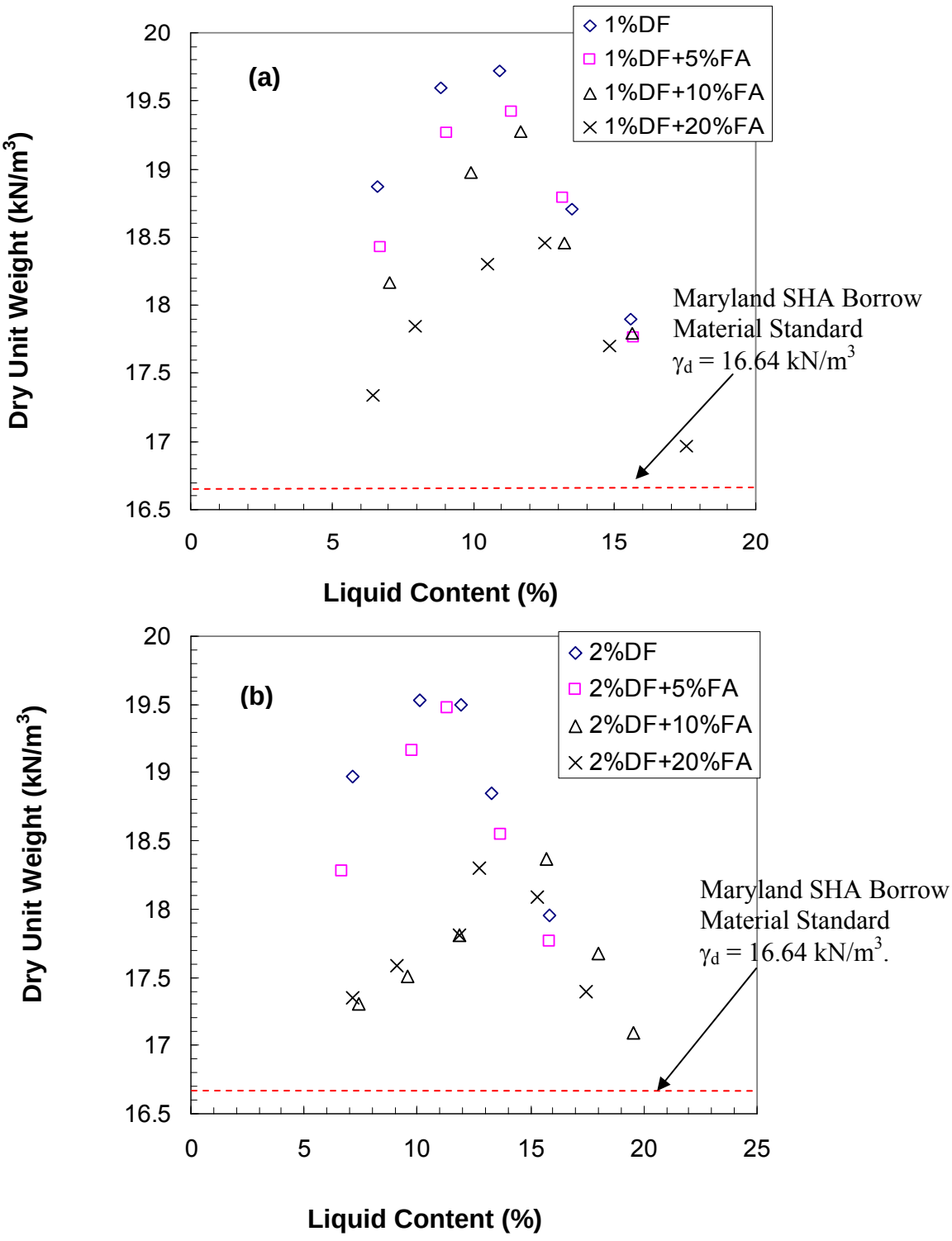

Figure 4. 6 The effect of fly ash content on the compaction properties (a) 1% DF contaminated soils mixed with different fly ash ratio, and (b) 2% DF contaminated soils (DF= diesel fuel, FA=fly ash)

the borrow material. Similar trends were also reported in previous studies conducted on fly ash-soil mixtures (Indraratna 1992, Senol et al. 2002). The trend in Figure 4.6 is more visible when the fly ash content was increased from 5% to 20%. These curves suggest that the mixtures can be used as either a common borrow or a select borrow material in construction of roadway embankments in Maryland because their maximum unit weight values satisfy the requirements of Section 916 of the Maryland State Highway Standard and Specification for Construction and Materials (MDSHA 2001).

4.3.2 Column Leaching Tests Results

4.3.2.1 Determination of Contaminant Mass inside the Columns during Specimen Preparation

The extraction of the NAPL compounds from the column specimens was performed in order to determine the mass of each pollutant that remained inside the column specimens to facilitate a mass balance analysis. The mass loss of each compound occurred probably primarily due to volatilization during the spiking, aging and compaction process as well as possibly some biodegradation and sorption onto testing equipment. Subsequently, the percent loss of naphthalene, *o*-xylene and dodecane were calculated by subtracting the measured compound loss from known initial mass added for all three pollutants.

The amount of losses of each organic compound that occurred from the 2% NAPL contaminated soil after the spiking, aging and compaction steps, which were performed by using hexane as the extraction solvent, are summarized in. Table 4.4. The results indicate that the mass losses increased going from spiking to compaction.

Table 4.4 Percent losses in columns contaminated with 2% NAPL by weight following spiking, aging, and compaction

Column Type	**Extraction Step**	**Percent Losses**		
		***O*-xylene**	**Naphthalene**	**Dodecane**
Control Column	Post Spiking	43.4	2.3	0.2
	Post Aging	46.4	8.4	4.5
	Post Compaction	56.6	6.3	24.3
5% Fly Ash amended Column	Post Spiking	42.1	2.9	0.0
	Post Aging	46.6	8.0	5.7
	Post Compaction	66.7	32.6	42.3
10% Fly Ash amended Column	Post Spiking	45.5	9.9	7.3
	Post Aging	44.1	6.9	5.8
	Post Compaction	71.8	34.5	46.7

This was the case for the control as well as the fly ash-amended soil columns. The post-compaction losses were significantly higher than the losses experienced after spiking or aging for any of the fly ash columns. The same post-compaction losses were also higher than the ones experienced during the preparation of the fly ash-amended columns. It is believed that the increased optimum water contents of the fly ash-amended soils as compared to the borrow material may have contributed to these losses, whereas being exposed to air during compaction inevitably increased the losses due to partitioning into air.

The results presented in Table 4.4 also indicate that naphthalene and dodecane losses were much less than the mass losses experienced with *o*-xylene. For example, the pre-compaction losses ranged from 2.3 to 9.9% and from 0 to 7.3% for naphthalene and dodecane, respectively, whereas the same losses remained in a range of 42.1 to 46.6% for *o*-xylene (Figure 4.7 to Figure 4.9). The values indicate that the highly volatile nature of *o*-xylene promoted losses even under confined conditions (i.e., aging). The post-compaction losses changed similarly, with naphthalene and dodecane losses ranging from 6.3 to 34.5% and 24.3 to 46.7%, respectively, while *o*-xylene losses ranged from 56.6 to 71.8%.

In all cases, mass losses were greater with the fly ash-amended soil than with borrow material alone. The losses due to volatilization were also calculated for the columns contaminated with 0.5% NAPL. However, losses were only calculated after compaction in that series of tests because that was the value of interest in terms of the mass loading onto the columns.

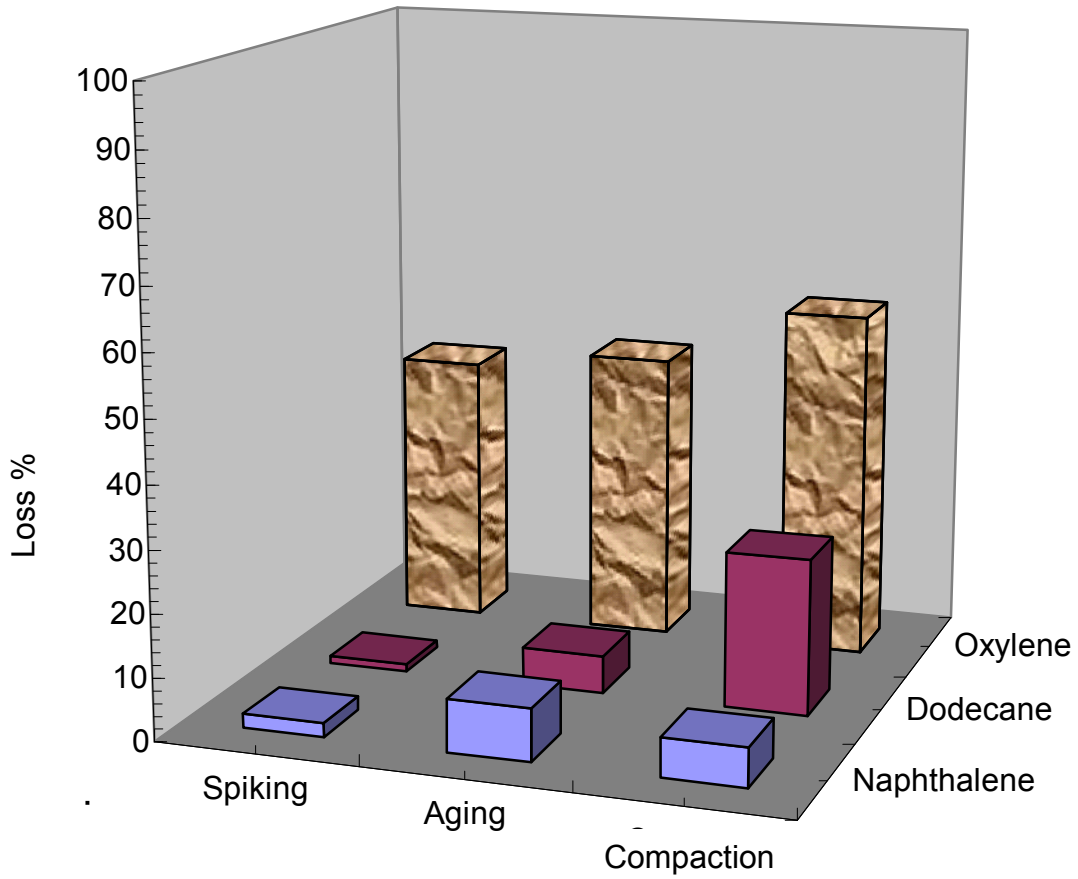

Figure 4.7 Percent losses in a control specimen contaminated with 2% NAPL by weight at each experimental step

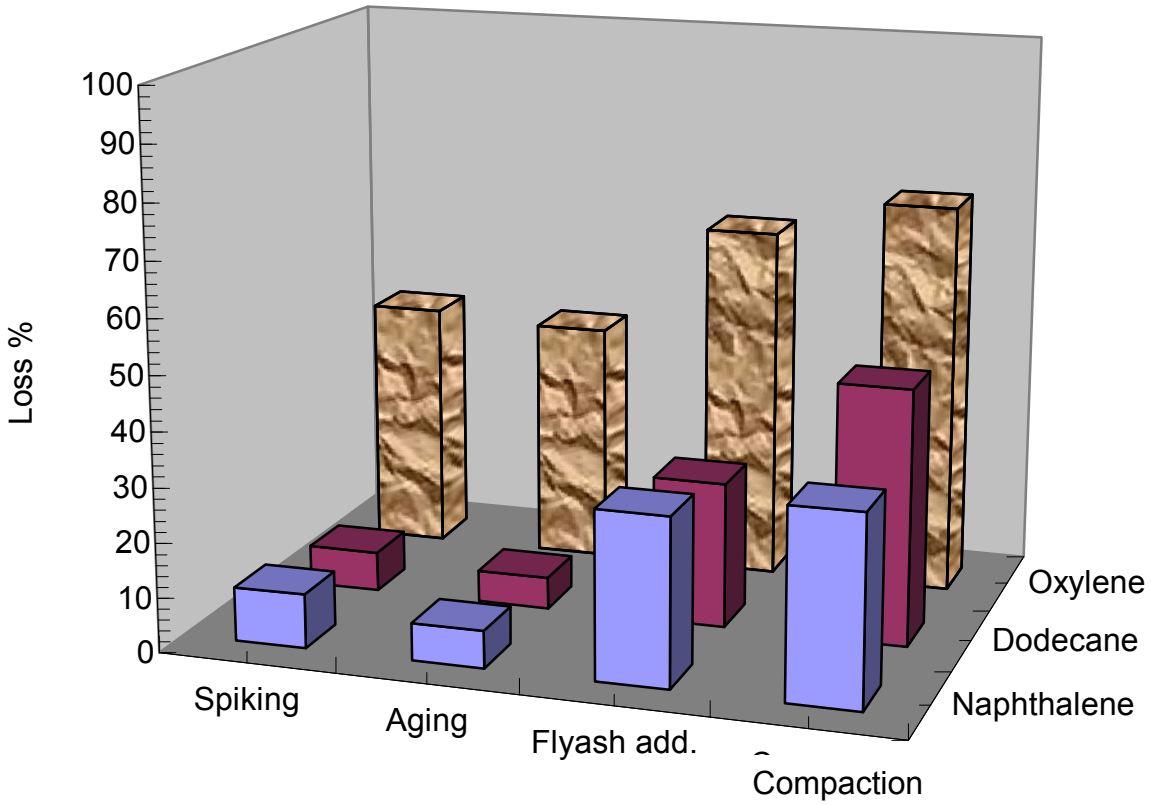

Figure 4.8 Percent losses in a 10% fly ash-amended column at each experimental step

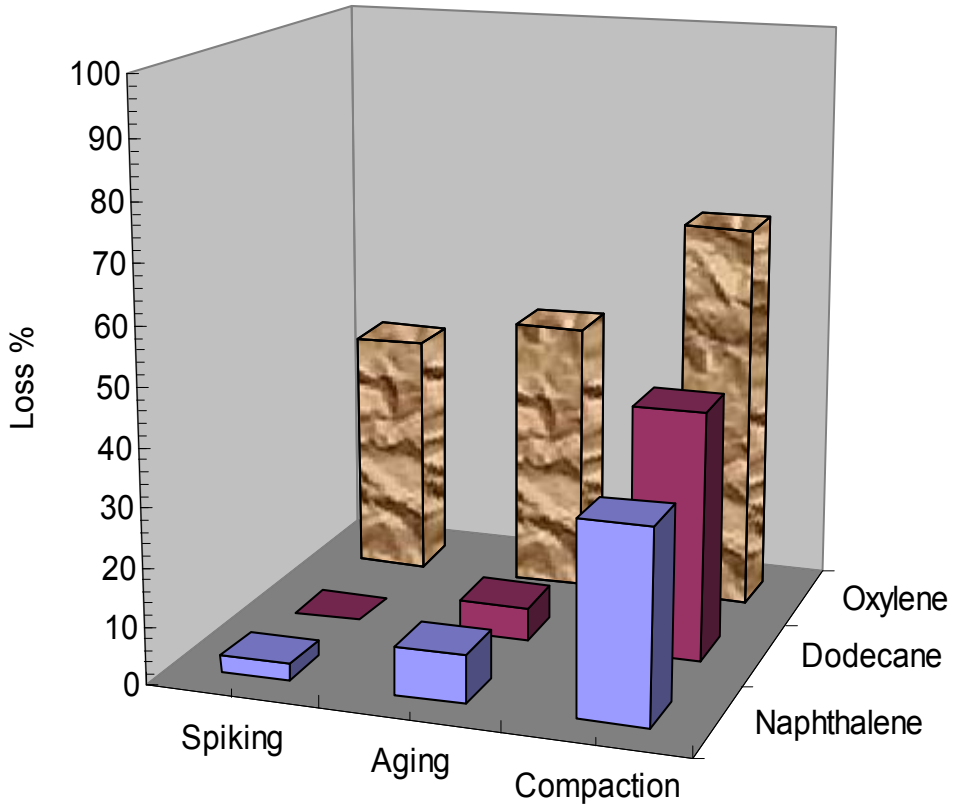

Figure 4.9 Percent losses in a 5% fly ash-amended column at each experimental step

As mentioned previously, the extractions of the compounds from the second set columns were performed by using acetone as the solvent. The results summarized in Table 4.5 indicate that addition of fly ash generally increased the amount of mass loss, similar to the observations made for the 0.5% NAPL columns, although less dramatically than for 2% NAPL.

4.3.2.2 Column Leaching Results

The concentrations of naphthalene and *o*-xylene were measured in the effluent samples from the nine test columns. Sample collection began once the full saturation of the column specimens occurred, which took about 8 to 10 days due to the low hydraulic gradient applied during testing. The temporal variations in the measured o-xylene and naphthalene effluent concentrations for the 2% NAPL contaminated columns are shown in Figure 4.10 to 4.12.

For both naphthalene and o-xylene, the concentrations released from the control column are generally higher than the concentrations released from the columns with fly ash-amended borrow material. The fluctuations in the concentrations observed in Figures 4.10 through 4.12 are attributed to the changes in water head due to refilling of the influent tank and their impact on mass transfer process. However, under the applied hydraulic gradients (4 to 5), mobilization of o-xylene and naphthalene from the borrow material (clayey sand) was expected to be extremely slow (Mercer and Cohen 1990). Hence, the fluctuations in the applied hydraulic gradient are believed to have a very limited effect on NAPL mobilization.

The data in Figures 4.10 through 4.12 also reveal that there was a large initial release of o-xylene and naphthalene in the control column. Specifically, the initial

Table 4.5 Post-compaction percent losses in columns contaminated with 0.5% NAPL by weight

Column Type	Extraction Step	*O*-xylene (%)	Naphthalene (%)	Dodecane (%)
Control Column 1	Post Compaction	78.9	52.4	25.5
Control Column 2	Post Compaction	79.6	51.2	22.1
5% Fly Ash Amended Column	Post Compaction	86	47.3	20
10% Fly Ash Amended Column	Post Compaction	95.2	60	31
20% Fly Ash Amended Column	Post Compaction	99.1	77.8	49.9

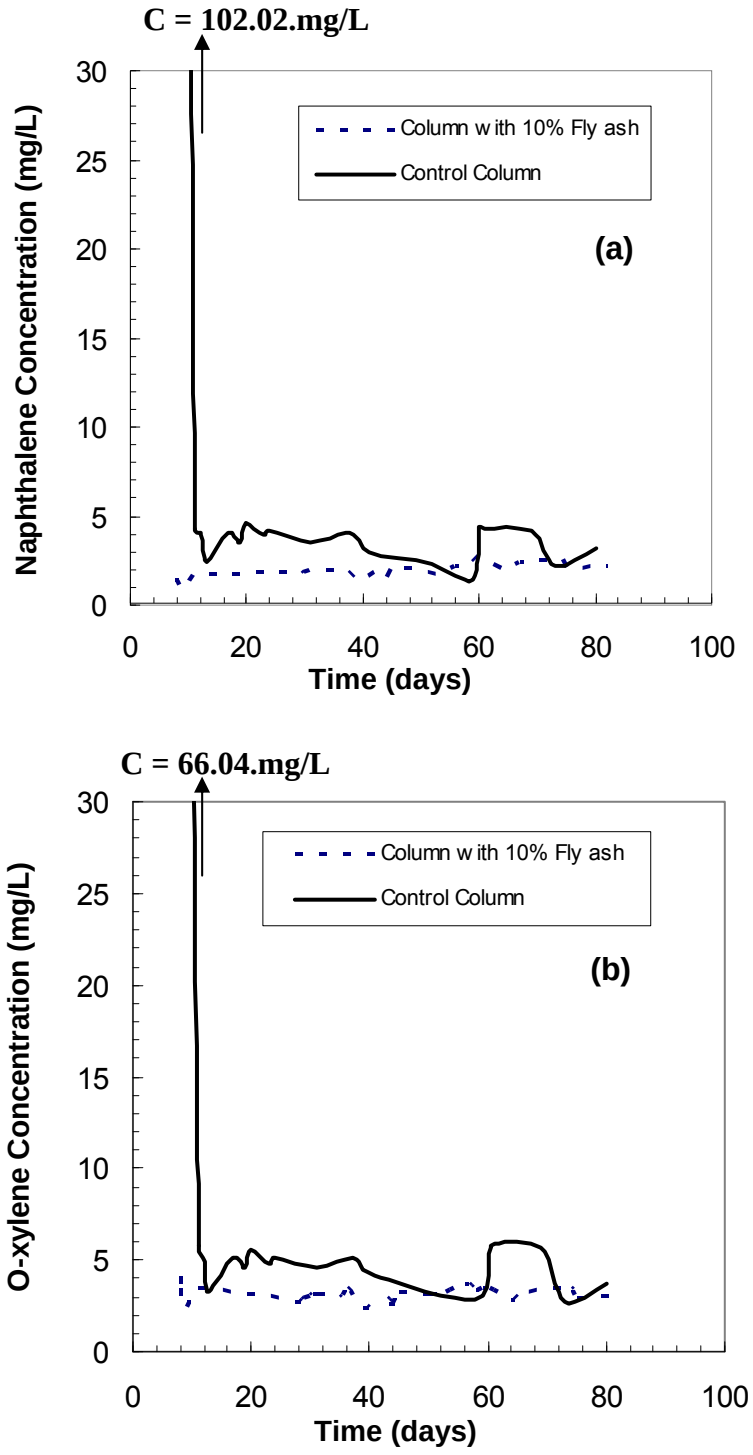

Figure 4. 10 (a) Naphthalene, and (b) *o*-xylene concentrations, measured in the effluents, collected from control and 10% fly ash-amended column (both columns are contaminated with 2% NAPL by weight).

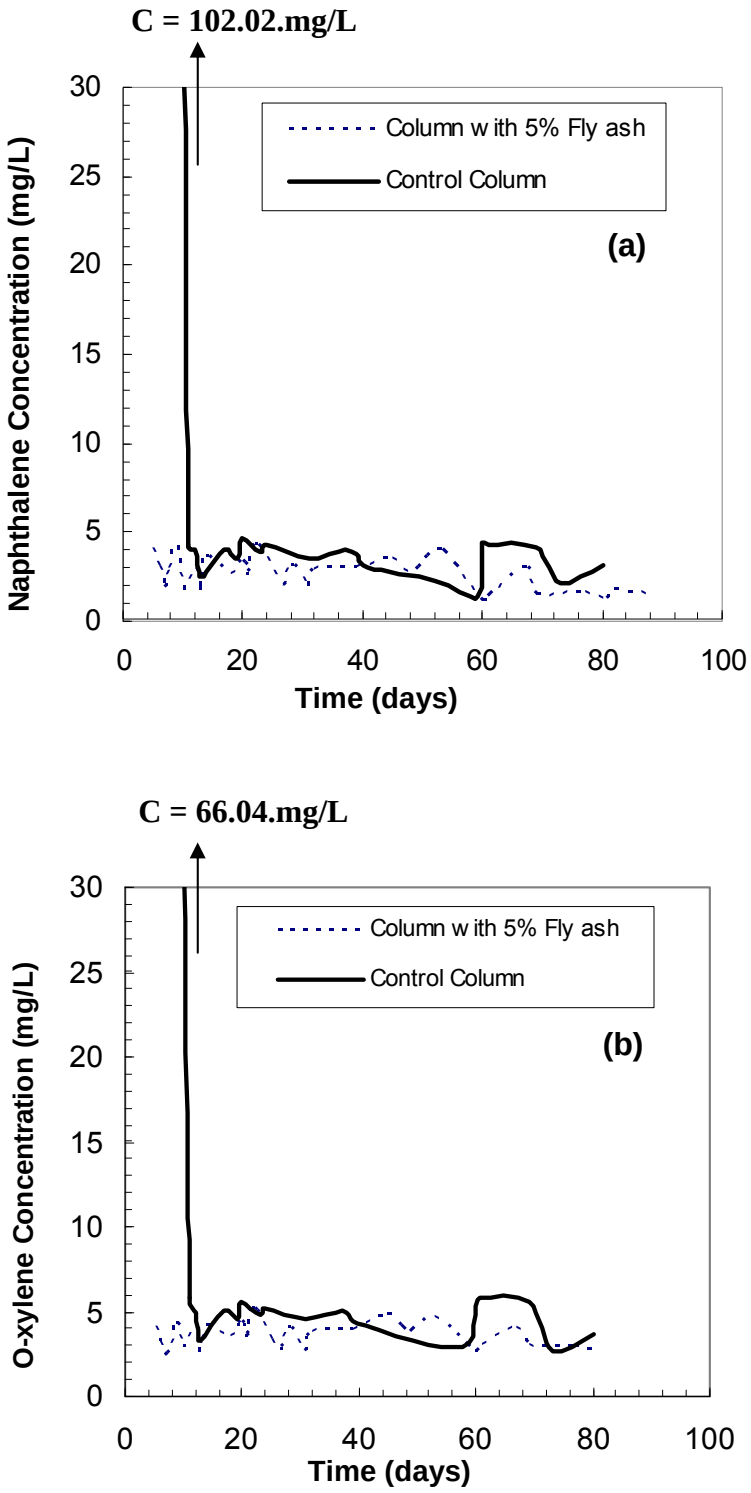

Figure 4. 11 (a) Naphthalene, and (b) o-xylene concentrations measured in the effluents collected from control and 5% fly ash amended column (both columns are contaminated with 2% NAPL by weight).

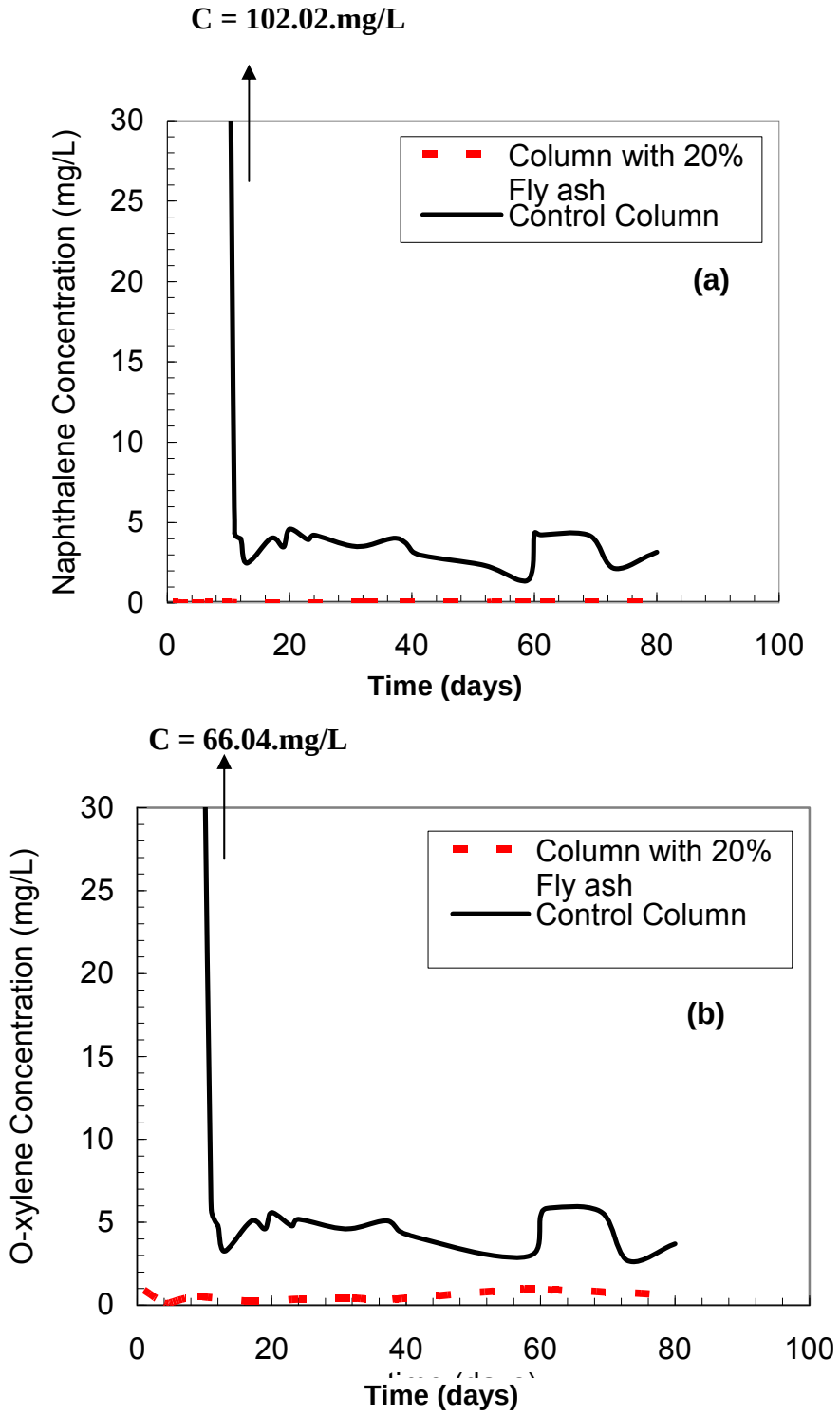

Figure 4.12 (a) Naphthalene, and (b) o-xylene concentrations measured in the effluents collected from control and 20 % fly ash-amended column (both columns are contaminated with 2% NAPL by weight).

concentrations in the control column were measured as 66.04 mg/L and 102.02 mg/L for o-xylene and naphthalene, respectively, and dropped to about 5 mg/L within 8 days. The low sorptive capacity of the borrow material is believed to have caused this effect. The fly ash, on the other hand, limited this release and immobilized the contaminants due to its high sorptive capacity. As a result, the initial effluent concentrations from the fly ash-amended specimens are quite low as compared to those measured in the effluent collected from the borrow material.

The concentrations of o-xylene and naphthalene in the first effluent samples were, respectively, 4.2 mg/L and 4.3 mg/L, for the column with 5% fly ash, 4.17 mg/L and 1.58 mg/L, for the column with 10% fly ash, and 0.92 mg/L and 0.03 mg/L, for the column with 20% fly ash. The differences between the concentration in the control and fly ash-amended columns, and the very high initial control concentrations indicate that there was probably an initial release of NAPL in the control column, because the measured naphthalene concentration was much higher than the water solubility of this chemical organic chemical.

An initial NAPL release from the 2% NAPL control column is also supported by the dodecane data (data not shown). The initial dodecane concentrations were relatively high in the effluents of the 2% NAPL columns (533 mg/L and 3 mg/L for control and borrow material/fly ash columns, respectively).The quasi-steady state dodecane concentrations in the effluent collected from the 2% NAPL columns were also higher than expected, based on dodecane's solubility, suggesting that the source of dodecane may have been the NAPL blobs inside the column. It is believed that these NAPL blobs coated the soil particles and caused high organic concentrations in the effluent.

Accordingly, the results for the 2% NAPL columns suggest that the high carbon content in the fly ash is suitable for immobilization of organic constituents in soils contaminated with petroleum residues.

The effluent concentrations of naphthalene and *o*-xylene for the 5%, 10% and 20% fly ash-amended columns contaminated with 0.5% NAPL are shown in Figures 4.13 4.14, and 4.15, respectively. One important effect of lowering the contamination level was that no initial NAPL release was observed from any of the 0.5% NAPL columns, based on the low initial naphthalene and *o*-xylene concentrations in the effluent. Furthermore, no dodecane was observed in the effluent collected from the 0.5% NAPL columns, which supports this conclusion.

Figures 4.13 through 4.15 show that naphthalene and *o*-xylene effluent concentrations in the 5%, 10%, and 20 % fly ash-amended columns were consistently lower than those measured in the control columns. The results again suggest that the high carbon content in the fly ash is suitable for immobilization of organic constituents in soils contaminated with petroleum residues especially for lower levels of NAPL contamination.

4.3.2.3 Effect of Biodegradation on Column Leaching Tests

During the column leaching tests, the gradual reduction in the contaminant concentration by time could have been due to biodegradation of these compounds by naturally-occurring microorganism. In order to evaluate the effect of biodegradation on the petroleum contaminated soils, petroleum hydrocarbon degrader bacterial populations were determined in the effluent from the 0.5% NAPL contaminated columns. The effluent samples were collected following the same procedure with the concentration determination and bacterial population was determined following the MPN procedure.

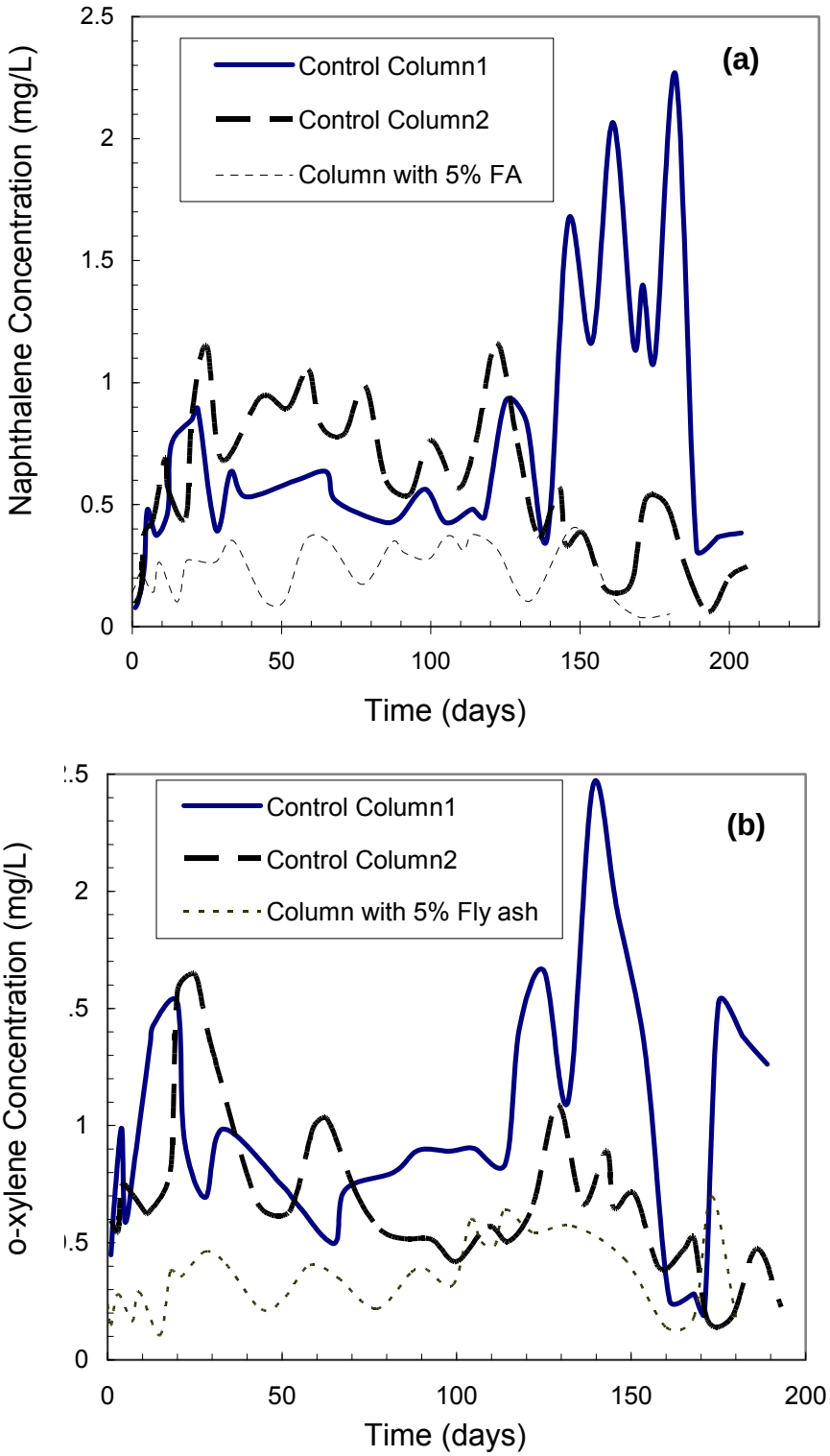

Figure 4.13 (a) Naphthalene, and (b) o-xylene concentrations measured in the effluents collected from control and 5% fly ash amended column (both columns are contaminated with 0.5% NAPL by weight).

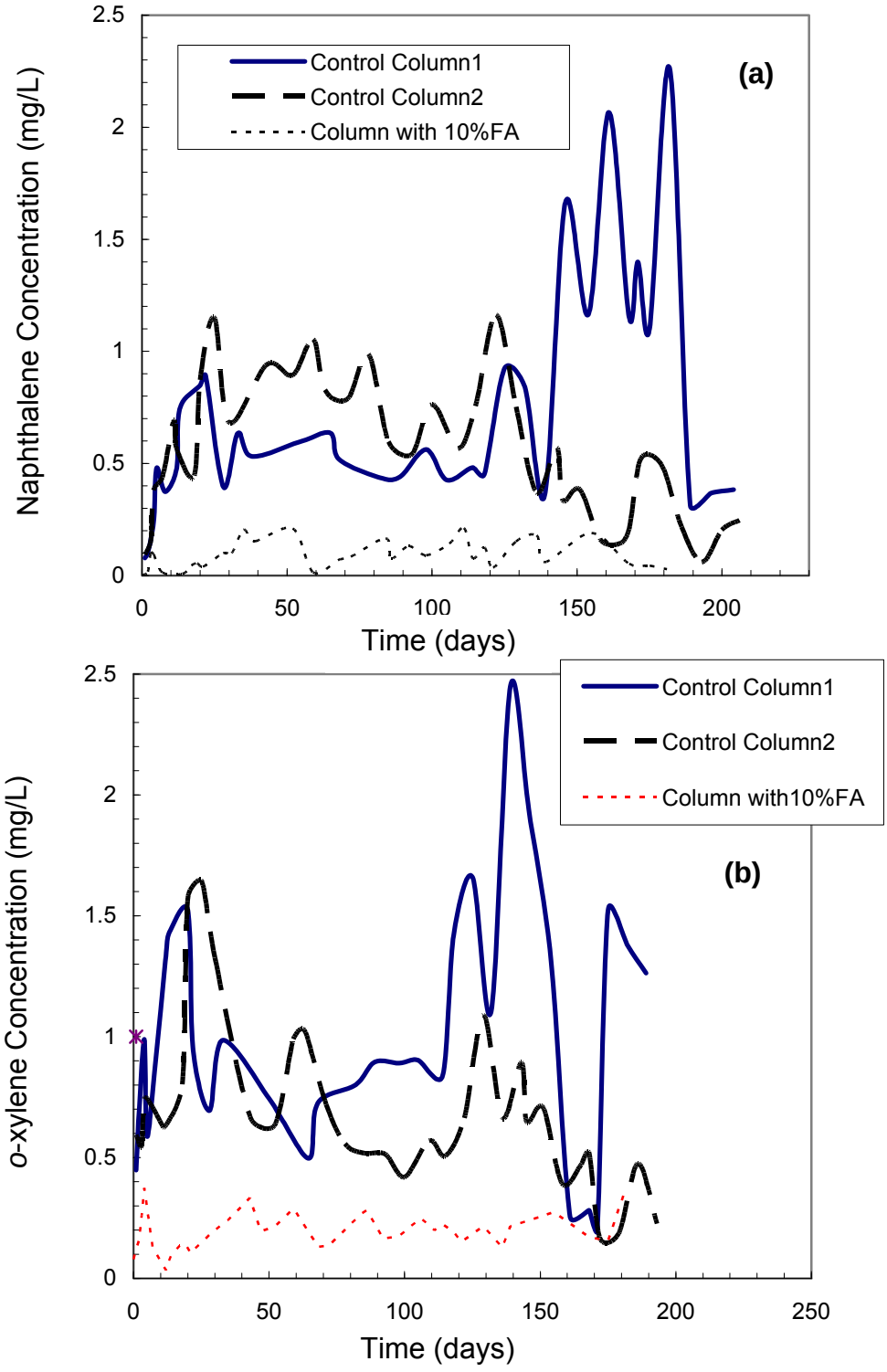

Figure 4. 14 (a) Naphthalene, and (b) *o*-xylene concentrations measured in the effluents collected from control and 10% fly ash amended column (both columns are contaminated with 0.5% NAPL by weight).

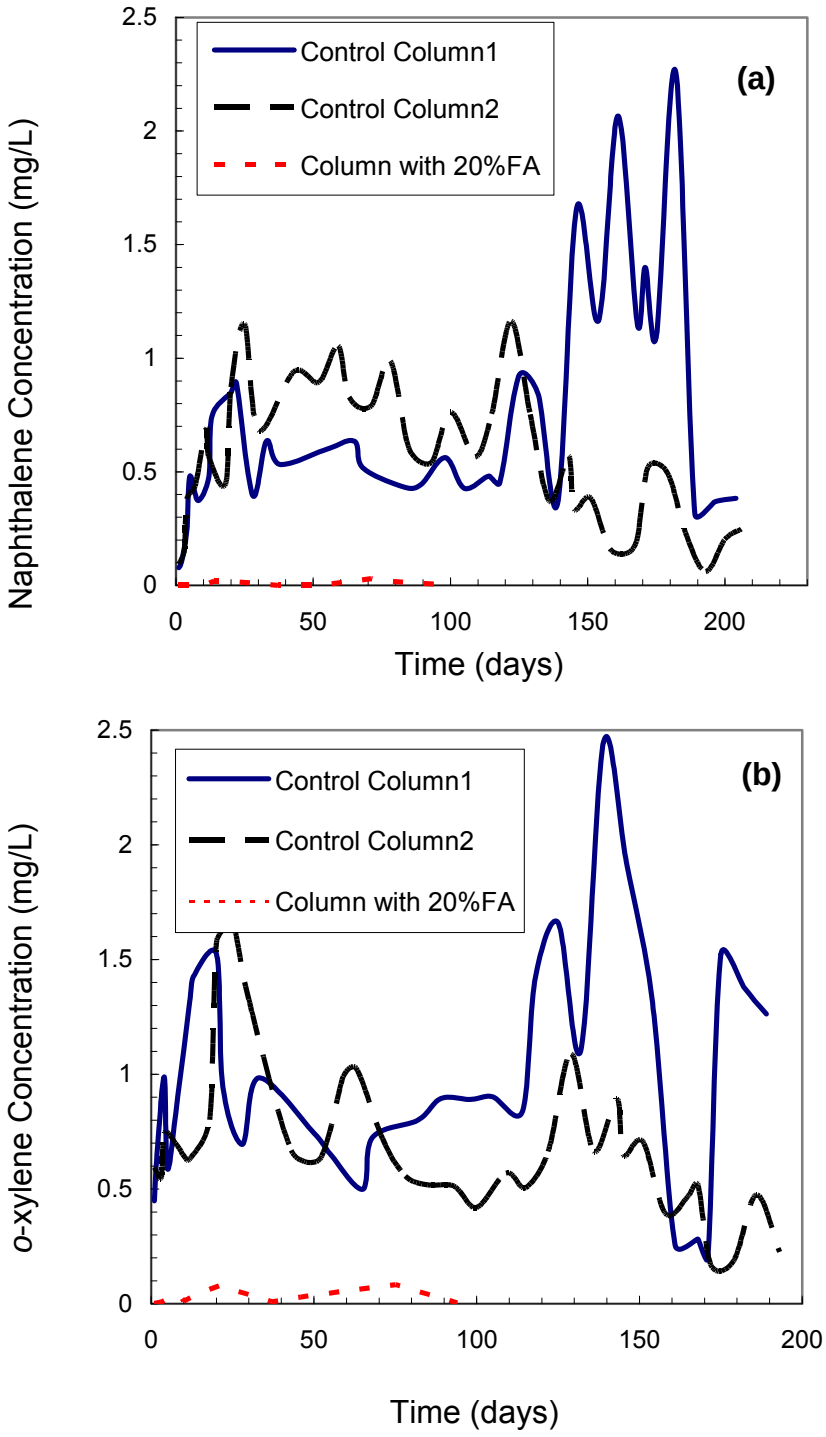

Figure 4. 15 (a) Naphthalene, and (b) *o*-xylene concentrations measured in the effluents collected from control and 20% fly ash amended column (both columns are contaminated with 0.5% NAPL by weight).

As mentioned earlier there were two control columns with 0.5% NAPL contamination. The MPN numbers that are corrected for bias are shown in Figure 4.16. During the first of 175 days of testing, the levels (changing between log 2 to log 5) of NAPL degrader population exists in both columns (Haines et al. 1996). On the 175th day, to investigate the degree of biodegradation observed in the contaminated soils, 400 mg/L mercury chloride ($HgCl_2$) was added to the influent solution of the Control Column 1. This concentration level of $HgCl_2$ was chosen by following the recommendations of Mihelcic and Luthy (1988). A slight reduction in the MPN numbers after the $HgCl_2$ application is evident for Control Column 1 (Figure 4.16). In comparison, the MPN values were generally greater for the Control Column 2 effluent during the same period. Nevertheless, the data suggest that the $HgCl_2$ concentrations were not high enough to eliminate the microbial activity in the columns. Consequently, it was not possible to distinguish how much of the overall contaminant removal process was due to biodegradation versus sorption.

In order to better determine effect of biodegradation in the fly ash-amended contaminated soils, the 20% fly ash-amended columns contaminated with 0.5% and 2% NAPL contaminations were subjected to the $HgCl_2$ addition after 86 days of testing. The MPN results corrected for bias during the column leaching tests are shown in Figure 4.17. During the first 86 days of the experiments the 2% NAPL column generally had higher levels of bacterial populations than the 0.5% NAPL column. This is attributed to the higher level of bioavailability of the contaminant compounds, which would have yielded higher microbial activity in the column.

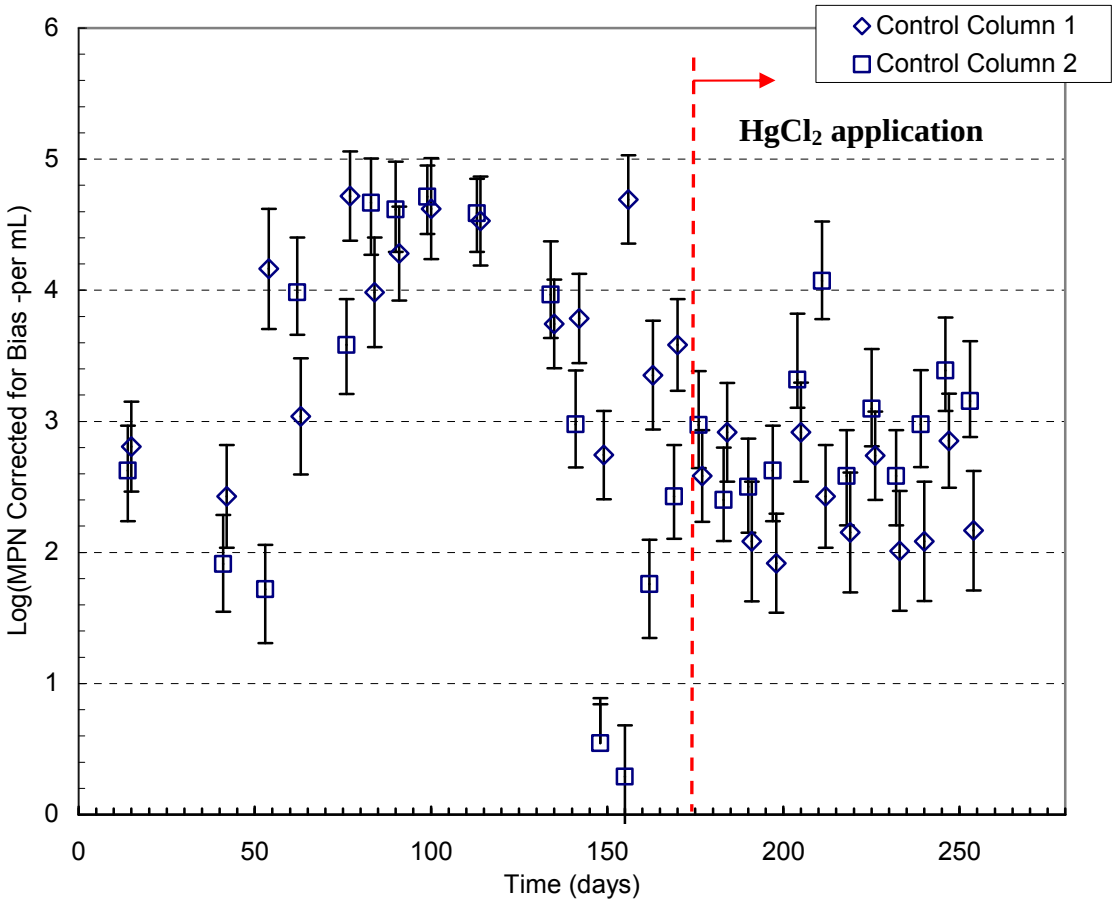

Figure 4.16 The logarithmic MPN numbers corrected for bias per mL of effluent during experiment period from control columns of 0.5 % NAPL contamination ($HgCl_2$ was applied to Control Column 1 after 175 days)

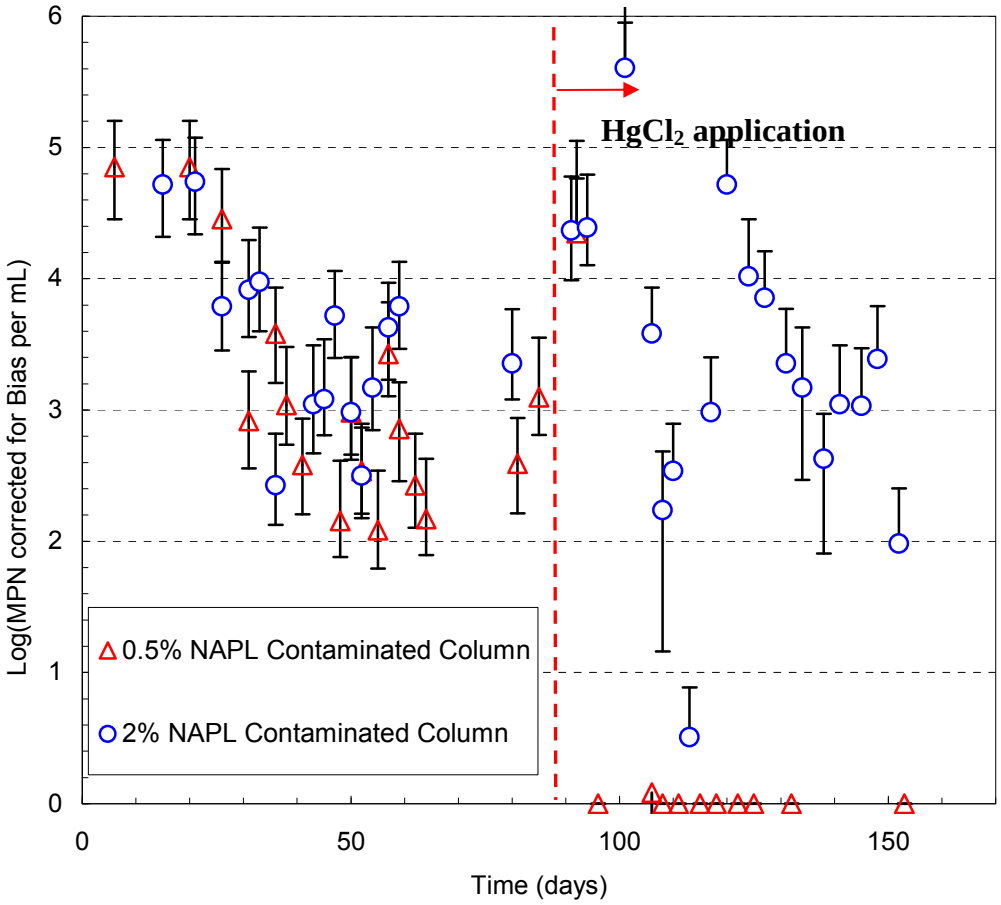

Figure 4. 17 Logarithmic MPN numbers corrected for bias per mL of effluent during experiment period from 20% fly ash-amended column with 0.5% and 2% NAPL contaminations

After 86 days of testing, 400 mg/L $HgCl_2$ was added to both columns. The log MPN value dropped to 0 (zero) upon application of the inhibitor for the 0.5% NAPL column (Figure 4.17). However, same observations can not be made for the 2% NAPL column. This continuing biodegradation process is most probably due to the higher bioavailability of the NAPL compounds to the microorganisms in the 2% NAPL column. As mentioned above, the higher levels of contamination yielded a higher degree of microbial activity and, therefore, the applied inhibition was not capable of eliminating it completely. On the other hand, a comparison of Figures 4.16 and 4.17 shows that the 20 % fly ash addition limited the bioavailability of the contaminants, which was confirmed by lower microbial levels in the fly ash-amended column compared to the control columns. Consequently, the presence (and probably amount) of fly ash and the degree of contamination are two important factors that play a major role in the biodegradation process during remediation of petroleum contaminated soils.

The above mentioned effects of biodegradation are also supported by examining the concentrations of the contaminants in the effluent during the test period. Figure 4.18 shows the aqueous concentrations of naphthalene and *o*-xylene from the 0.5% and 2% NAPL columns with 20 % fly ash addition. As discussed above, before the application of $HgCl_2$ to both columns, the hydrocarbon levels in the column effluents strongly depend on the levels of contaminations, with the 2% NAPL column having consistently higher aqueous naphthalene and *o*-xylene concentrations. This trend continues after the application of the inhibitor. However, in both columns the aqueous concentrations of both compounds were elevated due to the inhibition of biodegradation. The increases in

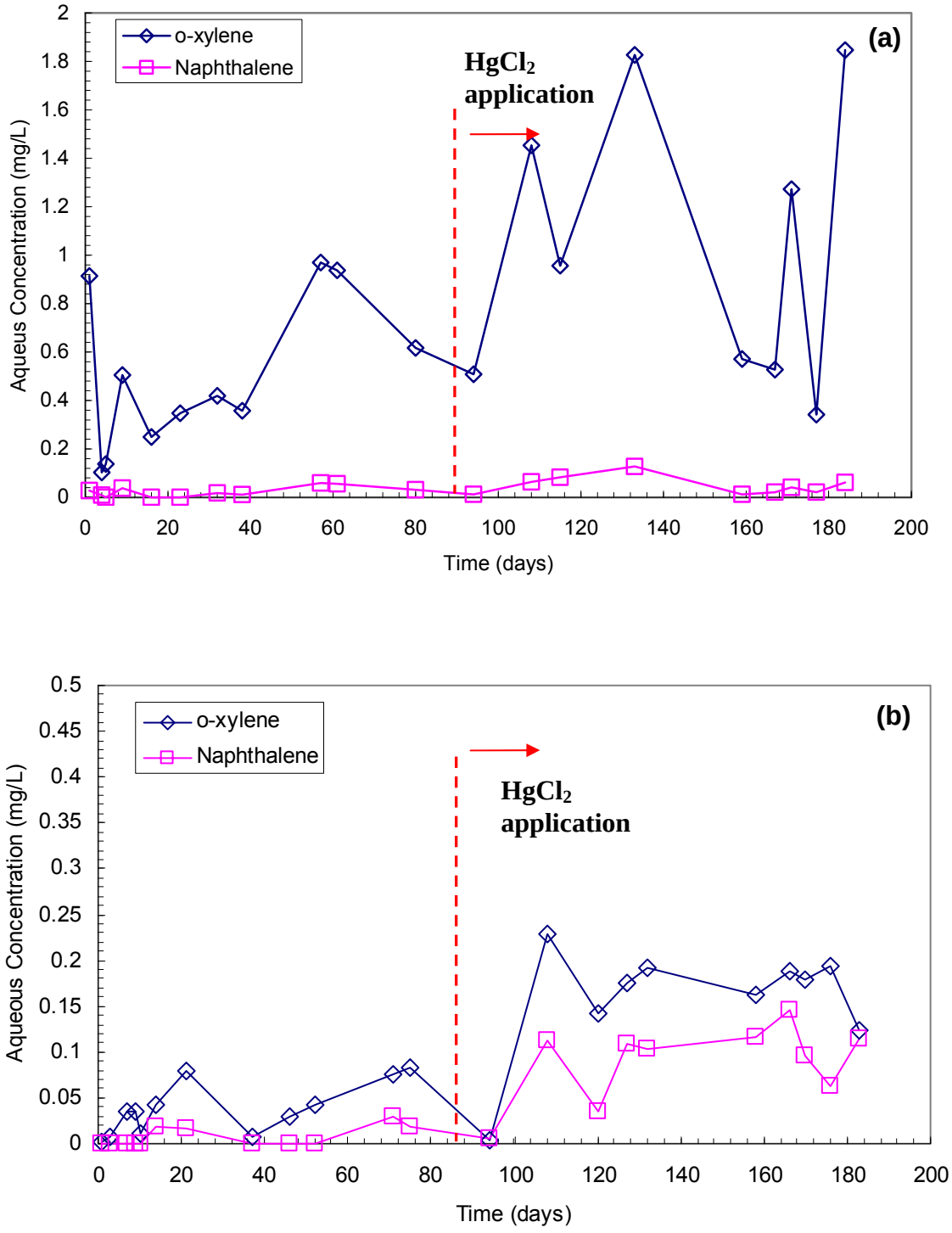

Figure 4.18 Naphthalene and *o*-xylene concentrations from (a) 2% NAPL column with 20% fly ash addition, and (b) 0.5% NAPL column with 20 % fly ash addition

the aqueous phase concentrations were more obvious in 0.5 % NAPL contaminated column, consistent with the fact that in this column there is no biodegradation (log MPN equal to zero).

One of the reasons behind addition an inhibitor with to the control and fly ash amended columns was to determine the column behavior under no microbial activity so that the difference between the control and fly ash amended column was solely due to adsorption of compounds on to fly ash. Unfortunately, the insufficient level of inhibition in the control column prevented us from doing so. Nonetheless, the positive effect of fly ash addition is clear from comparison of the biodegradation levels (MPN results) and compound concentration in the effluent.

4.3.2.4 Comparison of Column Leaching Test Results and Allowable Limits

Before the application of the microbial inhibitor, a quasi-steady state period for each column test was defined when the effluent solute concentration was relatively constant. Therefore, the average effluent concentrations during that period were calculated. A summary of these steady state average effluent concentrations along with the groundwater contamination limits set by the Maryland Department of Environment (MDE) is presented in Table 4.6 (MDE 2001). The concentrations of naphthalene leached from the columns are above the MDE groundwater protection limits for all cases, except for the 0.5% NAPL tests with 10% and 20% fly ash. On the other hand, *o*-xylene concentrations are constantly below the much higher MDE groundwater protection limit for all columns. These findings suggest that a minimum of 10% high carbon content fly ash should be added to the soils contaminated with petroleum residues in order to control their leachability.

The data in Table 4.6 also suggest that the NAPL amounts should be limited to or reduced to 0.5% (or less) by weight (e.g., by aging or aerating) before using fly ash for chemical stabilization. This recommendation was also supported when the concentrations of the measured pollutants are compared with the limits set by the MDE for soil clean-up in residential areas (Table 4.7). The concentrations are below the limits for non-residential areas in all cases (Table 4.8).

It should be noted that the fly ash addition does not reduce the mass of contaminant in the soil but rather the pollutant is blocked in the material due to high sorption capacity of the fly ash. Therefore, it is more appropriate to compare the mass of organics with the MDE-based soil limits rather than making comparison with the MDE groundwater protection limits provided that successful encapsulation of the organic is achieved.

These findings indicate that the high-carbon content fly ashes can be good sorptive agents for remediation of petroleum contaminated soils due to their low cost and presence of high carbon content. However, caution should be exercised when extending these laboratory results to field conditions, because the level of contamination may have a significant effect on leaching properties. For instance, the NAPL was added to the soils at 2% by weight in the current study, and the observed naphthalene concentrations in the effluent were generally higher than Maryland Department of Environment groundwater protection limits. On the other hand, the *o*-xylene concentrations were lower than those limits, and the naphthalene amounts in the effluent were also significantly lower than the Maryland Department of Environment soil clean-up limits for non-residential areas.

Table 4. 6 Comparison of steady state NAPL compound concentrations with MDE groundwater protection limits.

Contamination Level	Column Type	Compound	Steady State Conc. of Organic (mg/L)	MDE groundwater protection limits (mg/L)	Exceed MDE Standards?
2%	Control	Naphthalene	3.54	0.01	**YES**
		o-xylene	4.57	10	NO
	20% Fly ash - amended	Naphthalene	0.03	0.01	**YES**
		o-xylene	0.51	10	NO
	10% Fly ash- amended	Naphthalene	1.85	0.01	**YES**
		o-xylene	3.01	10	NO
	5% Fly ash- amended	Naphthalene	2.67	0.01	**YES**
		o-xylene	3.54	10	NO
0.5%	Control 1	Naphthalene	0.43	0.01	**YES**
		o-xylene	0.94	10	NO
	Control 2	Naphthalene	0.55	0.01	**YES**
		o-xylene	0.91	10	NO
	20% Fly ash- amended	Naphthalene	0.018	0.01	NO
		o-xylene	0.035	10	NO
	10% Fly ash- amended	Naphthalene	0.029	0.01	NO
		o-xylene	0.10	10	NO
	5% Fly ash- amended	Naphthalene	0.20	0.01	**YES**
		o-xylene	0.25	10	NO

Table 4. 7 Comparison of initial mass of NAPL compounds with MDE residential cleanup limits

Contamination Level	Column Type	Compound	Initial Mass of Organic (mg/kg)	MDE Residential Cleanup limits (mg/kg)	Exceed MDE Standards ?
2%	Control	Naphthalene	367	160	**YES**
		o-xylene	267	16000	NO
	20% Fly ash-amended	Naphthalene	150	160	NO
		o-xylene	124	16000	NO
	10% Fly ash-amended	Naphthalene	261	160	**YES**
		o-xylene	170	16000	NO
	5% Fly ash-amended	Naphthalene	269	160	**YES**
		o-xylene	201	16000	NO
0.5%	Control 1	Naphthalene	48	160	NO
		o-xylene	34	16000	NO
	Control 2	Naphthalene	50	160	NO
		o-xylene	31	16000	NO
	20% Fly ash-amended	Naphthalene	23	160	NO
		o-xylene	1	16000	NO
	10% Fly ash-amended	Naphthalene	41	160	NO
		o-xylene	6	16000	NO
	5% Fly ash-amended	Naphthalene	47	160	NO
		o-xylene	14	16000	NO

Table 4. 8 Comparison of initial mass of NAPL compounds with MDE non-residential cleanup limits

Contamination Level	Column Type	Compound	Initial Mass of Organic (mg/kg)	MDE Non-Residential Cleanup limits (mg/kg)	Exceed MDE Standards ?
2%	Control	Naphthalene	367	4300	NO
		o-xylene	267	410000	NO
	20% Fly ash-amended	Naphthalene	150	4300	NO
		o-xylene	124	410000	NO
	10% Fly ash-amended	Naphthalene	261	4300	NO
		o-xylene	170	410000	NO
	5% Fly ash-amended	Naphthalene	269	4300	NO
		o-xylene	201	410000	NO
0.5%	Control 1	Naphthalene	48	4300	NO
		o-xylene	34	410000	NO
	Control 2	Naphthalene	50	4300	NO
		o-xylene	31	410000	NO
	20% Fly ash-amended	Naphthalene	23	4300	NO
		o-xylene	1	410000	NO
	10% Fly ash-amended	Naphthalene	41	4300	NO
		o-xylene	6	410000	NO
	5% Fly ash-amended	Naphthalene	47	4300	NO
		o-xylene	14	410000	NO

The hydraulic gradients applied onto the column specimens in the current study varied from 4 to 5. Although use of such hydraulic gradients were necessary to trigger the flow from the low permeability clayey sandy soils in the laboratory, it is known that the field hydraulic gradients in embankment applications are typically 3 to 4 times lower than these values. Therefore, it is believed that the field concentrations of petroleum hydrocarbons in leachate from fly-ash stabilized soils are likely to be below the laboratory measured values.

4.3. Conclusions

Based on the results of a battery of compaction tests and column leaching experiments on petroleum contaminated soils stabilized with high carbon content fly ash the following findings can be reported; The laboratory test procedures indicated that the traditional approaches undertaken for preparation and testing of soils for their geotechnical and environmental analyses may not be applicable to petroleum contaminated soils. Deviations from the standard procedures, such as usage of liquid content instead of water content for evaluating the compaction test data, aging of specimens before compaction, and proper selection of the solid-to-solution ratio for batch-scale adsorption tests, should be considered.

The column leaching tests performed on the Brandon Shores fly ash-stabilized specimens indicate that the naphthalene and *o*-xylene concentrations in the effluents collected from the fly ash stabilized specimens were lower than those collected from the control specimen. The addition of this high carbon content fly ash (LOI= 13.4%) limited the initial release of the contaminants from the specimen, compared to a longer release

observed from the control column. Finally, the presence of fly ash and the degree of contamination were two important factors that played a major role in the biodegradation process during remediation of petroleum contaminated soils.

The findings indicate that the high-carbon content fly ash can be a good sorptive agent for remediation of petroleum contaminated soils due to its low cost and presence of high carbon content. However, caution should be exercised when extending these laboratory results to field conditions, because the level of contamination may have a significant effect on leaching properties. For instance, the NAPL was added to the soils at 2% by weight in the current study and the observed naphthalene concentrations in the effluent were generally higher than the U.S. EPA maximum concentration limits or Maryland Department of Environment groundwater protection limits. On the other hand, the o-xylene concentrations were lower than those limits, and the naphthalene amounts in the effluent were also significantly lower than the Maryland Department of Environment soil clean-up limits for non-residential areas.

Chapter 5 High Carbon Content Fly ash as a Reactive Medium in a PRB: Column Sorption Desorption Experiments

Remediation of groundwater contaminated with petroleum-based products has been an important task for engineers and scientists in recent years. The challenges associated with reducing subsurface contamination levels have led to research and development resulting in several innovative in-situ treatment technologies. One of the passive remediation technologies that is gaining wide acceptance is the use of permeable reactive barriers (PRB). In this technology, the pollutants are immobilized permanently or their levels are reduced to the Maximum Contamination Limits (MCL) while the plume is passing through an underground barrier system.

One relatively new variation on the PRB concept is to use an immobilization process, in which the organic pollutants are adsorbed onto the sorptive surface of the barrier material. The reaction mechanism in these PRBs is often adsorption, and the term "permeable sorptive barriers (PSB)" has been recently introduced (Woinarski et al. 2003) to describe these systems. Typical compounds that are targeted for treatment with such systems include trichloroethylene (TCE), petroleum hydrocarbons, as well as radioactive solutes (e.g., Strontium Sr^{90}) (Rabideau et al. 2001).

Laboratory studies have demonstrated the effectiveness of various natural and synthetic sorbents as potential reactive/sorptive media for treatment of groundwater containing both organic and inorganic pollutants. Specific examples of reactive and sorptive materials that have been investigated include such as wood chips, limestone, manure (USEPA 2006), peat (Guerin et al. 2002), lignitic coal (Jenk et al. 2003), and

activated carbon (Schad and Gratwohl 1998). Furthermore, there is growing interest in the utilization of recycled materials for remediation of contaminated groundwater as a part of sorptive barrier investigations. Recycled materials, such as tire chips (Kim et al 1997) and foundry sand (Lee et al. 2004) have also been studied to investigate their feasibility as sorptive medium in these barrier systems.

As discussed in Chapter 3, the batch adsorption data revealed that high carbon content fly ash (HCCFA) could potentially be a good sorptive medium for a reactive barrier application for mitigation of petroleum hydrocarbon contamination in the subsurface. However, batch adsorption tests do not entirely simulate the field conditions, and a more quantitative analysis of the sorption-desorption phenomena in the environment is expected from the column sorption tests. Column tests have been widely used in previous studies to evaluate the sorptive material as a barrier medium, to estimate the rate and capacity of contaminant retardation, and to evaluate the working life of the barrier (e.g., Cantrell and Kaplan 2001, Patterson et al 2002, Rasmussen et al. 2002, Su and Puls 2003, Gusmao et al 2004, Lee and Benson 2004, Rabideau et al. 2005). Therefore, to investigate the adsorption characteristics of HCCFA for its potential use as a PSB medium for removal of petroleum residues from groundwater, a series of column sorption experiments were conducted with three HCCFAs and PAC, and two potential groundwater contaminants (naphthalene and o-xylene). A sorptive barrier design is described using the column derived parameters and considering the barrier dimensions and barrier life expectancies.

5.1 Experimental Materials and Methods

5.1.1. Sorptive Media

Column sorption-desorption tests were conducted using three different fly ashes and PAC as the reactive media. The three fly ashes were selected so as to cover the whole range of LOI in the Maryland fly ashes: Dickerson Precipitator (DP) with 20.5 %LOI, Paul Smith (PS) with 10.7 % LOI, and Morgantown (MT) with 3.1 % LOI. The properties of these fly ashes were described in detail in Chapter 3.

5.1.2 Sand

The sand used in the reactive medium was #1 Q-Roc silica sand (US Silica, Berkeley Springs, West Virginia). The grain size distribution of the sand is given in Figure 5.1. The chemical composition of the sand is given in Table 5.1 by the manufacturer. The specific gravity, pH and hardness of the sand are 2.65, 6.5 and 7 mohs, respectively.

5.1.3 Synthetic Groundwater and Target Contaminants

All the column sorption-desorption experiments were conducted using a dilute mineral salt solution. This aqueous solution, here after referred to as the synthetic groundwater was adopted from artificial similar groundwater solutions used by Murphy et al. (1997) and Song (2005) except for the addition of potassium chloride (KCl) as an essential macronutrient for bacterial growth. The synthetic groundwater was prepared using deionized water generated by the Hydro Service reverse osmosis ion exchange system (model L2PRO-20). The constituents of the synthetic groundwater are given in Table 5.2.

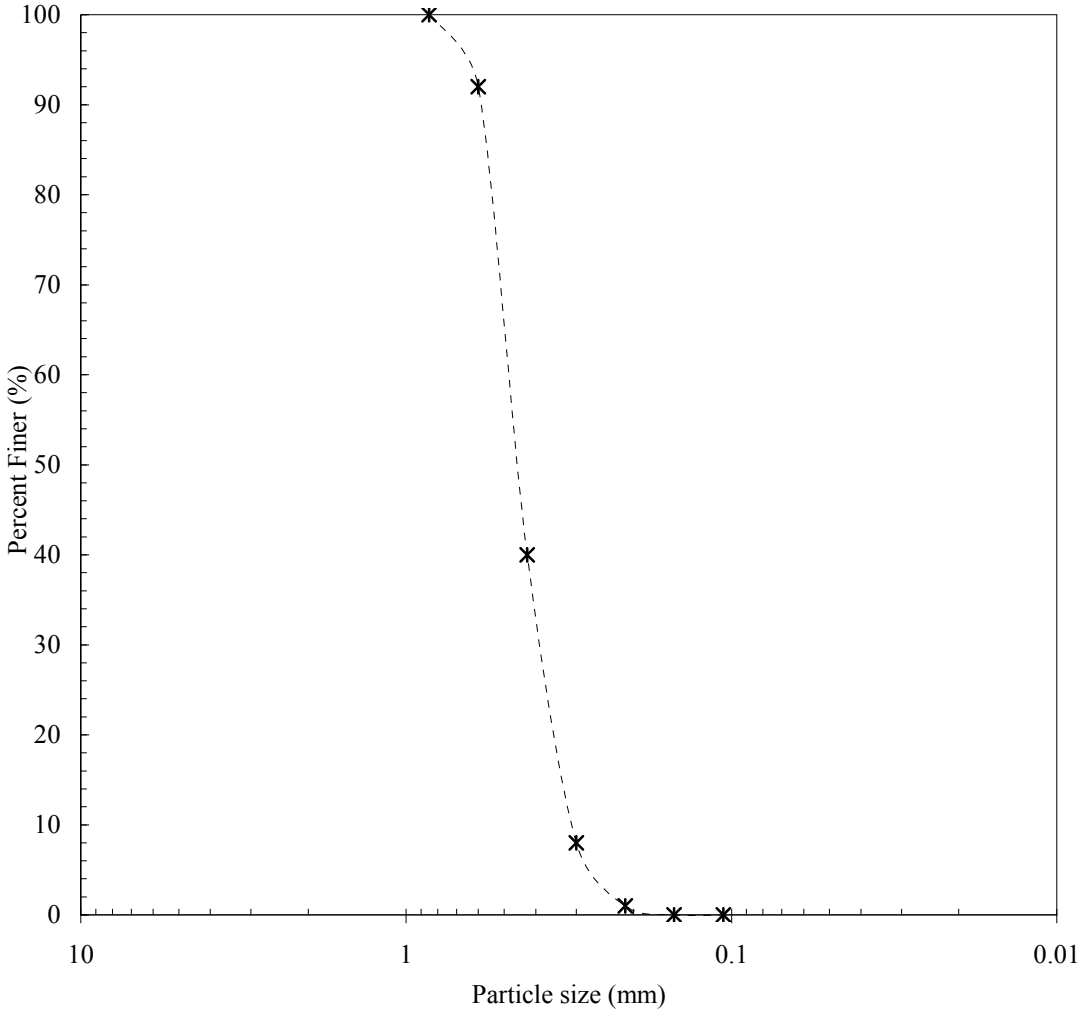

Figure 5.1 Grain size distribution of the sand used in the column experiments

Table 5.1 Chemical composition of the sand used in the study (US Silica, Berkeley Springs, West Virginia).

Compound	**% (by weight)**
SiO_2 (Silicon Dioxide)	99.7
Fe_2O_3 (Iron Oxide)	0.022
Al_2O_3 (Aluminum Oxide)	0.07
TiO_2 (Titanium Oxide)	0.02
CaO (Calcium Oxide)	0.01
MgO (Magnesium Oxide)	<0.01
Na_2O (Sodium Oxide)	<0.01
K_2O (Potassium Oxide)	0.01
LOI (Loss on Ignition)	0.2

The synthetic groundwater was prepared using three different stock solutions. The first was a macronutrient solution, which was prepared at 100 times the final solution concentrations by adding 10 mg of $FeSO_4 \cdot 7H_2O$, 200 mg of $MgSO_4 \cdot 7H_2O$, 300 mg NH_4Cl, 60 mg $NaH_2PO_4 \cdot H_2O$, and 60 mg KCl to 1 L deionized water. The second solution was the micronutrient solution and was prepared by first dissolving 50 mg each of $MnCl_2$, Na_2SeO_3, H_3BO_3, $Na_2MoO_4 \cdot 2H_2O$, $CoCl_2 \cdot 6H_2O$, $NiSO_4 \cdot 6H_2O$, $CaSO_4 \cdot 5H_2O$, and $ZnSO_4 \cdot 7H_2O$ into 1 L deionized water, from which 10 ml was taken out and diluted into 1 L with deionized water to obtain the trace stock solution. The third stock solution was the PIPES (Sigma Chemical Co., 99%) stock buffer solution, which was prepared by dissolving 151.2 g PIPES into 2L deionized water, and then adjusting the pH to 6.8 with 4 N NaOH. The synthetic groundwater was prepared by diluting 10 mL from each of the macronutrient and micro nutrient stock solutions, and 40 mL from PIPES stock solution in 1 L deionized water. The pH of the prepared synthetic groundwater was recorded and set to 6.9. All synthetic groundwater solutions were autoclaved for 20 minutes at 121 ^{0}C and 21 psi to eliminate any bacterial activity during tests.

Naphthalene and *o*-xylene were the target contaminants. Aqueous naphthalene and *o*-xylene solutions were prepared either from methanol stock solutions stock solutions. The stock solutions were initially prepared by dissolving solid target contaminant in methanol. These methanolic solutions were then used to prepare the aqueous solutions as column influent solution by transferring through a 2 mm sterilized syringe PTFE filters aseptically. . In all cases, it was ensured that the resulting concentration of methanol in the aqueous solutions was lower than 4 % by volume.

Table 5. 2 Synthetic groundwater constituents

Macro Nutrient Compounds	Concentration (mg/L)
$FeSO_47H_2O$	0.1
$MgSO_47H_2O$	2
NH_4Cl	3
$NaH_2PO_4H_2O$	0.6
KCl	0.6
Micro Nutrient Compunds	Concentration (μg /L)
$MnCl_2$	5
Na_2SeO_3	5
H_3BO_3	5
$Na_2MoO_42H_2O$	5
$CoCl_26H_2O$	5
$NiSO_46H_2O$	5
$CaSO_45H_2O$,	5
$ZnSO_47H_2O$	5
Buffer Solution	Concentration (mM)
PIPES	10

5.1.4 Column Test Set Up and Procedures

Rabideau et al. (2001) indicated that the characterization of strongly sorbing materials can best be accomplished by generating complete contaminant breakthrough curves by conducting the column tests in relative short columns, at realistic flow rates and long experimental periods. Alternatively, column experiments can be performed so as to accelerate the breakthrough by running the tests with artificially high flow rates, which may create artifacts due to non-equilibrium sorption, and measuring the sorbed contaminant concentration from the solid medium rather than temporal contaminant distributions. The latter involves indirect measurement of volatile contaminants (i.e., *o*-xylene), which may result in mass balance errors. In this study, the method of realistic flow rates with long experimental runs were chosen because of drawbacks mentioned above for other type of methods.

As described in Chapter 3, the three fly ashes that were used in the column sorption-desorption experiments (i.e., MT, PS, and DP fly ashes) have a fine particle size distribution. Based on the correspondingly low hydraulic conductivity values of three fly ashes ($<10^{-7}$ cm/sec), a mixture of sand and fly ash was prepared as a reactive medium for the column tests. Initially, a commonly adopted mixture ratio of 50% sand and 50 % fly ash (by weight) was prepared and constant head permeability tests were conducted to measure the hydraulic conductivity of the mixture. The results of these initial tests indicated that the hydraulic conductivity was less than 10^{-5} cm/sec, which is one order of magnitude of lower than a typical design value of 10^{-4} cm/sec for PRBs (Gavaskar et al. 1998, Lee and Benson 2004). Furthermore, excess pore water pressures were observed during the tests indicating an impediment of the flow. Therefore, a mixture of 60% sand

and 40% fly ash (by weight) was prepared and subjected to hydraulic conductivity testing. As discussed further below, the measured hydraulic conductivity was on the order of 10^{-4} cm/sec, and all column sorption desorption tests were performed using specimens prepared with 60% sand and 40% fly ash (by weight).

Several issues had to be considered in selecting the column dimensions. First, the column should be large enough to be a representative of the reactive medium in one dimensional flow, so the desired parameters can be determined under controlled conditions. Second, the column set-up should contain sufficient material to minimize the impact of heterogeneity in the fly ash. Third, the column diameter should be sufficiently greater than the porous media particle diameter to minimize short circuiting.

Table 5.3 summarizes the dimensions of columns used in previous studies. The column dimensions and the flow condition vary from one study to another depending on the purpose of the study. In order to keep the flow in one dimensional condition, the diameter was selected as 48 mm in the current study, an intermediate value compared to those used in the literature, and > 20 x diameter of the porous media particles. The height of the column was chosen as 300 mm which provided a volume of 543 cm^3 and holds enough reactive medium to overcome the material heterogeneity.

The tests were performed in CHROMAFLEX® glass columns (Kimble-Kontes #420830-3020). PTFE bed supports with 50 μm stainless steel screens were placed at the bottom and top ends of the columns. Leak-free seals were provided by the screw caps which also held flangeless fittings. All the columns were equipped with three sampling ports along the column at 70, 150 and 230 mm. The sampling ports were fabricated by the Kimble-Kontes custom glass shop using glass tubing with an outer diameter of ¼",

Table 5.3 Column sorption test parameters from recent literature

References	Reactive Material	Target Comp.	Dimension (ID/H) (cm)	Column Material	Flow rate	Seepage velocity	Duration
Lee et al. (2004)	Foundry Sand-Sand (50%-50%)	TCE	2.5x20 2.5x45	Glass	20-60 mL/h	0.8-4.3 m/day	200 PVE
Baciocchi et al. (2003)	ZVI 100%	TCE	5x100	Plexiglass	15 mL/h	0.37 m/d	20 PVE
Su and Puls (2003)	Peerless Iron - Sand(50%-50%)	Arsenic	2.5x31	Glass	28 mL/h	4.3 m/d	1800 PVE
Gusmao et al. (2004)	ZVI	TCE	6x51.5	Acrylic	55.14 mL/h	3.79 cm/h	2.7 PVE
Patterson et al. (2002)	Polymer mats	Atrazine Benzene	NA/200	NA	NA	NA	NA

NA= Not applicable, ZVI= Zero valent iron, PVE= Pore volume of equivalent

which were sealed with compression fittings from Swagelok Inc. (Part # SS-400-6). A PTFE 1/8" female mini-inert septum (Alltech # 631204) was used in the sampling port to hold the sampling needless (VWR Cat. # 20068-696). The sampling needles were originally 70 mm long, but were cut down to a length of 40 mm so that the end could be positioned at the center of the column. The outer surface of the columns was covered with aluminum foil to eliminate photodecomposition and inhibit algae growth.

The feed reservoir was connected to the column inlet via ¼" Teflon Tubing (Cole Parmer Cat. # 31320-50). The columns were operated in an up-flow mode with the influent flow from the feed reservoir provided by a peristaltic pump (Cole Parmer Cat. # 07553-70), which was equipped with a Teflon pump head (Cole Parmer cat. # 078520-40). The Teflon pump head tubing (Cole Parmer Cat. # 77390-50) was connected to ¼" Teflon tubing (Cole Parmer Cat. # 31320-50) by a 4 mm O.D. Teflon tubing (Cole Parmer Cat. # 31321-62). Influent and effluent samples were collected from sampling ports constructed using mini-inert valves with PTFE septum (Alltech Cat. # 654051). A break tube was fabricated to eliminate the contamination of the aspirator bottle (Sigma Aldrich Cat. # Z556017), which was used as a feed (influent) reservoir for the system. On the effluent end, PTFE tubing provided the connection between the column and the effluent reservoir. All other tubings and valves in the system were made of Teflon. All the tubing and sampling port equipment was autoclaved for 20 minutes at 121 ºC and 21 psi before each test. The details of the column set-up are shown in Figure 5.2.

All the column specimens were packed with 3 layers of porous medium. The lower 80-mm of the column was packed with sand only in order to maintain a uniform flow and to prevent the very fine fly ash particles from migrating downward due to the

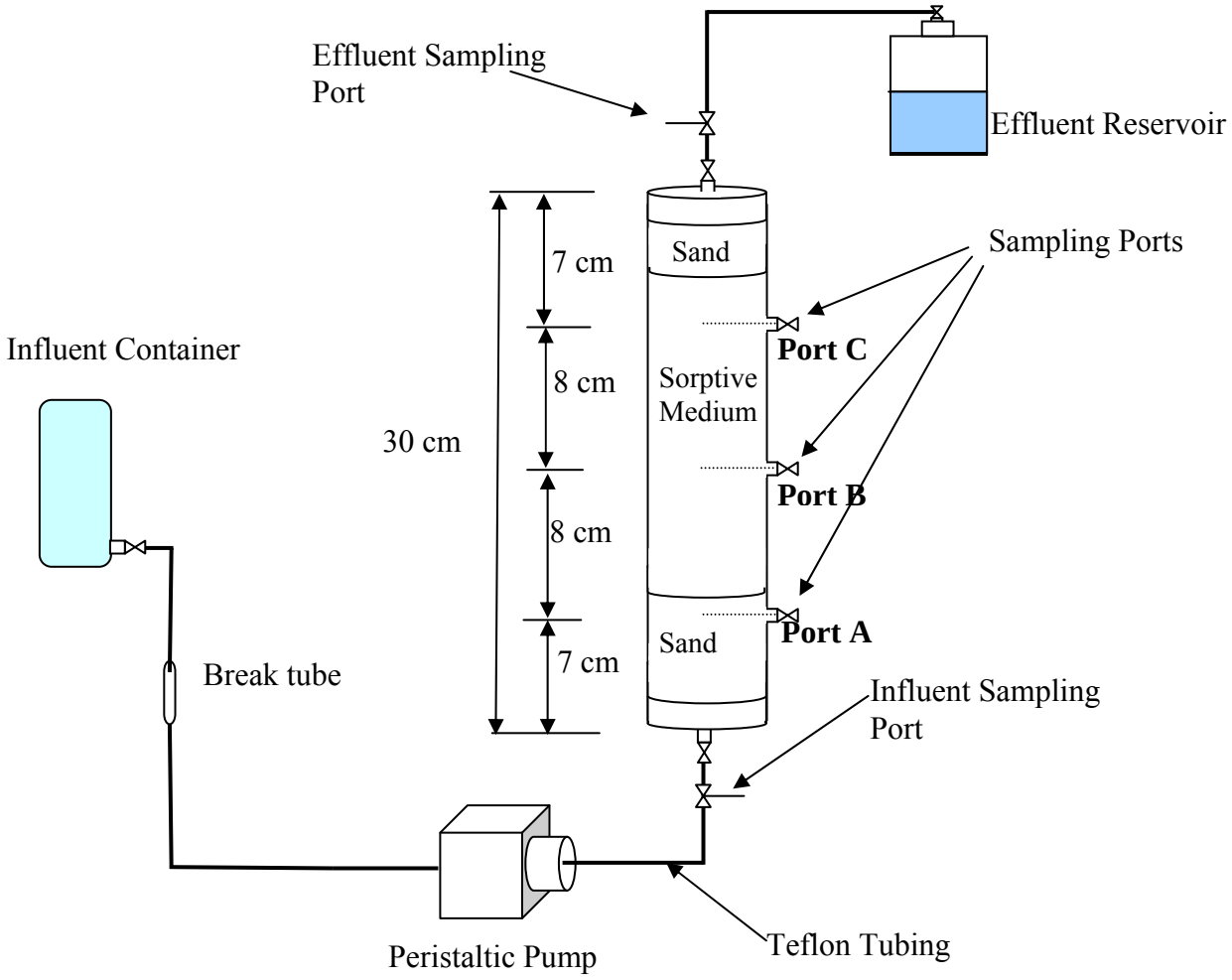

Figure 5.2 Column test set up schematic

gravitational forces and clogging the influent tubing. A height of 80 mm was chosen so that the sand would reach 10 mm above the first sampling port, and help monitoring the influent concentration right before it flows into the sorptive medium. The 190-mm sorptive medium located above this sand layer was a mixture of 60% sand and 40% HCC fly ash by weight overlain by another 30-mm layer of uniform sand. The top sand layer was design to prevent the fine and lighter particles from migrating upward and clogging the effluent. The 190-mm height of the sorptive medium provided reasonable mass between two sampling ports as well as geometrical symmetry between two sampling ports in the fly ash sand mixture. This geometrical symmetry will enable to compare the results of the two consecutive ports.

The media were tamped into the glass column in 5 mm layers by following the procedures outlined by Oliviera et al. (1996). Primary objectives of the packing procedure were to reproducibly achieve a homogenous porosity and bulk density along the column, and a dry density, typical of that expected under field placement conditions. Before packing, the sand and fly ash were sieved through a mess with an opening size of 2 mm, to remove larger size particles. Known quantities of the sieved and well-mixed sand and fly ash-sand mixture were prepared before packing. Then, the material was added to the column using a funnel, 300 mm in length with an 8 mm inner diameter neck, which could hold enough material to form a 5 mm thick layer in the column. Gradually, 5 mm thick batches of material were added during column packing to prevent the segregation and the preferential deposition of larger grained particles. For each layer, the funnel was introduced into the column, with the bottom tip resting on the last layer formed. Then the funnel was filled to capacity with dry material, which was slowly and

uniformly released into the column until the funnel was completely emptied. A heavy, stainless-steel flat pestle, with a diameter of 46 mm and weight of 1.5 kg, was subsequently used for gentle compaction of each layer with a controlled number of tamps. The compaction surface of the pestle was leveled in order to get equal pressure input over the freshly deposited layer. This packing sequence was repeated until the column was filled to the top, using the three types of medium described above. The uniformity of the packing was monitored after every 50 mm of material was deposited. At those points, the material remaining was weighed and mass subtracted from the known amount of initial mass, so that the mass of packed material and the bulk density of the 50 mm layer could be calculated. In this way, a uniform density along the column in the medium density was achieved during packing procedure. Typical packed column orientation is shown in Figure 5.3.

Before the start of sorption-desorption tests, the columns were sterilized by gamma irradiation in one of two ways. In most cases, after packing of the medium inside the column, the columns were exposed to gamma irradiation at a dose of 30 kGw for 48 hours at the University of Maryland, Department of Chemical and Nuclear Engineering gamma irradiation facility. This dosage was previously reported as being sufficient to provide complete sterilization while not changing the physical and chemical properties of the exposed medium (McNamara et al. 2003), and a similar dosage was used to sterilize reactive media by Ramussen et al. (2002). However, four of the columns were prepared using fly ash and sand that had been previously gamma irradiated using the same dosage, packed into the column under a laminar flow hood.

Figure 5.3 Typical sorption column medium orientations

Sterilized columns were connected to the sterilized influent and effluent assemblies. Before starting the sorption-desorption tests, columns were saturated with water by applying a 10 mL/hr flow of synthetic groundwater for four pore volume equivalents of flow (PVE). Similar low-flow-rate saturation methods were reported for soil column tests by Su and Puls (2003).

Separate column sorption-desorption tests were conducted for each contaminant (i.e., naphthalene and *o*-xylene) and sorptive material-sand mixtures (MT, PS, and DP fly ashes, and PAC). A flow rate of 45-53 mL/hr was selected based on previous column studies (Table 5.3) to simulate a typical groundwater flow in up-flow condition. During the experiments, column flow rates were measured daily using flow-meters (Cole Parmer # 03269-76) and pump speeds were adjusted accordingly if any deviations occurred in the flow rate. For tests with long durations (i.e., PAC, naphthalene) the pump head tubing was replaced and flow rates were adjusted to the original levels. The step input during the column sorption experiments, the contaminant was introduced in the influent as a step input in the synthetic groundwater solution. The step input concentrations ranged from 8.9-9.6 mg/L for the naphthalene experiments between 30.3 and 38.9 mg/L and for the *o*-xylene experiments. Influent solutions were prepared in the synthetic groundwater by adding naphthalene or *o*-xylene in methanol stock solutions, as described above. All sorption experiments were continued until the effluent organic concentrations reached to the input concentrations (i.e., complete saturation of the medium with the tested contaminant occurred).

During sorption tests, aqueous sampling was conducted through the periodic sampling from the three ports using a 2.5 mL luer-lock gas tight syringe (VWR Cat.#

60375-522) and a syringe pump (Harvard Apparatus Model 22). Measures were taken to ensure that the sampling rate was sufficiently low as not to impact the flow uniformity along the column. Specifically, the sampling flow rate was chosen as 5 mL/hr, and 2 mL samples were collected for concentration measurements. The frequency of the sampling was different for each column, depending on the changes in the sampling concentrations of the organics. Columns with high LOI fly ash (i.e., DP fly ash) did not require frequent sampling, and daily sampling was usually sufficient. Columns with medium LOI fly ash (i.e., PS fly ash) necessitated more frequent sampling at every 6 to 9 hours. Columns with low LOI fly ash (i.e., MT fly ash) required sampling every two hours and the tests were usually completed in less than two days. The sampling frequency of the ports was increased when the contaminant concentrations were higher than zero and less than input concentration, which in turn, enabled to capture of the breakthrough curve for that particular port.

After complete contaminant saturation of the columns, the desorption experiments were initiated. For the desorption experiments, the columns were fed with sterilized synthetic groundwater solution that contained no organic contaminant. The desorption of organics was monitored by periodic sampling from the three ports similar to the monitoring conducted during sorption phase, and the samples were again analyzed using the spectroflorophotometer. Tests were terminated when the organic contaminant concentrations reached an undetectable level (i.e., the detection level of the instrument).

The sorption-desorption tests were followed by non-reactive tracer tests in for determination of the flow parameters (dispersivity, pore water velocity, hydrodynamic

dispersion coefficient). Constant head hydraulic conductivity tests were also conducted after the tracer tests. Both sets of measurements are described in the paragraphs below.

5.1.5 Non reactive Tracer Experiments

A series of non-reactive tracer tests were performed to define the porosity, pore water velocity and hydrodynamic dispersion coefficient for each column specimens. The influent tracer solution for these tests was a 1000 mg/L sodium bromide (NaBr) solution prepared using synthetic groundwater at a concentration approximating the ionic strength of infiltrating water in the field. This solution was injected into the up-flow column system as a step input at time zero. The flow rate was kept constant during the tracer tests. Aqueous sampling from all sampling ports was conducted for every 15-20 minutes to monitor the breakthrough of bromide throughout the depth of the column. The measurement of the bromide concentration were performed within 24 hours of sample collection using an ion-specific electrode.

The breakthrough curves were evaluated using an absolute non-linear least-square regression to obtain the best fit estimates for the pore water velocity and hydrodynamic dispersion coefficient values. Hydrodynamic dispersion in porous media is commonly defined as being comprised of mechanical dispersion and molecular diffusion and is given as:

$$D_H = \alpha v + D^* \tag{5.3}$$

where D_H is the hydrodynamic dispersion coefficient (L^2T^{-1}), α is the longitudinal dispersivity (L), v is the average pore water velocity (LT^{-1}), and D^* is the effective

diffusion coefficient in porous media (L^2T^{-1}). The longitudinal hydrodynamic dispersion coefficients for the reactive medium in the column sorption-desorption tests were determined by using the tracer breakthrough curve at the sampling port and the following equation (Fetter 1993):

$$\frac{C}{C_o} = \frac{1}{2}\left[erfc\left(\frac{\left(x - v\ t\right)}{\left(2\left(DH \cdot t\right)^{1/2}\right)} \right) \right] \tag{5.4}$$

where C is the tracer concentration measured down gradient at distance x over time, t, until steady state is achieved, and D_H is the longitudinal hydrodynamic dispersion coefficient. Only v and D_H are unknown terms in Equation 5.4. Therefore, the best-fit values for V and DH were obtained by using non-linear regression to fit Equation 5.4 to the experimental breakthrough curves.

The non-linear regression was performed using a FORTRAN program "trafit3d", which calculates the sum of the squares of either the absolute or relative residuals between the normalized model predictions and the experimental conservative tracer data. The program gives outputs of the best fit longitudinal hydrodynamic dispersion coefficient, and the average pore-water velocity and the porosity (Song 2005). The best fit v and D_H parameters were obtained using a modified Levenberg-Marquardt method to minimize the sums of the squares of the residuals between the observed and calculated concentrations. Subsequently, α_x was calculated from $\alpha_x = D_H/v$.

5.1.6 Constant Head Hydraulic Conductivity Tests

Upon completion of the non reactive tracer tests, the column specimens were subjected to constant head hydraulic conductivity tests. Laminar steady-state flow with no change in the volume of the saturated specimen was maintained during the tests. Two transparent piezometer tubes were connected to the sampling ports using Teflon sealing and compression fittings. Constant flow was maintained, similar to the sorption-desorption and non-reactive tracer tests, and constant head measurements were made through the piezometers. The head readings were taken at different time intervals along with the flow rate (Q). Using the head readings, the head loss (Δh) (the difference in the piezometer levels) was determined, and the coefficient of hydraulic conductivity (k) for each specimen was calculated by using the Darcy's law:

$$k = \frac{Q.L}{A.\Delta h} \tag{5.5}$$

where Q is the flow rate (L^3T^{-1}), L is the height between sampling ports (L), A is the cross sectional area of the specimen (L^2)and Δh is the head loss between the sampling ports(LL^{-1}).

After all the tests were completed, the homogeneity and the isotropic characteristics of the column specimens were visually inspected. This was done after draining the specimens and removing them from the column and carefully cutting the specimens across their transversal directions. Finally, the column specimens were inspected for evidence of segregation of fine particles.

5.2 Numerical Modeling Methods

The laboratory sorption-desorption test data were modeled using a reactive transport modeling tool called Modular Three-Dimensional Multi-species Transport Model (MT3DMS). This computer program simulates the reactive multi-species transport in groundwater aquifers (Zhang and Wang 1998) and is coupled with a groundwater flow program named MODFLOW, which was developed by the U.S. Geological Survey (USGS) for computing temporal variations in groundwater heads and flow velocities. In this study, a graphical user interface program, Visual MODFLOW (VMOD) (Version 2.8.2; Waterloo Hydrogeologic Inc), was selected to operate MT3DMS and MODFLOW together. There are two main reasons MT3DMS has selected as the numerical modeling tool. First, it includes well-verified numerical algorithms and has been widely used by researchers for a variety of applications (e.g, Mehl and Hill 2001, Elder et al. 2002). Second, its implicit finite difference reaction solver method enables the simulation of various types of reactions, including nonlinear sorption.

5.2.1 Governing Equations

The general macroscopic advection-dispersion reaction equations describing the fate and transport of a single contaminant in three-dimensional, transient groundwater flow systems can be written as follows:

$$\theta \frac{\partial C}{\partial t} = \frac{\partial}{\partial x_i}\left(\theta D_{ij} \frac{\partial C}{\partial x}\right) - \frac{\partial}{\partial x_i}\left(q_i . C\right) + q_s C_s - q'_s C + \Sigma R_n \qquad (5.6)$$

where C is the dissolved contaminant concentration (ML^{-3}), θ is the porosity of the subsurface medium (L^3/L^3), t is time (T), x_i is the distance along the respective Cartesian

coordinate axis (L), D_{ij} is the hydrodynamic dispersion coefficient tensor(L^2T^{-1}), v_i is the seepage or linear pore water velocity (LT^{-1}), C_s is the concentration of the source or sink flux (ML^{-3}), q'_s is the rate of change in transient groundwater storage (T^{-1}), and $\sum R_n$ is the chemical reaction term ($ML^{-3}T^{-1}$). v_i is related to the specific discharge or Darcy flux through the relationship ($v = q_i/\theta$), and q_s is the volumetric flow rate per unit volume of aquifer representing fluid sources (positive) and sinks (negative) (T^{-1}).

5.2.2 Reaction Terms

The chemical reaction terms in Equation (5.6) includes equilibrium sorption and first-order decay for both aqueous and sorbed concentration, which is required for the biodegradation reaction modeling (discussed in detail in Chapter 6). After substitution of these reaction terms, the equation can be written as:

$$\theta \frac{\partial C}{\partial t} = \frac{\partial}{\partial x_i}\left(\theta D_{ij} \frac{\partial C}{\partial x}\right) - \frac{\partial}{\partial x_i}(q_i.C) + q_s C_s - q'_s\, C_s - \rho \frac{\partial q}{\partial t} - \lambda_1 \theta C - \lambda_2 \rho q_s \quad (5.7)$$

where ρ is the bulk density of the medium (ML^{-1}), q is the concentration of sorbed contaminant (MM^{-1}), and λ_1 and λ_2 are the first order reaction rate constants for aqueous and sorbed phase, respectively (T^{-1}).

The term $\frac{\partial q}{\partial t}$ in equation 5,7 represents the rate of contaminant adsorbed, and $(\frac{l}{\theta})(\frac{\partial q}{\partial t})$ gives the corresponding change in this aqueous concentration caused by sorption- desorption (Freeze and Cherry 1979). Assuming that the sorption process is in

local equilibrium, i.e., sorption is relatively fast when compared to the transport time scale, and noting that the sorbed concentration is typically a function of the aqueous concentration, where $\frac{\partial q}{\partial t} = \frac{\partial q}{\partial c}\frac{\partial C}{\partial t}$. Substituting this relationship into Equation 5.7 results in the following equation:

$$R.\theta \frac{\partial C}{\partial t} = \frac{\partial}{\partial x_i}\left(\theta D_{ij} \frac{\partial C}{\partial x}\right) - \frac{\partial}{\partial x_i}\left(v_i.C\right) + q_s C_s - q'_s C_s - \lambda_1 \theta C - \lambda_2 \rho q \qquad (5.8)$$

where R is dimensionless retardation factor and can be defined as:

$$R = 1 + \frac{\rho}{\theta}\frac{\partial q}{\partial C} \qquad (5.9)$$

Equilibrium-controlled sorption mechanisms are often incorporated into contaminant transport models through the use of a retardation factor as defined in Equation 5.9. The functional relationship between the aqueous and sorbed phases of the contaminants at constant temperature is called the sorption isotherm. Among the sorption isotherms discussed in Chapter 3, the Freundlich and Langmuir sorption isotherm models were considered in the modeling of column sorption desorption experiments described herein. As discussed in Chapter 3, these two nonlinear isotherm models are the most commonly employed ones for practical purposes. The other isotherm models applied in Chapter 3 such as the Polanyi, Fritz Schulender, Freundlich-Langmuir combined models,

are not available within the MT3DMS solver and were not used in evaluating the column data.

The Freundlich isotherm is a nonlinear isotherm and can be expressed in the following form:

$$q = K_f.C^n \tag{5.10}$$

where K_f is the Freundlich isotherm constant $(L^3M^{-1})^n$ and n is the dimensionless Freundlich exponent, taking the differential of $\frac{\partial q}{\partial C}$ and substituting into Equation 5.9, the retardation factor for a Freundlich sorption isotherm is defined as:

$$R = 1 + \frac{\rho}{\theta}\frac{\partial q}{\partial C} = 1 + \frac{\rho}{\theta} n K_f C^{n-1} \tag{5.11}$$

The nonlinear Langmuir isotherm can be expressed as:

$$q = \frac{K_L Q_{\max}.C^n}{1 + K_L C} \tag{5.12}$$

where K_L is the Langmuir isotherm constant (L^3M^{-1}), Q_{max} is the sorption capacity of the solid surface(MM^{-1}). The retardation factor for the Langmuir sorption isotherm is then:

$$R = 1 + \frac{\rho}{\theta}\frac{\partial q}{\partial C} = 1 + \frac{\rho}{\theta}\frac{K_L Q_{\max}}{(1 + K_L C)^2} \tag{5.13}$$

These chemical reaction models as well the advection-dispersion part of the model were solved using an Operator-Splitting (OS) strategy embedded in the MT3DMS. The advection part was solved by using the Upstream Finite Difference (UFD) method, because it is virtually free of numerical dispersion and provides the mass balance precisely. The OS strategy and UFD method were described in detail by Zhang and Wang (1998). The dispersion and source-sink mixing packages use explicit finite-difference approximations, while the reaction package has an improved implicit reaction solver.

5.3 Analytical Methods

5.3.1 Organic Contaminant Analysis

The concentrations of the organic contaminants (i.e., naphthalene and *o*-xylene) in the collected aqueous samples were determined using the spectrofluorophotometry technique described in Chapter 3.3.1.

5.3.2 pH Measurements

pH of the fly ashes as-received were determined by following the EPA SW 846 Method 9045. The fly ashes were first sieved through a No.10 sieve and 20 grams of the sieved material was transferred into a 50 mL beaker. Then, 20 mL of deionized water were added to the beaker to achieve a solid-to-liquid ratio of 1:1. The suspension in the beaker was mixed using a spatula for 30 minutes with 10-minute intervals between each mixing. Then, the suspension was left stagnant to equilibrate for one hour. The pH meter

(Cole Parmer Cat. # 05718-76) was calibrated using three standard buffer solutions at pH values of 4, 7, and 10. After the equilibration period, the pH of the suspension was measured by immersing the pH meter tip and recording the value after the reading became constant. All pH measurements were performed at room temperature (24 ±2 °C). The mean values of the two replicate measurements were reported as the pH of that particular fly ash.

The samples extracted from the ports of the columns were also monitored for pH. The pH measurements were conducted by following the procedure outlined in ASTM D 1293. The pH meter used was the smear described above.

5.3.3 Non-reactive tracer analysis

During the non-reactive tracer tests, the samples extracted from the effluent port, as well as from the ports located along the height of the column, were analyzed for bromide concentrations. An aqueous sample volume of 2.5 mL was collected and the samples were kept in the refrigerator at 4 °C for 24 hours. The samples were then allowed to reach room temperature before performing the bromide measurements using a bromide electrode (Cole Palmer # 27502-05) connected to an ion meter (Orion Model 520A). Filling solutions were added to inner chamber and outer chamber of the electrode before each use. A 5 M $NaNO_3$ solution was prepared as the ionic strength adjustor (ISA) to ensure a constant background ionic strength. The calibration of the bromide electrode was conducted prior to the sample measurements using standard bromide solution concentrations of 0.1, 1, 10 50 and 100 mg/L, which were prepared by appropriate dilution of a 1000 mg/L stock solution. Each solution was measured once and a logarithmic relationship between mV and concentration was constructed.

In order to perform the bromide analysis, a 1-mL sample was taken using a pipette, and then transferred into a 10-mL volumetric flask. The sample was then diluted to 10 mL using DI water, and 0.2-mL ISA solution was added to adjust the ionic strength. The diluted solution was stirred thoroughly at a moderate speed. The electrodes were rinsed with DI water, blotted dry and placed into the beaker containing the diluted sample. When a stable reading was displayed, the milivolt (mV) reading was recorded. The milivolt readings were converted to Br^- concentration using the standard calibration curves.

5.4 *Results and Discussion of Column Sorption-Desorption Experiments*

5.4.1 Non-reactive Tracer Experiment Results

Non-reactive tracer column test data were used to calculate the hydrodynamic dispersion coefficients and pore velocities. Two sets of column tracer tests were conducted. The first set of experiments, named Column Set 1, were performed after the testing of naphthalene transport through the three fly ashes and PAC, whereas the Column Set 2 experiments were conducted after testing the transport of *o*-xylene through these materials. The breakthrough curves from port B and port C of the fly ash-sand mixture columns are shown in Figure 5.3., 5.4, and 5.5 for the MT, PS, and DP fly ash-sand mixtures, respectively. The best fits to the laboratory data was obtained using the "trafit3d" program described above and are shown as solid lines in the figures. A generally close match between the data and the regressed curves suggests successful determination of D_H and V values by using the "trafit3d" program. The optimization algorithm always yielded the same parameter estimates even if different initial estimates

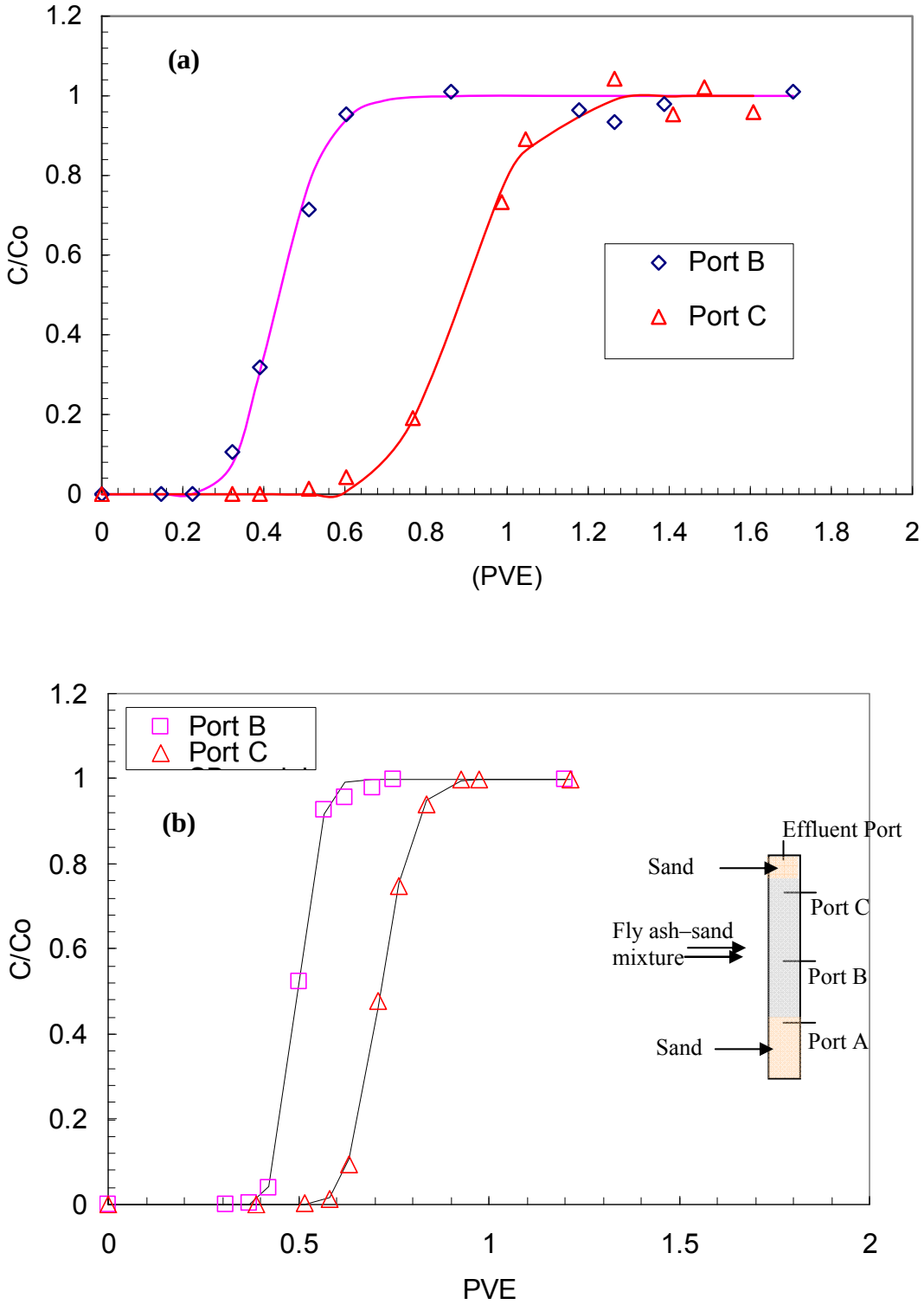

Figure 5.4 Breakthrough Curves (BTC) from non reactive tracer test conducted on MT fly ash-sand mixture: (a) Column 1 and (b) Column 2. A schematic of typical locations of the ports along the column is shown. Symbols represent experimental measurements. Lines represent the best-fit model predictions.

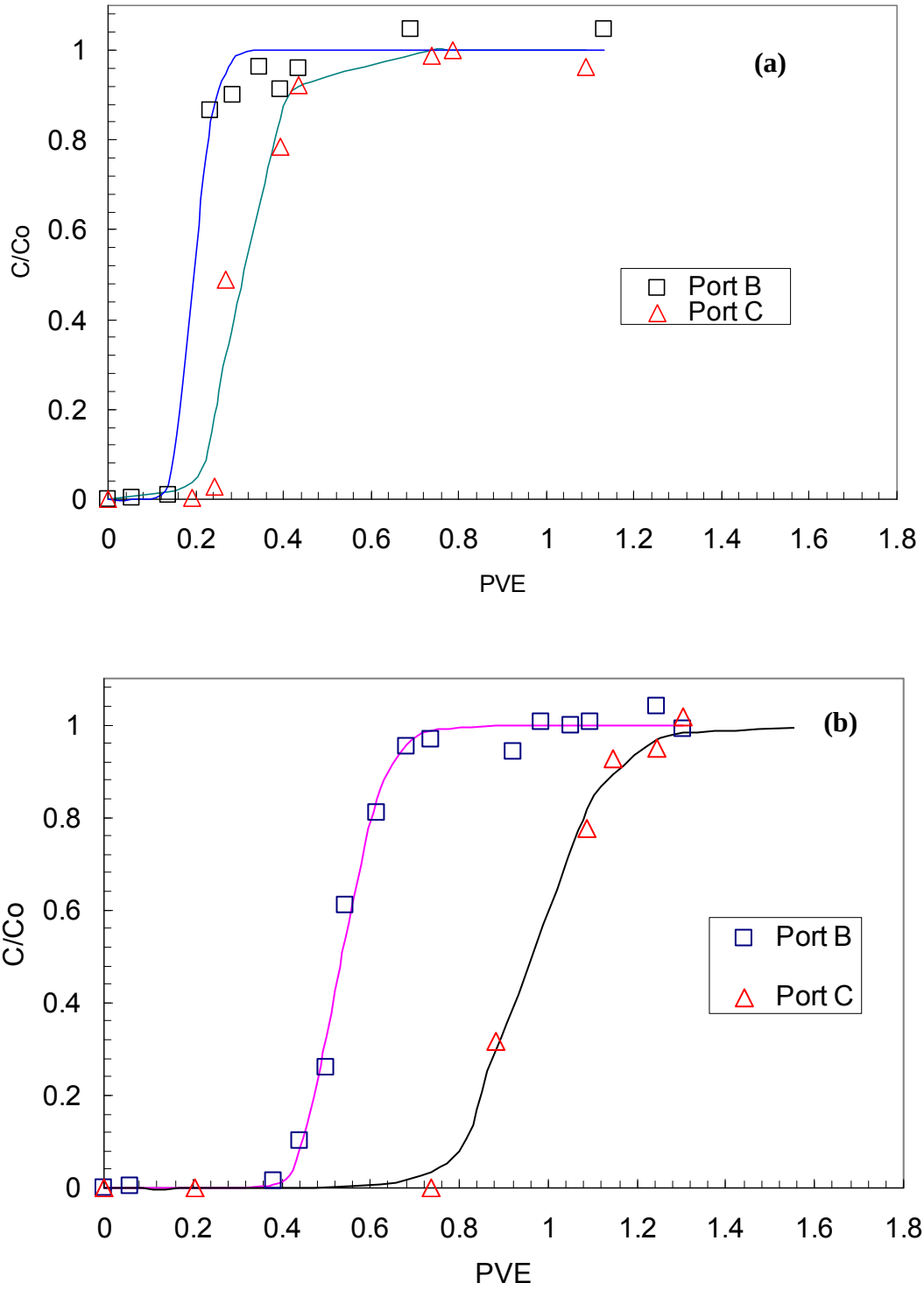

Figure 5.5 Breakthrough Curves (BTC) from non reactive tracer test conducted on PS fly ash-sand mixture: (a) Column 1 and (b) Column 2. Symbols represent experimental measurements. Lines represent the best-fit model predictions.

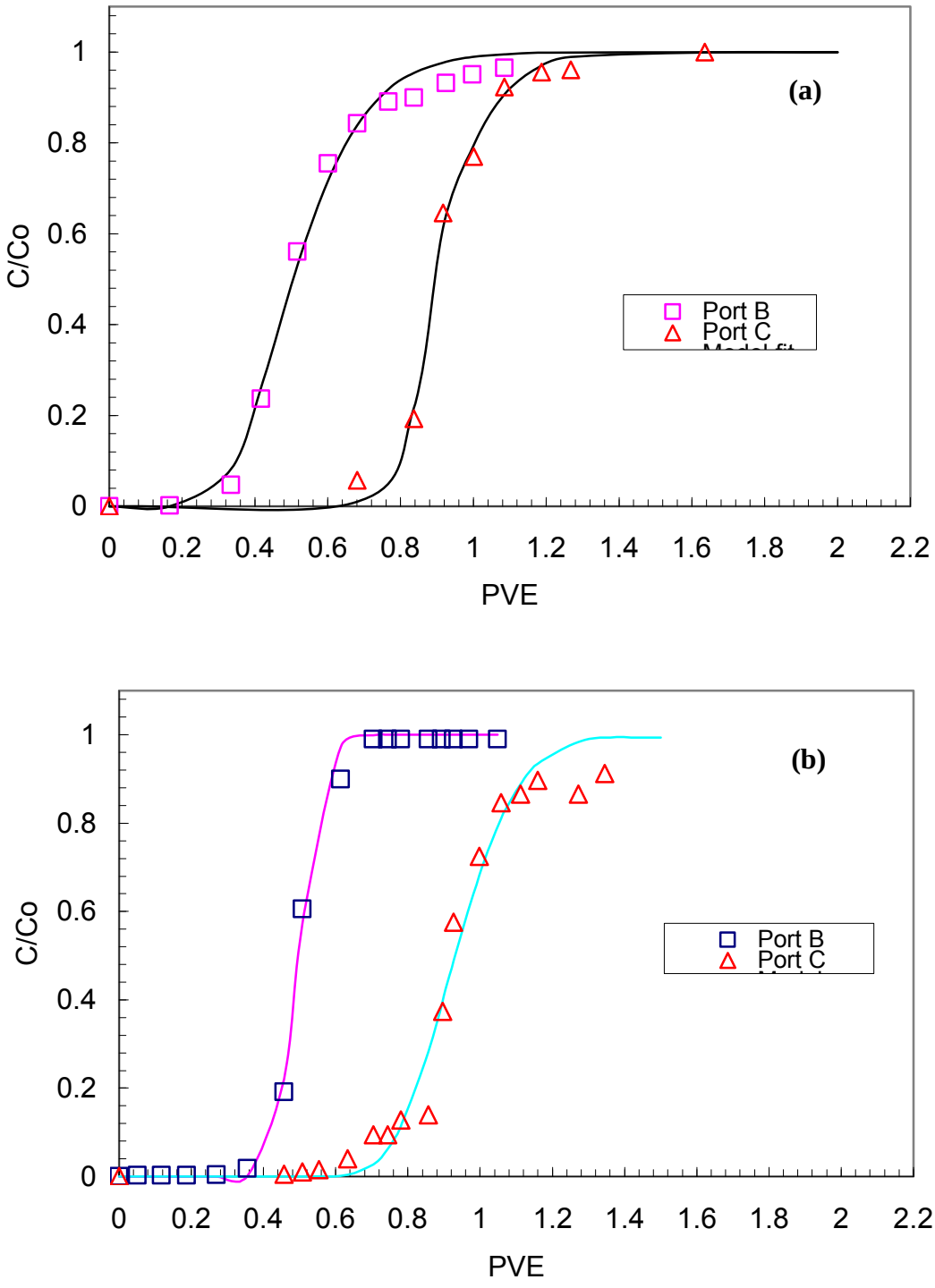

Figure 5.6 Breakthrough Curves (BTC) from non reactive tracer test conducted on DP fly ash-sand mixture: (a) Column 1 and (b) Column 2. Symbols represent experimental measurements. Lines represent the best-fit model predictions.

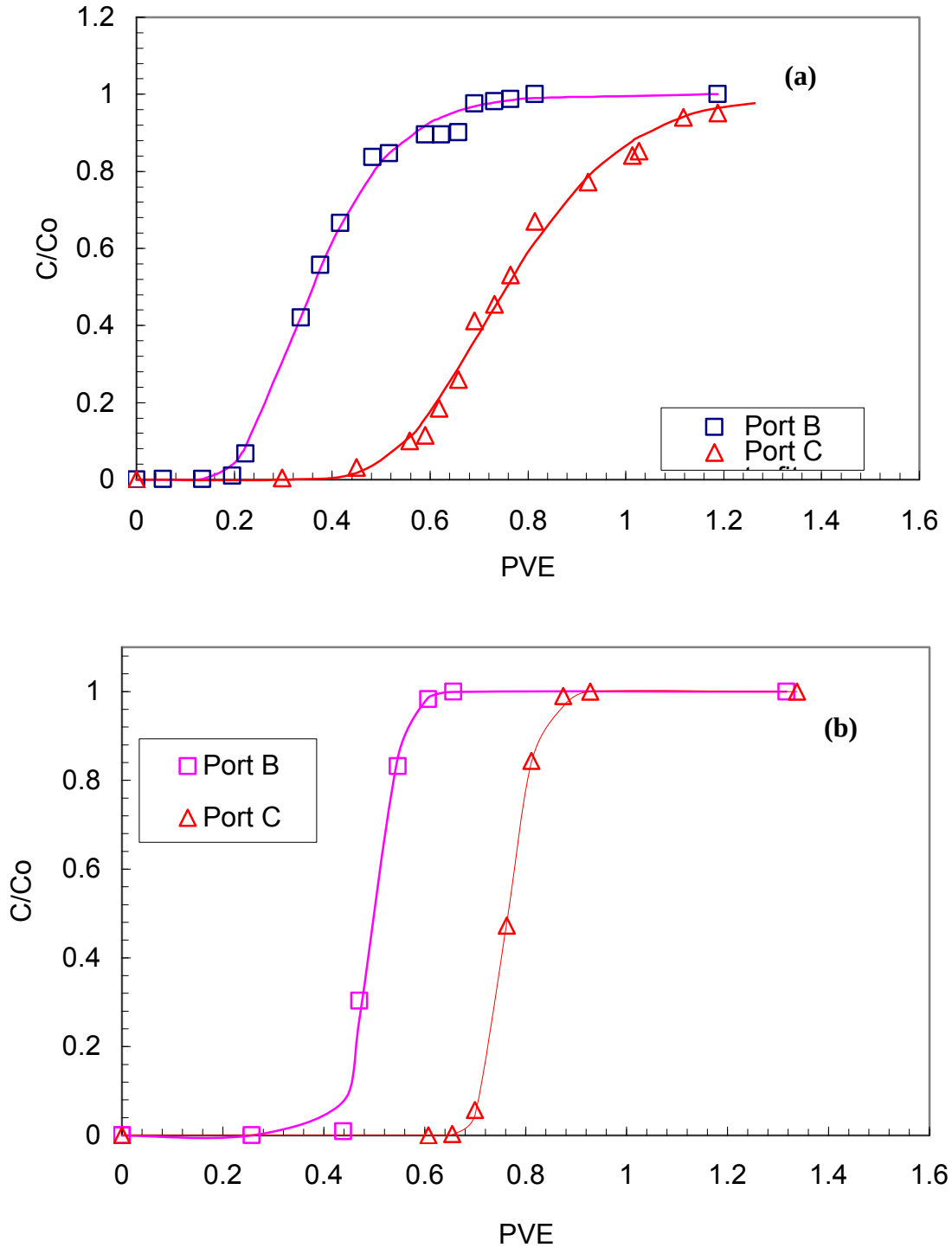

Figure 5.7 Breakthrough Curves (BTC) from non reactive tracer test conducted on PAC-sand mixture: (a) Column 1 and (b) Column 2. Symbols represent experimental measurements. Lines represent the best-fit model predictions.

were inputted; therefore the best fit D_H and V values were assumed to be unique. Table 5.4 summarizes the best fit values of D_H and V along with the calculated α (longitudinal dispersivity) values per Equation 5.3. During the numerical modeling of the sorption desorption experiments with VMOD-MT3DMS, the average of the pore water velocities at ports B and C were used.

As seen in Table 5.4, the pore water velocities in the fly ash-sand and PAC-sand mixtures ranged between 4.96 and 7.40 cm/hr, and 5.32 and 8.48 cm/hr, respectively. The variation in the pore velocities are most probably due to distribution of pores within each medium. The dispersivity values range between 0.07 and 0.74 cm, and 0.04-0.96 cm for fly ash-sand and PAC-sand mixtures, respectively. These values fall in a range typical of values reported for sorptive media with relatively high fines content (Rabideau et. al. 2005).

As shown in Figure 5.3, the reactive medium in three columns was sandwiched between two sand layers to assist with the development of uniform flow through the column. To investigate the effect of the two sand layers on the flow parameters (i.e., D_H and V), a separate column was filled completely with the PS fly ash-sand mixture, and a tracer test was performed. The breakthrough curves for this test are shown in Figure 5.8a, and the best-fit estimates for the parameters V and D_H obtained using the non-linear regression are listed in Table 5.5. Both parameters are very comparable to the ones obtained from the columns that included reactive media between two sand layers (Table 5.4). Thus, the effect of initial sand layer on flow parameters was limited.

A fourth column tracer test was conducted on pure sand to further investigate the effect of the two sand layers on the flow parameters. The breakthrough curves from all

Table 5.4 Summary of transport parameters obtained from tracer tests

Column set number	Sorptive Medium	Port	Q[a] (cm^3/hr)	*V* (cm/hr)	D_H (cm^2/hr)	α (cm)
Column Set 1	**MT fly ash**	B	45	7.40	2.51	0.37
		C		5.66	1.54	0.23
	PS fly ash	B	45	6.27	1.63	0.26
		C		6.06	4.62	0.74
	DP fly ash	B	45	5.68	3.96	0.7
		C		5.19	1.59	0.3
	PAC	B	52.2	8.48	8.19	0.96
		C		6.40	4.69	0.73
Column Set 2	**MT fly ash**	B	52.9	6.67	0.45	0.07
		C		7.13	0.77	0.11
	PS fly ash	B	52.4	6.69	0.99	0.149
		C		5.74	1.40	0.244
	DP fly ash	B	53	6.084	0.56	0.09
		C		4.96	1.22	0.25
	PAC	B	52	5.32	0.32	0.06
		C		5.41	0.20	0.04

[a]-The flow rate during the test

three ports of the sand column are shown in Figure 5.8b, and the best fit parameters are summarized in Table 5.6. The D_H values range from 0.548 to 1.435 cm^2/hr, indicating that the flow parameters for pure sand are comparable to those determined for the columns that included reactive media between the two sand layers (Table 5.4).

It is well-known that dispersivity is strongly related to the method and scale of testing (Gelhar et al. 1992). The commonly reported laboratory-scale longitudinal dispersivity values range between 0.1 mm to 1 mm (Song 2005). Generally, such laboratory-scale dispersivity values are strongly correlated to the average mean grain size diameter of the porous media (Rumer 1962). For the fly ash-sand mixture, it is well-understood that the dispersivity is controlled by the sand in the mixture. The sand used in the current column experiments, has a mean grain size diameter of 0.3 mm. This is very similar to the dispersivity values obtained from the breakthrough curves at port C and the effluent port of the sand column, which were 0.249 and 0.243 mm, respectively (Table 5.4). Therefore, these dispersivity values appear to be reasonable.

The column Peclet number ($P_L=vL/D_H$) is an important parameter that controls the flow conditions within a column (Freeze 1999). For all of the columns tested, the P_L ranged from 12.4 (PAC-sand column for naphthalene) to 249.1 (PAC-sand column for *o*-xylene) which indicated that the transport was dominated by advective flow. Based on the results from the tracer experiments, the assumption of negligible diffusion in the hydrodynamic dispersion was also evaluated. The effective diffusion coefficient for bromide is reported as 2.08 10^{-5} cm^2/sec (Kim et al. 1997). Based on this value, the error due to ignoring diffusion is small (1.6-7 % based on Equation 5.3) and indicates that diffusive flux does not contribute significantly to contaminant transport.

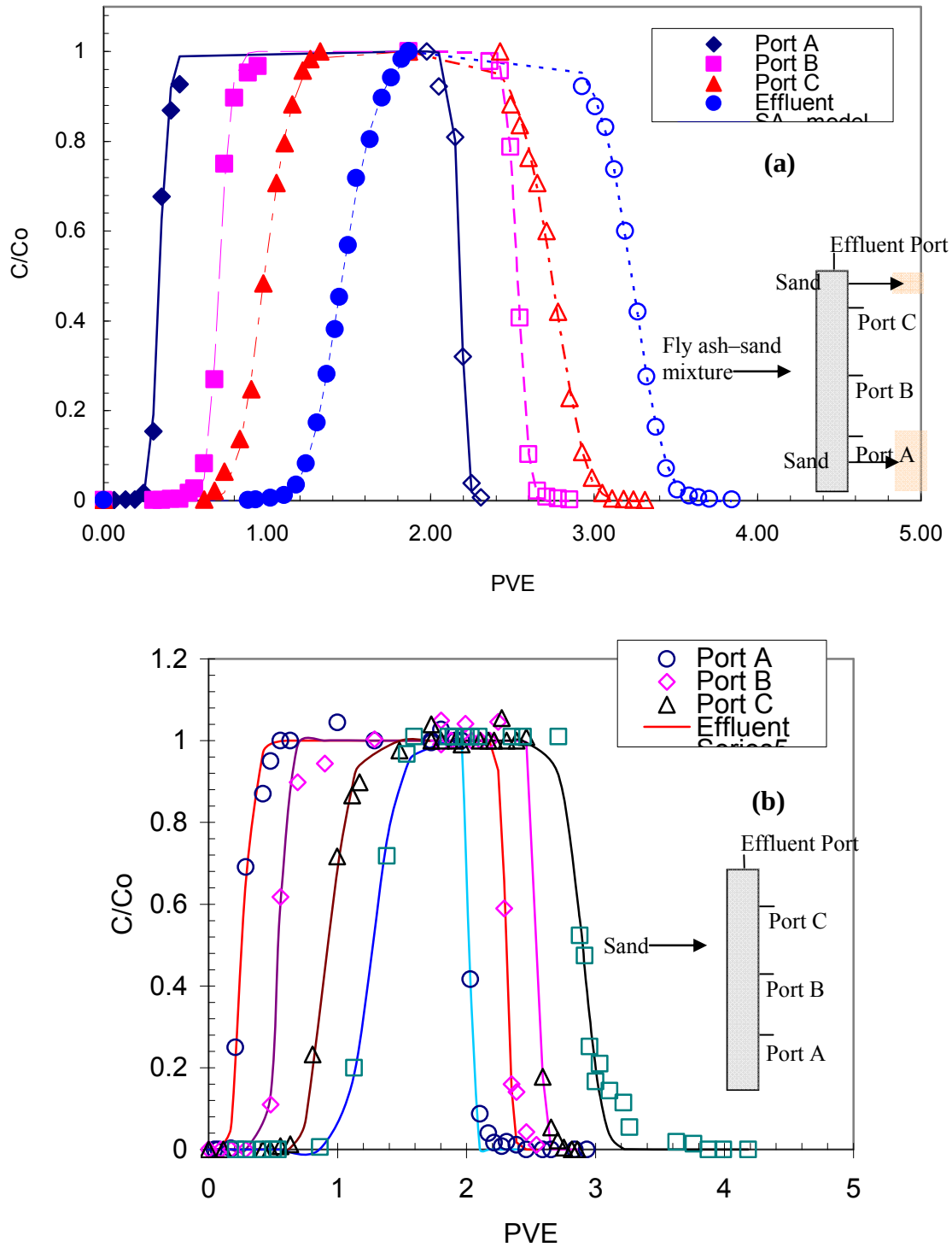

Figure 5.8 Breakthrough Curves (BTC) from non reactive tracer test conducted on (a) PS-sand mixture (b) sand only. Symbols represent experimental measurements. Lines represent the best-fit model predictions.

Table 5.5 Summary of transport parameters for the PS fly ash sand mixture

Sampling Point	Q (cm^3/hr)	Vx (cm/hr)	DH (cm2/hr)	α (cm)
Port A	54	5.3	0.33	0.062
Port B		5.5	0.28	0.051
Port C		6.0	ĩ.32	0.22
Effluent		5.3	1.11	0.21

Table 5.5 Summary of transport parameters for the sand

Sampling Point	Q (cm^3/hr)	*V* (cm/hr)	DH (cm2/hr)	α (cm)
Port A	50	5.99	1.435	0.187
Port B		6.34	0.548	0.086
Port C		5.62	ĩ.398	0.249
Effluent		5.416	1.317	0.243

5.4.2 Constant Head Hydraulic Conductivity Test Results

The constant head hydraulic conductivity results are summarized in Table 5.6. The hydraulic conductivity of the sand (no fly ash) is 4.5 10^{-2} cm/sec, which is comparable to hydraulic conductivities of 10^{-1} to 10^{-3} cm/sec reported for fine to medium sands (Bowles 1992). It is clear that the addition of 40% fly ash by weight to the sand caused an approximately two order of magnitude decrease in hydraulic conductivity. Mixing the sand with 2% PAC by weight also caused a 4.8 to 32 times reduction in hydraulic conductivity. The fine particle size of both the fly ash and the PAC is responsible for the observed decrease in hydraulic conductivities. Despite the reduction in hydraulic conduction, the measured values of the fly ash-sand mixtures range between 4.7 x 10^{-5} and 1.8 x 10^{-4} cm/sec and these are comparable with the typical field hydraulic conductivities reported for PRBs (Gavaskar et al. 1998). Therefore, it can be concluded that the hydraulic conductivity of the fly ash-sand mixture is reasonable for its use as a PRB medium.

5.4.3 pH results

Samples were periodically collected from the effluent ports during the sorption-desorption tests and evaluated for pH. The observed changes in the effluent pH of the MT, PS, and DP fly ashes/sand columns during the naphthalene sorption-desorption tests are plotted against PVE in Figure 5.9. Figure 5.9 shows that pH initially remains relatively constant and slightly basic for several pore volumes of flow, then decreases at the later stages, and eventually drops to a relatively constant level comparable to the pH of artificial groundwater solution (i.e, pH =6.9). The pH of the columns reached this equilibrium value typically within 15-35 pore volumes of flow. Similar trends were

Table 5.6 Hydraulic conductivities one fly ash-sand column specimens.

Fly ash Type	Column set number	Average hydraulic conductivity (cm/sec)	Sorptive Medium Bulk Density (g/cm^3)
MT	Column Set 1	$1.1\ 10^{-4}$	1.701
PS		$9.5\ 10^{-5}$	1.398
DP		$1.3\ 10^{-4}$	1.407
PAC		$1.4\ 10^{-3}$	1.582
MT	Column Set 2	$4.7\ 10^{-5}$	1.756
PS		$1.8\ 10^{-4}$	1.471
DP		$1.5\ 10^{-4}$	1.408
PAC		$9.4\ 10^{-3}$	1.649

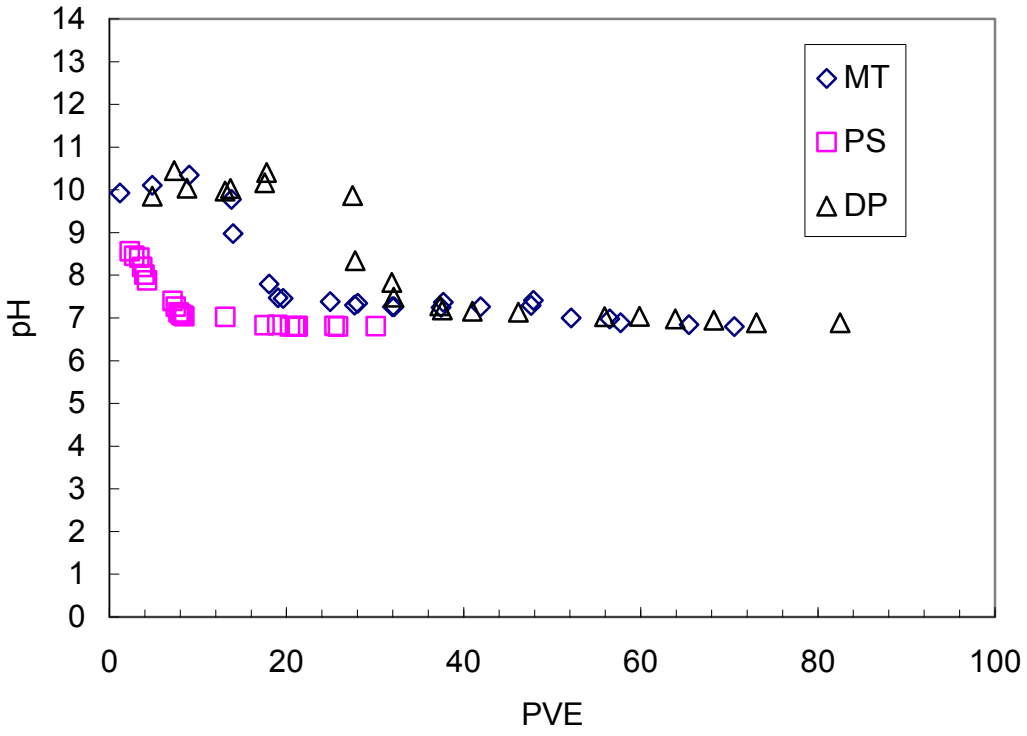

Figure 5.9 pH values during the naphthalene sorption-desorption tests for the three fly ashes tested. MT: Morgantown fly ash-sand mixture, PS: Paul Smith fly ash-sand mixture, DP: Dickerson Precipitator fly ash-sand mixture.

observed by Qiao et al (2005) in a study on use of fly ash in waste stabilization/solidification systems.

It is difficult to relate the shapes of the pH elution curves to any one single factor, but rather the curves are influenced by a series of factors, including flow rate, mineral composition of the fly ash, and percolating eluant solution. Fytianos and Tsaniklidi (1998) attributed the observed decrease in pH with the increasing liquid-to-solid ratio (i.e., the increasing pore volumes of flow) to the "depletion of materials controlling this parameter". For example, the elevated values for pH may be due to the buffering reactions initiated by the dissolution and/or decomposition of the minerals components of the fly ash (McBride et al. 1994 and Genc-Fuhrman et al. 2007). Over the time, the buffering capacities of the Maryland fly ashes tested in this study diminished and the pH in the system became governed by the PIPES buffer present in the groundwater recipe as more pore volumes of flow pass through the column and more fly ash mineral components were washed out from the column system.

5.4.4 Column Sorption-Desorption Test Results with Naphthalene

A series of column sorption-desorption tests were conducted on the fly ash-sand mixtures to determine the sorption parameters for these reactive media. Prior to these columns tests, a sorption-desorption column test was performed on sand (no fly ash) to determine sorption-desorption characteristics of sand alone. Figure 5.10 shows the relative naphthalene concentrations for sand sorption-desorption experiment. Also shown are the breakthrough curve simulations produced using MT3DMS with the transport

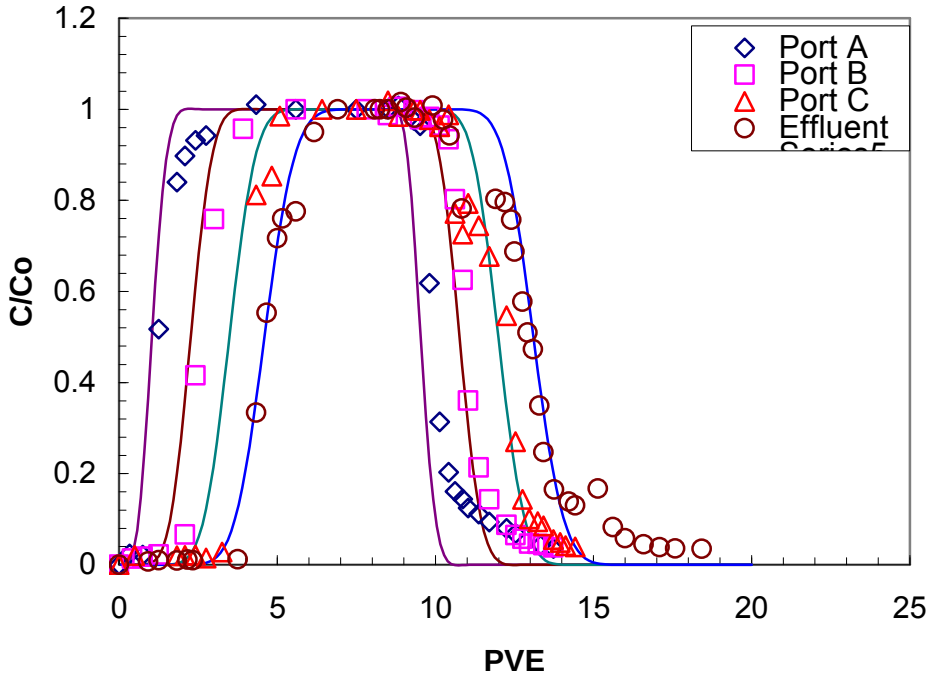

Figure 5.10 Naphthalene breakthrough in sand column sorption-desorption test. Solid line are the results from numerical analysis.

parameters obtained from the sand only tracer test and assuming no sorption. The tailing observed at the conclusion of the desorption part of breakthrough curve was probably mostly due to pore-scale variations in the sand medium (Fesch et al. 1998). Other then the observed tailing, the measured naphthalene concentrations agree well with those predicted through the MT3DMS simulations by assuming no sorption-induced uptake of naphthalene during flow. These column test data confirm the observations made in batch adsorption tests on sand that the material does not have any significant sorption capacity for naphthalene.

Following this test, the series of column sorption-desorption tests were conducted on fly ash-sand mixtures with naphthalene in the influent. Initially, the input (influent) concentrations were determined through the samples taken from the influent port as well as at port A. Port A was located in the sand portion of the column, 10 mm below the fly ash sand mixture (see the inset in Figure 5.11 for the port orientations). Typical naphthalene concentrations from the influent port and port A are shown in Figure 5.11, and suggest that no significant difference existed in the naphthalene concentrations. Thus, further measurements for the influent naphthalene concentrations were made through the samples collected at port A, which, because of its proximity to the sorptive medium, represented more accurate input concentration for the column data.

Upon completion of the column experiments, breakthrough curve simulations were first conducted using VMOD and MT3DMS, the transport parameters from the corresponding non-reactive tracer studies, and the sorption parameters determined from the batch adsorption test isotherm models. For example, the Freundlich isotherm was the best-fit sorption isotherm model for the MT fly ash data, therefore, the MT fly ash-sand

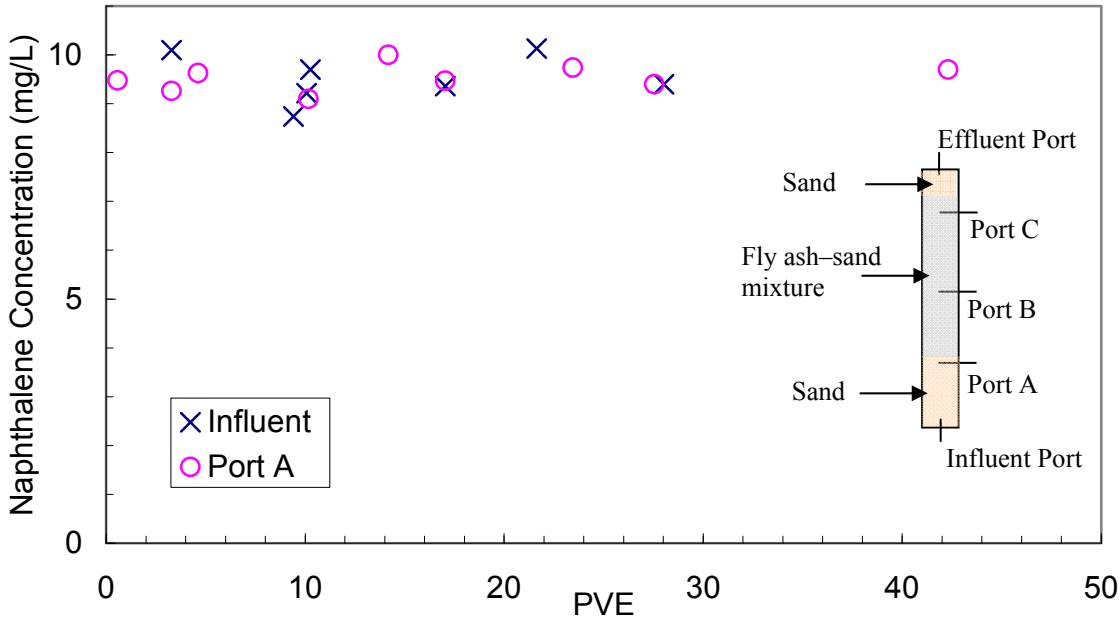

Figure 5.11 Typical naphthalene concentrations at the influent port and Port A during sorption tests (From PS-sand column)

mixture column tests were modeled using the Freundlich isotherm coefficients taken from the batch adsorption tests. The column data for the MT fly ash-sand column, generated using the batch parameters, and the breakthrough curves are given in Figure 5.12. The breakthrough curves determined using the batch parameters are shifted rightward implying that the naphthalene sorption is overpredicted by using these parameters. Similar observations were made in some previous studies that compared the batch and column sorption isotherms (Maraqa et al 1998, Fesch et al 1998, Allen-King et al 2001, Altfelder et al 2001, Maraqa 2001, Rabideau et al. 2001, Lee et al 2002). For example, it was reported that batch-determined isotherm coefficients overpredicted the column sorption data by 50 to 170% (Maraqa 2001, Rabideau et al. 2001), and in some cases the difference was over one order of magnitude (Altfelder et al. 2001).

The reasons behind the discrepancy between batch and column data for non-polar organic contaminant sorption are not completely understood (Altfelder et al. 2001, Maraqa 2001, Alllen-King et al. 2002). Various reasons have been reported to be responsible for the discrepancy, including the solid-to-liquid ratio, sorption nonlinearity, and nonequilibrium (rate-limited) sorption (Maraqa 2001). It is possible that a combination of these factors caused the observed discrepancy in the current experiments. Among these factors, the equilibrium state of sorption during column sorption-desorption was evaluated in this study using MOD flow-MT3MS, which is capable of modeling rate-limited sorption with a linear sorption isotherm.

In order to investigate the potential effect of sorption rate-limitations in the column experiments, the MT fly ash-sand mixture results were compared with MODFlow-MT3MS simulations with rate-limited sorption and an equivalent linear

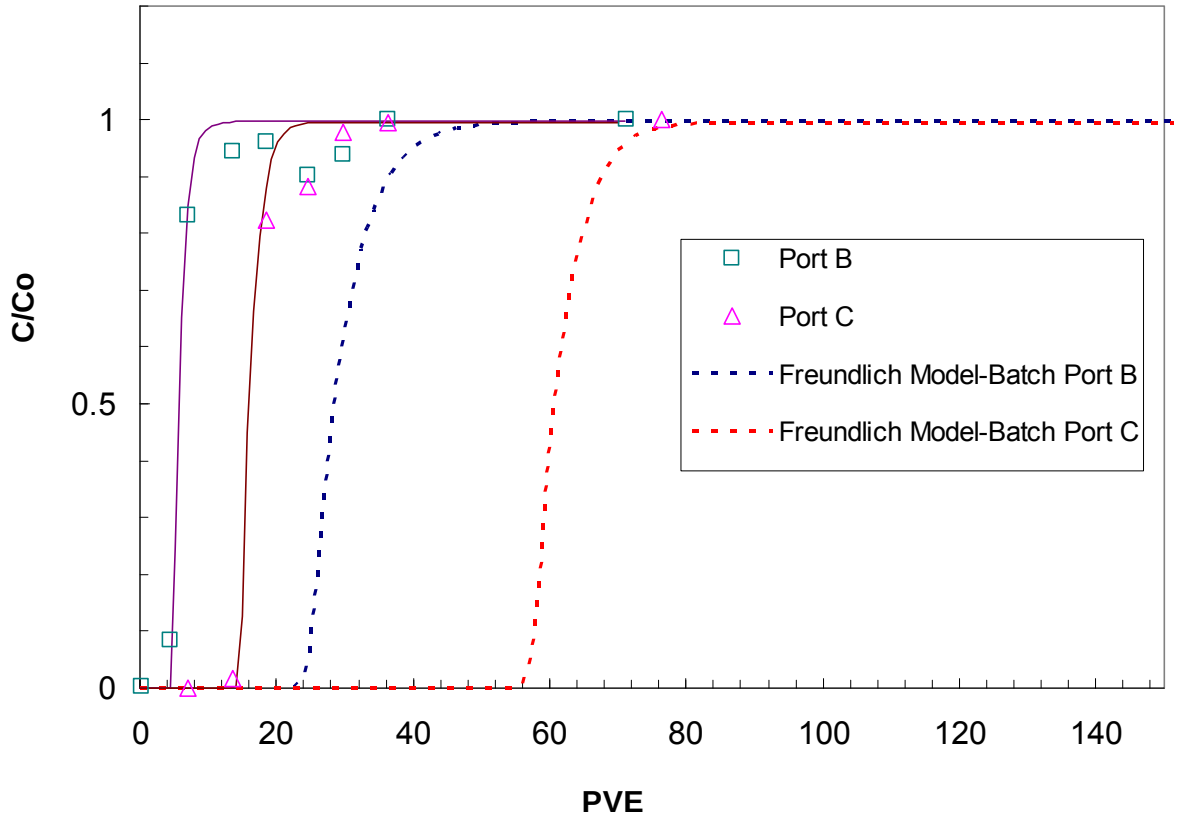

Figure 5.12 MT fly ash-sand mixture column breakthrough curves during naphthalene sorption. Dotted lines are breakthrough curves modeled with isotherm parameters taken from batch adsorption tests. Solid lines are from calibrated isotherm parameters. Symbols are from experimental measurements.

sorption isotherm. The equivalent linear isotherm coefficient for the MT fly ash was calculated by using the Freundlich isotherm coefficients obtained in the batch sorption tests and following the procedure described by Schwarzenbach et al (1999) and Maraqa (2007) in which the linear partition coefficient, K_d, is related to the Freundlich parameters as follows:

$$K_d = K_f C_e^{n-1} \tag{5.12}$$

where K_d is the equivalent linear partition coefficient (L/kg), K_f is the Freundlich isotherm coefficient $(mg/kg)/(L/mg)^{-n}$, C_e is the equilibrium concentration, and n is the Freundlich isotherm exponent. The mass transfer rate constant was not independently estimated in this work; therefore, numerical analyses were conducted with low rate constants ($<1\ hr^{-1}$) to ensure nonequilibrium conditions (Miller and Weber et al. 1988). Breakthrough curves generated from the rate-limited sorption modeling runs resulted in significant tailing in the sorption breakthrough. Similar tailing sorption breakthroughs with use of low sorption rate constants were also reported in previous studies (Mansell et al. 1977, Cameron and Klute et al. 1977, Liu et al. 1991, Spurlock et al 1995). However, as seen the Figure 5.12 the actual breakthrough curve data have relatively sharp fronts during the sorption phase. Due to the significant differences in the shape of the rate-limited sorption breakthrough curves and the experimental data, it was concluded that the sorption in the fly ash medium is not a rate-limited process, and a local equilibrium had been reached. Because a sharp front was observed in the sorption breakthrough curves

for all fly ashes and PAC (see below), no further investigation was conducted on the rate limitation.

As illustrated in Figure 5.12, the shape of the breakthrough curves using the batch parameters and the column test data had similar shapes, but the experimental data had an earlier breakthrough compared to the curves calculated using batch-determined sorption parameters. In other words, the column sorption experiments may yield same nonlinear sorption isotherm with lower sorption capacity (i.e., yielding the same shape with a rightward shift). For example, the results of Fesch et al. (1998) also revealed a similar breakthrough curve orientation, but the ones from their soil column experiments had earlier breakthrough points. Therefore, another possible explanation for the difference between the sorption capacities of the two test methods could be due to the fact that the number of sorption sites in the column was overestimated. Fesch et al. (1998), Rabideau et al. (2001), and Maraqa (2001) reported a similar overestimation when batch-derived parameters were used for column data. This overestimation could be due to the limited accessibility of carbon sorption sites in the column resulting from relatively denser packing as compared to a low solid-to-liquid ratio in the batch equilibrium tests (e.g., 0.5 g of HCCFA fly ash were tested in 60 mL naphthalene solutions in the batch tests). Similar observations were made by Burgisser et al. (1993) and Fesch et al. (1998) in comparing in the batch and column tests.

In order to determine the sorption isotherm coefficients for the flow through column conditions, the calibration procedure described by Fesch et al. (1998) was followed. Fesch and coworkers also studied a flow-through sorption column using a sorptive medium that was best described with nonlinear batch-determined isotherm

models (i.e., Freundlich and Langmuir). Their column results were described by nonlinear sorption isotherms with same isotherm coefficients (i.e., "K_L"of Langmuir isotherm, and n of Freundlich isotherm) as the batch data, but using different sorption capacity parameters (i.e., "Q_{max}" of Langmuir isotherm and K_f of Freundlich isotherm--see Chapter 3 for isotherm details). Similarly, Lee et al. (2002) determined Freundlich isotherm coefficients from batch and column studies and reported that same Freundlich exponents, n, were obtained in both cases, but the column sorption experiments yielded lower K_f values. Lee et.al. (2002) and Maraqa (2007) discussed the effect of the Freundlich exponent, n, on column breakthrough results. They indicated that a slight change in n has a significant effect on the breakthrough curve. Therefore, n can be considered to be a sorbent-specific parameter.

Following the approach of Fesch et al. (1999), the Freundlich exponent "n" obtained from the batch experiments was used to model the column data. However, new Freundlich isotherm coefficients, K_f, for column experiments were determined via numerical simulation. Specifically, the best estimate of K_f was evaluated via trial and error by minimization of the root mean-squared error (RMSE) between the experimental and numerical data. The calibrated (new) Freundlich isotherm parameters determined from the column breakthrough curves are summarized in Table 5.7. Freundlich isotherm coefficients calculated from the column data are 27.3 to 47.3% lower than the batch-determined ones. It can be seen in Table 5.7 that the fly ashes with relatively low LOI values (i.e,, MT and PS) generally have lower sorption medium efficiency. This difference can also be expressed as the efficiency of column sorption capacity. The

Table 5.7 Isotherm coefficients from batch and column studies

Sorptive Medium	n	Batch K_f (L/kg)	Column K_f (L/kg)	RMSE	K_F efficiency[a] (%)
MT	0.3062	102	28.75	0.73	28.2
PS	0.3389	696.4	190	1.44	27.3
DP	0.194	1416	670	0.75	47.3
PAC	0.169	72570	1110	0.89	1.5

[a] (Column K_f / Batch K_f)*100

resulting model simulation breakthrough curves using the batch and best-fit column K_f values for DP, PS and MT fly ash-sand mixture sorption desorption column results are shown in Figure 5.13, 5.14, 5 15, respectively along with the experimental data.

The nonlinear sorption of the organic compound was reflected in sharp adsorption and tailing desorption fronts of the breakthrough curves (Brusseau 1995).As seen in these figures, the MT3DMS simulations in general successfully model the experimental data using the new Freundlich isotherm coefficients for the sorption as well as the desorption phases. However, there are some discrepancies. For example, the data from the DP and PS fly ash-sand mixture columns (Figure 5.13 and 5.14) have relatively sharp sorption breakthrough fronts, which were predicted well by the MT3DMS nonlinear equilibrium isotherm model. However, the MT fly ash-sand mixture column data (Figure 5.15) exhibited a great degree of tailing in the sorption front. As mentioned earlier, a column breakthrough curve can indicate the sorption equilibrium based on the shape of the curve (Miller and Weber 1998).In this case, given the fact that MT fly ash has a low carbon content, equilibrium may not be satisfied at high naphthalene concentrations most probably due to the low sorption affinity of the MT fly ash. The effect of non-equilibrium sorption on the column breakthrough curves was also mentioned by others (e.g., Burgisser et. al. 1993, Miller and Weber 1988, Lee et al. 2002).

A tailing of the desorption front was observed for DP fly ash-sand mixture column (Figure 5.13), which was most probably caused by the nonlinearity of the sorption isotherm (Brusseau 1995, Spurlock et al. 1995, Fesch et al 1998). However, for both ports B and C, the nonlinear desorption MT3DMS model overpredicts the experimental naphthalene desorption data toward the end of the desorption process.

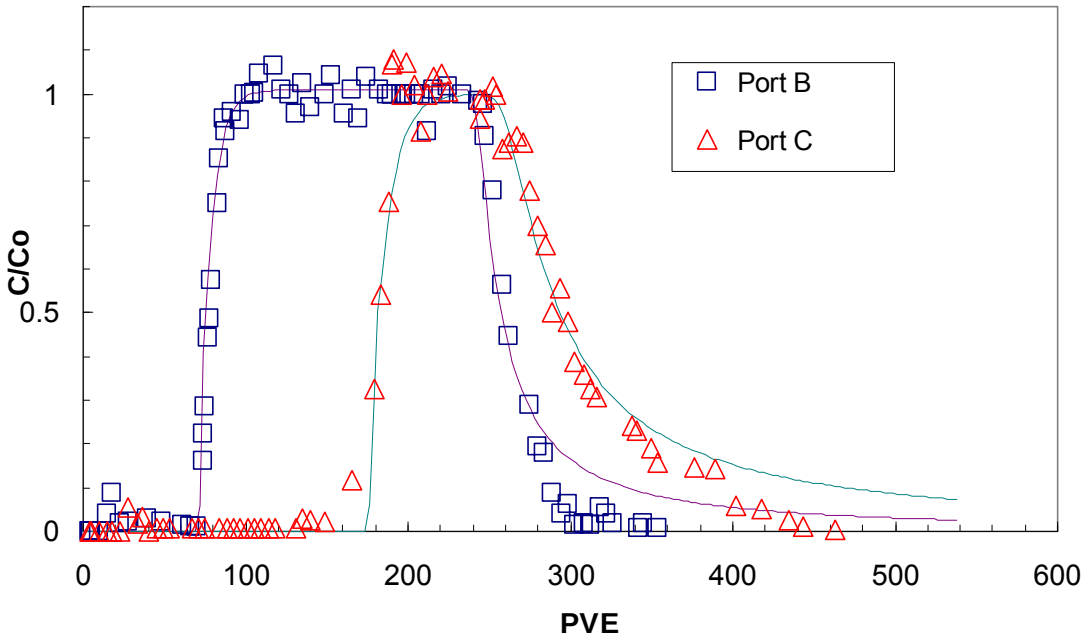

Figure 5.13 Breakthrough curves from Port B and Port C of Naphthalene sorption desorption column using DP fly ash as sorptive medium. Solid lines are from Numerical modeling using MT3DMS.

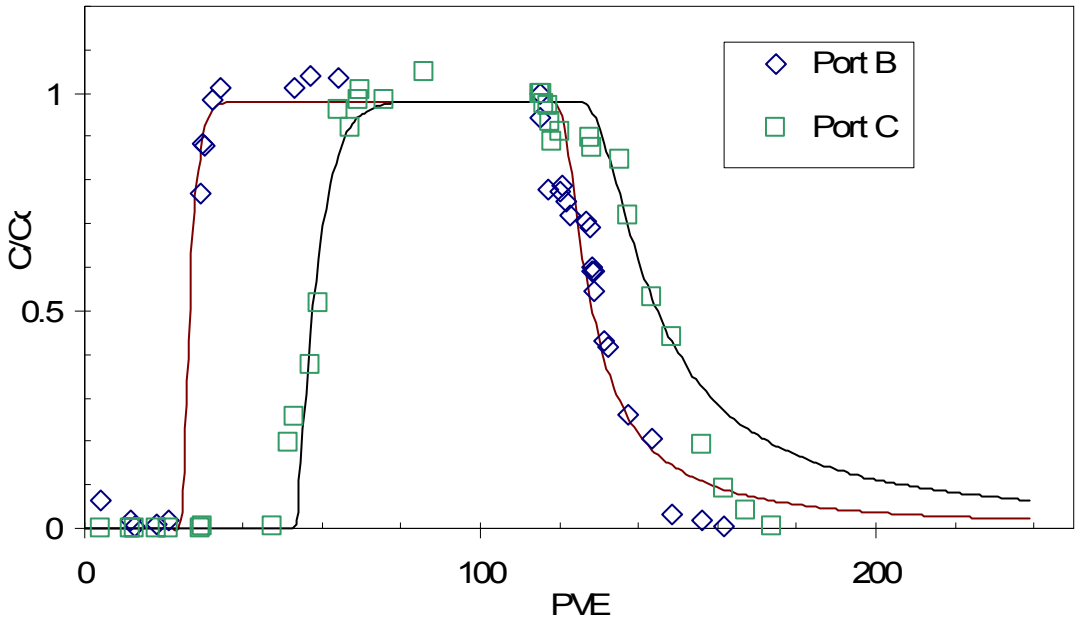

Figure 5.14 Breakthrough Curves from Port B and Port C of Naphthalene sorption desorption column using PS fly. Solid lines are from Numerical modeling using MT3DMS.

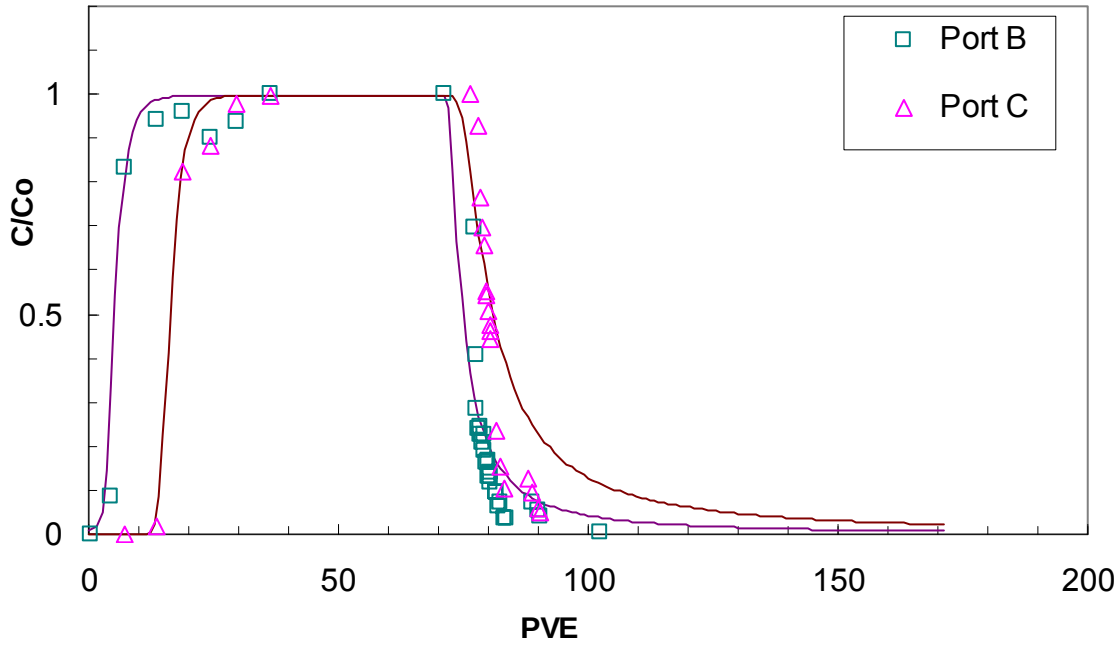

Figure 5.15 Breakthrough Curves from Port B and Port C of Naphthalene sorption desorption column using MT fly ash. Solid lines are from Numerical modeling using MT3DMS.

Similar deviations of the model predictions from the experimental data were also observed at the lower end of the desorption curve for the PS and MT fly ashes (Figure 5.14 and 5.15). Although, the Freundlich sorption isotherm is capable of capturing the column sorption-desorption processes at low naphthalene concentrations, the desorption process occurs faster than the model predictions. This is most probably due to an increase in the desorption deriving force created by the higher concentration gradient. It has also been reported that if the desorption part of the breakthrough curve has a sharp end (fast desorption), mass transfer processes are most likely to reach an equilibrium with a linear sorption isotherm (Altfelder et al 2001). In fact, it is well known that non-polar organic chemicals (i.e. naphthalene) exhibit equilibrium mass transfer behavior at relatively low concentrations (Chiou et al. 1998).

The batch test-determined isotherm model parameters for the PAC were also re-calibrated through the column sorption-desorption tests a using MT3DMS analysis to define new isotherm coefficients in the same manner as described above for the fly ashes. As discussed in Chapter 3, the PAC batch data were best fit by the Langmuir isotherm model. Therefore, first, a new best estimate of Q_{max} was obtained by trial and error minimization of RMSE between the experimental and numerical data, keeping the same K_L value as from the batch data analysis. Then the PAC-naphthalene sorption desorption data from the column tests were compared with the MT3DMS simulations using the new Langmuir isotherm coefficient (Figure 5.16). However, there was not a good match between the model prediction and the data set. Similar to the fly ash column breakthrough curves, the experimental data for the PAC-sand mixture have a relatively sharp sorption front and a slight tailing during desorption. In comparison, the Langmuir

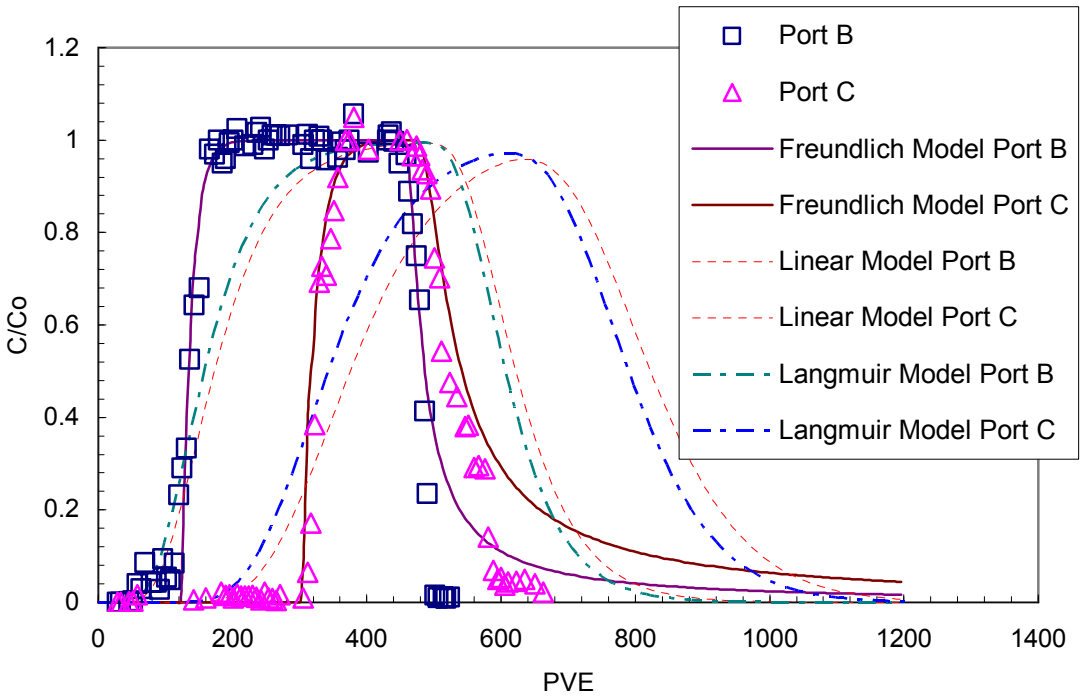

Figure 5.16 Breakthrough Curves from Port B and Port C of Naphthalene sorption desorption column experiment using PAC-sand as the sorptive medium. Lines are the numerical modeling prediction using MT3DMS for the Linear, Freundlich and Langmuir sorption isotherms.

isotherm model, with the relatively slow sorption front, was unsuccessful in predicting the test data. Therefore, the Freundlich isotherm was calibrated to the experimental data, as described above for the fly ash data, to obtain new isotherm parameters for the PAC-sand mixture column data. In addition, an equivalent linear isotherm coefficient for PAC was calculated using Equation (5.12). The re-calibrated Freundlich isotherm parameters are presented in Table 5.7. Interestingly, compared to the fly ashes, the efficiency, is very low for PAC, a high carbon content material (LOI=99%). This is probably due to very low solid-to-liquid ratio used during batch adsorption tests on PAC (a ratio of 1/6000 for PAC as compared to a ratio of 1/120 for fly ashes),, which caused the sorption sites in PAC to be fully accessible for naphthalene.

It is clear from Figure 5.16 that the numerical simulations using the recalibrated Freundlich model provided a good prediction for the experimental data, whereas the equivalent linear isotherm coefficient did not. The reasons behind the superiority of the Freundlich isotherm model for the column tests predictions can be described as follows. First, the PAC-sand mixture exhibits a sorption behavior in the column similar to the fly ashes tested. Specifically, there is a sharp sorption front and a tailing desorption end of the breakthrough, as discussed for fly ash columns. This nonlinearity is successfully captured by Freundlich isotherm, although the model simulations overpredict the naphthalene concentration at the end of the desorption front for the fly ashes. Note that the difference in the goodness-of-fit for the batch adsorption test Freundlich and Langmuir isotherms was very small (RMSE=0.33). Therefore, it is not surprising that the PAC-naphthalene sorption can be modeled using a Freundlich isotherm.

5.4.5 Naphthalene Retardation from Column Experiments

In order to determine the retardation of naphthalene during advective-dispersive flow in the columns, the sorbed and desorbed masses were calculated. The area above the sorption front of the breakthrough curve was used to calculate the sorbed mass of the solute multiplied by the test flow rate (Burgisser et al. 1993, Fesch et al 1998). Similarly, the area under desorption breakthrough was used to determine the desorbed mass multiplied by the flow rate during desorption phase of the experiment (Figure 5.17). For all of the column tests conducted with naphthalene, the areas associated with the sorbed and desorbed naphthalene mass were calculated using Newton-Cotes integration methods (Chapra and Canale, 2002). These two areas are symmetrical and equal for a non-reactive solute (i.e., the injected solute mass is equal to the flushed solute mass). However, when the solute is retarded within the medium, the difference between the two masses provides the retarded solute mass in the sorptive medium. Sorbed and desorbed naphthalene masses as well as the retarded mass per gram of sorptive medium are given in Table 5.8. Several key observations can be made based on the retarded naphthalene mass amounts. First, retarded naphthalene mass increases with increasing LOI values (MT< PS< DP fly ashes< PAC). This observation is consistent with the hypothesis that the sorption and retardation capacity of the fly ashes are strongly dependent on the carbon content of the fly ashes. Second, retarded mass per gram sorptive medium calculated from Port C is generally higher than the one calculated at port B. This indicates that the retarded mass increases along the height of the column. Third, the percent retardation of the input naphthalene in the tested fly ashes varies between 48.14 to 77.87%, and this range is very comparable to the range observed in this study for retardation within PAC which varied

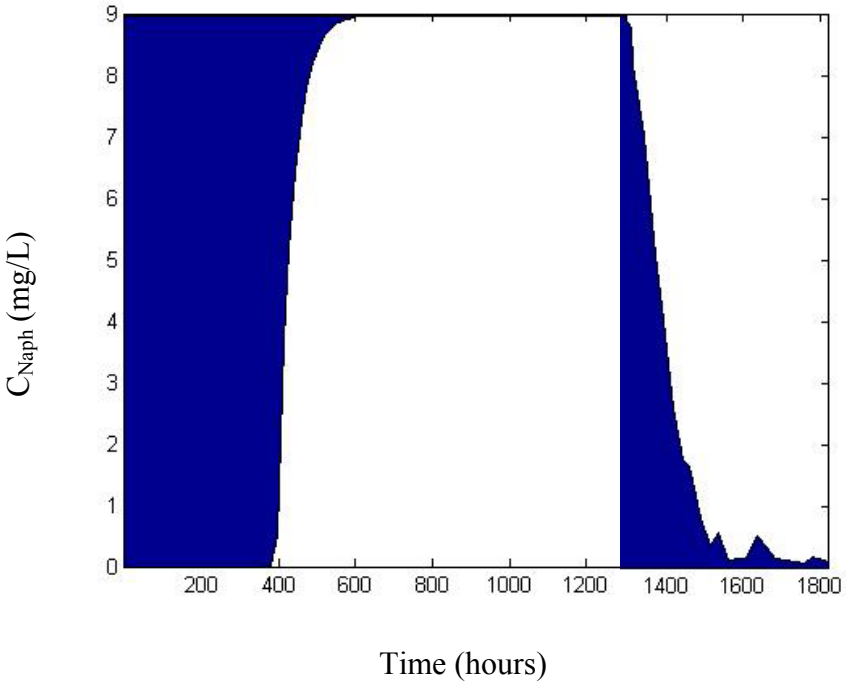

Figure 5. 17 Typical schematic of the area calculated from adsorption and desorption part of the column curves (DP-sand mixture naphthalene sorption desorption).

Table 5.8 Sorbed and desorbed naphthalene amounts in column tests

Sorptive Medium		**MT** (LOI=3.2%)	**PS** (LOI=10.7%)	**DP** (LOI=20.5%)	**PAC**
Port B	Mass Sorbed [a](mg)	10.32	47.47	174.36	321.59
	Mass Desorbed [b] (mg)	3.87	24.62	48.2	109.15
	Mass Retarded [c] (mg)	6.45	22.85	126.16	212.44
	Mass Retarded / Sorptive Medium Mass [d] (μg /g FA-sand mixture)	29.94	128.98	725.47	1071.31
	Percent Retarded [e] (%)	62.50	48.14	72.36	66.06
Port C	Mass Sorbed [a](mg)	28.01	103.92	411.57	749.47
	Mass Desorbed [b] (mg)	6.2	45.49	155.19	168.58
	Mass Retarded [c] (mg)	21.81	58.43	256.38	580.89
	Mass Retarded / Sorptive Medium Mass [f] (μg /g FA-sand mixture)	47.25	153.92	675.57	1350.28
	Percent Retarded [e] (%)	77.87	56.23	62.29	77.51

a- area calculated from adsorption curve, *b*-area calculated from desorption curve, c- the difference between *a* and *b,* d- retarded mass to sorptive medium mass ratio up to Port B, e- ratio of (c/*a*)*100, f- retarded mass to sorptive medium mass ratio up to Port C

between 66.06 and 77.51%. This observation further supports the previous findings that HCC fly ashes are strong sorbents with sorption properties comparable to a commercial PAC product.

5.4.6 Naphthalene Retardation Coefficients from Column Breakthrough Curves

Retardation coefficients from the column test results were determined for *o*-xylene using the column density, porosity, and the Freundlich isotherm parameters. These are plotted in Figure 5.18 as function of retardation coefficients calculated using the isotherm parameters from the batch adsorption tests. The retardation coefficients calculated from column tests are 2.3 to 3.6 times lower than ones calculated from batch tests. Altefelder et al. (2001), Maraqa et al. (2001) reported a difference in similar magnitude between the column- and batch-based retardation coefficients. Furthermore, both retardation coefficients increase with increasing LOI of the fly ash (Figure 5.19). Also the same figure reveals that the correlation for the column-derived retardation coefficients is favorable upon batch-derived retardation coefficients due to higher R^2 values.

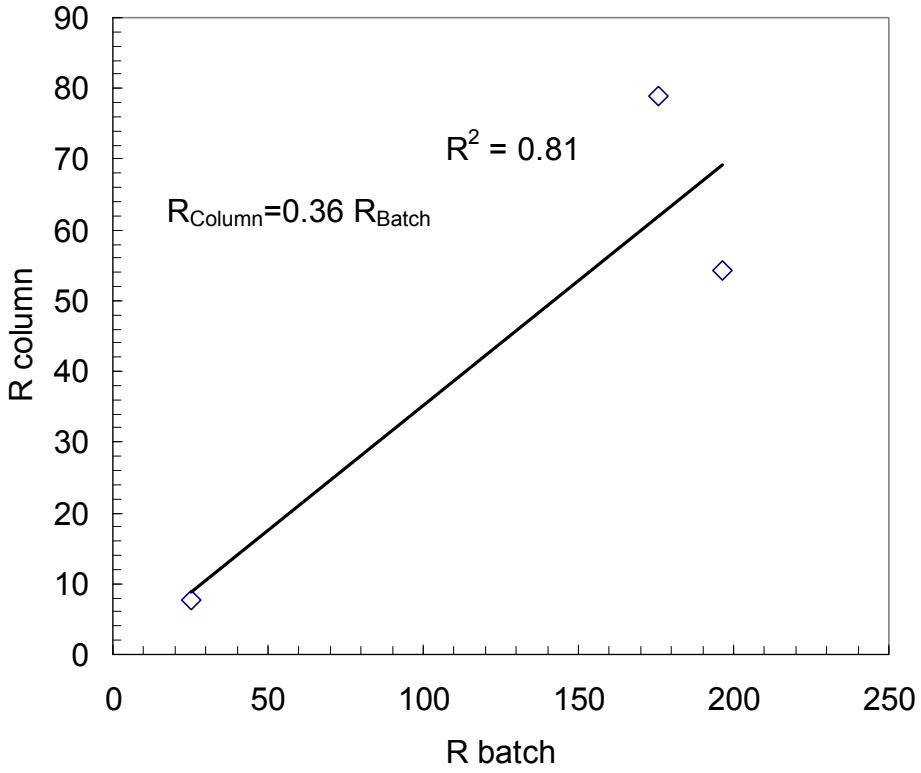

Figure 5.18 The relationship between the naphthalene retardation coefficients calculated using column and batch data for three fly ashes.

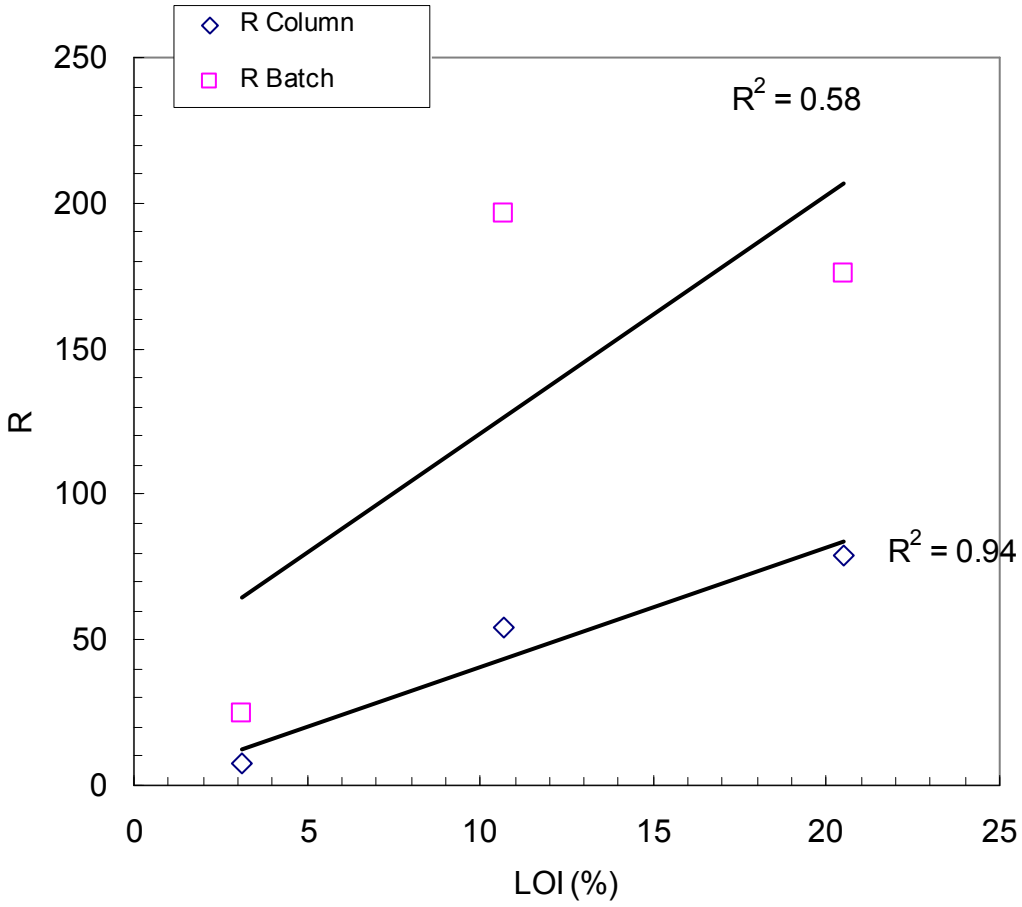

Figure 5. 19 Retardation coefficients for naphthalene from the column and batch data versus Loss in Ignition LOI (%)

5.4.7 Column Sorption-Desorption Test Results with *o*-xylene

Sorption-desorption performance of *o*-xylene was examined by running column experiments with MT, PS, DP fly ash-sand mixtures and PAC-sand mixture. The main objective of these tests was to investigate performance of the fly ashes with a less hydrophobic, and subsequently a more mobile (due to its high aqueous solubility) organic contaminant as compared to naphthalene.

In these experiments *o*-xylene solutions were prepared as step input in a constant concentration range of 30.3 to 38.9 mg/L. This range mimics typical concentration levels of BTEX compounds observed in contaminated field sites (Kelly et al. 1995). The column experiments for *o*-xylene sorption desorption were conducted following the same experimental set-up and conditions as for naphthalene (See Chapter 5.1.3). Similar to the experiments with naphthalene, numerical simulations of the experiments were conducted using VMOD-MT3DMS. The isotherm parameter estimation for the numerical modeling was conducted by following the same procedure as described above for the naphthalene tests, i.e., the K_F parameters were calculated from the MT3DMS simulations. The best-fit isotherm parameters used in the numerical analysis are tabulated in Table 5.9, along with the ones taken from batch tests. The experimental breakthrough curves and numerical modeling simulations are shown in Figures 5.20 and 5.21 for fly ash-sand and PAC-sand mixtures, respectively. As seen in Figures 5.20 and 5.21, the column performance was successfully predicted by the numerical simulations using the column test-derived isotherm parameters.

Table 5.9 Isotherm coefficients from batch and column studies

Column	n	Batch K_f	Column K_f	RMSE	K_F efficiency [a] (%)
MT	0.388	79.08	17.58	3.49	22.3
PS	0.3796	305.2	85.6	2.18	28.1
DP	0.26	803.4	284	2.38	35.4
PAC	0.2	46940	445.8	2.81	1.0

[a] (Column K_f / Batch K_f)*100

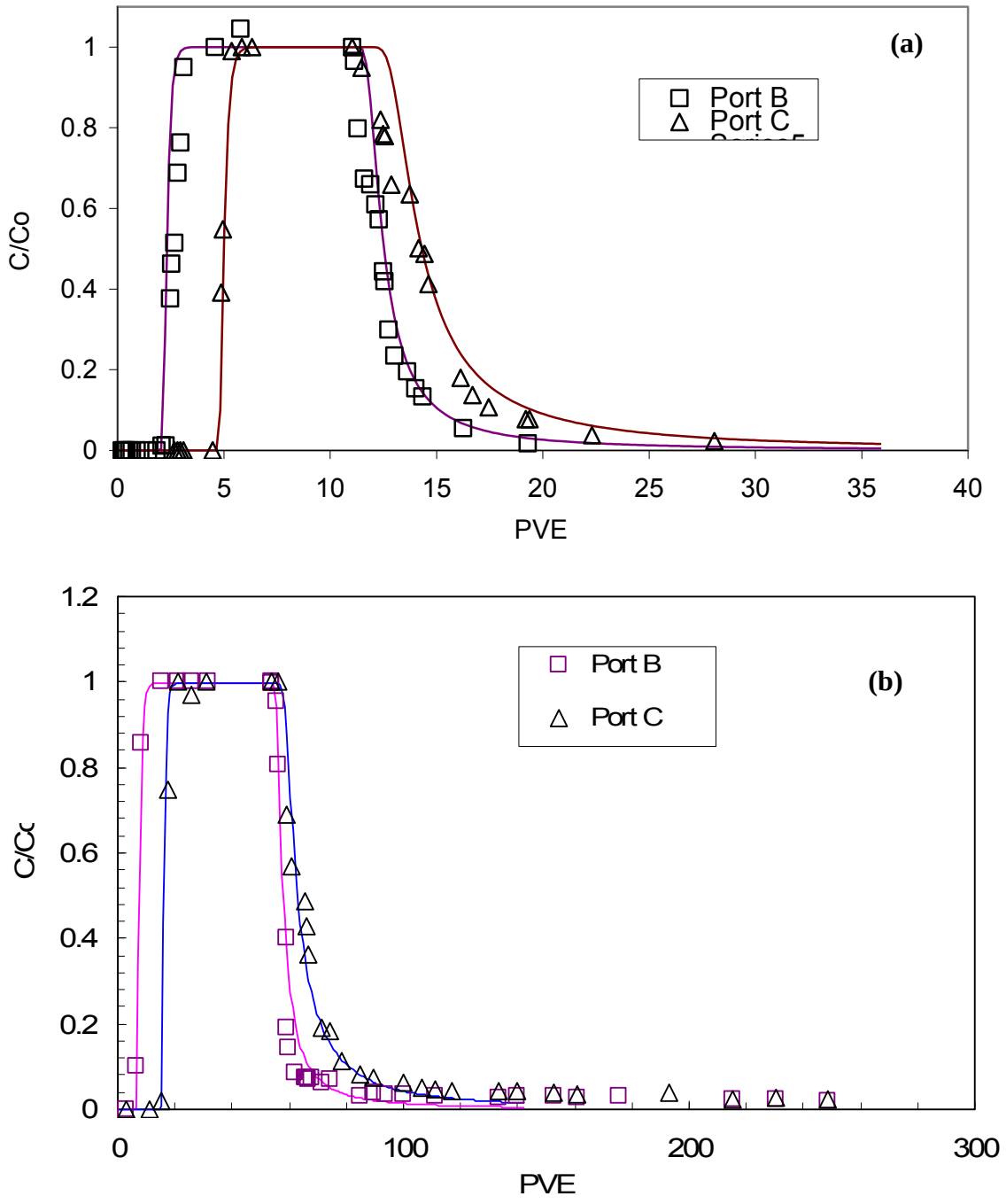

Figure 5. 20 Breakthrough curves from Port B and Port C for the *o*-xylene sorption desorption column studies using a)MT, and b)PS fly ash as sorptive medium. Solid lines are from the numerical modeling conducted using MT3DMS.

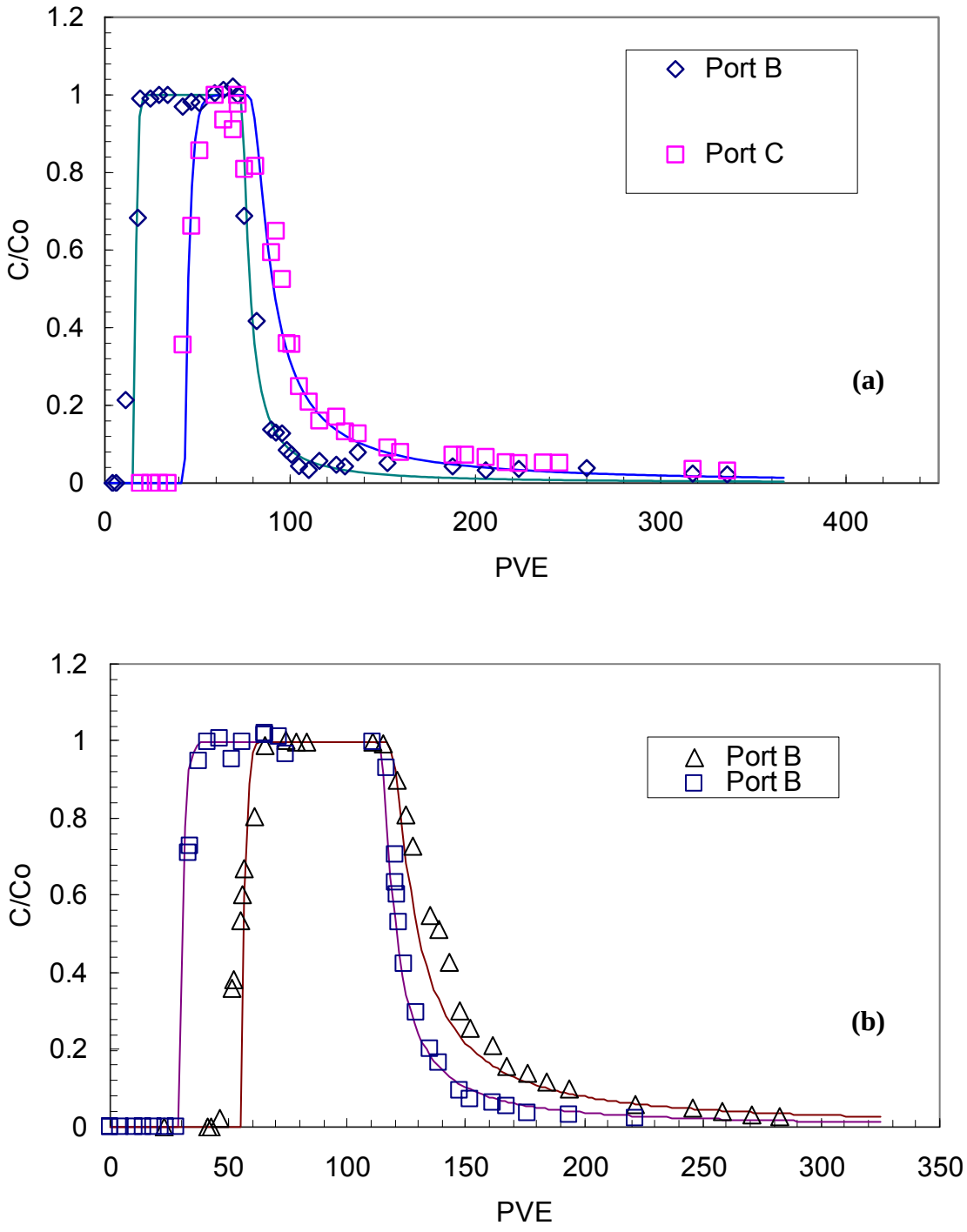

Figure 5. 21 Breakthrough curves from Port B and Port C of *o*-xylene sorption desorption column using a)DP fly ash, and b)PAC as sorptive medium. Solid lines are from the numerical modeling conducted using MT3D.

Two observations can be made based on a visual comparison of the experimental and numerical data. First, similar to the naphthalene tests, *o*-xylene breakthrough curves have sharp adsorption fronts during the sorption phase of the experiments. Fesch et al. (1998) speculated that the effect of equilibrium sorption was most evident in the form of self-sharpened adsorption fronts of the breakthrough curve without any tailing. Thus, the sharp-front adsorption curves suggest that sorption equilibrium was achieved during the *o*-xylene adsorption onto all media. Second, a tailing of the conclusion of the desorption front was observed in all tests. A tailing front of the desorption breakthrough was also observed by several other researchers during column testing of organic contaminant transport (e.g., Brusseau et al. 1995, Spurlock et al. 1995, Altfelder et al. 2001, Lee et al. 2002). Altfelder et al. (2001) discussed several possible explanations for the tailing desorption front phenomenon. One possible reason for the observed long tailing is the nonlinear sorption characteristic of the sorbent. Fesch et al. (1998) performed column sorption-desorption experiments on sand-clay mixtures and also attributed the tailing desorption front to the nonlinear sorption characteristic of the medium. Alternatively, slow desorption kinetics can cause a tailing during desorption. This hypothesis was also supported by Maraqa et al. (1998), who attributed a tailing desorption breakthrough to the slow mass transfer processes. Consequently, a combination of non-equilibrium in the mass transfer process and nonlinear sorption characteristics could be possible reasons for long tailing of *o*-xylene breakthrough curves.

The hypothesis that the nonlinear sorption characteristics are responsible for the desorption tailing is supported by a comparison of the Freundlich exponent n of each fly ash. As noted by, Accardi-Dey and Gschwend (2002), n describes the degree of sorption

nonlinearity for the Freundlich isotherm. Specifically, for n<1, the affinity of the sorbents sites for the sorbate decreases as the sorbed concentration increases. The HCC fly ashes tested for *o*-xylene sorption exhibited n values of 0.388, 0.3796, 0.26 for the MT (LOI=3.2%), PS (LOI=10.7%), and DP (LOI=20.5%) fly ashes, respectively. It is clear from the data that fly ashes with the higher LOI values have lower n values, which, in turn, indicate a high degree of nonlinearity. Furthermore, note that PAC has an n value of 0.20, the lowest n among all the sorbents tested consistent with its higher LOI value (99%). Spurlock et al. (1995) discussed the effect of n on the desorption tailing. According to their experimental study, the sorbents with low n values had longer tailing during column desorption tests. Consistent with their observation, the sorbents tested in this study with lowest n values (i.e., PAC and DP fly ash) exhibited relatively longer desorption tailings.

5.4.8 *O*-xylene Retardation from Column Experiments

The masses of the sorbed and desorbed *o*-xylene were calculated following the same integration method as used for the naphthalene data, as described in Section 5.6.1. The results of the numerical integration are given in Table 5.10. Note that because of the long tailing desorption breakthrough curves, observed during *o*-xylene tests, effluent concentrations did not reach to the detection limit before the tests were terminated, which resulted in some underestimation of the mass desorbed. However, the desorbing concentrations are all around 0.5 mg/L, which is substantially lower than the USEPA MCL level for *o*-xylene (10 mg/L). Several observations can be made based on the data in Table 5.10.

Table 5.10 Sorbed and desorbed *o*-xylene amounts from column test results

	Sorptive medium	**MT** (LOI=3.2%)	**PS** (LOI=10.7%)	**DP** (LOI=20.5%)	**PAC**
Port B	Mass Sorbed [a](mg)	20.55	69.63	123.26	372.9
	Mass Desorbed [b] (mg)	11.46	37.16	101.64	145.92
	Mass Retarded [c] (mg)	9.09	32.47	21.62	226.98
	Mass Retarded / Sorptive Medium Mass [d] (μg /g FA-sand mixture)	40.86	176.82	126.74	1123.67
	Percent Retarded [e] (%)	44.23	46.63	17.54	60.87
Port C	Mass Sorbed [a](mg)	44.19	144.63	321.77	689.71
	Mass Desorbed [b] (mg)	22.75	111.96	273.39	300.36
	Mass Retarded [c] (mg)	21.44	32.67	48.38	389.35
	Mass Retarded / Sorptive Medium Mass [f] (μg /g FA-sand mixture)	45.27	82.38	129.22	887.63
	Percent Retarded [e] (%)	48.52	22.59	15.04	56.45

a- area calculated from adsorption curve, *b*-area calculated from desorption curve, c- the difference between *a* and *b,* d- retarded mass to sorptive medium mass ratio up to Port B, e- ratio of (a/*c*)*100, f- retarded mass to sorptive medium mass ratio up to Port C

First, the retardation percentages determined for *o*-xylene are in all cases lower than calculated for naphthalene. This is probably related to the somewhat more hydrophobic nature of naphthalene compared to o-xylene. Second, as was observed for the naphthalene percent retarded o-xylene mass generally increases with increasing LOI value with the exception of DP.

5.4.9 *O*-xylene Retardation Coefficients from Column Breakthrough Curves

Following the same approach as for the naphthalene column data, retardation coefficients from the column test results were determined for *o*-xylene using Equation 5.9 and the column density, porosity, and the Freundlich isotherm parameters. Additionally, retardation coefficients using isotherm parameters from batch adsorption tests were also calculated. Again, as was observed with naphthalene, The retardation coefficients calculated from column tests are 2.7 to 3.6 times lower than ones calculated from batch tests (Figure 5.21). As illustrated in Figure 5.22, the batch and column retardation coefficients increase with increasing LOI of the fly ash, as expected although there is a stronger correlation for the column-derived retardation coefficients with LOI that for the batch-derived retardation coefficients based on the higher R^2 values.

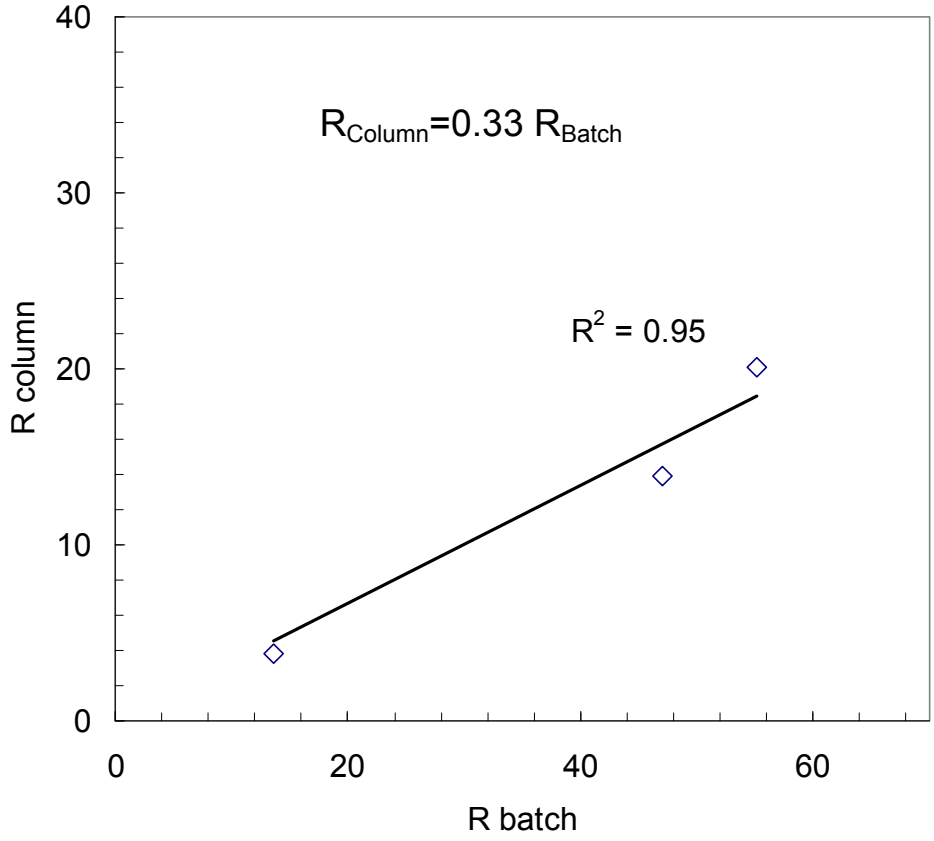

Figure 5.22 The relationship between the retardation coefficients calculated using column and batch data for *o*-xylene

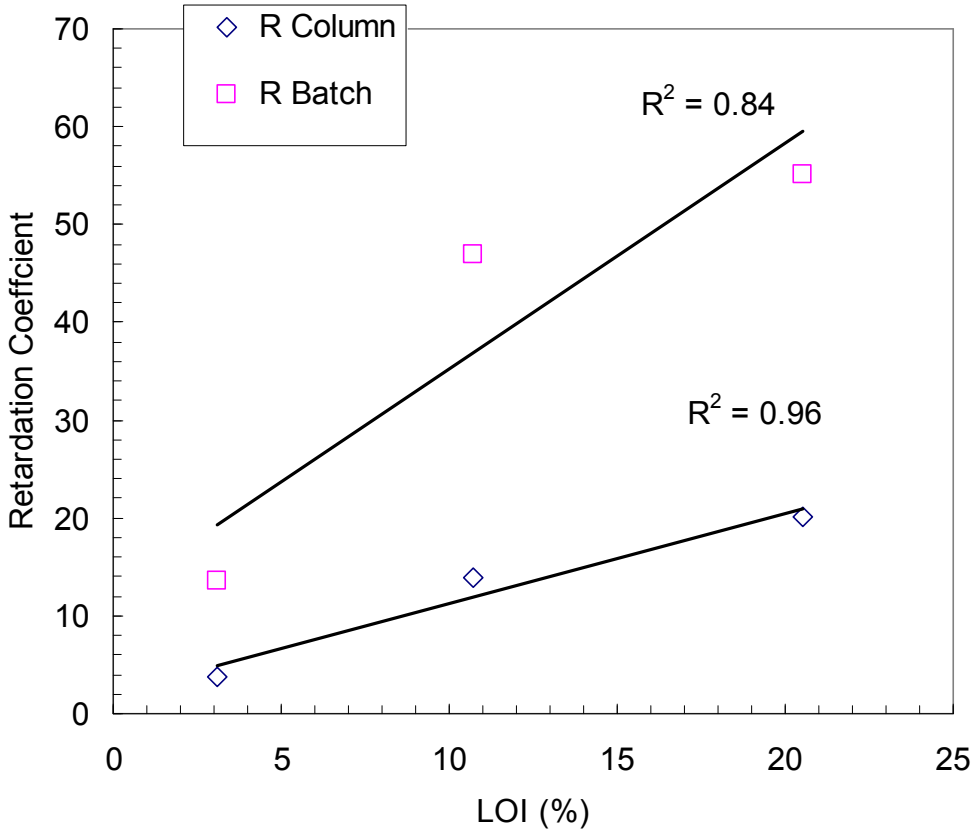

Figure 5.23 Retardation coefficients from column and batch data versus Loss in Ignition LOI (%) for *o*-xylene

5.5. *Conclusions*

The findings of the column sorption desorption tests on the mixtures of sand with three fly ashes, DP, PS, and MT, with LOI content of 20.5%, 10.7%, and 3.1%, respectively, and PAC have shown that high carbon content fly ashes are strong sorbents with sorption properties comparable to a commercially powder activated carbon with retardation capacity of 48 to 78% for naphthalene and 15 to 48% for *o*-xylene. These ranges were very comparable to the range observed for retardation within PAC. Retarded naphthalene and *o*-xylene amounts increased with increasing LOI content (MT, PS, DP fly ashes and PAC, respectively) in the column tests. For example, the DP fly ash exhibited sorption properties comparable to a commercially powder activated carbon

The measured hydraulic conductivities of fly ash-sand mixtures in the column sorption-desorption tests were comparable with the typical field hydraulic conductivities reported for PRBs. The bromide tracer test data indicated that dispersivity values range between 0.09 and 0.76 cm, and 0.04-0.96 cm for fly ash-sand and PAC-sand mixtures, respectively. These values fall in a typical range of values reported for sorptive media with relatively high fines content.

pH readings during column experiments showed that pH initially remained constant for several pore volumes of flow, then decreased at the later stages, and eventually dropped to a level comparable to the pH of artificial groundwater solution (i.e., pH =6.9). The buffering capacities of the Maryland fly ashes tested in this study were diminished and the pH in the system was governed by the PIPES buffer.

Numerical simulations conducted on the column sorption desorption data revealed that the breakthrough curves determined using the batch parameters shifted rightward

implying that the naphthalene sorption is overpredicted by using batch adsorption test derived parameters. It is possible that a combination of factors such as solid-to-liquid ratio, sorption nonlinearity, and nonequilibrium (rate-limited) sorption caused the observed discrepancy between the batch and column-derived parameters.

Freundlich isotherm coefficients calculated from the column data were 27.3 to 47.3% lower than the batch-determined ones. Column sorption-desorption data was successfully described using a Freundlich isotherm. The areas under the contaminant breakthrough curves were used to calculate the retarded contaminant mass during the experiment. The calculations revealed that the retarded naphthalene amount increased with increasing LOI values (MT, PS, DP fly ashes and PAC, respectively). The retarded mass per gram sorptive medium calculated from Port C is consistently higher than the one calculated at port B, which indicated that the retarded mass increased along the height of the column.

Similar to the naphthalene tests, *o*-xylene breakthrough curves have sharp adsorption fronts during the sorption phase of the experiments. A tailing of desorption front was observed in all tests. Fesch et al. (1998) speculated that the effects of equilibrium sorption-desorption was most evident from the self-sharpened adsorption fronts of the breakthrough curve without any tailing. Thus, the sharp front adsorption curves suggested that the sorption equilibrium was achieved during the *o*-xylene adsorption onto all media. *O*-xylene breakthrough curves also exhibited tailing at the desorption front.

Chapter 6 : Bioreactive Barrier Design: An Integrated Approach Using Aerobic Biodegradation and Sorption

Biodegradation is the most important destructive mechanism for contaminant removal in bioreactive barrier applications. Therefore, prior knowledge of the biodegradation kinetics is essential for designing bioreactive barriers. Correctly representing the impact of biokinetics on contaminant fate confers several advantages, including the minimization of errors in predicting the biodegradation rate, and a more complete understanding of the effect of attenuation processes on the contaminant (Bekins et al. 1998).

The influence of sorption on biodegradation is complex, with a variety of positive and negative effects having been observed (Rittmann et al. 1994). For example, if the sorption rate is significant, it can reduce the contaminant concentration in solution that is available for biodegradation. Furthermore, if the rate of mass transfer from the soil particles is slower than the biokinetics, then the biodegradation rate is limited by the desorption rate. However, if the solute concentrations are toxic to the microorganisms, then sorption may sufficiently lower the contaminant concentration to allow biodegradation. Furthermore, in some cases, increased biological growth will occur when sorbed substrate is later become available for biodegradation by desorption. Which of these effects, if any, occurs, and to what degree depends on the concentration of the contaminant, sorbent, and microorganism.

The effects of sorption coupled with biodegradation in a reactive barrier design have been evaluated by several researchers. Consistent with the previous research

discussed above, both positive and negative influences have been observed. For example, Guerin and Boyd (1992), and Park et al (2001) reported an increase in the biodegradation potential when sorptive soils were employed. Famisan and Brusseau (2002) reported that while local bioavailability may have been reduced for the soils tested, the overall biodegradation was increased due to sorption. However, McBride et al. (1992) reported no change in the biodegradation rate of the sorptive medium tested in the laboratory. Relevant to HCC fly ashes studied in this research, with their highly nonlinear sorption properties (See Chapter 3), Brusseau (1995) suggested that rate of biodegradation in a highly sorptive medium can be affected by the sorption nonlinearity

The research presented in this chapter had three objectives: 1) to determine the appropriate biodegradation rates for naphthalene, 2) to investigate the biodegradation of naphthalene in the fly ash medium in a column set-up, and 3) to evaluate the life expectancies of the bioreactive barrier for different barrier dimensions and aquifer conditions. In the following section, a brief review of biodegradation kinetics is presented. Subsequently, the methodology for the biodegradation-sorption column studies is presented, followed by a presentation and discussion of the experimental and modeling results.

6.1.1 Biodegradation Kinetics

Mathematical description and evaluation of the transport and biodegradation of organic compounds in a sorptive medium requires selection of an appropriate model of the biodegradation rate (Bekins et al. 1998). Several mathematical expressions have been proposed for describing biodegradation kinetics as a function of substrate concentration

in subsurface systems. The most commonly used ones are Monod equation, and first- and zero-order approximations, of which first two are the focus here. The classical Monod equation is given as:

$$\frac{dC}{dt} = -\frac{\mu_{\max} \cdot X \cdot C_i}{Y \cdot (K_s + C_i)} \tag{6.1}$$

where μ_{max} is the maximum specific growth rate (T^{-1}), X is the biomass concentration (ML^{-3}), C_i is the contaminant concentration (M_sL^{-3}), Y is the yield coefficient of bacteria (MM_s^{-3}), and K_s is the half saturation constant (M_sL^{-3}). The Monod equation models the interdependence of the degradation of rate limiting compound and biomass growth. Although many studies have been conducted to determine Monod parameters, the general applicability of these parameters are unclear. Furthermore, parameterization of the Monod model is challenging due to inherent correlations between μ_{max} and Ks, and the impact of culture history and conditions, the experimental data quality, and the regression technique on the parameter estimates (Haws et al. 2006).

Because of the challenges associated with the Monod model, as well as general ease of use, the first-order rate model is the most commonly employed one for both field and laboratory biodegradation kinetic determinations (Rifai et al. 1995, Warith et al. 1999). Specifically, when modeling the biodegradation of an organic compound, if the aqueous compound concentration is much lower than the K_s value, (Haws et al 2006) then the Monod model reduces to first-order kinetics with respect to C:

$$\lambda = -\left(\frac{\mu_{\max} \cdot}{K_s \cdot Y}\right) X \cdot C_i \tag{6.2}$$

where the biomass, X_s, is constant, it can be included with the kinetic coefficients into a lumped first order degradation constant (λ) that can be defined as follows:

$$\lambda = \frac{\mu_{\max} \cdot X}{K_s \cdot Y} \tag{6.3}$$

Therefore, equation 6.2 can be written as:

$$\frac{dC}{dt} = -\lambda \cdot C_i \tag{6.4}$$

It should be noted that the biomass concentration (X_s) may not be constant and depends on the laboratory or field conditions including the availability of the contaminant as a growth substrate. This limits application of the Equation (6.4).

Numerical modeling of the biodegradation experiments in this work was conducted by using the VMOD-MT3DMS computer program. During this numerical modeling of the biodegradation experiments, Equation 6.4 was used as the biodegradation sink term in the transport equation (Equation 5.7). As discussed by Brusseau (1995), biodegradation of organic contaminants is conventionally assumed to take place only in solute phase, therefore, only biodegradation in the aqueous phase was modeled in this study. The first-order kinetic parameters, for microbial degradation of naphthalene were estimated in column experiments, as described below.

6.2 *Materials and Methods*

6.2.1 Microorganism and Inoculum preparation

The microorganism used in the column biodegradation experiments was *Pseudomonas fluorescens* Uper-1, which as obtained from Dr. Lueking of the Department of Biological Sciences at Michigan Technological University. Under aerobic conditions, this microorganism utilizes naphthalene as a carbon source for growth and

requires no other growth factors (Song 2005). An Uper-1 stock culture was maintained by periodically preparing streak plates and transferring existing cultures to freshly prepared plates containing nutrient agar (Difco Granulated agar), which were incubated in the presence of naphthalene vapor. The plates were subsequently stored in a refrigerator at 4 ºC.

As a first step in the inoculum preparation, a batch culture of Uper-1 was grown in four 50 mL side arm flasks containing 50 ml of basal salt medium (BSM). The BSM contained 4 g KH_2PO_4, 4 g Na_2HPO_4, 2 g $(NH_4)_2SO_4$, 0.2 g $MgSO_47H_2O$, 0.001 g $CaCl_2$ $2H_2O$, 0.001 g $FeSO_47H_2O$ and 1.5 % w/v (0.75g / 50 mL) glycerol (Acros 99+%) (Song 2005). The inoculum was grown on glycerol first in BSM and followed by growth on naphthalene in synthetic groundwater, which was described in Chapter 3. The flasks were prepared aseptically by capping with cotton balls wrapped with aluminum foil and autoclaving for 20 minutes at 121 ºC. After keeping the autoclaved flasks in room temperature for two hours, Uper-1 was transferred ascetically to inoculate triplicate flasks. The fourth glass of BSM with glycerol was used as a abiotic control. All the flasks were incubated with shaking (110 rpm) in a water bath at 30 ºC for 24 to 48 hours. Growth of the batch culture in the side arm flasks was monitored turbidimetrically (wavelength = 510 nm) utilizing a Spectronic 21 spectrophotometer (Bausch and Lomb, Inc.). A typical growth curve for Uper-1 grown on BMS with glycerol is shown in Figure 6.1. Once the biomass reached the late exponential phase (around 20 hours), 0.5 mL of the primary culture was transferred into three autoclaved side-arm flask contained BSM with 1.5 % glycerol (w/v). These three flasks with one control flask were also incubated in the water bath with shaking for 24 hours and, similar to the primary culture, the

biomass in the BSM was monitored turbidimetrically. A typical growth curve for the secondary culture is shown in Figure 6.2. When the culture reached the middle exponential phase, the biomass in the secondary culture was harvested by centrifugation at 3000g for 10 minutes. The supernatant from the centrifuged BSM was decanted and the remaining biomass was washed three times using autoclaved synthetic groundwater. This washing procedure enabled removal of any residual glycerol from the biomass. The washed culture was then aseptically resuspended in a 1000 mL aspirator bottle containing autoclaved synthetic groundwater with filter-sterilized solution of naphthalene in Dimethylformamide **(**DMF) to reach the desired concentration of 10 mg/L. The inoculum in the aspirator bottle was incubated for 24 hours at room temperature. The heterotrophic plate count (HPC) at that point was $8x10^{11}$ CFU/L. This inoculation procedure ensured fully adaptation to growth on naphthalene before inoculating the column. Column inoculation was carried out by pumping the inoculum from the aspirator bottle using same pumping set up as described in Chapter 5, at a flow rate of 40 mL/hr for 25 hours. The inoculated column was allowed to stand stagnant for 24 hours after the pumping, to provide the biomass time to attach on sand medium. Similar column inoculation techniques were used by Kelly et al. (1996) and Yolcubal et al. (2003).

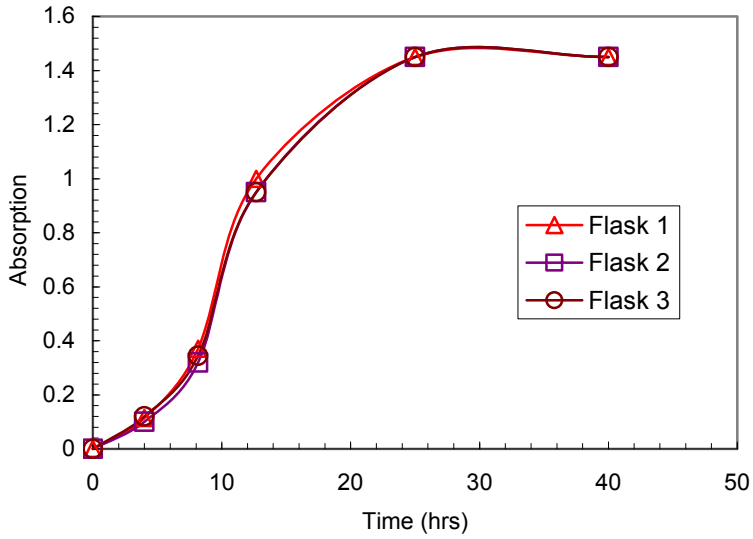

Figure 6.1 Typical Uper-1 growth curves (absorbance versus time) for the primary culture grown on BSM with glycerol

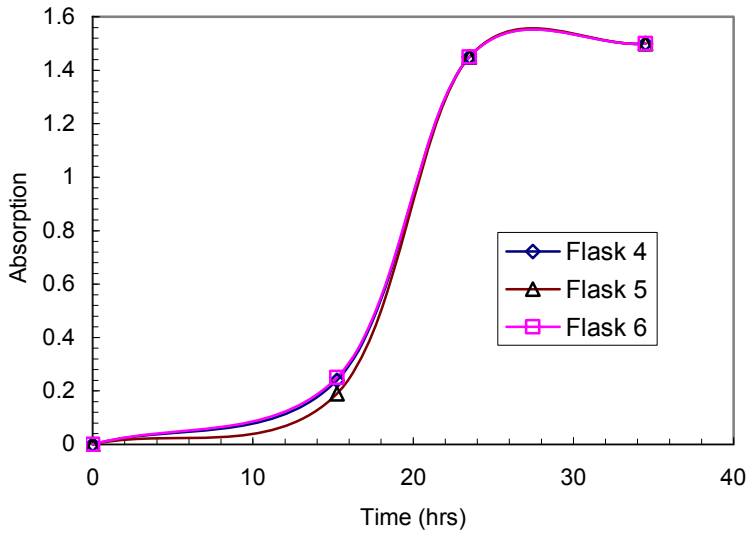

Figure 6.2 Typical Uper-1 growth curves (absorbance versus time) for the secondary culture grown on BSM with glycerol

6.2.2 Column Biodegradation Experiments

In order to investigate the naphthalene biodegradation kinetics of the Uper-1 culture, column biodegradation tests were conducted on the inoculated column. In these experiments, the non-sorptive sand used in the sorption-desorption experiments (Chapter 5) was the column medium. Thus, biodegradation was the only significant reaction mechanism in these experiments

The experimental column reactor design used in the sorption-desorption tests, as described in Chapter 5, was modified for the biodegradation experiments to allow accurate determination of the biokinetic parameters. As discussed by McBride et al. (1992), Kelly et al. (1996) and Chang and Rittmann (1987), shorter micro columns (e.g., lengths of 10 to 50 mm and for diameters of 5 to 25 mm) are often necessary for determination of rate parameters from inoculated soil columns, because of the relative rate of reaction. In this work, short column lengths provided for accurate measurements of naphthalene degradation with sufficient oxygen availability.

To achieve micro-column dimensions, the column reactor design described in Chapter 5 was modified by the addition of four new sampling ports near the column entrance for total of five ports. The four new ports were fabricated in the same manner as described in Chapter 5. The location of the sampling ports in the modified column used in biodegradation tests are shown in Figure 6.3. The first port (Port A) was located 10 mm from the column entrance with the distance between each remaining port set as 20 mm. Therefore all sampling during the experiments were taken after flow had traveled through at least 10 mm of column medium. Similar to the sorption experiments, sampling was accomplished using 25-gauge needles that extended to the center of the column. After

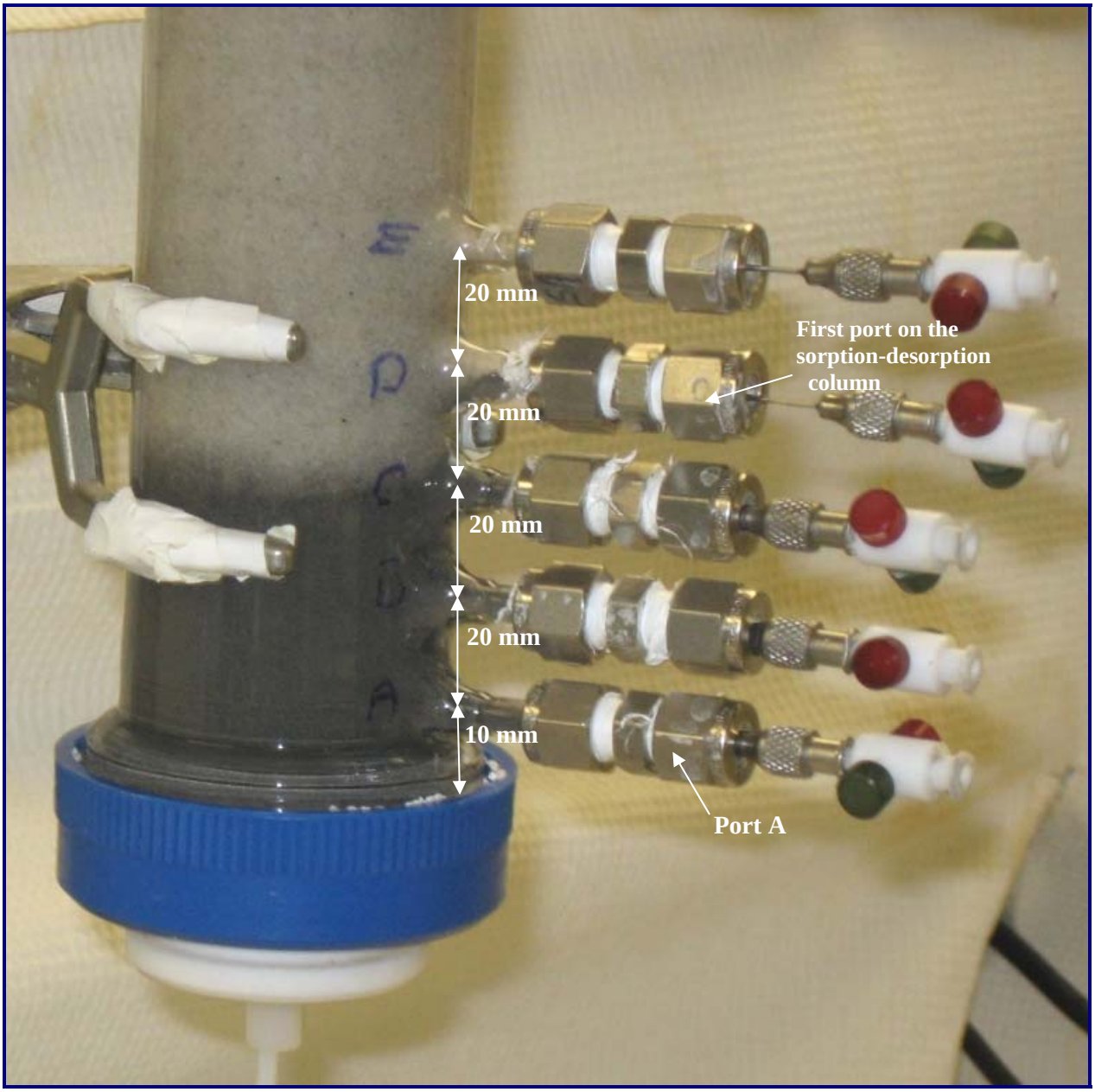

Figure 6.3 The column used in the PS fly ash-sand mixture biodegradation experiments

modification, the column was filled with sand by following the same aseptic packing procedure described in Chapter 5.1.3. The column was saturated with autoclaved synthetic groundwater as described in Chapter 5.1.4. Subsequently, the column was inoculated as described above. The influent solution was a three mg/L naphthalene in synthetic groundwater solution that was prepared aseptically as described in Chapter 5. To initiate the experiment, the naphthalene solution was used as a step input. The flow rate of the step input was 55 mL/hr.

After initiation of the experiment, the naphthalene concentration was maintained at the sampling ports until the system reached a steady-state with respect to naphthalene removal. To evaluate the approach to steady-state, the mean square successive differences in naphthalene concentrations were calculated for consecutive PVEs. Specifically, naphthalene losses were determined by taking the difference in concentration between the influent and sampling ports and dividing by the influent concentration. Once the steady state transport was achieved, samples from the ports were periodically analyzed for naphthalene, biomass, and dissolved oxygen concentrations.

The lumped first-order biodegradation rate constant, l, was determined during steady state naphthalene removal by varing method described by Buscheck and Alcantar (1995). This method has been commonly used for estimating first-order biodegradation rate constants when accurate determination of dispersivity and pore velocity are available (Bedient et al. 1999). Following this methodology, the naphthalene concentration has plotted on a logarithmic scale versus distance along column length on a linear scale, based on an analytical solution for one-dimensional steady state transport due to

advection, dispersion and biodegradation. The first-order biodegradation rate was then approximated by:

$$\lambda = \frac{Vc}{4\alpha}\left(\left[1+2\alpha\left(\frac{k}{Vx}\right)\right]^2 - 1\right) \tag{6.5}$$

where λ is first-order rate constant (T^{-1}), V_c is the retarded contaminant velocity (LT^{-1}), α is the dispersivity (L^{-1}), and k/V_x is the slope of line formed by making a log-linear plot of contaminant concentration versus distance downgradient along the flow path.

6.2.3 Combined Sorption-Biodegradation Experiments

Column sorption-biodegradation experiments were conducted using a Paul Smith (PS) fly ash-sand mixture in order to investigate the biodegradation performance of Uper-1 in the sorptive medium. The mixture consisted of 60% sand and 40% fly ash by weight and it was packed into the modified column following the procedures outlined in Chapter 5.1.3. Following packing, the column was inoculated with Uper-1 following the approach described above. The experiments were performed following the same basic protocol described for the biodegradation only columns, using a three mg/L naphthalene as a step input, with flow rate of 55.6 mg/L.

6.2.4 Non-reactive Tracer Experiments

In a solute transport system, in which biodegradation is coupled with sorption processes, the magnitude and rate of biodegradation is influenced by not only properties of microorganism and substrate organic compound, but also by hydrodynamic flow properties such as residence time and dispersivity (Brusseau et al. 1999). Therefore, non-reactive tracer (bromide) experiments were conducted after naphthalene concentrations reached steady-state levels to determine the hydrodynamic flow properties (average pore water velocity, dispersivity) of the medium tested. The bromide tracer solution (1000 mg/L Br) was autoclaved (20 minutes at 120 ºC) and prepared as described in Chapter 5.1.4 and. The autoclaved tracer solution was applied as step input with 55 ml/hr, following the procedure in Chapter 5. In order to determine the pore water velocities and hydrodynamic dispersion coefficients from the biodegradation column test results, the FORTRAN program "'trafit1d" was utilized. Details of the program are given in Chapter 5.1.4.

6.2.5 Analytical Methods

Performance of the biodegradation and sorption-biodegradation experiments required measurement of naphthalene, dissolved oxygen, biomass, and bromide. Naphthalene and bromide were measured as discussed in Chapter 5 and not discussed here. The methods for dissolved oxygen and biomass are outlined below.

6.2.5.1 Dissolved Oxygen Measurements

Dissolved oxygen (DO) concentrations were monitored at the influent and column ports using an oxygen microelectrode (Microelectrodes, Inc., Bedford, NH USA), connected to an OM-4 oxygen meter. Two sampling techniques were used. In case of the influent port, in which the influent solution flowed continuously, by using a 22-gauge hypodermic needle with a luer-hub, which was inserted into a female mininert valve on the sampling port and connected via a male-luer fitting to a section of Tygon tubing that was connected on the other-end to a barbed fitting on the flow cell of the DO microelectrode. The other barbed fitting on the flow all was attached via Tygon tubing to a syringe. A 0.3 mL of sample was slowly withdrawn using the syringe, the needle was disconnected from the mininert valve, and allowed to sit on the bench until a steady reading occurred.

In order to sample from the ports located along the length of the column, the mininert valves were opened and the sample was slowly withdrawn from the port by following the same procedure described for sampling from the influent port, except that 0.6 mL of sample was taken. The first 0.3 mL sample was discarded as it passed the flow cell, flushing the sampling, port, needle, and the sampling line, and the following 0.3 mL sample was used for DO measurements.

The oxygen percentage was recorded by the OM-4 meter and later converted into mg/L using the following equation:

$$S = (a / 22.414) \times ((760 - p) / 760) \times (r\%/100) \times 32000 \qquad (6.6)$$

where *S* is the solubility of gas (mg/L) mg per liter; *a* is the absorption coefficient of gas at temperature; *p* is the vapor pressure of water at temperature; and *r%* is the actual reading of DO meter in percent of oxygen.

A two-point method was used to calibrate the microelectrode using ambient air as well as a sample with zero DO. The calibration with ambient air was performed each time when the microelectrode was used during the experiments. The calibration with a sample of zero DO was carried out once a week. The zero DO solution was prepared by adding excess sodium sulfite, Na_2SO_3, and a trace of cobalt chloride, $CoCl_2$, to bring the DO to zero. The relative accuracy of microelectrode was reported as ±0.04 mg/L at 24°C by the manufacturer (Song 2005).

6.2.5.2 Heterotrophic Plate Counts

Heterotrophic plate counts (HPC) were performed to determine the biomass concentration in the aqueous samples during column biodegradation tests. The experimental procedures used in this method were adapted from Standard Method 9215 (APHA et al. 1995). During the HPC steps, aseptic techniques were employed and all the equipment used (e.g., test tubes with caps, dilution bottles, pipette tips, and filter papers) were autoclaved before use.

Agar plates for the HPC, were prepared using sterilized disposable petri dishes and R2A agar (Difco No: DF1826-17). A solution of R2A agar (18 grams in 1 L deionized water) was mixed and autoclaved for 20 minutes at 121 ºC. When the medium cooled to 45 to 50 ºC it was aseptically poured into the bottom of the Petri dishes. After the solidification of the agar, the plates were pre-dried at 30 ºC for 24 hours before using.

The plates that were not used immediately were stored in sealed bags at 4ºC in the refrigerator.

The dilution of the aqueous samples required for the HPC procedure was conducted using the phosphate and magnesium chloride-based dilution water. This solution was autoclaved for 20 minutes at 121 ºC before use.

Aqueous samples were serially diluted as follows. First, 1 mL of the samples taken from during the column tests (including inoculum preparation and column biodegradation tests) was asceptically transferred into 9 mL dilution water establishing a 10^{-1} dilution and shaken for 15 seconds vigorously using a 140 mini vortexer (VWR Scientific Products). The sample solution was further diluted by transferring 0.1 mL of sample from the first test tube into a second test tube containing 9.9 mL of dilution water, to prepare a 10^{-3} solution. The same procedures were followed to obtain a series of test tubes with a range of dilutions. Finally, taking 1 mL or 0.1 mL of each suspension and spreading it on the agar plate provided the desired dilution, or a one order of magnitude lower dilution, respectively. For example, if 1 mL and 0.1 mL of the 10^{-3} dilution solution were spread onto plates, the dilutions were 10^{-3} and 10^{-4}, respectively. HPC tests were conducted in this fashion with dilutions ranging between 10^{-3} and 10^{-8}. The R2A agar plates for each dilution were prepared in duplicates or triplicates.

The edges of the spread plates were wrapped with parafilm, and the plates inverted and incubated at 30°C for 72 hours. After incubation, plates having 30 to 300 colonies were considered in determining the plate count. All colonies in plates with appropriate range were counted and averaged. The bacterial count per milliliter (colony-forming units (CFU)/mL) was computed by using the following equation:

$$CFU / mL = \frac{ColoniesCounted}{actualsamplevolumeindish, mL} \quad (6.7)$$

Upon termination of the column experiments, the attached biomass concentrations were determined using the bacterial extraction technique described by Gagliardi and Karns (2000). Column media (sand or fly ash-sand mixture) samples were removed from the columns and diluted 1:10 in sterile synthetic groundwater (using a solid-to-liquid ratio of 10 g /100 mL). Then the attached biomass was extracted by using a Waring blender with a 1 L glass container that was operated at the top speed (22,000 rpm) for 2 min. After mixing, the contents were allowed to settle for 1 min before HPCs were conducted on dilutions of the supernatant collected from the middle fraction of the blender container. The blender and all necessary tools were autoclaved at 120 ºC for 20 minutes before use. The same extraction technique was used by Kelly et al. (1996) who observed a 95% efficiency of cell recovery.

6.3 *Results*

6.3.1 Non-reactive Tracer Results

The breakthrough curves from tracer experiments for biodegradation only column (sand) and combined biodegradation sorption column (PS fly ash-sand) are shown in Figures 6.4a and 6.4b, respectively. Note that these measurements were taken from port A of the modified column, which is located 10 mm down-gradient of the column inlet.

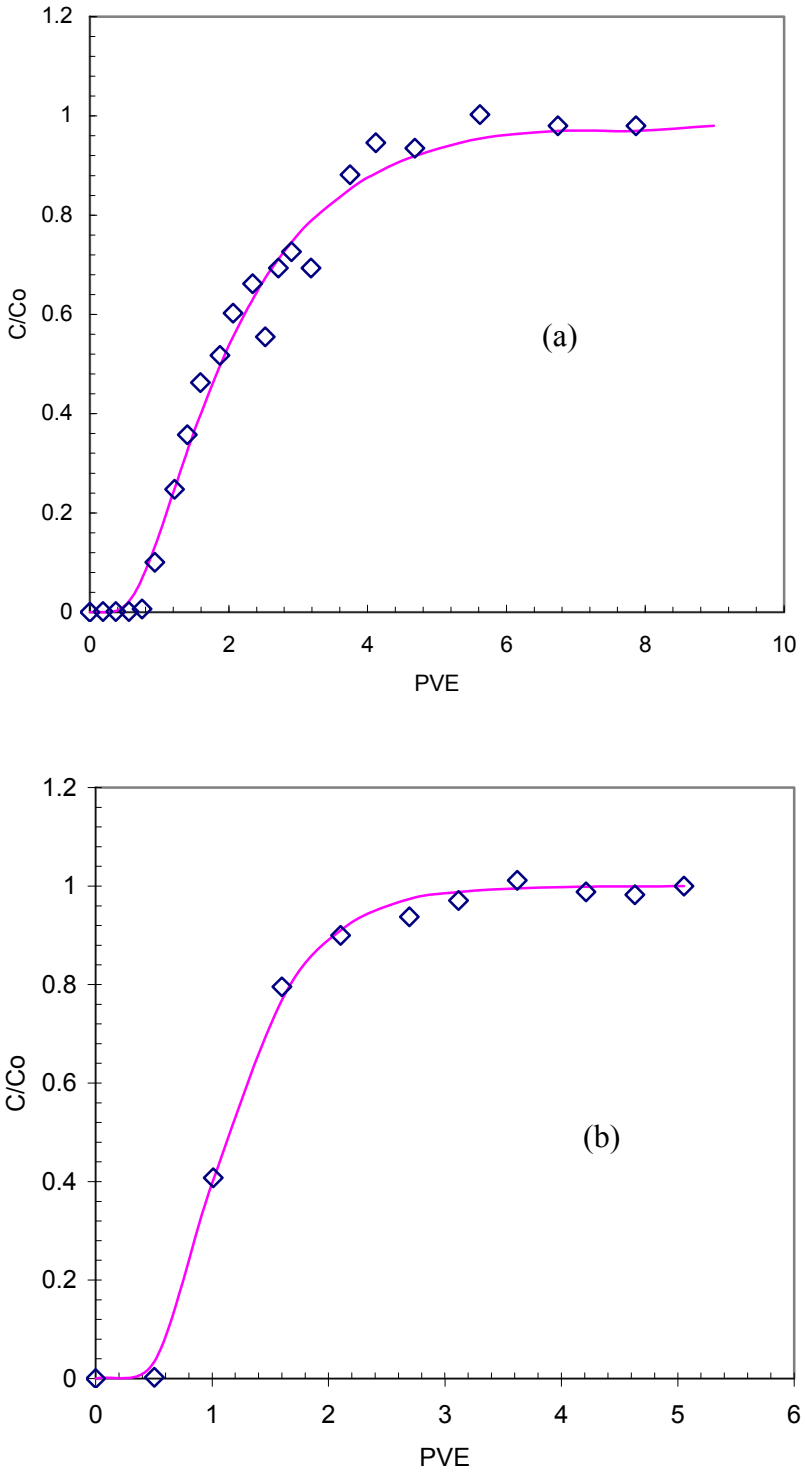

Figure 6.4 Bromide tracer breakthrough curves for (a) sand column, and (b) PS fly ash-sand mixture column

The results of bromide analysis for all biodegradation columns are shown in Table 6.1. The dispersivity was calculated by assuming molecular diffusion was negligible compared to mechanical dispersion. The hydrodynamic flow properties of the modified column (first port located at 10mm) are shown along with the result from a regular column (first port located at 70 mm). Previous studies have indicated that the predicted performance of any passive barrier systems (i.e., PRBs, bioreactive barriers) is quite sensitive to the dispersion coefficient (Rabideau et al. 2006). As seen in Table 6.1, the dispersion coefficients as well as dispersivities are very comparable for both the sand and sand-fly ash columns, although the biodegradation column with the PS-fly ash-sand mixture has slightly lower D_H and α values compared to those obtained for sand.

6.3.2 Column Biodegradation Test Results

The naphthalene breakthrough curve for Port A during the biodegradation test in the sand medium is shown in Figure 6.5. Once the sorption reached steady-state, the date were analyzed using the method of Buscheck and Alcantar (1995). Using the slope of 0.369, and α 0.24 cm of from Table 6.1 and V_c of 6,84 cm/sec and λ of 2.83 1/h was calculated using Equation 6.5.

The MT3DMS simulations using the λ value determined using the Buscheck and Alcantar method is presented with the experimental breakthrough at Port A in Figure 6.5. Three observations can be made based on Figure 6.5. First, a lag period can be observed before naphthalene removal starts due to biodegradation, which occurs at about 40 PVE (9 hours). Experiencing an initial lag is typical for most of the organic hydrocarbon degraders (Kelly et al. 1996) as the microbes adapt to their new environment, although the Uper-1 culture should have been reacclimatized to naphthalene degradation.

Table 6. 1 Results determined from Non-reactive tracer tests on biodegradation columns

Column Medium Type	Sampling Port Location (mm)	Q(cm^3/hr)	*V* (cm/hr)	D_H (cm^2/hr)	α (cm)	ρ (kg/cm^3)	Porosity (n)
Sand	**10**	55.6	6.84	1.677	0.24	1.410	0.47
Sand	**70**	45.0	6.10	1.630	0.27	1.560	0.41
PS fly ash-Sand Mixture	**15**	55.6	6.45	1.144	0.18	1.570	0.41

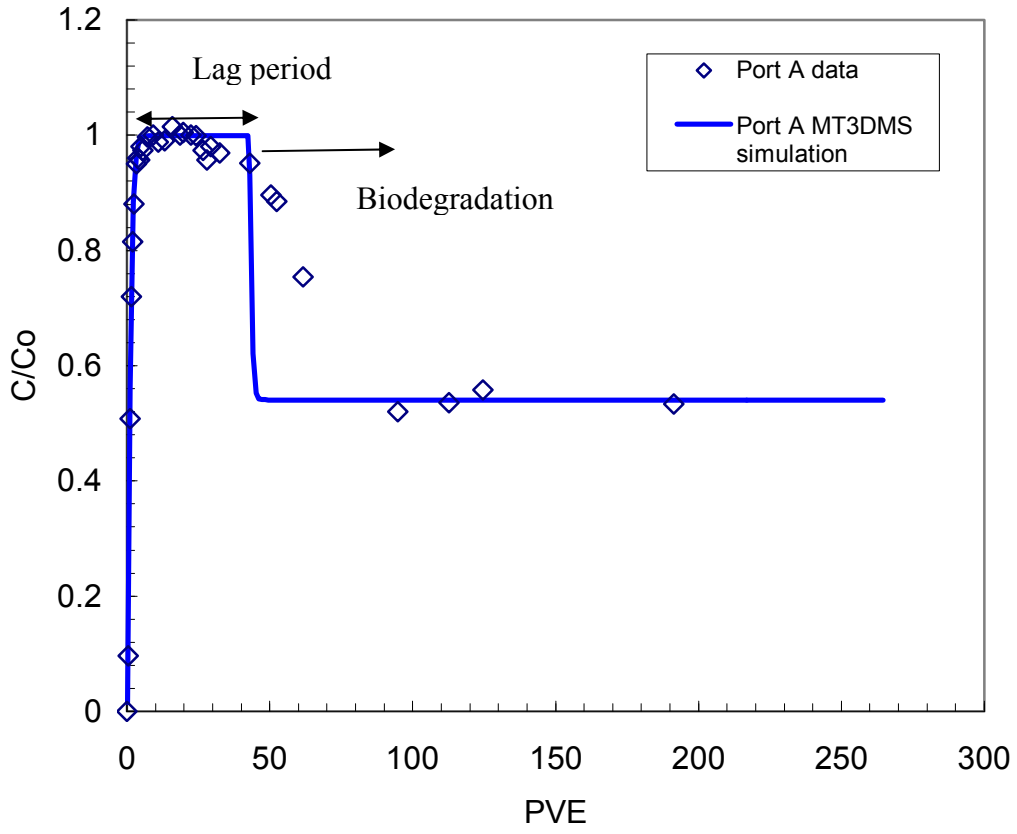

Figure 6.5 Naphthalene breakthrough at Port A during the naphthalene biodegradation test in the sand column. Column sampling length was 10mm. Solid lines are from MT3DMS simulation breakthrough using λ of 2.83 1/hr.

Second, the numerical simulations overpredict the biodegradation in the initial phase (between 55 to 95 PVE). Finally, the numerical simulations successfully predict the steady-state naphthalene removal using the biodegradation rate constant in the steady-state phase determined based on the Buscheck and Alcantar (1995) method.

During the biodegradation experiments, aqueous solutions from port A were analyzed for any intermediate compounds of naphthalene biodegradation. Fluorescence and GC chromatography scans on these samples did not indicate any peak other than naphthalene peaks, which in turn, indicated that naphthalene was completely mineralized in the degradation process.

DO concentrations from influent port and sampling ports along the column length are shown in Figure 6.6. The average DO at the influent port was about 6.9 mg/L during this experiment. The initial DO concentration at port A, however, was 0.91 mg/L, which is mostly due to the consumption of available O_2 during the column inoculation. Subsequently, the DO levels increased with application of the step input of the naphthalene solution to about 5 to 6 mg/L, indicating a low level of biological activity during that period although apparently not much naphthalene degradation observed (Figure 6.5). Then as the naphthalene levels decreased, the DO levels decreased as well. During the steady-state naphthalene removal period (>100 PVE), DO level averaged around 2.8 mg/L and, corresponding to a DO removal of 5.0 mg/L. During the same period, about 46% of initial naphthalene concentration (3.94 mg/L) was removed due to biodegradation (Figure 6.5) resulting in a DO concentration of about 2.2. mg/L, where naphthalene concentration was about 1.7 mg/L. Based on the naphthalene degradation stoichiometry including biomass growth (Equation 2.1), 1.5 mg DO is required per mg of

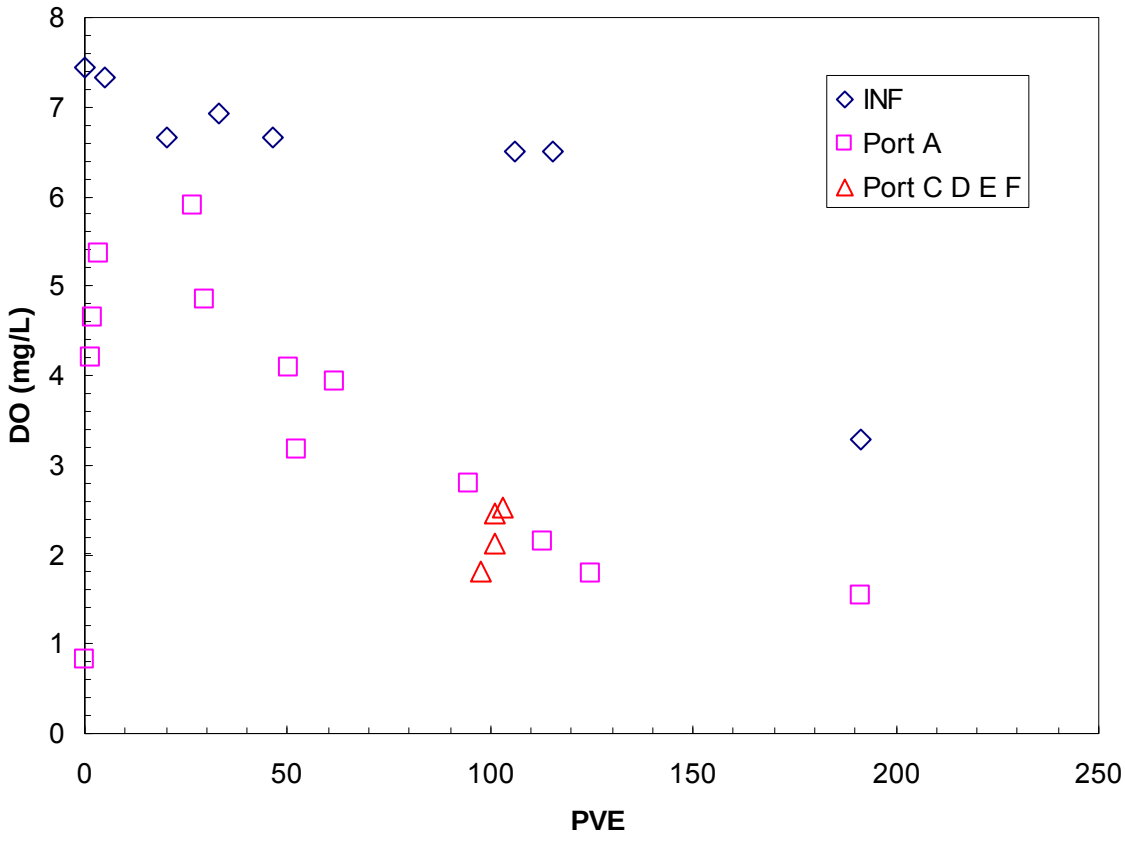

Figure 6.6 DO measurements from influent and sampling ports of biodegradation test on sand medium. INF: influent port, Port locations for A, C, D, E, F are 15, 55, 70, 90, 150 mm, respectively.

naphthalene mineralized. Assuming a naphthalene concentration of 1.7 mg/L, based on this stoichiometry we would predict ~ 2.6 mg/L DO required, which is less than the DO amount used up during biodegradation. If biomass sythethisis is ignored the naphthalene mineralization can be shown as:

$$C_{10}H_8 + 12O_2 \rightarrow 4H_20 + 10CO_2 \quad (6.8)$$

where the stoichiometry predicted 3.0 mg DO per mg naphthalene. Based on this, a DO loss of 5.1 mg/L is predicted. So the actual DO removal is reasonable given the naphthalene degradation observed.

Interestingly, the DO readings from other ports (Port C, D, E, F) were very close (~2.2.mg/L) to the values at port A (Figure 6.6), which indicates that no further biodegradation occurred above port A. These DO measurements suggest that the level of oxygen in the system may be critical. According to Kelly et al. (1996), DO levels above 1.3 mg/L in the aqueous samples should be high enough to prevent oxygen limitation during contaminant biodegradation and reaction rates in the columns would not be limited by availability of dissolved oxygen with this level of DO. The DO level in the sand column was averaged at around 2.8 mg/L, which is similar to but greater than the limit of 1.3 mg/L stated by Kelly et al. (1996). Therefore, it is unclear what is the main reason behind biodegradation leveling at 0.54 C/Co naphthalene removal and essentially stopping by Port A.It may be an oxygen limitation problem, or some other factor may be limiting the microbes. Biomass was measured attached to the sand at lower levels at ports above A (Figure 6.7), but this would not explain an absence of biodegradation above port A.

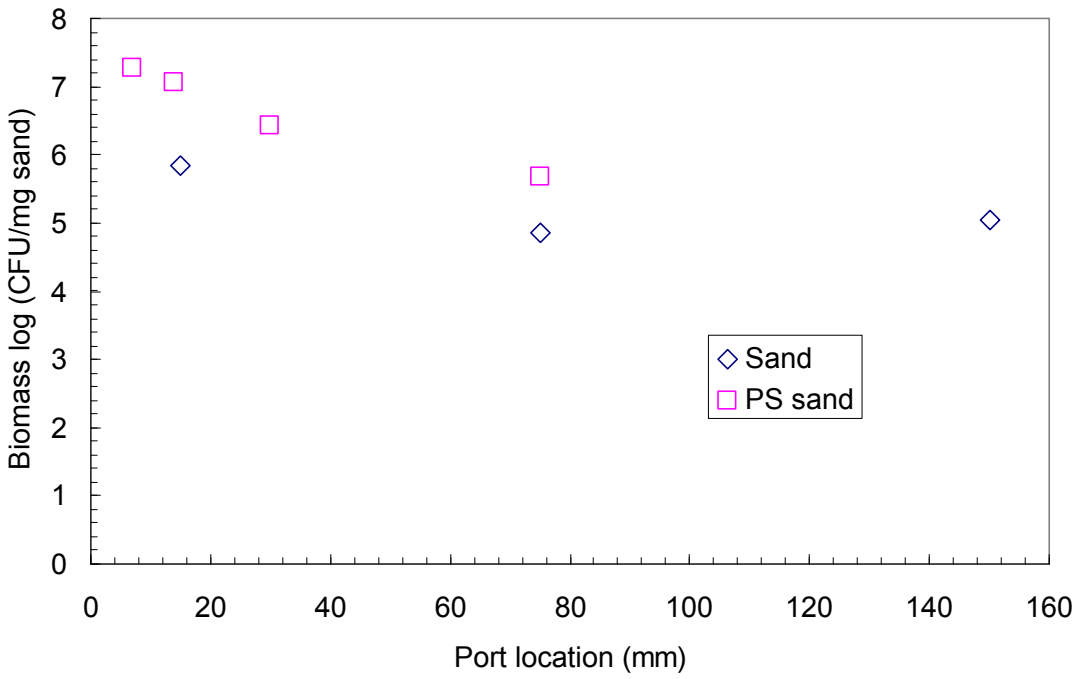

Figure 6.7 Attached biomass concentration along the column length for sand and PS-sand mixture column biodegradation experiments

The lack of biodegradation after port A is confirmed by the data in Figure 6.8. This figure shows the results of another biodegradation experiment using the sand medium, but conducted in a regular column (i.e., with Port A located at 70mm) by following the same inoculation and experimental procedure with the previously mentioned experiment. A similar lag period and steady state concentration phase were also observed in this experiment. Based on the level of steady state naphthalene degradation with this relatively longer column, it is quite clear that biodegradation occurred in the initial parts of the column. The Buscheck- Alcantar method derived biodegradation rate constant for this column is 3.32 1/hr. This value is close to the rate constant determined from the short biodegradation column data, and confirms the biodegradation occurrence at the column entrance.

6.3.3 Combined Sorption-Biodegradation Test Results

The experimental results of the combined sorption-biodegradation test using PS fly ash-sand mixture in the modified columns are shown in Figure 6.9 for port A. Several observations can be made based on Figure 6.9. First, a period was observed at the beginning of the test during which there was no breakthrough at Port A due to sorption, and possibly biodegradation, of the naphthalene on the PS fly ash- sand medium. Next, when the available surface of the fly ash was saturated, naphthalene breakthrough started to occur around 250 PVE. . However, as seen from the figure, that naphthalene concentration only reached a maximum concentration of 0.16 C/Co which implies

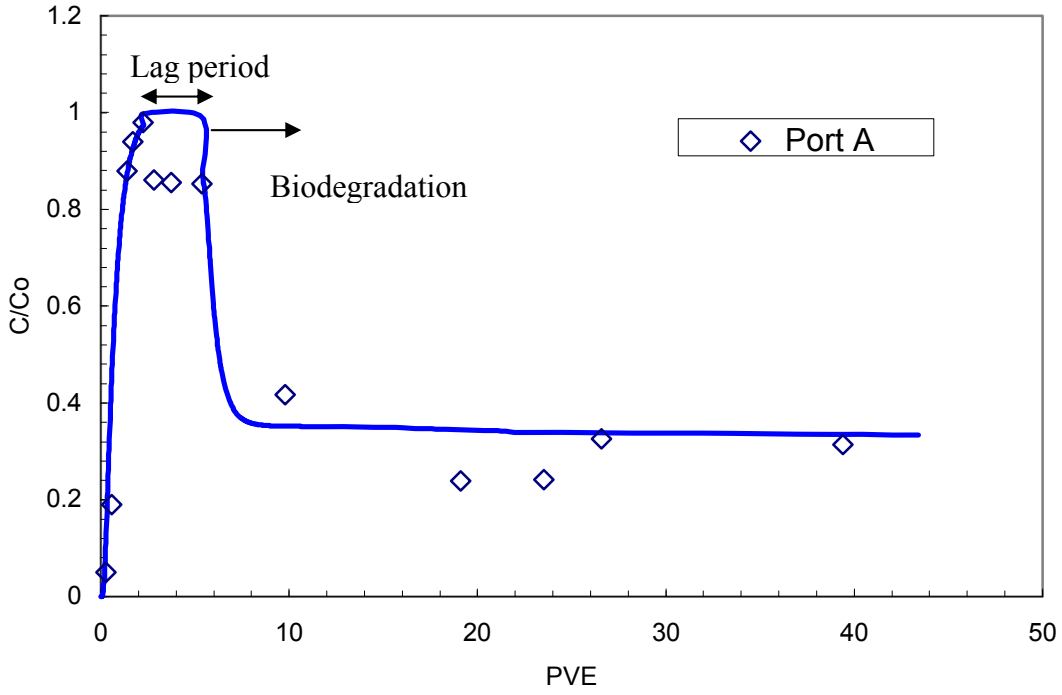

Figure 6.8 Breakthrough curve for the naphthalene biodegradation test in a sand column with a column sampling length of 70 mm. Solid lines are from MT3DMS simulation breakthrough using λ of 3.32 1/hr.

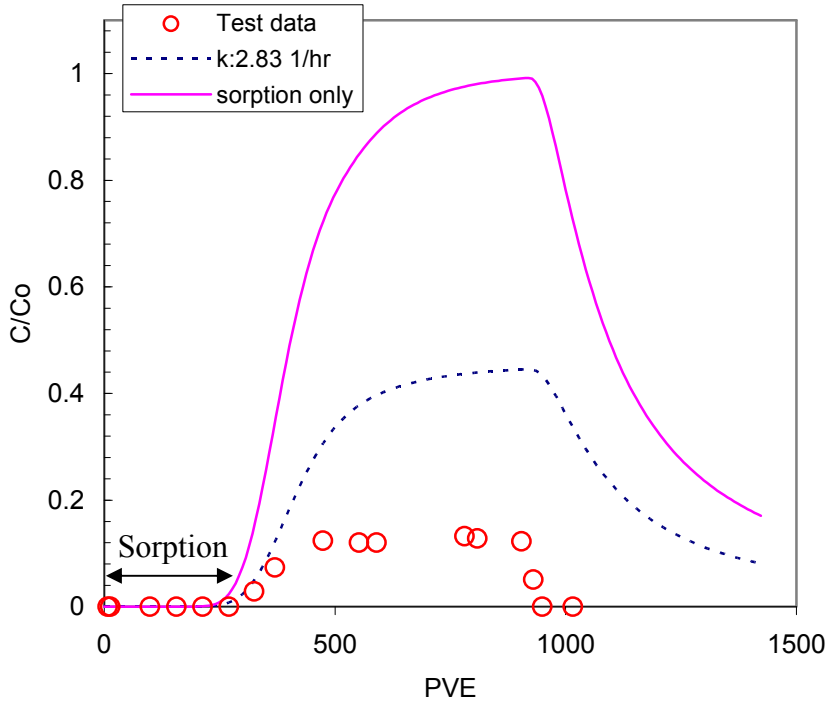

Figure 6. 9 Breakthrough curve at port A for PS sand medium biodegradation test. MT3DMS simulation results for sorption only (solid line), sorption plus biodegradation using λ=2.83 1/hr from the sand test (dotted line).Column sampling length =10 mm

that a 84% naphthalene removal has occurred during the steady state transport period, presumably due to a combination of sorption plus biodegradation.

Figure 6.9 also presents three MT3MS simulation results. First, the solid line is the modeling result for advection, dispersion with sorption only, and no biodegradation. The experimentally-derived column partition coefficients described in Chapter 5 were used in this modeling simulation. A visual comparison of the simulated and experimental data reveals that the data are comparable before a complete saturation of the PS fly ash-sand medium occurred. However, the data start to deviate when naphthalene breakthrough started and naphthalene became more readily available for the microorganisms.

The dashed line in Figure 6.9 is the modeling result for the columns with transport plus biodegradation and sorption. The biodegradation rate constant (λ) derived from the modified sand medium column was used in the modeling (Chapter 6.3.2), along with the sorption parameters described above. The trend is initially similar to the one observed for the sorption-only column; however, the effect of biodegradation on the solute concentration can be observed when the solid and dashed lines are compared. However, these model simulations predicted a maximum C/C_o value of ~0.44, which is almost 3 times greater than the actual maximum breakthrough concentration observed. This suggests that the amount biodegradation has been underestimated. Famisan and Brusseau (2003) also observed greater magnitude of biodegradation and an absence of lag phase before biodegradation begin in the presence of sorptive medium. They attributed this to sorption of naphthalene onto sorptive media, and the attendant retardation due to this

sorption. Specifically, they suggested that the high level of biodegradation was a result of the increased residence time associated with the retardation. This also implies that sorption was a key factor affecting dynamics of the biodegradation process. Therefore, although that there may be a reduction of the local bioavailability of the substrate due to sorption, the residence time associated with biodegradation was enhanced for systems undergoing a sorptive transport. Similar high biodegradation potentials in sorptive media were reported by Guerin and Boyd (1992) and Park et al. (2001).

Once the steady-state transport of naphthalene was observed, the influent solution was switched to contaminant-free synthetic groundwater to study the desorption of naphthalene from the medium. As seen in Figure 6.9, MT3DMS simulations with sorption and sorption plus biodegradation overestimates the naphthalene concentrations and under estimates the desorption rates. The steep desorption front that was observed suggests that as the naphthalene is desorbed, it is rapidly degraded.

DO measurements were also conducted during the PS-sand mixture sorption-biodegradation experiment and presented in Figure 6.10. The average DO level in the column influent was 7.85 mg/L and stayed within a narrow range during the experiment. The DO levels at Port A were depressed compared to the influent from the first measurement, suggesting that biodegradation of naphthalene was occurring from early in the experiment. DO measurements at port A exhibited more scatter than the influent, averaging around 4.2 mg/L. This indicates a consumption of 3.65 mg/L DO due to biodegradation. Meanwhile, 2.2 mg/L of naphthalene was removed due to biodegradation. Thus, based on the stoichiometry (Equation 2.1) assuming biomass formation, and the 2.2. mg/L naphthalene from the system, a removal of 3.3 mg/L DO is

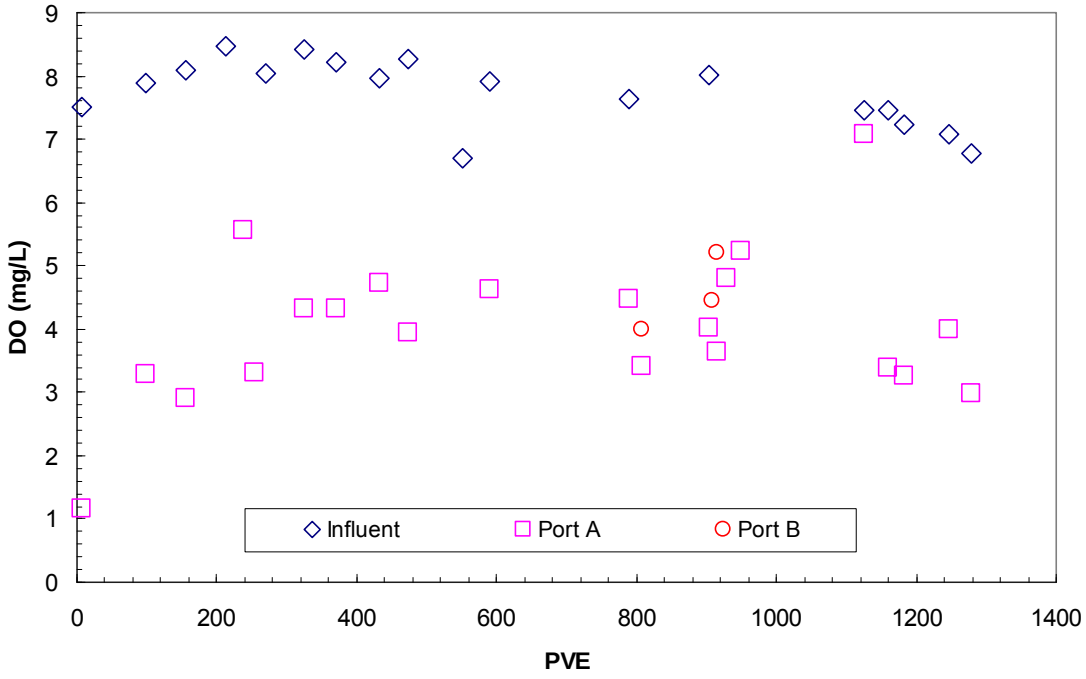

Figure 6.10 DO measurements during PS-sand mixture biodegradation experiments.

predicted. If biomass formation is ignored (Equation 6.8), a removal of 6.6 mg/L Do is predicted. The former prediction is very comparable to the actual DO consumption amount of 3.65 mg/L. DO measurements at Port B, the port located 20 mm above Port A, are also shown in Figure 6.10. DO readings at Port B are close to the ones measured at Port A, indicating that no active biodegradation accruing in the zone above Port A. this is consistent with the sand column results.

The aqueous biomass concentrations measured from the sampling ports located along the height of the PS fly ash-sand column (port A at 10 mm, port B at 35 mm, port D at 70 mm) are summarized in Table 6.2. Several observations can be made based on these data, First, during the initial stage when no naphthalene was observed in the aqueous phase, biomass levels were 6.9 10^5 CFU/mL, but no biomass was observed in the upper ports (Ports B and D). Once the naphthalene breakthrough was observed, the aqueous biomass levels increased to 1.66 10^5 CFU/mL at port A. However, again no aqueous biomass was observed at ports B or D. On the other hand, biomass was measured from port B and D during the desorption stage suggesting that downgradient biomass levels increased as desorbing naphthalene become available for biodegradation.

In addition to the aqueous biomass measurement, attached biomass concentrations were measured at Ports A, C, D and F of sand and PS-sand column biodegradation tests following the completion of the sorption-desorption phase. Figure 6.7 shows these concentration measurements along the column moving down-gradient. The biomass concentrations were relatively high near the initial of the column (at Port A). In addition, the HPC concentrations measured for the PS-sand mixture were one order of magnitude higher than the ones measured for the sand column consistent with greater removal of

Table 6.2 HPC counts from aqueous samples during PS-sand mixture napahthelene biodegradation

Sampling PVE	Port	HPC (CFU/mL)	Test Stage
213	A	6.90E+05	Sorption (No Biodegradation)
	B	0	
	D	0	
704	A	1.66E+06	Biodegradation
	B	0	
	D	0	
1016	A	6.50E+07	Desorption
	B	6.00E+07	
	D	5.50E+07	

naphthalene via biodegradation observed during the mixed sorption- biodegradation experiments. At upper column locations (port C, port E, Port F) relatively low biomass concentrations were measured. The accumulation of the attached biomass on sand was also reported by Yolcubal et al. (2003). They reported that the majority of the microbial activity occurred between the inlet and midpoint of the column and attributed these results to the location and size of the bioactive zones which, in turn, influenced the substrate and DO availability.

6.4 *PRB Design and Sensitivity Analysis*

The data collected in the experiments were used in designing PRBs. More specifically, model simulation were performed to examine the life expectancies of PRBs considering sorption only, and sorption-biodegradation processes. Three assumptions were made during these model simulations of barrier behavior: 1) both barrier and aquifer are homogenous, 2) groundwater flow is uniform in the longitudinal direction, and 3) a barrier length-to-width ratio of 5 is always satisfied (Rabideau et al. 2006).

To perform these model analyses, a one-dimensional model was prepared using VMOD-MT3DMS. The width and depth of the barrier were set at 30 m and 3 m, respectively, in order to capture the plume completely. These dimensions are typically used in designing barriers (Gavaskar et al. 1998). The average pore water velocity and barrier thickness (i.e., the barrier dimension in the longitudinal flow direction) were considered to be design variables, and the barrier life expectancy was calculated accordingly. Dispersivity of the barrier medium was taken as one-tenth of the barrier thickness following the suggestions of Gelhar et al. (1992) and Lee and Benson (2004).

The sorption-desorption parameters derived from the column tests, and the bulk density and porosity determined from the non-reactive tracer tests were also used as model inputs. Three fly ash-sand mixtures and PAC were used as the PRB sorptive media.

6.4.1 PRB design based on sorption only

6.4.1.1 PRB for Naphthalene Mitigation

Based on the column sorption-desorption test results, a PRB was designed using the column test-derived sorption parameters. A contaminant plume originating from a creosote source described by Godsy et al. (1992) was used in the design to simulate a typical naphthalene contamination scenario in the field. Godsy et al. (1992) reported that the naphthalene concentration of the plume varied between 0.93 and 9.38 mg/L, with an average field concentration of 3.63 mg/L. This average concentration was selected as the step input concentration for the PRB design. The reported field groundwater velocities ranged from 0.3 m/d to1.2 m/d, and both the lower and upper limits were used in the design to account for seasonal groundwater fluctuations. Barrier life was calculated as the time required to first observe a naphthalene concentration of 0.01 mg/L in the barrier effluent. This contamination level is the Maryland Department of Environment's maximum contaminant limit (MCL) for naphthalene in drinking water. This value is also slightly less than the naphthalene detection limit (0.016 mg/L) of the analytical instruments used in this study. Using these conditions, the barrier life expectancies were determined.

The expected barrier life is plotted against the barrier thickness in Figure 6.11 for all fly ash-sand and PAC- sand mixtures at the two average pore water velocities. The

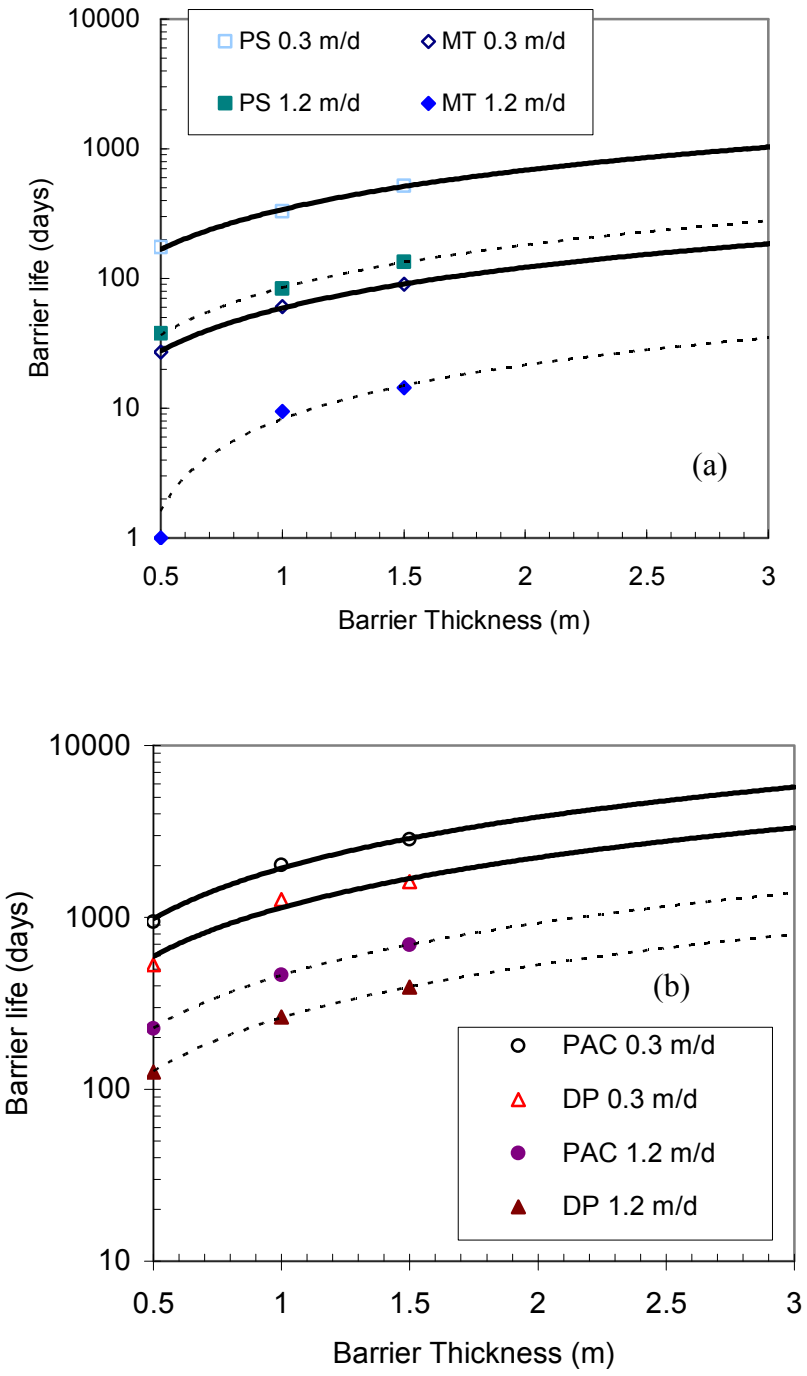

Figure 6.11 Barrier life expectancies for naphthalene as a function of barrier thickness and groundwater velocity for a) for PS and MT fly ash-sand mixtures as reactive medium, b) DP fly ash and PAC fly ash-sand mixtures as reactive medium

observed trends suggest that a longer time is required for the fly ashes with a high sorption potential (i.e., high LOI) to reach the MCL levels in the barrier effluent. Furthermore, groundwater velocity has a significant effect on the overall fate of the contaminant treated in the barrier. Higher groundwater flows resulted in shorter barrier lives. Note that the design influent naphthalene concentration can be considered as relatively high when compared to the allowable limits. However, higher concentrations were actually measured at the model site and the magnitude is typical of aqueous equilibrium naphthalene concentrations observed at coal tar contamination sites (Lee et al.1992). It is also important to note that the plume delineation plays a significant role in the design life of a barrier, but these parameters were not varied during these one-dimensional simulations.

6.4.1.2 PRB for *o*-xylene Mitigation

PRB life expectancies for *o*-xylene were determined by following the same basic procedures as used for naphthalene. Three fly ashes and PAC were the sorptive media in the design. A contaminant plume originating from a petroleum storage facility described by McGovern et al. (2002) was considered in the design to simulate typical *o*-xylene contamination in the field. The average *o*-xylene concentration of the plume was reported as 2.8 mg/L and this value is used in the PRB design herein. Barrier life was calculated conservatively as the time required to observe 0.06 mg/L of *o*-xylene in the barrier effluent after the plume hits the barrier, instead of the U.S. EPA and Maryland Department of Environment MCL limit of 10 mg/L. This value is the detection limit of

the analytical instrument used in the experiment. Therefore, barrier lives were determined with respect to the time when *o*-xylene would first be observed in the barrier effluent.

The expected barrier life is plotted against the barrier thickness in Figure 6.12 for all fly ash-sand and PAC-sand mixtures at the two selected average pore water velocities. As expected, barrier life increases substantially with higher fly ash carbon contents, although barriers with activated carbon and DP fly ash (LOI%=20.5) have very similar life times. Similar to naphthalene, higher groundwater flows resulted in shorter barrier lives.

6.4.2 PRB design based on sorption plus biodegradation

Passive treatment barriers may have great potential for remediation if right biological conditions are present in the environment for natural attenuation. As described in Chapter 6.3.3, high carbon content fly ashes not provide a good sorptive medium but may also enhance the biodegradation potential of the petroleum hydrocarbons, Therefore the modeling for designing PRBs in this section followed the approach outlined for the sorption only process above, except that, in addition, biodegradation was modeled using a first-order biodegradation constant.

The effectiveness of biodegradation is often dictated by the ability of native microbial culture to take up and metabolize the contaminant (Haws et al. 2006). For example, in this work the biodegradation decay constants determined using the fly ash-sand column experiments were relatively high compared to the ones obtained with the sand only columns. Such measurement of high biodegradation constants under

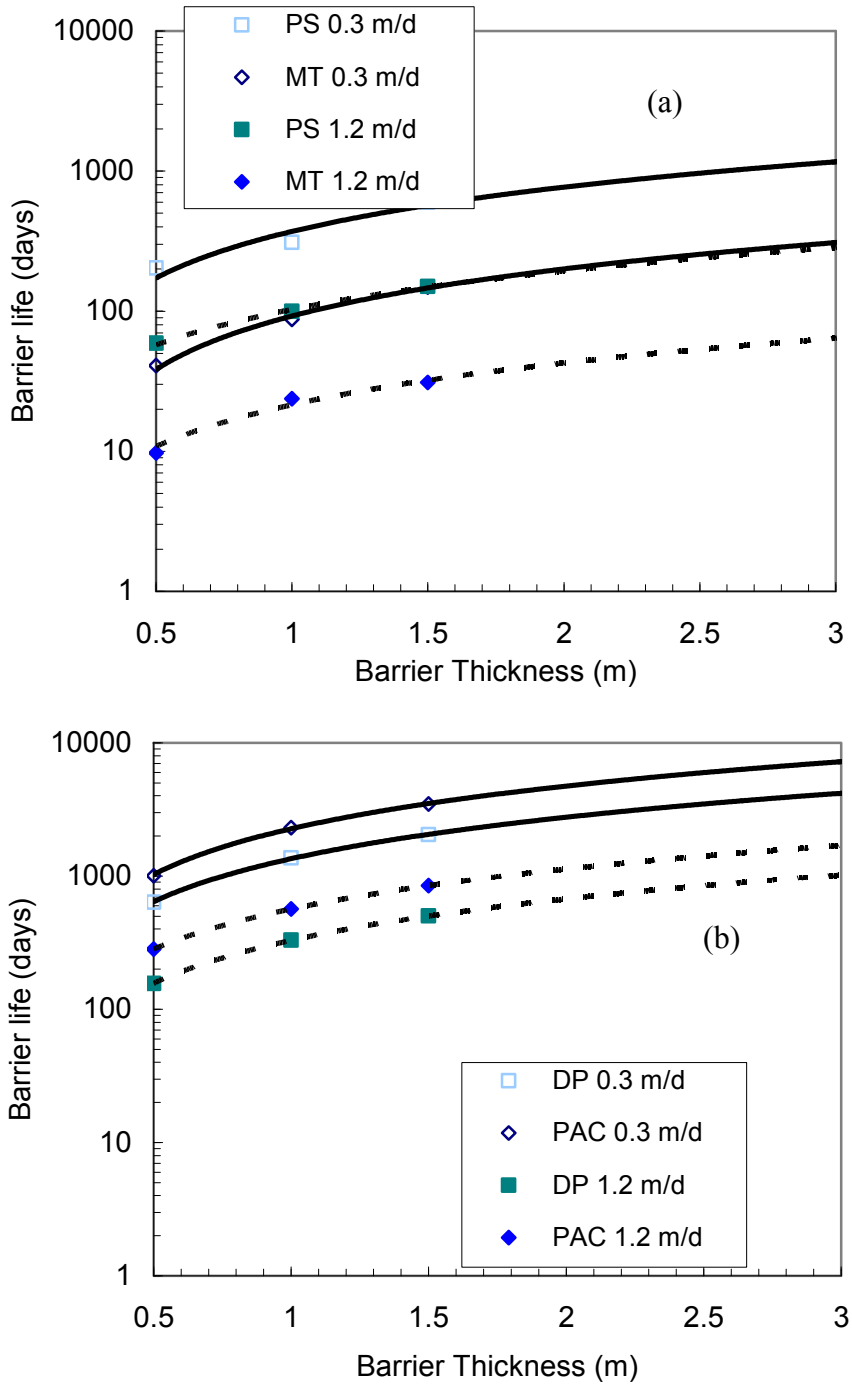

Figure 6.12 Barrier life expectancies for *o*-xylene as a function of barrier thickness and groundwater velocity for a) for PS and MT fly ash-sand mixtures as reactive medium, b)DP fly ash and PAC fly ash-sand mixtures as reactive medium.

laboratory conditions is common; however, one must be careful in choosing the appropriate biodegradation constant for field conditions. Bekins et al. (1998) states that first-order rates measured in the laboratory microcosms are frequently one order of magnitude higher than the field rates. This may be due to several reasons, including spatial and temporal issues associated with upscaling from a batch or column system to a more complex subsurface domain (Haws et al. 2006). The reduction in the field rate constants may be obtained solely by fitting first-order models to laboratory and field data with different initial concentrations. Therefore, for each contaminant of concern in this study (i.e., naphthalene and *o*-xylene), first-order rate constants reported from field related studies were adopted rather than using the laboratory-derived values from this study.

6.4.2.1 PRB for Naphthalene Mitigation

Barrier life expectancies for naphthalene contamination with different barrier thicknesses were determined using a first-order rate constant for naphthalene degradation of 0.9 1/day. This rate constant was selected because it is within the range observed by several researchers (Nielsen et al. 1996, Warith et al. 1999, Alshafie and Ghoshal 2003).

The expected barrier life is plotted against the barrier thickness in Figure 6.13 for all fly ash-sand and PAC-sand mixtures and two different average pore water velocities. Barrier life time increases substantially with higher fly ash carbon contents. A comparison of Figures 6.11 and 6.13 indicates that the influence of groundwater is much stronger when biodegradation is considered. Specifically, barriers exposed to slower

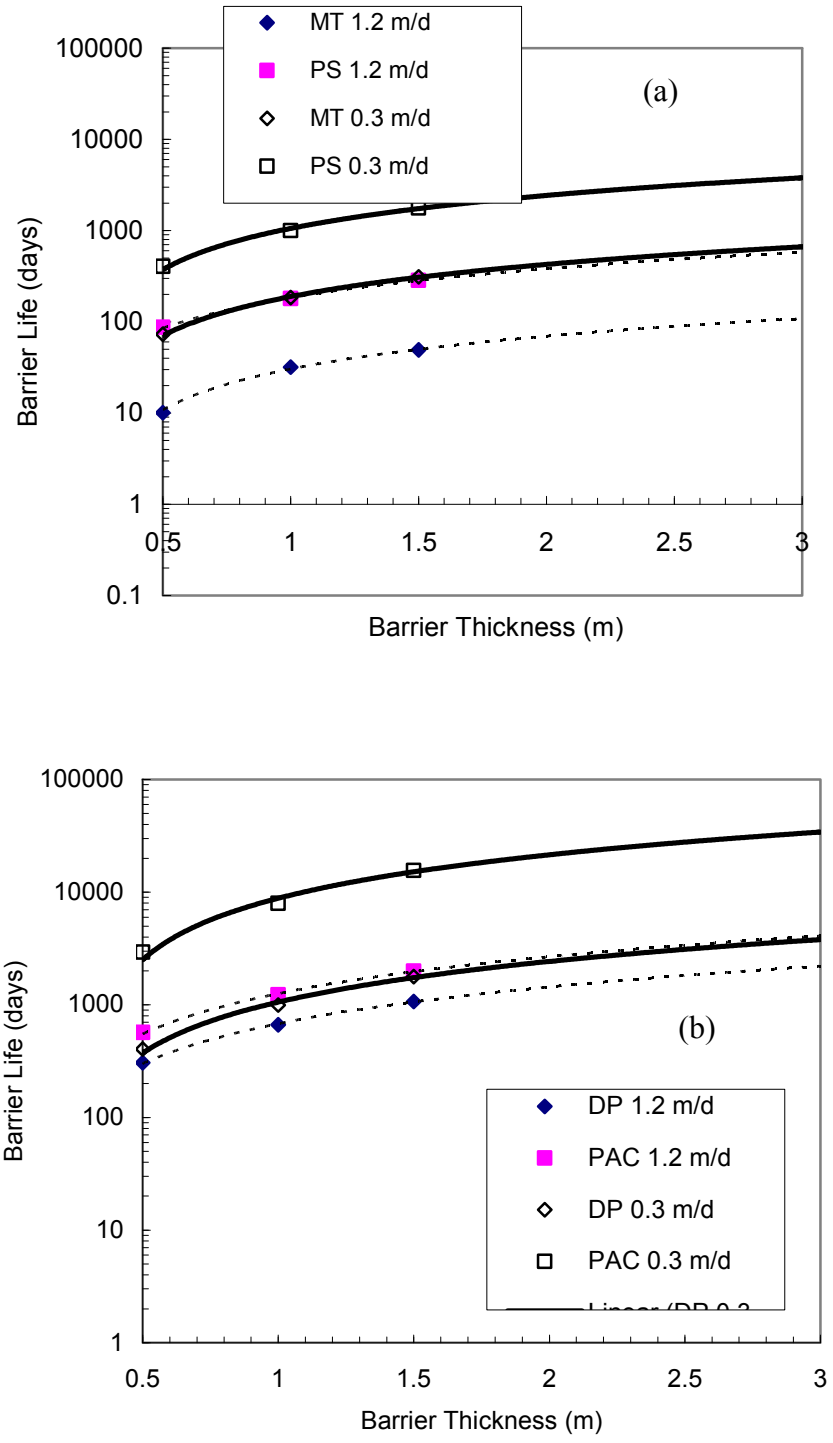

Figure 6.13 Barrier life expectancies for naphthalene as a function barrier thickness and groundwater velocity for a) for PS and MT fly ash-sand mixtures as reactive medium, b)DP fly ash and PAC fly ash-sand mixtures as reactive medium. First-order rate constant was 0.9 1/day.

groundwater velocity will have a better performance when microbial decay is occurring in the barrier. This is consistent with the experimental observation that greater residence time leads to greater biodegradation.

Figure 6.14 compares the expected barrier life of a DP fly ash-sand PRB with sorption plus biodegradation compared to with sorption only. When sorption plus biodegradation are active (referred to here as integrated remediation), the barrier has a longer life when compared to a sorption only scenario. This effect is most dramatic when the barrier has a thickness of 1.5 m and groundwater velocity is 0.3 m/d. As expected, the slower groundwater velocity and greater sorption material increased the residence time and caused an enhancement in the biodegradation levels. For barriers experiencing faster flow rates, the positive effect of biodegradation is relatively insignificant, because under these conditions the rate of advection is much greater than the biokinetics. In other words, the contaminant is moving through the barrier faster than the microbes can degrade it.

6.4.2.2. PRB for *o*-xylene Mitigation

Similar to the approach undertaken for naphthalene, a field derived first-order rate constant of 0.08 1/day was used in designing PRBs to mitigate *o*-xylene. This value was reported as a typical rate constant for *o*-xylene decay in the field (Bedient et al. 1998). Figure 6.15 shows the life expectancies for various barrier thicknesses with an *o*-xylene contaminant plume. As observed with naphthalene, fly ash mixtures containing higher carbon amounts have longer barrier life expectancies before breakthrough. Again the groundwater velocity has a significant effect on the barrier life, with the slower

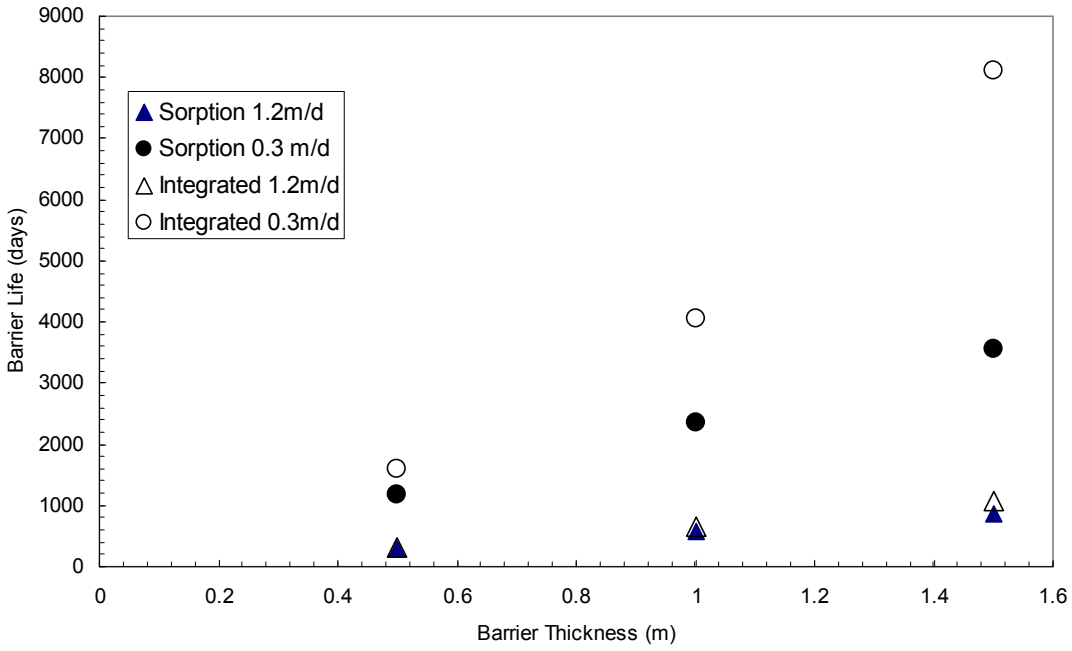

Figure 6.14 The comparison of barrier life expectancies as a function of barrier thickness for sorption and sorption plus biodegradation (integrated) barriers containing DP fly ash sand mixture

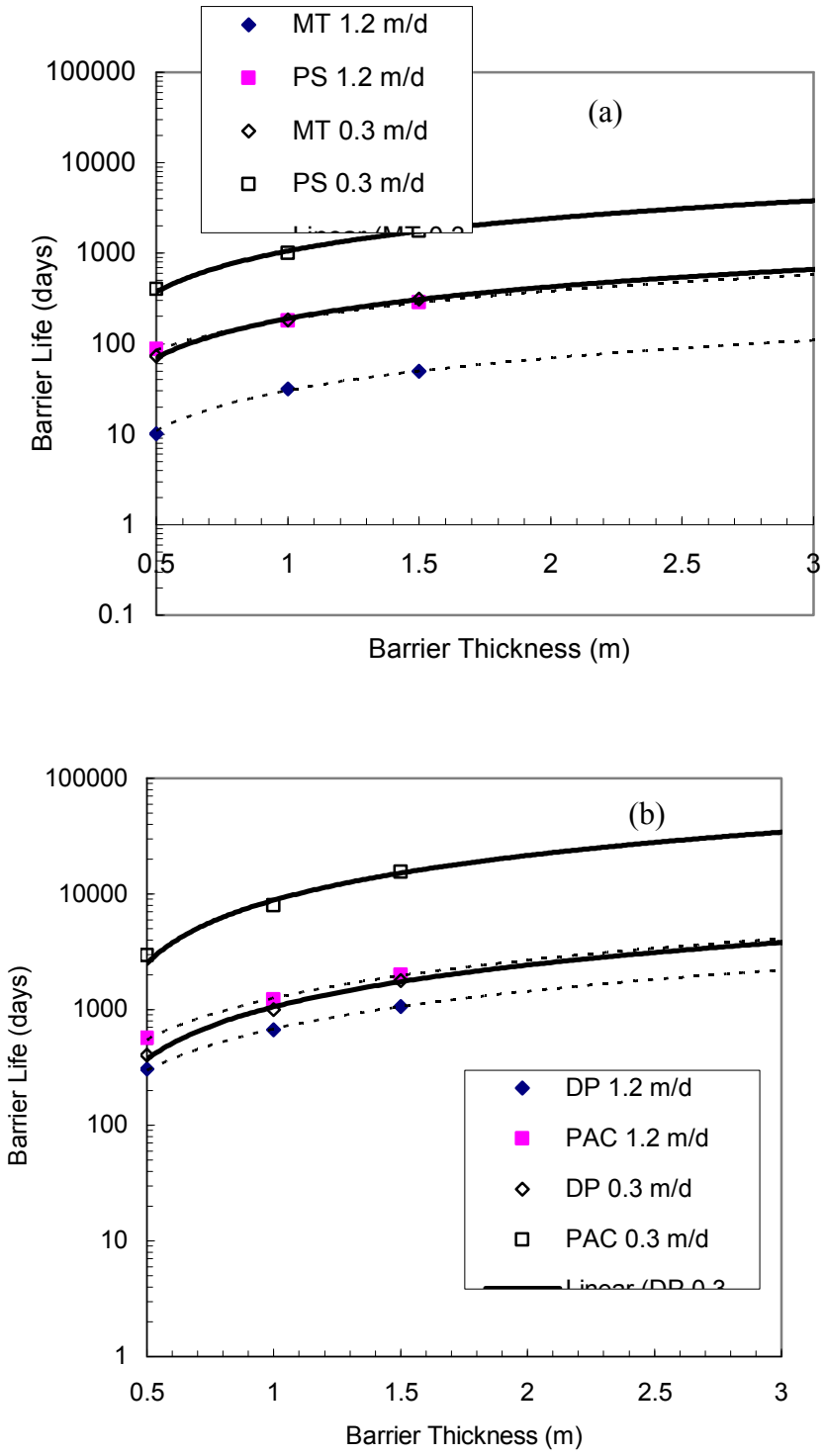

Figure 6.15 Barrier life expectancies for *o*-xylene according to barrier thickness and groundwater velocity for a) for PS and MT fly ash-sand mixture as reactive medium, and b)DP fly ash and PAC fly ash-sand mixture as reactive medium. First-order rate constant was 0.08 1/day.

groundwater velocity resulting in the greatest enhancement in contaminant loss via biodegradation.

6.4.3 Sensitivity Analysis

The analysis above for barriers utilizing sorption and biodegradation processes shows that several parameters are likely to have an influence on the performance of a PRB. To investigate which of these parameters have the greatest impact on barrier life, the sensitivity of the model prediction to several key variables (groundwater velocity, input concentrations, first-order rate constant) was evaluated for a DP fly ash-sand PRB. Naphthalene was selected as the model contaminant. The barrier life was calculated as the time at which the effluent concentration reached the allowable limit defined above.

Groundwater velocity was varied from 0.075 m/d to 1.2m/d. The resulting predictions for barrier life are plotted against the velocity normalized by the design velocity (0.3 m/d) in Figure 6.16(a). Clearly, the barrier life is strongly influenced by the groundwater velocity. In particular, barrier life increases significantly when the 1m thick barrier is compared to a barrier with a 0.5m thickness for the slower velocities. Note that the barrier life at 1.5 m thickness has essentially infinite capacity for naphthalene mitigation when a relatively slower velocity of 0.075 m/d is considered and this data point is not shown in Figure 6.16(a).

Figure 6.16(b) depicts the effect of input concentration on barrier life expectancies. As expected, the barriers exposed to lower input concentrations are likely to have longer performance. The influence of input concentration as a function of the barrier thickness was diminished when barriers were designed for relatively high input concentrations. Figure 6.16(c) shows the dependence of the barrier life on the first-order

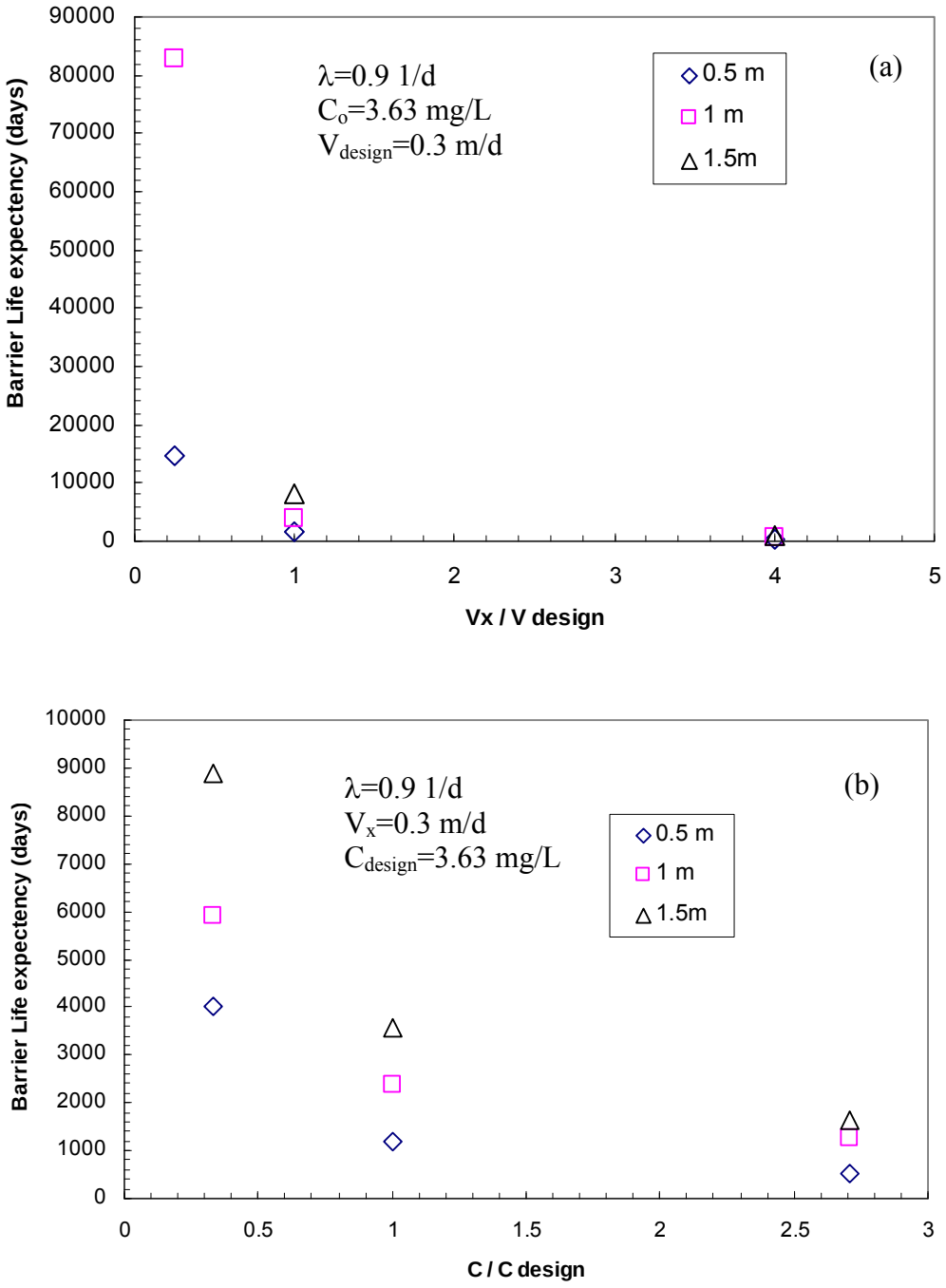

Figure 6.16 Sensitivity analysis results for barrier life expectancy as a function of (a) groundwater velocity, (b) the input concentration, and (c) the first-order biodegradation rate constant.

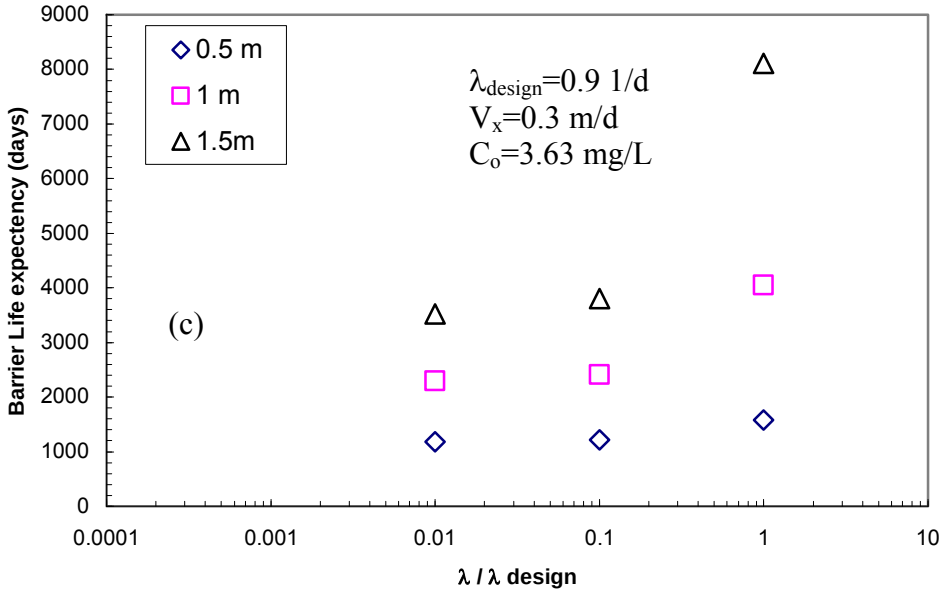

Figure 6.16 (continued)

rate constant. It is clear from the figure that varying the rate constant within the range tested does not have a significant effect on barrier life except at relatively high λ values and barrier thicknesses.

6.5. *Conclusions*

The results of the biodegradation test revealed high levels of biodegradation occurred when fly ash was employed as the reactive medium. These high levels of biodegradation were a result of increased residence time associated with retardation of the contaminant due to sorption onto fly ash. This finding implies that sorption was a key factor in the biodegradation dynamics of the substrates during the biodegradation process. Therefore, even though there may be concerns about the reduction of the local bioavailability of the substrate due to sorption, the resistance time associated with biodegradation was enhanced for systems undergoing a sorptive transport. Attached biomass and DO measurements conducted during the experiments supported that the increase in the biodegradation was due to sorption-derived long retention times.

Life expectancies of the bioreactive barriers were calculated for different barrier dimensions and aquifer conditions using a numerical model. Fly ashes with higher sorption potential (i.e., higher LOI) performed better as greater amounts of contaminant were captured by the barrier. The groundwater velocity had a significant effect on the overall fate of the contaminant treated in the barrier, and higher groundwater flows resulted in shorter barrier lives. Barriers exposed to slower groundwater velocities had a better performance when microbial decay is occurring in the barrier.

Chapter 7 Conclusions and Recommendations

7.1 Summary and Conclusions

A research study was conducted to investigate subsurface remediation of petroleum hydrocarbons using high carbon content fly ash as a sorptive agent. The study had two components: stabilization of petroleum contaminated soils and remediation of groundwater with petroleum hydrocarbons. Conventional in-situ treatment methods (i.e., pump and treat) suffer from high operational costs, generation of secondary wastes and long time periods of operation. Therefore, the difficulty of reducing subsurface contamination levels economically and removing and/or immobilizing the contaminants permanently has led to research and development of an innovative technology. In this research, the utilization of a waste material was incorporated as reactive medium rather than using commercial products (i.e., zero valent iron, activated carbon), which constitute the major cost of these structures. Continuous landfilling of high carbon content fly ashes is a recent problem that coal burning electrical power plants must confront. These ashes are generated in large quantities all around the nation due to the adaptation of the plants to new regulatory laws on nitrogen oxide emissions. They contain significant amounts of unburned carbon (i.e., high loss on ignition) and cannot be used as a concrete additive. The only alternative for this byproduct is to landfill unless no beneficial reuse is offered.

It was hypothesized that the unburned carbon contained in the fly ash can be used as a sorptive medium for petroleum hydrocarbons in the subsurface. The overall goal of this study was to evaluate the effectiveness of high carbon content fly ash as a sorptive agent for subsurface remediation of petroleum-contaminated soils and groundwater. To

accomplish this goal, experimental and numerical analyses were conducted in three primary phases. During these phases, naphthalene and *o*-xylene were employed as model subsurface contaminants.

First phase of this study started with examining the physical and chemical properties of the fly ashes taken from several power plants in Maryland. In the second phase, the geotechnical performance and environmental suitability of petroleum contaminated soils stabilized with high carbon content fly ash was investigated. A battery of laboratory tests that included compaction, batch-sorption and column leaching tests were performed on the mixtures to evaluate the effectiveness of the stabilization process. The third phase included investigation of the performance of high carbon content as a reactive medium in a permeable reactive barrier through column sorption-desorption experiments, column biodegradation experiments, and numerical design of reactive barriers. Column sorption-desorption tests were conducted on fly ash-sand mixtures (40% fly ash and 60% sand by weight) in sterile conditions. After completion of the experiments, the data was modeled using VMOD-MT3DMS. For the column biodegradation experiments, an isolated culture was used for inoculation and to simulate the biodegradation process in sand and fly ash-sand mixture columns. The results of the biodegradation experiments were also numerically modeled in order to assess effectiveness of the biokinetic parameters estimated from experiments. Following the column experiments, a numerical model of typical PRB was constructed in order to investigate the barrier life expectancies. The model output for different fly ash types and groundwater velocities were used to develop design charts for practical applications. The following conclusions were drawn from the results of the study:

1) The loss on ignition (LOI) of the Maryland high carbon content Class F fly ashes varied between 3.1% and 20.5% and contain three distinct carbon forms. Batch adsorption tests indicated that the naphthalene and *o*-xylene adsorption capacity of these fly ashes was strongly correlated with LOI.
2) The chemical and physical of structure of the fly ash promoted adsorption and yielded nonlinear sorption isotherms that are characterized by high sorption capacity at low concentrations. Furthermore, fly ashes with higher surface area generally exhibited high sorption capacities.
3) Among the adsorption isotherm models used to evaluate adsorption test data. Polanyi-Dubinin-Manes (PDM) model posed great potential for explaining the petroleum contaminant adsorption on to fly ash. Pore filling mechanism, explained by PDM isotherm, believed to be the dominant mechanism for adsorption of non-polar organic chemical onto highly heterogonous sorbents like fly ash. One of the practical advantages of the PDM model is the normalization of the aqueous concentrations to water solubilities of the organic compounds. This provides unified sorption isotherm for a group of similar organic compounds for specific sorbent material (i.e, activated carbon, fly ash). By use of PDM isotherm (usually referred to as correlation curve when used for multiple sorbates), sorption capacity of a particular sorbent can be determined for a group of chemicals.
4) The laboratory test procedures indicated that the traditional approaches undertaken for preparation and testing of soils for their geotechnical and environmental analyses may not be applicable to petroleum contaminated soils. Deviations from the standard

procedures, such as usage of liquid content instead of water content for evaluating the compaction test data, aging of specimens before compaction, and proper selection of the solid-to-solution ratio for batch-scale adsorption tests, should be considered. The column leaching tests performed on the Brandon Shores fly ash-stabilized specimens indicate that the naphthalene and *o*-xylene concentrations in the effluents collected from the fly ash stabilized specimens were lower than those collected from the control specimen. The addition of this high carbon content fly ash (LOI= 13.4%) limited the initial release of the contaminants from the specimen, compared to a longer release observed from the control column. Finally, the presence of fly ash and the degree of contamination were two important factors that played a major role in the biodegradation process during remediation of petroleum contaminated soils.

5) The mixtures of sand with three fly ashes, DP, PS, and MT, with LOI content of 20.5%, 10.7%, and 3.1%, respectively, and PAC were subjected to column sorption-desorption testing. The bromide tracer test data indicated that dispersivity values range between 0.09 and 0.76 cm, and 0.04-0.96 cm for fly ash-sand and PAC-sand mixtures, respectively. These values fall in a typical range of values reported for sorptive media with relatively high fines content. Moreover, the measured hydraulic conductivities of fly ash-sand mixtures in the column sorption-desorption tests were comparable with the typical field hydraulic conductivities reported for PRBs.
6) pH readings during column experiments showed that pH initially remained constant for several pore volumes of flow, then decreased at the later stages, and eventually dropped to a level comparable to the pH of artificial groundwater solution (i.e., pH

=6.9). The buffering capacities of the Maryland fly ashes tested in this study were diminished and the pH in the system was governed by the PIPES buffer.

7) Retarded naphthalene and *o*-xylene amounts increased with increasing LOI content (MT, PS, DP fly ashes and PAC, respectively) in the column tests. The DP fly ash exhibited sorption properties comparable to a commercially powder activated carbon. Freundlich isotherm coefficients calculated from the column data were 27.3 to 47.3% lower than the batch-determined ones.

8) Numerical simulations conducted on the column sorption desorption data revealed that the breakthrough curves determined using the batch parameters shifted rightward implying that the naphthalene sorption is overpredicted by using batch adsorption test derived parameters. It is possible that a combination of factors such as solid-to-liquid ratio, sorption nonlinearity, and nonequilibrium (rate-limited) sorption caused the observed discrepancy between the batch and column-derived parameters.

9) Column sorption-desorption data was successfully described using a Freundlich isotherm. The areas under the contaminant breakthrough curves were used to calculate the retarded contaminant mass during the experiment. The calculations revealed that the retarded naphthalene amount increased with increasing LOI values (MT, PS, DP fly ashes and PAC, respectively). The retarded mass per gram sorptive medium calculated from Port C is consistently higher than the one calculated at port B, which indicated that the retarded mass increased along the height of the column. Furthermore, the percent retardation of naphthalene in the tested fly ashes varied from 48 to 78%, and this range is very comparable to the range observed for retardation within PAC (retardation in PAC varies between 66 and 77.5%).. These observations

further supported the previous findings that high carbon content fly ashes are strong sorbents with sorption properties comparable to a commercially powder activated carbon.

10) Similar to the naphthalene tests, *o*-xylene breakthrough curves have sharp adsorption fronts during the sorption phase of the experiments. A tailing of desorption front was observed in all tests. Fesch et al. (1998) speculated that the effects of equilibrium sorption-desorption was most evident from the self-sharpened adsorption fronts of the breakthrough curve without any tailing. Thus, the sharp front adsorption curves suggested that the sorption equilibrium was achieved during the *o*-xylene adsorption onto all media. *O*-xylene breakthrough curves also exhibited tailing at the desorption front.

11) The results of the biodegradation test revealed high levels of biodegradation occurred when fly ash was employed as the reactive medium. These high levels of biodegradation were a result of increased residence time associated with retardation of the contaminant due to sorption onto fly ash. This finding implies that sorption was a key factor in the biodegradation dynamics of the substrates during the biodegradation process. Therefore, even though there may be concerns about the reduction of the local bioavailability of the substrate due to sorption, the resistance time associated with biodegradation was enhanced for systems undergoing a sorptive transport. Attached biomass and DO measurements conducted during the experiments supported that the increase in the biodegradation was due to sorption-derived long retention times.

12) Life expectancies of the bioreactive barriers were calculated for different barrier dimensions and aquifer conditions using a numerical model. Fly ashes with higher sorption potential (i.e., higher LOI) performed better as greater amounts of contaminant were captured by the barrier. The groundwater velocity had a significant effect on the overall fate of the contaminant treated in the barrier, and higher groundwater flows resulted in shorter barrier lives. Barriers exposed to slower groundwater velocities had a better performance when microbial decay is occurring in the barrier.

This study represents an important step towards implementation of a currently landfilled waste material in an environmental clean-up process. The performance and the environmental impact of the material were tested with respect to various applications. Experimental and numerical analyses indicated that high carbon content fly ash has a great potential as a remediation medium for petroleum-contaminated soils and groundwater.

There is an increasing need in using sustainable technologies in environmental remediation, and as a result, recycled materials are increasingly being more incorporated into design. This study also increases the understanding of the role of standard testing procedures on recycled materials. The current study enhances the understanding of the role of standard testing procedures on recycled materials and provides information to facilitate sustainable engineering applications.

7.2 Recommendations for Future Work

Although the overall sorption performance of the high carbon content fly ashes was satisfactory, the efficiency of the high and medium carbon content fly ashes can be enhanced by pre-washing as cleaning the dust on the particle surface is likely to increase the available sorption sites. The carbon percent can also be increased by separating the carbon by simple means, such as sieving. A cost analysis should be conducted for pre-washing of large quantities of fly ash or separating carbon for field PRB applications that employ fly ashes.

Petroleum contamination occurs in a more complex phenomenon in situ than the one represented in the current laboratory study. Fate of contaminants can be influenced by the presence of other compounds. Limited information is available on the effects of competition of multiple solutes during sorption and biodegradation processes. It has been known that the multiple solutes can increase the competition for adsorption sites and may reduce the intrinsic biodegradation rates of individual compounds (Haws et al. 2006). Experimental determination of the co-solutes on specific fate processes can enhance the prediction capabilities. Therefore, sorption-desorption experiments using multiple solute can be conducted by carefully manipulating the level of co-solutes and measuring them using advanced analytical instrumentation (i.e., GC-MS).

Finally, a successful implementation of this study at the field scale would help to study the effect of others factors, such aquifer heterogeneity, local variabilities in sorption and hydraulic conductivity of fly ash, on in situ chemical and microbiological processes.

Chapter 8 References

Accardi-Dey, A., and Gschwend, P.M., (2002). "Assessing the combined roles of natural organic matter and black carbon as sorbents in sediments." *Environmental Science and Technology*, Vol.36, No.1, pp.21-29.

Agency for Toxic Substances and Disease Registry, (2001) *Top 20 hazardous substances from the CERCLA Priority List of Hazardous Substances for 2001*, ATSDR, Div. of Toxicology, Atlanta.

Ahmad, F., Schnitker, S.P., and Newell, C.J. (2007) "Remediation of RDX- and HMX-contaminated groundwater using organic mulch permeable reactive barriers" *Journal of Contaminant Hydrology*, Vol. 90, pp. 1-20.

Akgerman, A., and Zardkoohi, M. (1996). "Adsorption of phenolic compounds on fly ash." *J.Chem. Eng. Data*, Vol.41, pp. 185-187.

Alexander, M. (1999). "Biodegradation and bioremediation." *Academic Press.* Newyork, NY

Allen-King, R.M., Grathwohl, P., Ball, W.P. (2002). "New modeling paradigms for the sorption of hydrophobic organic chemicals to heterogeneous carbonaceous matter in soils, sediments, and rocks," *Advances in water resources* Vol. 25, pp. 985-1016

Alshafie, M., and Ghoshal, S., (2003). "Naphthalene biodegradation from non-aqueous-phase liquids in batch and column systems: comparison of biokinetic rate coefficients." *Biotechnology Progress*, Vol. 19, pp. 844-852.

Altfelder, S., Streck, T., Maraqa, M.A., and Voice, T.C., (20010. "Nonequilibrium sorption of Dimethylphthalate Compatibility of Batch and Column Techniques" Soil Sci. Soc. Ame. Journal, Vol. 65 pp. 102-111.

APHA, AWWA, and WEF. (1995). "*Standard Methods for the Examination of Water and Wastewater*," American Public Health Association, American Water
Works Association, and Water Environment Federation, Washington, D.C.

ASTM E1676, (1998). Standard Guide for Conducting Laboratory Soil Toxicity or Bioaccumulation Tests With the Lumbricid Earthworm Eisenia Fetida. *In the Annual Book of ASTM Standards*, Vol 11.05 Philadelphia PA, pp 1056-1074.

ASTM D1292, (1999). Standard Test Methods for pH of water. *In the Annual Book of ASTM Standards*, Philadelphia PA

ASTM D4319. (2001). Standard Test Method for Distribution Ratios by the Short-Term Batch Method. *In the Annual Book of ASTM Standards*, Philadelphia PA.

ASTM C1254 (2002) Standard Test Method for Water-Extractable Chloride in Aggregate (Soxhlet Method). *In the Annual Book of ASTM Standards*, Philadelphia PA

ASTM D4646. (2003). Standard Test Method for 24-h Batch-Type Measurement of Contaminant Sorption by Soils and Sediments *In the Annual Book of ASTM Standards*, Vol 11.04 Philadelphia PA.

ASTM C618-05, (2005). Standard specification for coal fly ash and raw or calcined natural pozzolan for use in concrete. *In the Annual Book of ASTM Standards*, 2005. Philadelphia PA.

ASTM D 5285 (2003) Test Method for 24-Hour Batch-Type Measurement of Volatile Organic Sorption by Soils and Sediments, *In the Annual Book of ASTM Standards*, 2003. Philadelphia PA.

Baltrus, J.P, Wells, A.W., Fauth D.J., Diehl, J.R., and White, C.M., (2001).”Characterization of carbon concentrates from coal-combustion fly ash.” *Energy&Fuel*, Vol. 15, pp. 455-462.

Bartelt-Hunt, S.L., Smith, J.A., Burns, S.E., and Rabideau, A.J. (2005). “Evaluation of granular activated carbon, shale, and two organoclays for use as sorptive amendments in clay landfill liners.” *Journal of Geotechnical and Geoenvironmental Eng*., Vol.131, No.7, pp.848-856.

Banerjee, K., Cheremininoff, P.N., and Cheng, S.L. (1995). “Sorption of contaminants by fly ash in a single solute system.” *Environmental Science and Technology*, Vol.29, No.9, pp.2243-2251.

Banerjee, K., Cheremininoff, P.N., and Cheng, S.L. (1997). “Adsorption Kinetics of *o*-xylene by fly ash.” Water Research, Vol.31, No.2, pp.249-261.

Bedient, P.B., Rifai, H.S., and Newell, C.J., (1999). “*Ground water Contamination Transport and Remediation*” 2nd ed., Prentice Hall, NJ.

Bekins, B.A., Warren, E., and Godsy, E.M. (1998). “A Comparison of Zero-order, First-order, and Monod Biotransformation Models.”, Ground Water, Vol.36, No.2, pp. 261-268.

Berthhouex, P.M., and L.C. Brown. (2000) *Statistics for Environmental Engine*ers. Lewis Publishers, Boca Raton, FL.

Bin-Shafique, S., Edil T.B., and Benson, C.H., (2002). *Leaching of heavy metals from fly ash stabilized soils used in highway embankments*. *Geo Eng. Rep. 02-14*. Dep. of Civil and Envronmenatal Eng., Univertsity of Wisconsin Madison.

Bin-Shafique, S., Benson, C.H., Edil, B.T., and Huang, K. (2006). "Leachate concentrations from water leach and column leach tests on fly ash-stabilized soils." *Environmental Engineering Science*, Vol. 23, No. 1, pp 53-67

Bowles, J. E. (1992), *"Engineering Properties of Soils and Their Measurement"*, 3rd ed.., McGraw Hill Book Company, NY.

Brinch, U. C., Ekuland, F., and Jacobsen, C. S. (2002). "Method for spiking soil samples with organic compounds." *Applied and Environmental Microbiology*, Vol. 68, pp. 1808-1816.

Brusseau, M. L. (1991). "Application of a multi-process non-equilibrium sorption model to solute transport in a stratified porous-medium." *Water Resources Research*, 27(4), 585-595.

Brusseau, M. L. (1995). "The effect of nonlinear sorption on transformation of contaminants during transport in porous media." *J. Contam. Hydrol.*, Vol.17, No. 4, pp. 277–291.

Brusseau, M.L., Hu, M.Q., Wang, J.M., Maier, R.M. (1999). "Biodegradation during contaminant transport in porous media. 2. The influence of physicochemical factors." *Environ. Sci. Technol.*, No.33, pp.96-103.

Burgisser, C.S., Cernik, M., Borkovec, M., and Sticher, H., (1993). "Determination of Nonlienar Adsorption Isotherms from Column Experiments: An Alternative to Batch Studies." *Environmental Science and Technology*, Vol.27, No.5, pp.943-948.

Buscheck, T.E., and Alcantar, C.M., (1995). "Regression Techniques and Analytical Solutions to Demonstrate Intrinsic Bioremediation" Proceedings, 1995 Battelle International Conference on In situ and On site Bioreclamation, Battelle Pres., Columbus OH.

Cameron, D.R., Klute, A. (1977). "Convective- Dispersive solute transport with a combined equilibrium and kinesthetic adsorption model." *Water Resources Research*. Vol.13, No.1, pp.183-188

Cantrell, K.J., and Kaplan, D.I., (2001). "Sorptive barriers for groundwater remediation." *In Encyclopedia of Environmental Analysis and Remediation,* Meyers. R.A., eds, John Wiley, New York, pp.4663-4677.

Carmo, A.C., Hundal, L.T., and Thompson, M.L. (2000). "Sorption of hydrophobic organic compounds by soil materials: application of unit equivalent Freundlich coefficients." *Environmental Science and Technology*, Vol.34, No.20, pp.4363-4369.

Chang, T.H., and Rittmann, B.E., (1987). "Verification of the Model of Biofilm on Activated Carbon", *Environmental Science and Technology*, Vol.21, No.3, pp.280-288.

Chapra, S.C., and Canale, R.P., (2002). " *Numerical Methods for Engineers*", McGraw Hill Book Company, NY.

Chiou, T.C., Mcgroddy, S.E., and Kile, D.E. (1998). "Partition characteristics of polycyclic aromatic hydrocarbons on soils and sediments" *Environmental Science and Technology*, Vol.32, No.2, pp.264-269.

Chiou, T.C., Kile, D.E., Rutherford, D.W., Sheng, G., Boyd, S.A. (2000). "Sorption of selected organic compounds from water to a peat soil and its humic-acid and humin fractions: potential sources of the sorption nonlinearity." *Environ. Sci. Technol.* Vol. 34, pp. 1254-1258

Chiou, C.T., (2002). *Partition and adsorption of organic contaminants in environmental systems,* John Wiley and Son, New Jersey.

Crittenden, J.C., Sanongraj, S., Bulloch, J.L., Hand, D.W., Speth, T.F., and Ulmer, M. (1999). "Correlation of aqueous-phase adsorption isotherms." *Environ. Sci. Technol.* Vol. 33, pp. 2926- 2933

Czurda, K., and Haus, R., (2002). "Reactive barriers with fly ash zeolites for in situ groundwater remediation". *Appl. Clay Sci*. Vol. 21, pp.13–20.

Doherty, R., Phillips, D.H., McGeough, K.L., Walsh, K.P., Kalin, R.M. (2006). "Development of modified flyash as a permeable reactive barrier medium for a former manufactured gas plant site, Northern Irelend." *Environ. Geol*. Vol.50, pp.37-46

Doick, K. J., Lee, H.P. and Semple, K.T. (2003). "Assessment of spiking procedures for the introduction of a phenanthrene-LNAPL mixture into field wet soil." *Environmental Pollution,* Vol.126, pp.399-406.

Elder, C.R., C.H. Benson, and G.R. Eykholt, (2002), "Effects of heterogeneity on influent and effluent concentrations from horizontal permeable reactive barriers," *Water Resour. Res*., 38(8), DOI 10.1029/2001WR001259.

Ezeldin, A. Z, Vaccari. D. A., Bradford, L., Dilcer, S., Farouz, E., and Mueller, R.T., (1992). "Stabilization and solidification of hydrocarbon-contaminated soils in concrete." *J. of Soil Contamination*, Vol.1, No.1, pp.61-79.

Famisan, G. B., and Brusseau, M. L. (2003). "Biodegradation during contaminant transport in porous media: 6. Impact of sorption on coupled degradation transport behavior." *Environmental Toxicology and Chemistry*, 22(3), 510- 517.

Fesch, C., Simon, W., Haderlein, S.B., Reichert, P., and Schwarzenbach, R.P., (1998). "Nonlienar sorption and nonequilibrium solute transport in aggregated porous media:

Experiments, process identification and modeling," Journal of Contaminant Hydrology, Vol. 31, pp. 373-407.

Fetter, C.W. (1992), "*Contaminant Hydrology*", Macmillan Publishing, Ontario, Canada.

Freeze, R.A., and Cherry, J.A., (1979). *Groundwater*. Prentice-Hall. Englewood Cliffs, New Jersey.

Friend, D., (1996). Remediation of petroleum-contaminated soils, *National Cooperative Highway Research Program Synthesis 226,* Transportation Research Board publication , Washington D.C.

Fritz, W., and Schluender, E.U. (1974). "Simultaneous adsorption equilibria of organic solutes in dilute aqueous solution on activated carbon." *Ceram. Eng. Sci. Proc.,* Vol. 29, No. 5, pp. 1279-1282

FRTR, (1999). *In situ solidification/stabilization*. Federal Remediation Technologies Roundtable, (http://www.frtr.gov/matrix2/section4/4_10.html).

Fytianos, K., Tsaniklidi, B., and Voudrias, E., (1998). "Leachability of heavy metals in Greek fly ash from coal combustion", *Environment International,* Vol. 24, No. 4, pp. 477-486.

Gagliardi, J.V., Karns, J.S. (2000). "Leaching of Escherichia coli O157:H7 in diverse soils under various agricultural management practices." *Appl. Environ. Microbiol*. 66, 877-883.

Gavaskar, A.R., Gupta, N., Sass, B., Janosy, R.J., Sullivan, D. (1998). "Permeable barriers for groundwater remediation." *Battelle Press*.

Genc-Fuhrman, H., Mikkelsen, P.S., and Ledin, A., (2007). " Simultaneous removal of As, Cd, Cr, Cu, Ni and Zn from stormwater: Experimental comparison pf 11 disserent sorbents", *Water Research*, Vol. 41, pp. 591-602.

Gelhar, L. W., Welty, C., and Rehfeldt, K. R. (1992). "A critical review of data on field-scale dispersion in aquifers." *Water Resources Research*, 28(7), 1955-1974. 287

Ghoshal, S., and Luthy, R. G. (1998). "Biodegradation Kinetics of Naphthalene in Nonaqueous Liquid-Water Mixed Batch Systems: Comparson of Model Predictions and Experimental Results." *Biotechnology and Bioengineering*, 57(3), 356-366.

Godsy, E.M., Goerlitz, D.F., and Grbic-Galic, D., (1992) "Methanogenic biodegradation of creosote contamination in natural and simulated groundwater ecosystems" Ground Water Vol. 30, No. 2, pp. 232-242.

Guerin, W.F., Boyd, S.A. (1992). “Differential bioavailability of soil sorbed naphthalene to two bacterial species.” *Appl. Environ. Microbiol*. No.58, pp.1142,1152.

Guerin, T.F., Horner, S., McGovern, T., Davey, B. (2002). “ An application of permeable reactive barrier technology to petroleum hydrocarbon contaminated groundwater.” *Water Research*, Vol.36, pp.15-24.

Gullick, R. W., and Weber, Jr. W.J., (2001) “ Evaluation of Shale and Organoclays as Sorbent Additives for low-permeability soil Containment barriers” *Environmental Science and Technology.* Vol.35, No.7, pp. 1523-1530.

Gusmao, A.D., Campos, T.M.P., Nobre, M.M.M., Vargas, E.A. (2004). “Laboratory tests for reactive barrier design.” *Journal of Hazardous Materials.* Vol.110, pp.105-112

Haines, J.R., Wrenn, B.A., Holder, E.L., Strohmeier, K.L., Herrington, R.T., Venosa, A.D. (1996). “Measurement of hydrocarbon-degrading microbial populations by a 96-well plate most-probable-number procedure.”
Journal of Industrial Microbiology., Vol. 16, pp. 36-41.

Haines, J.R., Wrenn, B.A., Holder, E.L., et al. (1996) “Measurement of hydrocarbon-degrading microbial populations by a 96-well plate most-probable-number procedure” *Journal of Industrial Microbiology,* Vol. 16 (1), pp.36-41

Haws, N.W., Ball, W.P., Bouwer, E.J. (2006). “Modeling and interpreting bioavailability of organic contaminant mixtures in subsurface environments.” *Journal of Contaminant Hydrology.* Vol. 82, pp. 255-292

Headley, J.V., Bolldt-Leppin, B.E.J., Haug, M.D., and Peng, J. (2001). “Determination of Diffusion and Adsorption Coefficients for Volatile Organics in an Organophilic Clay-Sand-Bentonite Liner.” *Canadian Geotech. Journal*, Vol. 38, pp. 809-817.

Hong, E. (2003). “Sustainable Oil and Grease Removal from Stormwater Runoff Hotspots using Bioretention.” *M.S thesis*,. University of Maryland-Collegepark, Department of Civil and Environmental Engineering.

Hong, E.Y., Seagren, E.A., Davis, A.P., (2006) “Sustainable oil and grease removal from synthetic stormwater runoff using bench-scale bioretention studies.” *WATER ENVIRONMENT RESEARCH* . VOL.78 (2): 141-155 FEB 2006

Hower, J.C., Mastalerz, M. (2001). "An Approach Towards a Combined Scheme for the Petrographic Classification of Fly Ash," *Energy and Fuels*, Vol.15, pp. 1319-1321.

Indraratna, B. (1992). Problems Related to Disposal of Fly Ash and Its Utilization as a Structural Fill, *Utilization of waste materials in civil engineering construction:*

proceeding of sessions sponsored by the Materials Eng. Division of ASCE, H. I.,Inyang and K. L. Bergson ed., pp. 274-285, ASCE, New York.

Jackson, D. R., Garrett, B. C. and Bishop, T. A. (1984). "Comparison of batch and column methods for assessing leachability of hazardous waste." *Environmental Science and Technology.* Vol.18, pp. 668-673.

Janos, P., Buchova, H., and Ryznarova, M. (2003). "Sorption of Dyes from Aqueous Solutions onto Fly Ash." *Water Research*, Vol. 37, 2003, pp. 4938-4944.

Jenk, U., Schreyer, J., and Klinger, C. (2003). " Fe(0)/lignitic coal: an efficient and mechanically stable reactive material for purification of water containing heavy metals, radionuclides, and nitroaromatics." *Environmental Science and Technology*, Vol.37, No.3, pp.644-651.

Kalin, R.M. (2004). "Engineered passive bioreactive barriers: risk-managing the legacy of industrial soil and groundwater pollution." *Current Opinion in Microbiology*. Vol.7, pp.227-238.

Kalyoncu, R., (2001). *Coal Combustion Products*, (http://minerals.usgs.gov/ minerals/pubs/commodity/coal/coalmyb01.pdf).

Kamnikar, B. (2001). "Managing Petroleum Contaminated Soil: Department of Transportation Perspective." *J. Environ. Eng.*, Vol. 127, No. 12, pp.1080-1088.

Kelly, W.R., Hornberger, G.M., Herman, J.S., Mills, A.L. (1996). "Kinetics of BTX biodegradation and mineralization in batch and column studies." *Journal of Contaminant Hydrology* 23, No.1/2, pp.113,132.

Kershaw, D., Culik, C., and Pamukcu, S. (1997). "Ground rubber: sorptive media for groundwater containing benzene and *o*-xylene." *Journal of Geotechnical and Geoenvironmental Eng*., Vol.123, No.4, pp.324-334.

Khan, F. I., Husain, T., and Hejazi, R., (2004). An overview and analysis of site remediation technologies, *Journal of Environmental Management*, Vol.71, pp.95-122.

Kim, J.Y., Edil, T.B., and Park, J.K. (1997). "Sorption of Organic Compounds in the Aqueous Phase onto Tire Rubber." *Journal of Environmental Management,* Vol. 123, No. 9, pp. 827-835.

Kim, J.Y., Edil, T.B., and Park, J.K. (2001). "Volatile Organic Compound Transport Through Compacted Clay." *Journal of Geotechnical and Geoenvironmental Eng*., Vol. 127, No. 2, pp. 126-134.

Kleineidam, S., Schuth, C., Grathwohl, P., (2002). "Solubility normalized adsorption-partitioning sorption isotherms for organic pollutants." *Environ. Sci. Technol.* Vol. 36, No. 21, pp. 4689– 4697.

Konstantinou, I. K., and Albanis, T. A. "Adsorption – Desorption Studies of Selected Herbicides in Soil – Fly Ash Mixtures." *J. Agric. Food Chem.,* Vol. 48, pp. 4780-4790.

Komnitsas, K., Bartzas, G., and Paspaliaris, I., (2006). " Modeling of reaction front in fly ash permeable reactive barrier." *Environmental Forensics*, Vol. 7, pp. 219-231.

Kulaots, I., Hsu, A., Hurt, H.R., and Suuberg, E.M. (2003). "Adsorption of surfactants on unburned carbon in fly ash and development of standardized foam index." *Cement and Concrete Research*, Vol. 33, pp. 2091-2099.

Kulaots, I., Hurt, H.R., and Suuberg, E.M. (2004). "Size and distribution of unburned carbon fly ash and its implications." *Fuel*, Vol.83, pp.223-230.

Lee, S. L., Hagwall, M., Delfino, J. J., and Rao, P.S.C. (1992). "Partitioning of Polycyclic Aromatic Hydrocarbons from Diesel Fuel into Water. *Environmental Science and Technology,* Vol. 26, pp. 2104-2110.

Lee, J., Hundal, L.S., Horton, R. and Thompson, M.L. (2002) " Sorption and transport behavior of naphthlane in an aggregated soil" Journal of Environmental Quality, Vol. 31, pp. 1716-1721

Lee, T., and Benson, C.H., (2002). Using foundry sands as reactive madia in permeable reactive barriers. *Geo Eng. Rep. 02-01*. Dep. of Civil and Envronmenatal Eng., Univertsity of Wisconsin Madison.

Lee T., Benson, C.H. and Eykholt G.R. (2004). "Waste green sands as reactive media for groundwater contaminated with trichloroethylene (TCE)". *Journal of Hazardous Materials*, Vol. 109, No.1-3, pp. 25-36

Leglize, P., Saada, A., Berthelin, J., Leyval, C. (2006). "Evaluation of matrices for the sorption and biodegradation of phenanthrene*." Water Research*. Vol.40, pp.2397-2404

Limousin, G., Gaudet, J.P., Charlet, L., Szenknect, S., Barthes, V., Krimissa, M. (2007). "Sorption isotherms: A review on physical bases, modeling and measurement." *Applied Geochemistry,* Vol. 22, pp. 249-275

Liu, K., Enfield, C.G., and Mravik, S.C., (1991)."Evaluation of sorption models in the simulation of naphthalene transport through saturated soils" *Ground Water*, Vol.29, No.5, pp. 686-692.

Liu, S.J., Jiang, B., Huang, G.Q., Li, X.G. (2006). "Laboratory column study for remediation of MTBE-contaminated groundwater using a biological two-layer permeable barrier." *Water Research*. Vol.40, pp.3401-3408

Lorbeer, H., Starke, S., Gozan, M., Tiehm, A., Werner, P. (2002). "Bioremediation of chlorobenzene-contaminated groundwater on granular activated carbon barriers, water, air, and soil pollution." *Focus*. Vol.2, pp.183-193

Luthy, R.G., Aiken, G.R., Brusseau, M.L., Cunningham, S.D., Gschwend, P.M., Pignatella, J.J., Reinhard, M., Traina, S.J., Weber, Jr.W.J., and Westall, J.C. (1997). "Sequestration of hydrophobic organic contaminants by geosorbents." *Environmental Science and Technology*, Vol.31, No.12, pp.3341-3347.

Malek, A., and Farooq, S. (1996). "Comparison of isotherm models for hydrocarbon adsorption on activated carbon." *Al ChE J.* Vol.42, No.11, pp.3191-3201

Manes, M., (1998). "Activated carbon adsorption fundamentals." *Meyers, R.A. (Ed.), Encyclopedia of Environmental Analysis and Remediation. John Wiley, New York.* pp. 26-67

Mansell, R.S., Selim, H.M., Kanchanasut, P., Davidson, J.M, and Fiskell, J.G.A., (1997). "Experimental and simulated transport of phosphorus through sandy soils." *Water Resources Research*, Vol.13, No.1, pp. 189194.

Mata-Sandoval, J. C., Karns, J., and Torrents, A. (2002). "Influence of Rhamnolipid and Triton X-100 on the desorption of pesticides from soils." *Environmental Science and Technology.,* Vol. 36, pp.4669-4675.

Matott, L. (2004). *IsoFit documentation and user's guide, version 1.0*, Dept. of Civil, Structural, and Environmental Engineering, Univ. at Buffalo, Buffalo, N.Y.

Maraqa, M.A., Zhao, X., Wallace, R.B., Voice, T.C. (1998). "Retardation coefficients of nonionic organic compounds determined by batch and column techniques", *Soil Sci. Soc. Am. J*. No.62, pp.142, 152.

Maraqa, M. A., (2001) " Effects of fundamental differences between batch and miscible displacement techniques in sorption distribution coefficient" Environmental Geology Vol. 41. pp. 219-228.

Maraqa, M. A. (2007) " Retrdation of Nonlinearly Sorbed Solutes in Porous Media" ASCE Journal of Environmental Eng. Vol. 133, No. 12, pp. 1080-1087.

Maroto-Valer, M.M., Taulbee, D.N., and Hower, J.C. (2001). "Characterization of differinf forms of unburned carbon present in fly ash separated by density gradient centrifugation." *Fuel*, Vol. 80, pp.795-800.

Maroto-Valer, M.M., Taulbee, D.N., and Hower, J.C. (1999). "Novel separation of the differing forms of unburned carbon in fly ash using density gradient centrifugation." *Energy&Fuels*, Vol.13, No.13, pp.947-953.

Maurya, N.S., and Mittal, A.K. (2006). "Applicability of equilibrium isotherm models for the biosorptive uptakes in comparison to activated carbon-based adsorption." *Journal of Environmental Engineering ASCE*. Vol. December, 2006, pp.1589-1599.

McBride, J.F., Brockman, F.J., Szecsody, J.E., Streile, G.P. (1992). "Kinetics of quinoline biodegradation, sorption and desorption in a clay coated model soil containing a quinoline-degrading bacterium." *J. Contam. Hydrol*., No.9, pp.133-154.

McBride, M., (1994). "Environmental chemistry of soils*"*, *Oxford University Press, New York.*

McGovern, T., Guerin, T. F., Horner, S., and Davey, B. (2002). "Design, construction and operation of a funnel and gate in-situ permeable reactive barrier for remediation of petroleum hydrocarbons in groundwater." *Water, Air and Soil Pollution*, Vol. 136, pp. 11.31.

McNamara, N.P., Black, H.I.J., Beresford, N. A. Parekh, N.R., (2003)." Effects of acute gamma irradiation on chemical, physical and biological properties of soils." *Applied Soil Ecology*, Vol. 24,No. 2, pp. 117-132

Meegoda J. N. and Ratnaweera, P. (1995). "Treatment of Oil Contaminated Soils for Identification and Classification." *ASTM Geotechnical Testing Journal*, Vol. 18, No. 1, pp. 41-49.

Meegoda, J. N., Chen, B., Gunasekera, S. D., and Pederson, P. (1998). "Compaction characteristics of contaminated soils-reuse as an road base material**."** *Recycled materials in geotechnical applications: proceedings of sessions of Geo-Congress 98*, C. Vipulanandan and David J. Elton, ed., ASCE Geotechnical special publication ;No. 79. pp.195-209, Reston, VA.

Meegoda, J. N., (1999). "Stabilization/Solidification of Petroleum Contaminated Soils with Asphalt Emulsion." *Practice Periodical of Hazardous, Toxic and Radioactive Waste Management,* ASCE, Vol. 3, No. 46, pp. 46-55.

Mehl, S.W. and M.C. Hill, 2001, Comparison of solute transport solution techniques and their effect on sensitivity analysis and inverse modeling results, *Ground Water*, 39(2), 300-307.

Mercer J.W., and Cohen. R.M., (1990). "A Review of Immiscible Fluids in the Subsurface Properties, Models, Characterization and remediation." *Journal of Contaminant Hydrology*, Vol. 6, pp. 107 – 163.

Mendenhall, W., and Sincich T. (1984). *Statistics fro the Engineering and Computer Sciences*. Dellen Publishing Company, San Francisco, CA.

Mihelcic, J. R., and Luthy, R. G. "Degradation of PAH compounds under varios redox conditions in Soil water systems" *Applied Environmental Microbiology May* 1988 1182-1187 Vol 54 No.5

Miller, C. T., and Weber, W. J. (1988). "Modeling the sorption of hydrophobic contaminant by aquifer material 2. column reactor systems." *Water Research*, Vol. 22, pp. 465-474.

MDE, (2001). Maryland Department of Environment Cleanup Standards for Soils and Groundwater, (http ://www. mde. state. md. us/ assets / document / hazcleanup Dec2000. pdf

Moo-Young, H.K, and Zimmie, T.F., (1996). "Waste minimization and re-use of paper sludges in landfill covers: A case study." *Waste Manage. Res.* Vol. 15, pp. 593–605.

Mott, H.V., and Weber, W.J. (1992). "Sorption of low molecular weight organic contaminants by fly ash: considerations for the enhancement of cutoff barrier performance" *Environmental Science and Technology*. Vol.26, pp.1234-1241

Mullah, A.H., and Robinson, C.W. (1996). "Pentachlorophenol adsorption and desorption characteristics of granular activated carbon-I isotherms." *Water Res*., Vol. 30, No. 12, pp. 2901-2906

Murphy, E. M., Ginn, T. R., Chilakapati, A., Resch, C. T., Phillips, J. L., Wietsma, T. W., and Spadoni, C. M. (1997). "The influence of physical hetergeneity on microbial degradation and distribution in porous media." *Water Resources Research*, 33(5), 1087-1103.

Nguyen, T.H., Sabbah, I., Ball, W.P. (2004). "Sorption nonlinearity for organic contaminants with diesel soot: method development and isotherm interpretation." *Environ. Sci. Technol.* Vol. 38, pp. 3595-3603

Nguyen, T.H., Cho, H., Poster, D.L., Ball, W.P. (2007). "Evidence for a pore-filling mechanism in the adsorption of aromatic hydrocarbons to a natural wood char." *Environ. Sci. Technol*. Vol. 41, pp. 1212-1217

Nollet, H., Roels, M., Lutgen, P., Van der Meeren, P., and Verstraete W. (2003). "Removal of PCBs from Wastewater Using Fly ash." *Chemosphere*, Vol. 53, pp.655-665.

Nielsen, P. H., Bjerg, P.L, Nielsen, P., Smith, P, and Christensen, T, H, (1996). " Insitu and laboratory determined first-order degradation rate constants of specific organic compounds in an aerobic aquifer." *Environ. Sci. Technol*. Vol. 30, No. 1 pp. 31-37

Northcott, G.L., and Jones. C.J. (2000). "Spiking Hydrophobic Organic Compounds into Soil and Sediment: A Review and Critique of Adopted Procedures." *Environmental Toxicology and Chemistry*, Vol. 19, No. 10, pp. 2418-2430.

Norit Americas Inc. (2007). Hydrodarco®B Datasheet, http://www.norit-americas.com/pdf/HDB_rev6.pdf.

Oliviera, I.B., Demand, A.H., and Salehzadeh, A. (1996). "Packing of sands for the production of homogeneous porous media." *Soil Science Society of America Journal*, Vol. 60, No. 1, pp.49-53.

Pankow, J. F., and Cherry, J.A., (1996). *Dense chlorinated solvents and other DNAPLs in groundwater*, Waterloo Press, Oregon.

Park, J., Zhao, X., and Voice, T.C, (2001)." Biodegradation of non-desorbable Naphthalene in soils." *Environ. Sci. Technol*. Vol. 35, No. 13, pp. 2734-2740.

Patterson, B.M., Grassi, M.E., Davis, G.B., Robertson, B.S., McKinley, A.J. (2002). "Use of polymer mats in series for sequential reactive barrier remediation of ammonium-contaminated groundwater: laboratory column evaluation." *Environ. Sci. Technol*. Vol. 36, pp. 3439-3445

Petzrick, P. (2001). "The Use Power Plant Coal Combustion Products in Maryland." *Proceedings of International Ash Utilization Symposium*, Paper #51, pp. 7, Lexington, Kentucky.

Qiao, X.C., Poon, C.S., and Cheeseman, C., (2005). "Use of flue gas desulphurization (FGD) waste and rejected fly ash in waste stabilization/solidification systems", *Waste Management*, Vol. 26, Issue 2, pp. 141-149.

Rabideau, A.J., Benschoten, J.V., Khandelwal, A., Repp, C.R. (2001). "Sorbing vertical barriers." *Physicochemical Groundwater Remediation.*

Rabideau, A.J., Suribhatla, R., Craig, J.R. (2005). "Analytical models for the design of iron-based permeable reactive barriers." *Journal of Environmental Engineering.* Vol. 131, No.11, pp.1589-1597

Ramussen, G., Fremmersvik, G., Olsen, R.A. (2002). "Treatment of creosote-contaminated groundwater in a peat/sand permeable barrier, a column study." *Journal of Hazardous Materials*. Vol.B93, pp.285-306

Reemtsma T. and Mehrtens J. (1997). "Determination of polycyclic aromatic hydrocarbon (PAH) leaching from contaminated soil by a column test with on-line solid phase extraction." *Chemosphere* Vol.35, pp.2491-2501.

Reid, B.J., Northcott, G.L., and Semple K.T. (1998). "Evaluation of Spiking Procedures for the Introduction of Poorly Water Soluble Contaminants into Soils." *Environmental Science and Technology*, Vol. 32, pp. 3224-3227.

Rifai, H.S., Newell, C.J., Miller, R., Taffinder, S., and Rounsaville, M, (1995)."Intrinsic Bioattenuation for subsurface restoration" *Proceedings, 1995 Battelle International Conference on In situ and On site Bioreclamation,* Battelle Pres., Columbus OH.

Rittmann, B. E., Seagren, E. A., Wrenn, B. A., Valocchi, A. J., Ray, C., and Raskin, L. (1994). *In situ bioremediation*, Noyes Publishers, Park Ridge, NJ.

Rumer, R. R., Jr. (1962). "Longitudinal dispersion in stready and unsteady flow." *J. Hydraulics Div., Proc. Amer. Soc. Civil Eng.*, 88, 147-172.

Salanitro, J.P, Spinnler, G.E., Maner, P.M., Tharpe, D.L., Pickle, D.W., Wisniewski, H.L., Johnson, P.C., and Bruce, C. (2001), "Insitu bioremediation of MTBE using biobarriers of single or mixed cultures" *International in situ and on-site bioremediation symposium, Bioaugmentation, biobarriers, and biogeochemistry ed. Leeson, A,Alleman, B.C, Alvarez, P. J and Megar V .C* , Battelle press Columbus OH.

Schad, H., and Gratwohl, P. (1998). "Funnel-and-gate systems for in situ treatment of contaminated groundwater at former manufactured gas sites." Proceeding of NATO/CMS Phase III meeting, 23-24 February, 1998, Vienna, Austria.

Schwab, A.P., Su, J., Wetzel, S., Pekarek, S., and Banks, M. K. (1999). "Extraction of Petroleum Hydrocarbons from Soils by Mechanical Shaking." *Environmental Science and Technology*, Vol. 33, pp. 1940 – 1945.

Schwarz, L.G., Krizek, R.J. (2006). "Hydrocarbon Residuals and containment in microfine cement grouted sand." *Journal of Materials in Civil Engineering, ASCE.* Vol. March/April 2006, pp. 214-228

Schwarzenbach, R.P., Gschwend, P.M., and Imboden, D.M. (1993). *Environmental Organic Chemistry*, Wiley, New York.

Schwarzenbach, R.P., Gschwend, P.M., and Imboden, D.M. (1999). *Environmental Organic Chemistry-2nd Edition*, Wiley, New York.

Seagren, E.A., Rittmann, B.E., and Valocchi, A.J. (1994). "Quantitative evaluation of the enhancement of NAPL-pool dissolution by flushing and biodegradation." *Environmental Science and Technology*, Vol.28, No.5, pp.833–839.

Seagren, E.A., and Moore. T.O. (2003). "Nonaqueous phase liquid pool dissolution as a function of average pore water velocity." *Journal of Environmental Engineering*, 1Vol.29, No.9: pp.786-799.

Semple K.T., Moriss, A.W.J., Paton, G.I. (2003). "Bioavailability of Hydrophobic Organic Contaminants in Soils: Fundamental Concepts and Techniques for Analysis." *European Journal of Soil Science*, Vol.54, pp. 809–818.

Senol, A., Binshafique, S., Edil, T.B., Benson, C.H. (2002). "Use of Class C Fly Ash For Stabilization of Soft Subgrade", *Fifth International Congress on Advances in Civil Engineering,* Istanbul Technical University, Istanbul, Turkey, 25-27 September, pp.89 – 95.

Shirazi, F. H., (2001), "Comparative cost and performance of two novel biological permeable barriers (BPBs)." *International in situ and on-site bioremediation symposium, Bioaugmentation, biobarriers, and biogeochemistry ed. Leeson, A,Alleman, B.C, Alvarez, P. J and Megar V .C* , Battelle press Columbus OH.

Song, X., (2005) Subsurface Heterogeneities, Interfaces and Biodegradation Defining the Limits on In Situ Bioremediation, Ph.D Dissertation, University of Maryland College Park.

Spurlock, F. C., Huang, K. and van Genuchten. M. Th.(1995). Isotherm nonlinearity and nonequilibrium sorption effects on transport of fenuron and monuron in soil columns. *Environ. Sci. Techn*., 29(4): 1000-1007.

Su, C., and Puls, R.W. (2003). "In situ remediation of arsenic in simulated groundwater using zerovalent iron: laboratory column tests on combined effects of phosphate and silicate." *Environ. Sci. Technol*. Vol.37, pp.2582-2587

Tiehm, A., Gozan, M, Muller, A., Bockle, K, Schell, H, Lorbeer, H. and Werner, P., (2001). "Biologoval activated carbon barriers for the reoval of chloroorganics/BTEX Mixtures." *International in situ and on-site bioremediation symposium, Bioaugmentation, biobarriers, and biogeochemistry ed. Leeson, A,Alleman, B.C, Alvarez, P. J and Megar V .C* , Battelle press Columbus OH.

Tuncan, A., Tuncan, M., and Koyuncu, H. (2000). "Use of Petroleum Contaminated Drilling Wastes as Subbase Material for Road Construction." *Waste Management and Research,* Vol. 18, pp. 489-505.

USEPA, (1999). "Understanding Variation in Partition Coefficient Kd Values" *EPA United States Office of Research EPA/402/R-99/004A* Environmental Protection and Development Agency, 1999, Washington, DC 20460.

USEPA (2004). "*Underground storage tanks: Building on the past to protect the future*" 510-R-04-001 http://www.epa.gov /oust/pubs / 20rpt508.pdf

USEPA, (2006a). *Performance Evaluation of an Organic Carbon/Zero-Valent Iron Based PRB for Treatment of Arsenic and Heavy Metals,* (http://www.epa.gov/ada/research/waste/research_01.pdf).

USEPA, (2006b). Performance Evaluation of Organic Carbon + Limestone Based PRB for Treatment of Pb and Acidity, (http://www.epa.gov/ada/ research/waste/research_02.pdf).

USGS, (2006). *Modular three-dimensional finite-difference ground-water mode,* http://water.usgs.gov/nrp/gwsoftware/modflow2000/Mf2k.txt.

van Genuchten, M.T., and Alves, W.J. (1982). "Analytical solution for the one dimentional convective-dispersive solute transport equation." Tech. Bull. No.1661, U.S. Dept of Agric., Washington, D.C.

Wang, S., Li, L., Wu, H., and Zhu, Z. (2005a). "Unburned carbon as a low-cost adsorbent for treatment of methylene blue-containing wastewater*." Journal of Colloid and Interface Science*, Vol.292, pp.336-343.

Wang, S., Boyjoo, Y., Choueib, A., Ng, E., Wu, H., and Zhu, Z. (2005b). "Role of unburnt carbon in adsorption of dyes on fly ash" *Journal of Chemical Technology and Biotechnology*, Vol.80, pp.1204-1209.

Warith, M., Fernandes, L., Gaudet, N. (1999). "Design of in-situ microbial filter for the remediation of naphthalene." *Waste Management*. Vol.19, pp.9-25

Woinarski, A.Z., Snape, I., Stevens, G.W., Stark, S.C. (2003). "The effects of cold temperature on copper ion exchange by natural zeolite for use in a permeable reactive barrier in Antarctica." *Cold Regions Science and Technology*, Vol.37, pp.159-168.

Xia, G. and Ball, W.P., (1999). "Adsorption-partitioning uptake of nine low-polarity organic chemicals on a natural sorbent." *Environmental Science and Technology*, Vol.33, No.2, pp.262-269.

Xing, B., and Pignatello, J.J. (1997). "Dual-Mode sorption of low-polarity compounds in glassy poly (vinyl chloride) and soil organic matter." *Environmental Science and Technology*, Vol.31, No.3, pp.792-799.

Xia, G.S., Pignatello, J.J., (2001). "Detailed sorption isotherms of polar and apolar compounds in a high-organic soil." *Environ. Sci. Technol*. Vol. 35, No.1, pp. 84–94.

Yang, X.Y., and Al-Duri, B. (2000). "Application of branched pore diffusion model in the adsorption of reactive dyes on activated carbon." *Chem. Eng. J.,* Vol.83, No.1, pp. 15-23

Yolcubal, I., Dorn, J.G., Maier. M. R., and Brusseau, M.L, (2003) "The influence of substrate and electron acceptor availability on bioactive zonedynamics in porous media" *Journal of Contaminant Hydrology*, Vol. 66, pp. 219 – 237.

You, C.N., and Liu, J.C. (1996). "Desorptive behavior of chlorophenols in contaminated soils." *Water Sci. Tech.*, Vol.33, No.6, pp.263-270.

Yukselen, Y., and Kaya, A., (2006) "Comparison of methods for determining specific surface area of soils." *ASCE Journal of Geotechnical and Geoenvironmental Engineering* Vol. 132,No. 7, pp. 931-936

Zheng, C., and Wang P.P., (1999). "*MT3DMS, A modular three-dimensional multi-species transport model for simulation of advection, dispersion and chemical reactions of contaminants in groundwater systems; documentation and user's guide"* U.S. Army Engineer Research and Development Center Contract Report SERDP-99-1, Vicksburg, MS.

Zhu, L., Chen, B., and Tao, S. (2004). "Sorption behavior of polycyclic aromatic hydrocarbons soil – water containing nonionic surfactant." *Environmental Engineering Science*, Vol.21, No.2, pp.263-272.